ISSN 1927-0461 (Print)
ISSN 1927-047X (Online)

Journal of Plant Studies

Vol. 6, No. 2 September 2017

CANADIAN CENTER OF SCIENCE AND EDUCATION

Journal of Plant Studies; Vol. 6, No. 2; 2017
ISSN 1927-0461 E-ISSN 1927-047X
Published by Canadian Center of Science and Education

EDITORIAL TEAM

Journal of Plant Studies; Vol. 6, No. 2; 2017
ISSN 1927-0461 E-ISSN 1927-047X
Published by Canadian Center of Science and Education

CONTENTS

Journal of Plant Studies; Vol. 6, No. 2; 2017
ISSN 1927-0461 E-ISSN 1927-047X
Published by Canadian Center of Science and Education

Antagonistic Activity of *Pseudomonas Fluorescens* Against *Fusarium Oxysporum* f. sp. *Nievum* Isolated from Soil Samples in Palestine

Mazen Salman[1], Nabil Shahin[1], Nawaf Abu-Khalaf[1], Mohammad Jawabrih[1], Basima Abu Rumaileh[1], Ruba Abuamsha[2] & Sameer A. Barghouthi[3]

[1]College of Agricultural Sciences and Technology, Palestine Technical University-Kadoorie (PTUK), Tulkarm, State of Palestine

[2]National Agriculture Research Centre (NARC), Ministry of Agriculture, Qabatya, Jenin, State of Palestine

[3]Department of Medical Laboratory Sciences, Faculty of Health Professions, Al Quds University, Jerusalem, State of Palestine

Correspondence: Mazen Salman, College of Agricultural Sciences and Technology, Palestine Technical University-Kadoorie (PTUK), Tulkarm, State of Palestine. E-mail: salman_mazen@daad-alumni.de

Received: January 23, 2017 Accepted: February 20, 2017 Online Published: March 6, 2017

doi:10.5539/jps.v6n2p1 URL: https://doi.org/10.5539/jps.v6n2p1

Abstract

Watermelon is an important summer crop in Palestine, for several decades filling the needs of local market and some Arab countries. The yield of watermelon decreased dramatically in recent years due to severe infections with the soil borne fungal pathogen *Fusarium oxysporum f. sp. niveum* (FON). Soil fumigation with methyl bromide was commonly applied by Palestinian farmers until it was recently legally banned. Different control mechanisms were not feasible to overcome problems caused by the disease resulting in decreased watermelon cultivation in Palestine for the past 30 years. In this work, we have experimentally shown that *Pseudomonas fluorescens* was efficient in controlling FON infection and allowing normal seedling growth of both the root and shoot systems. Field experiments are necessary to further confirm the efficacy of biocontrol application.

Keywords: Biological Control, Watermelon, Fungi, Bacteria

1. Introduction

Watermelon (*Citrullus lanatus* L.) is an economically important vegetable crop in many parts of the world. In Palestine, it is one of the most important summer fruit crops. According to FAOSTAT (2014), the watermelon cultivated area was estimated to be 356 ha during the period from 2001-2008 with an average yield of 13,777 tons. In the following years, the watermelon area decreased by more than 65% and the total annual production was reduced by more than 75% (FAOSTAT, 2014). A number of reasons caused the dramatic decline in watermelon cultivation, of which Fusarium Wilts caused by formae speciales of *Fusarium oxysporum* that are generally considered host specific (Martyn, 2012; Ren et al., 2015; Meyer et al., 2016). *Fusarium oxysporum* f. sp. *niveum* (FON) is one of the most severe diseases in watermelon and a major limiting factor for watermelon production in the world (Martyn & McLanghlin, 1983; Peng et al., 2013). Due to high infestation rates of the disease in different regions in Palestine, farmers have abandoned growing watermelon. The use of fungicides is not always feasible due to economic and ecological reasons.

Currently, no effective fungicides or chemical disinfectants are available because FON can generate thick-walled chlamydospores that are highly resistant to soil fumigation (Besri, 2008; Peng et al., 2013). FON can survive in soil as saprophyte for many years (Notz, Maurhofer, Dubach, Haas, & Defago, 2002). Therefore, watermelons can only be replanted in locations with infected soil, after FON has been eradicated by preplan treatments with soil fumigants. However, the most effective soil fumigant, methyl bromide, has been phased out, and FON can transform itself into thick-walled chlamydospores, highly resistant to chemical fumigation (Lin, Chen, Liou, Huang & Chang, 2009), leaving hardly any means to control the soilborne FON safely, economically and effectively (Ren et al., 2015).

With increasing public awareness of the environmental implications of the extensive use of fungicides in agricultural practices, alternative strategies for the control of plant disease are being sought (Weller, 1988; Ellis et al., 1999). Biological control using antagonistic microorganisms alone, or as supplements to minimize the use

of chemical pesticides in a system of integrated plant disease management, has become more important in recent years (Hwang, 1993; Mao, Lewis, Hebber, & Lumsden, 1997).

Soilborne, non-pathogenic fast growing bacteria that are capable of antagonizing fungal phytopathogens might represent first choice biocontrol method. They show great promise with respect to protecting plant roots from fungal-induced diseases (O'Sullivan & Ogara, 1992; Walsh, Morrissey, & O'Gara, 2001). These bacteria are known by several generic names, including biological control agents (BCAs), plant growth promoting rhizobacteria (PGPR) and biopesticides (Walsh et al., 2001). The aim of this study was to test the activity of *P. fluorescens* isolate against the watermelon fungal pathogen *F. oxysporum* f. sp. *nievum* (FON).

2. Methods

2.1 Isolation of FON Plant Pathogens

Soil and plant samples naturally infested with FON were used for the isolation of pathogenic strains of the fungus. Isolation from soil samples was conducted using the soil dilution plate technique modified from Nishimura (2007). One gram of soil was suspended in 99 ml of 0.05% water agar. Serial dilutions (10^{-3}, 10^{-4} and 10^{-5}) were prepared and 100 µl from each solution were spread on selective medium for FON isolation; selective medium was prepared as described by Leslie and Summerell (2006).

For isolation of the pathogen from plant materials and debris, samples were washed thoroughly under running tap water, blotted to remove excess water, cut into 0.5 cm pieces that were placed on the selective medium.

2.2 Selection of Biological Control Agents (BCAs) to FON

Bacteria were isolated from healthy and infected watermelon plants as well as from infested and non-infested soil samples. Bacterial extracts were suspended in 0.085% NaCl, diluted serially and 100 µl were spread on Nutrient Agar media supplemented with 50 µg ml^{-1} cyclohexamide.

Four-day old cultures of FON grown on 7-mm diameter disks were placed centrally on potato dextrose agar (PDA) plates were used as targets for bacterial mediated antagonism. Bacterial suspensions (~ 5 x 10^9 cfu ml^{-1}) in 20 µl of 24 hrs old broth cultures were placed on 0.5 cm sterile paper disks. The assembled test cultures were incubated for 48 hrs at 22°C and inhibition of mycelial growth was noted. Bacteria that inhibit fungal growth were selected for further greenhouse studies. Identification of *P. fluorescens* was done as mentioned in Barghouthi (2010).

2.3 Pathogenicity of Bacteria to Host Plant (Wtermelon)

In order to test whether the selected bacteria were pathogenic to host plants, 2-3 true leaf stage plants (grown in peat moss vermiculite mix 2:1, v/v) were treated by root drench with different concentrations of bacterial suspensions (10^7-10^9 cfu ml^{-1}). Control was done by treatment of seedlings with sterile water. Seedlings were incubated in climate rooms of 12 hrs day length and day-night temperature of 26°C and 16°C. Plant height, fresh and dry weights of root and shoot, and damage were assessed and recorded after the plant reached a stage of development of 4-5 true leaves (Montealegre et al., 2003).

The pathogenicity of bacterium was tested on watermelon seeds as well. Seeds were immersed in bacterial suspensions (10^7-10^9 cfu ml^{-1} in 2% methylcellulose, pH 7.0) for 60 seconds (Abuamsha, Salman, & Ehlers, 2011). Seeds were sown in peat moss vermiculite mix (2:1, v/v) at the above mentioned conditions. Measurements of time of emergence, heights and fresh and dry weights of shoots and roots were recorded when the seedling reached the 2-3 true leaf stage (Montealegre et al., 2003).

2.4 Molecular Identification of Isolated Fusarium Spp

Isolated fungal strains were identified using PCR according to the method of Z. Zhang, J. Zhang, Wang, and Zheng (2005). Specific primers for FON Fn-1 (5'-TACCACTTGTTGCCTCGGC-3') and Fn-2 (5'-TTGAGGAACGCGAATTAAC-3') were used to produce a 327 bp PCR product. PCR was performed in 25 µl reaction mixtures containing 1 µl genomic DNA, 0.5 µM primers, a 0.5-µl mixture that contained 50 mM of each dNTP, 2.5 µl 10 PCR buffer, 2 mM Mg^{2+}, 2.5 µl 1% BSA, 0.25 µl Tw-20, and 1.25 U of Taq DNA polymerase. Amplification was performed using PCR System DNA thermal cycler programmed for one cycle at 94°C for 5 min, followed by 35 cycles at 94°C for 30 s, 54°C for 30 s, and 72°C for 30 s. A final 7-min extension at 72°C was conducted. PCR products were separated on 1.5% agarose (in TAE buffer) for 60 min at 70V and visualized after staining with ethidium bromide (0.2 µg) under UV transilluminator.

2.5 In Vitro Inhibition of Fungal Growth

The antagonistic activity of bacteria against FON was determined using the dual culture technique (Salman,

2010). Each bacterial strain was streaked on the center line of a PDA plate and incubated for 24 hrs at 28°C. Then two disks of FON grown for 4 days on PDA medium were placed about 3 cm apart from the bacterial streak. Cultures were then incubated at 22°C for 48 hrs. Control experiments used sterile distilled water instead of bacteria. The distance between the bacterial streaks was recorded and the effect of the bacteria was determined by measuring the inhibition zone of mycelial growth.

2.6 Greenhouse Pot Experiments

Watermelon (*Citrullus lanatus* (Thunb)) was used as the target test plant species. Seed treatment with the bacteria was done as mentioned above. For infesting soil with *F. oxysporum* sp. *niveum*, pots (9 cm diameter; 450 cm^3) were 66% filled with peat moss vermiculite mix (2:1, v/v). Small agar pieces (1/16 of an agar plate; 3 (7 mm diameter) discs from plates grown with FON (4-days old) were placed on the soil surface of each pot. Subsequently, the inoculum of each pot was then covered with a top layer of soil. The pots with infested soil and control-non-infested soil were watered and incubated for 3-days under greenhouse conditions as mentioned above, before sowing five watermelon seeds per pot (Vogt & Buchenauer, 1997). Disease development was recorded by examining a cross section of water melon stems after three weeks of sowing the seeds. During experimental period, all plants were fertilized weekly with commercial N:P:K (8:8:6) fertilizer.

2.7 Statistical Analysis

All experiments were done in triplicates and repeated three times. Statistical analysis was done using XlStat (Adinosoft). Significant differences were computed using ANOVA after Tukeys HSD test at $P< 0.05$.

3. Results

Six FON isolates (F161, F162, F163, F164, F241, and F243) were obtained from infected watermelon plants. All six isolates were shown to be FON based on PCR using *F. oxysporum* specific primers that produced a 327bp PCR amplicon (Fig. 1).

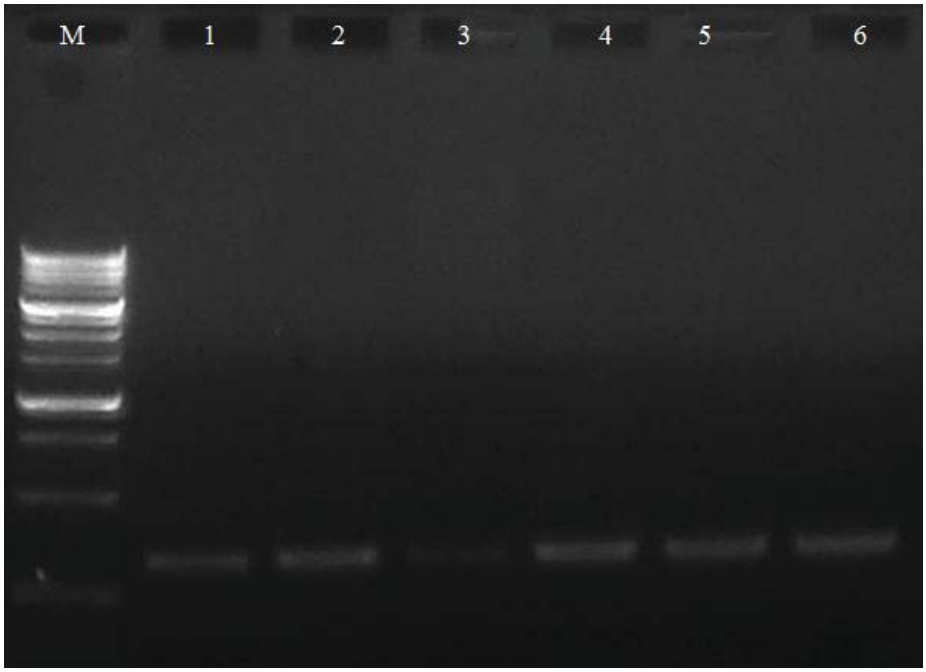

Figure 1. PCR products of 6 FON isolates F161 (lane 1), F162 (lane 2), F163 (lane 3), F164 (lane 4), F241 (lane 5) and F243 (lane 6) after amplification with FON specific primers Fn-1 and Fn-2. PCR products were separated on 1.5% agarose gel in 1X TAE buffer at 80 V for 1 h. Lane M, 100bp marker.

All fungal isolates were detected in reinfected watermelon seedlings. However, only isolate F161 showed browning symptoms in cross sections of the seedlings (Fig. 2). The isolate was used for further studies to evaluate the efficacy of bacteria against the pathogen. Inhibition zones on PDA against FON isolates were obvious in the presence of *P. fluorescens* (Fig. 3). A large inhibition zone (8 mm) in the presence of the bacteria was significantly higher ($P < 0.05$) against FON isolate F161 (Table 1). The lowest inhibition zone was recorded against FON isolate F162.

Table 1. In vitro antagonistic effects of *P. fluorescens* isolates against six FON isolates on PDA medium.

FON isolate	Inhibition distance (mm)	Average diameter of FON (mm)
F161	8 [a]	9.7 [d]
F163	5.4 [b]	11.5 [c]
F241	5.4 [b]	13 [ab]
F243	4.1b [c]	11.6 [bc]
F164	3.6 [c]	13.1 [ab]
F162	2.9 [c]	12.4 [bc]
FON	0 [d]	14.2 [a]

Data with different letters in the same column are significantly different after ANOVA at $P < 0.05$ using Tukeys HSD test.

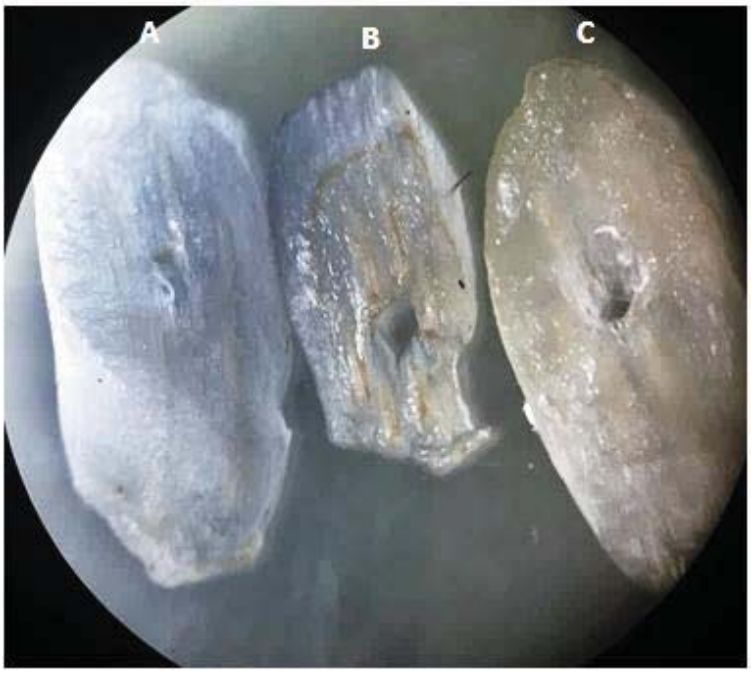

Figure 2. Stem Cross section showing vascular browning of watermelon stem (A) Control; (B) Infected with the FON isolate F161 and treated with of *P. fluorescens* and (C) Infected with FON isolate F161. Browning of tissue was due to fungal growth; indicating tissue infection.

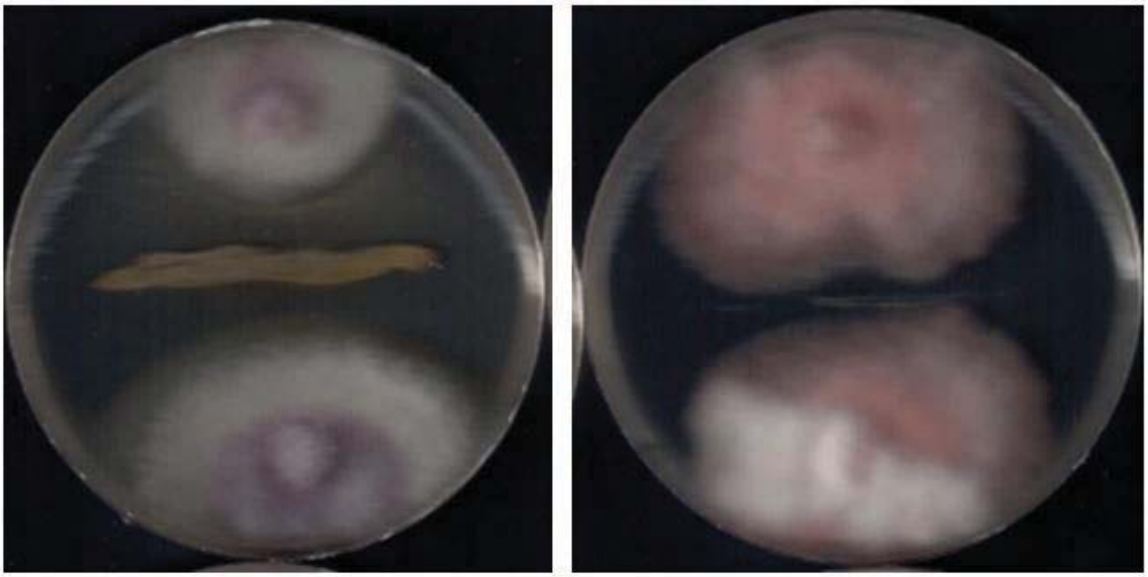

Figure 3. Inhibition caused by *P. fluorescens* against FON isolate 161 (left) on PDA medium.

Under pot experiments, watermelon seedling grown in the presence of the bacteria showed higher growth rates compared to control seedlings or seedlings infected with the pathogen (Fig. 4). Growth promotion effect of the bacteria was measured and the results proved the bacteria could enhance both fresh and dry weights of the plant (Table 2). Shoot fresh and dry weights of watermelon seedlings treated with the bacteria (5.112±0.159 and 1.03±0.105, respectively) were significantly higher ($P < 0.05$) than that in the control seedlings (3.40±0.448 and 0.52 ±0.116, respectively). Seedlings Infected with FON showed significantly lower ($P < 0.05$) fresh shoot and root dry weights (1.59±0.209 and 0.31±0.068, respectively). The same observations were recorded for dry shoot and root weights (Table 2).

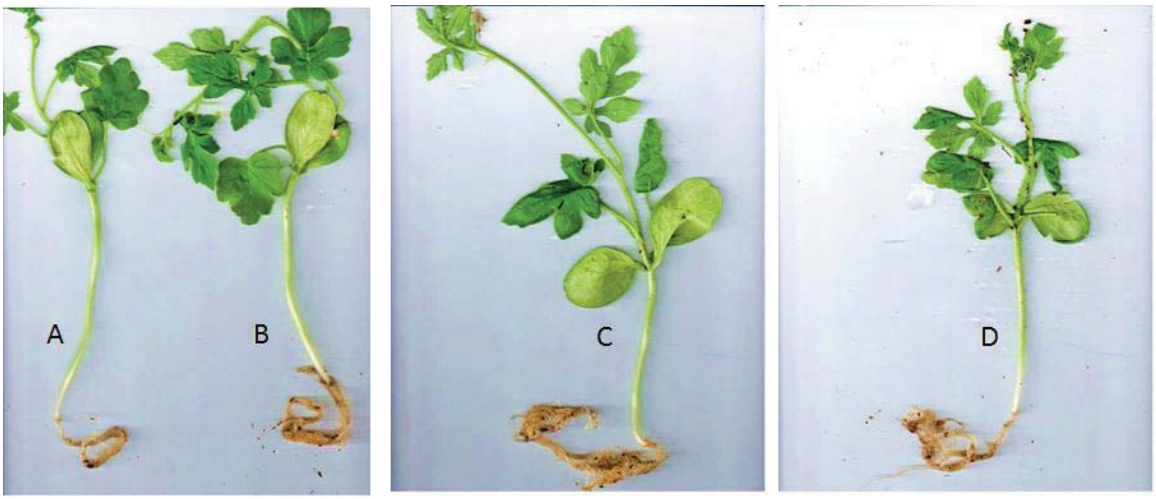

Figure 4. Seedlings of watermelon three weeks after sowing, (A) infected with FON isolate F161 (B) infected with isolate F161 and treated with *P. fluorescens* (C) treated only with *P. fluorescens* and (D) negative control, not treated. Notice that B, C, and D are well developed relative to A which is infected but not treated.

Table 2. Fresh and dry weight of water melon seedling three weeks after sowing growth promotion effect of *P. fluorescens* on watermelon.

	Shoot fresh weight (g)	Shoot dry weight (g)	Root fresh weight (g)	Root dry weight (g)
Control	3.40±0.448 [b]	0.20±0.047 [cd]	0.52±0.116 [bc]	0.03±0.006 [ab]
P. fluorescens	5.112±0.159 [a]	0.35±0.024 [ab]	1.03±0.105 [a]	0.05±0.012 [a]
F161	1.59±0.209 [c]	0.08±0.009 [d]	0.31±0.068 [c]	0.01±0.008 [b]
F161+*P. fluorescens*	4.28±1.0138 [ab]	0.25±0.041 [bc]	0.64 ±0.140 [b]	0.03±0.017 [ab]

Data with different letters in the same column are significantly different after ANOVA at $P < 0.05$ using Tukeys HSD test.

4. Discussion

In this study, it was found that some bacterial isolates were capable of preventing the growth of *F. oxysporum* f. sp. *niveum* under *in vitro* conditions and in pot experiments, respectively. Reports on using bacteria as biocontrol agents against plant pathogens and pests have increased in recent decades. In this work, screening bacterial isolates for anti- *F. oxysporum* activity; 167 bacterial isolates were screened as described in methods section for anti *F. oxysporum* activity. The biological control approach of plant pathogens and diseases has been studied for many years, and the introduction of beneficial microorganisms into soil or the rhizosphere has been proposed for the biological control of soilborne crop diseases (Joffe, 1986; Burge, 1988; Cook, 1993). Many studies have been conducted on the application of antagonistic microbes, such as Pseudomonas spp., for the control of Fusarium wilt (Tu & Chang, 1983; Duijff et al., 1999).

The ability of *P. fluorescens* to control the growth of *F. oxysporum* pathogenic isolates as represented by F161 was demonstrated *in vitro* assay and confirmed by pot experiments. The biocontrol activity of *P. fluorescens* observed in vitro experiments were reproduced in pot experiments.

P. fluorescens has shown great potential to controlling fungal infection. In addition, a significant ($P < 0.05$) enhancement of the growth of control seedlings treated with the bacterium relative to untreated control indicates that in addition to controlling infection, *P. fluorescens* somehow stimulated seedling growth either by provision or solubilization of nutrients and/or further protection of plants against an invisible plant pathogen.

Seedling wet or dry weight produced consistent results that were significantly different for each applied combination; poor growth of infected seedlings, enhanced growth of *F. oxysporum* infected or non-infected seedlings receiving *P. fluorescens* treatment.

Wet or dry weight of shoot and root systems revealed that significant difference existed between infected and bio-controlled seedlings. The *P. flueorescens* protected seedlings; fresh shoot weight was 4.28±1.0138 g which was higher than the F161 infected seedlings vs. 1.59 ± 0.209 for the infected seedlings ($p < 0.05$; $n \geqslant 9$). Protection allowed >2.6 folds enhancement in seedling shoot weight and enhanced growth >1.6 folds. *P. fluorescens* enhanced growth of seedlings in the absence of experimental infections possibly through the provision of other plant promoting factors or extended protection against unseen microbes or factors. The results are illustrated in Figs. 2-4 and Table 2.

Non-chemical strategies for the control of crop diseases are of considerable interest due to environmental and health concerns about the adverse effects of synthetic pesticides (Reuveni, 1995). Therefore, it is likely that there will be greater reliance on the use of microorganisms as antagonists of plant pathogens in the future (Hall, 1995; De Cal, Sztejnberg, Sabuquillo, & Melgarejo, 2009). However, the spectrum of activity of microorganisms as biocontrol agents is usually narrower than that of chemical pesticides (Baker, 1991; Janisiewicz, 1996). In addition, the inconsistent performance of microorganisms in commercial agriculture has limited their use as agents for controlling plant pathogens (Backman, Wilson, & Murphy, 1997; De Cal et al. 2009).

Application of Pseudomonas or its byproducts to field crops (before, during, and/or after sawing) such as watermelon and other similar crops that are afflicted by Fusarium, may improve the productivity and yields of such crops. Successful field biocontrol application will contribute to better agricultural methods. Furthermore, this method is cost effective, easily applicable and may accumulate beneficiary results on the long run; i.e. each successive year should be an improvement over the preceding year. Moreover, environmentally, it is a better choice than chemically based control methods.

Acknowledgments

This research was supported by Palestine Technical University-Kadoorie (PTUK).

References

Abuamsha, R., Salman, M., & Ehlers, R. U. (2011). Effect of seed priming with *Serratia plymuthica* and *Pseudomonas chlororaphis* to control *Leptosphaeria maculans* in different oilseed rape cultivars. *European Journal of Plant Pathology, 130*, 287-295. https://doi.org/10.1007/s10658-011-9753-y

Backman, P. A., Wilson, M., & Murphy, J. F. (1997). Bacteria for biological control of plant diseases. In: Recheigl, N.A., Recheigl, J. E. (Eds.), Environmentally safe approaches to crop Disease control. CRC Lewis Publishers, Boca Raton, FL, pp. 95-109.

Baker, R. (1991). Diversity in biological control. *Crop Protection, 10*, 85-94. https://doi.org/10.1016/0261-2194(91)90054-U

Barghouthi, S. (2010). A Universal Method for the Identification of Bacteria Based on General PCR Primers. *Indian Journal of Microbiology, 51*(4), 430-444. https://doi.org/10.1007/s12088-011-0122-5

Besri, M. (2008). Cucurbits grafting as alternative to methyl bromide for cucurbits production in Morocco. Proceedings of the 14th International Research Conference on Methyl Bromide Alternatives and Emissions Reduction, Orlando, pp. 60-61

Burge, M. N. (1988). The scope of fungi in biological control. In: Burge M.N. (Ed), Fungi in biological control systems. Manchester University Press, Manchester, 1-18

Cook, R. J. (1993). Making greater use of introduced microorganisms for biological control of plant pathogens. *Annual Review of Phytopathology, 31*, 53-80. https://doi.org/10.1146/annurev.py.31.090193.000413

De Cal, A., Sztejnberg, A., Sabuquillo, P., & Melgarejo, P. (2009). Management Fusarium wilt on melon and watermelon by *Penicillium oxalicum*. *Biological Control*, *51*, 480-486 https://doi.org/10.1016/j.biocontrol.2009.08.011

Duijff, B. J., Recorbet, G., Peter, A., Bakker, H. M., Loper, J. E., & Lemanceau, P. (1999). Microbial antagonism at the root level is involved in the suppression of Fusarium wilt by the combination of nonpathogenic *Fusarium oxysporum* Fo47 and *Pseudomonas putida* WCS358. *Phytopathology, 89*, 1073-1079. https://doi.org/10.1094/PHYTO.1999.89.11.1073

Ellis, R. J., Timms-Wilson, T. M., Beringer, J. E., Rhodes, D., Renwick, A., Stevenson, L., & Bailey, M. J. (1999). Ecological basis for biocontrol of damping-off disease by *Pseudomonas fluorescens* 54/96. *Journal of Applied Microbiology, 87*(3), 454-463. https://doi.org/10.1046/j.1365-2672.1999.00851.x

FAOSTAT, (2014). http://faostat3.fao.org/faostat-gateway/go/to/download/Q/QC/E

Hall, R. (1995). Challenges and prospects of integrated pest management. In: Reveuni, E. (Ed.), Novel approaches to integrated pest management. Lewis Publishers, CRC Press Inc., Boca Raton, FL, pp. 1-21

Hwang, S. F., Chakravarty, P., & Prevost, D. (1993). Effects of rhizobia, metalaxyl, and VA mycorrrhizal fungi on growth, nitrogen fixation, and development of Pythium root rot of Sainfoin. *Plant Disease, 77*, 1093-1098. https://doi.org/10.1094/PD-77-1093

Janisiewicz, W. J. (1996). Ecological diversity, niche overlap, and coexistence of antagonists use in developing mixtures for biocontrol of postharvest diseases of apples. *Phytopathology, 86*, 473-479. https://doi.org/10.1094/Phyto-86-473

Joffe, A. Z. (1986). Fusarium species: their biology and toxicology. Wiley, New York.

Leslie, J. F., & Summerell B. A. (2006). The Fusarium laboratory manual. Blackwell Publishing, Oxford.

Lin, Y. H., Chen, K. S., Liou, T. D., Huang, J. W., & Chang, P. F. L. (2009). Development of a molecular method for rapid differentiation of watermelon lines resistant to *Fusarium oxysporum* f. sp. *niveum*. *Botanical Studies, 50*, 273-280. https://doi.org/10.1016/j.nbt.2010.05.005

Mao, W., Lewis, J. A., Hebber, P. K., & Lumsden, R. D. (1997). Seed treatment with a fungal or a bacterial antagonist for reducing corn damping-off caused by species of Pythium and Fusarium. *Plant Disease, 81*, 450-454. https://doi.org/10.1094/PDIS.1997.81.5.450

Martyn, R. D. (2012). Fusarium wilt of watermelon: A Historical review. In: Cucurbitaceae 2012, Proceedings of

the 10th EUCARPIA meeting on genetics and breeding of Cucurbitaceae

Martyn, R. D., & McLanghlin, R. J. (1983). Effects of inoculum concentration on the apparent resistance of watermelons to *Fusarium oxysporum* f.sp. *niveum*. *Plant Disease, 67*, 493-495. https://doi.org/10.1094/PD-67-493

Meyer, S. L. F. Everts Kathryne L., Gardener B. M., Masler, E. P., Abdelnabby, H. M. E., & Skantar, A. M. (2016). Assessment of DAPG-producing *Pseudomonas fluorescens* for management of *meloidogyne incognita* and *Fusarium oxysporum* on watermelon. *Journal of Nematology, 48*(1), 43-53

Montealegre, J. R., Reyes, R., Perez, L. M., Herrera, R., Silva, P., & Besoain, X. (2003). Selection of bioantagonistic bacteria to be used in biological control of *Rhizoctonia solani* in tomato. *Electronic Journal of Biotechnology, 6*, 115-127. https://doi.org/10.2225/vol6-issue2-fulltext-8

Nishimura, N. (2007). Selective media for *Fusarium oxysporum*. *Journal of General Plant Pathology, 73*, 342-348. https://doi.org/10.1007/s10327-007-0031-y

Notz, R., Maurhofer, M., Dubach, H., Haas, D., & Defago, G. (2002). Fusaric acid-producing strains of *Fusarium oxysporum* alter 2,4-Diacetylphloroglucinol biosynthetic gene expression in *Pseudomonas fluorescens* CHA0 in vitro and in the rhizosphere of wheat. *Applied Environmental Microbiology, 68*, 2229-2235. https://doi.org/10.1128/AEM.68.5.2229-2235.2002

O'Sullivan, D. J., & O'Gara, F. (1992). Traits of *Fluorescent pseudomonas* spp. involved in suppression of plant root pathogens. *Microbiology Review, 56*(4), 662-676

Peng, J., Zhan, Y., Zeng, F., Long, H., Pei1, Y. &, Guo, J. (2013). Development of a real-time Fluorescence Loop-Mediated Isothermal amplification assay for rapid and quantitative detection of *Fusarium oxysporum* f. sp. *niveum* in Soil. *FEMS Microbiology Letters, 349*, 127-134. https://doi.org/10.1111/1574-6968.12305

Ren, Y., Jiao, D., Gong, G., Zhang, H., Guo, S., Zhang, J., & Xu, Y. (2015). Genetic analysis and chromosome mapping of resistance to *Fusarium oxysporum* f. sp. *niveum* (FON) race 1 and race 2 in watermelon (*Citrullus Lanatus* L.). *Molecular Breeding, 35*, 183. https://doi.org/10.1007/s11032-015-0375-5

Reuveni, R. (1995). Novel approaches to integrated pest management. Lewis Publishers, CRC Press Inc., Boca Raton, FL.

Salman, M. (2010). Determination of antibiotic activity on plasmids from Fluorescent pseudomonads isolates CW2, WB15 and WB52 against pre emergence damping-off caused by *Pythium ultimum* and *Rhizoctonia solani* in cucumber. *Biological Control, 53*(2), 161-167. https://doi.org/10.1016/j.biocontrol.2010.01.007

Tu, C. C., & Chang, Y. H. (1983). Soil microbial activity in relation to Fusarium wilt suppression soils and conducive soil. In: Proc Republic of China-Federal Republic of Germany Seminar Plant Nutrition Soil Sciences. National Science Council, Taipei, pp 189-196

Vogt, W., & Buchenauer, H. (1997). Enhancement of biological control by combination of antagonistic fluorescent Pseudomonas isolates and resistance inducers against damping-off and powdery mildew in cucumber. *Journal of Plant Diseases and Protection, 104*(3), 272-280.

Walsh, U. F., Morrissey, J. P., & O'Gara, F. (2001). Pseudomonas for biocontrol of phytopathogens: from functional genomics to commercial exploitation. *Current Opinion in Biotecholgy, 12*, 289-295. https://doi.org/10.1016/S0958-1669(00)00212-3

Weller, D. M. (1988). Biological control of soilborne plant pathogens in the rhizosphere with bacteria. *Annual Review of Phytopathology, 26*, 379-407. https://doi.org/10.1146/annurev.py.26.090188.002115

Zhang, Z., Zhang, J., Wang, Y., & Zheng, X. (2005). Molecular detection of *Fusarium oxysporum* f. sp. *niveum* and *Mycosphaerella melonis* in infected plant tissues and soil. *FEMS Microbiology Letters*, 249 (2005) 39-47. https://doi.org/10.1016/j.femsle.2005.05.057

Journal of Plant Studies; Vol. 6, No. 2; 2017
ISSN 1927-0461 E-ISSN 1927-047X
Published by Canadian Center of Science and Education

Survey of Foliar Trichomes in *Combretum* Loelf. (Combretaceae) in Parts of West Africa

Chimezie Ekeke[1] & Ikechukwu Ozoemena Agbagwa[1]

[1]Department of Plant Science and Biotechnology, Faculty of Science, University of Port Harcourt, PMB 5323, Choba, Nigeria

Correspondence: Chimezie Ekeke, Department of Plant Science and Biotechnology, Faculty of Science, University of Port Harcourt, PMB 5323, Choba, Nigeria. Email: ekeke.uche@uniport.edu.ng

Received: November 8, 2016 Accepted: January 16, 2017 Online Published: March 10, 2017

doi:10.5539/jps.v6n2p9 URL: https://doi.org/10.5539/jps.v6n2p9

Abstract

We studied the foliar trichome types, density and distribution among the genus *Combretum* Loelf. in parts of West Africa. Fresh and herbarium specimens were used. These specimens were fixed, peeled, trichome types identified and micro-photographed using a Leica WILD MPS 52 microscope camera on a Leitz Diaplan microscope. Generally, two major trichome groups were identified among these species studied. These include glandular trichomes: multicellular gland head with uniseriate stalk (MGU), cylindrical uniseriate clavate trichome (CUCT), unicellular gland with unisariate stalk (UGHU), cylindrical uniseriate trichome (CUT), paltate gland head (PGH) and combretaceous eglandular (non-glandular) conical trichome (long and short types). The eglandular trichome types were the most widely distributed trichome found in the species and could be used to distinguish the genus. They occurred in all the species studied except *C. glutinosum* and *C. micranthum.* Among the glandular trichomes, cylindrical uniseriate trichome was the most dominant occurring in 11 species namely; *C. aculeatum, C. bracteatum, C. collinum* subsp. *binderianum, C. collinum* subsp. *hypopilinum, C. constrictum*, *C. capitatum, C. hispidum, C. nigricans*, *C. panuculatum, C. platypterum* and *C. zenkeri.* This is followed by multicellular gland head with uniseriate stalk (MGU) trichome type which occurred in 9 species (*C. bracteatum, C. collinum* subsp. *binderianum, C. collinum* subsp. *hypopilinum, C. constrictum*, *C. excelsum*, *C. hispidum, C. mooreanum*, *C. platypterum* and *C. racemosum*). The trichome density varied from 1.25±0.44 trichomes per 100 cells to 600 trichomes per 100 cells. The distribution/occurrence, density and type of these trichomes formed dependable character for delimitating *Combretum* species. The findings of this study showed that trichomes provide good taxonomic characters useful for in differentiating the genus *Combretum* in West Africa.

Keywords: *Combretum*, eglandular trichome, foliar trichome, Gladular trichome and trichome density

1. Introduction

Leaves can be classified in various ways, for example their shape and size, their texture and colour and the degree of hairiness to name but a few. These variable features are frequently reflected in different internal tissue arrangement. Some modifications are typical of plants that can grow under particular conditions, but other features may owe more to the genome than to the habitat (Airy Shaw 1985). The foliar epidermis is one of the most taxonomic characters from the biosystematics point of view. Taxonomic studies have been made on number of plant families base on their leaf epidermal characteristics (Bhatia 1984; Baranova 1972). Although taxonomists lately realized the importance of microscopic features of the epidermis, taxonomic monographs are now considered incomplete without them (Rejdali 1991).

The comparative systematic investigations of angiosperms base on the variations in trichome types have long been reported (Cowan 1950; Metcalfe & Chalk 1950; Elena *et al.* 2003; Shaheen *et al.* 2009; Chadaporn and Pranom 2010; Ilkay *et al.* 2014). The morphology, types, shapes and sizes (Lawrence 1951; Stace 1980) are of taxonomic value. The use of uniseriate glandular trichomes and calcium oxalate crystals in distinguishing between the genera *Diathus* and *Silene* have been reported (Metcalfe & Chalk 1950). Presently, (Jafari, *et. al.,* 2002; Altaf, *et. al.,* 2003; Agbagwa & Okoli, 2006 ; Saheed & Iiloh, 2010 and Kiran, *et. al.,* 2011; Frehat, *et. al.,* 2011; Ahmed, *et. al.,* 2011; Abduhaman, *et. al.,* 2011) have stated the use trichomes, their morphology (shape, size, etc) and anatomy (number of glandular head, eglandular, serriated or non serriated, etc) in plant systematics. The length, size and density of trichomes have been described among the American *Combretum* and concluded

that the presence of particular type of trichome could be used to distinguish the genus (Stace 1969, 1980). However, West African species of *Combretum* have been basically classified based on their morphological attributes (Hutchinson & Dalziel 1954). Therefore, this work is aimed at surveying the types and distribution on trichomes among the *Combretum* as complementary data to delimiting the genus.

2. Materials and Methods

2.1 Source of Plant Materials

Leaves of herbarium and fresh specimens of *Combretum* species used for this study were collected from Forestry Research Institute of Nigeria Herbarium (FRIN) and University of Port Harcourt Herbarium. The list and herbarium numbers of the *Combretum* species studied is presented in Table 1.

2.2 Epidermal Studies

These leaf specimens were soaked in concentrated nitric acid or trioxonitrate (v) acid ($HN0_3$), rinsed in distilled water, peeled with forceps, stained in 1 % aqueous safranin solution and mounted in glycerin. Thereafter, the leaf epidermal characteristics were determined based on the methods of (Dilcher 1974; Cutler 1978; Metchalfe & Chalk 1979 and Okoli & Ndukwu 2002) and the trichome micro-photographed using a Leica WILD MPS 52 microscope camera on a Leitz Diaplan microscope.

The trichome density (abundance) is computed following the methods of Olowokudejo (1990) used in *Annona* species.

- 0 (No) Trichomes per 100 cells glabrous
- 1 – 10 „ „ „ „ glabrescent
- 11 – 29 „ „ „ „ sparsely hairy
- 30 – 49 „ „ „ „ densely hairy
- >50 „ „ „ „ very densely hairy

Table 1. Information about the West African Voucher Specimens studied

S/N	*Species name*	Voucher information	Country
1	*C. aculeatum* Vent.	Dikwa division; Miss. A. McClintock; FHI 38989; 30/11/1954.	Cameroon
		Yola; Girls Sch., Adamawa; M.G. Latilo; FHI 63521; 24/10/1971.	Nigeria
		Yankari game Reserve; Bauchi; C. Geerling; FHI 41147; 30/10/1970	Nigeria
2	*C. acutum* Laws	River Oyinmi egde, Kabba, Kogi; Daramola & Adebusiyi; FHI 38412; 24/10/1958.	Nigeria
		Gold Coast, 3miles above Ajena, Bawku; Moton; FHI 48692; 29/11/1953.	Ghana
		North Dagemba district; FHI 45036	Ghana
3	*C. bauchiense*	Platuea; Dogon; Platuea; Hilary; FHI 56997; 25/02/1966	Nigeria
	Hutch. & Diels.	Bauchi; Bauchi; Holely; FHI 2067; Jan. 1929	Nigeria
4	*C. bracteatum* (Laws)	Aponum F/R, Akure/Ondo; Odewo et al.; FHI 90845; 7/6/1979.	Nigeria
	Engl. & Diels.	Atim, Calabar, C/R state; H.D. Onyeachusim; FHI 48155; 13/2/1964	Nigeria
		Ndoro/Umudike, Abia; J.C. Okafor & Ariwodo; FHI 57617; 27/01/1966	Nigeria
		Owerri/Aba Rd, Imo State; Latilo; et al. FHI 71624; 17/09/1975	Nigeria
5	*C. collinum* Fresen. Subsp.	Zalanya, Bauchi; Wit; Gbile & Daramola; FHI 48905; 28/4/1972	Nigeria
	hypopilinum (Diels) Okafor	Nimbia F/R, Kaduna; Opayemi & others; FHI 79526; 30/11/1976	Nigeria
		Bode Sadu, Jebba, Kwara; Eimunjeze & Oguntayo; FHI 71461; 13/10/1974	Nigeria
6	*C. collinum* Fresen. subsp	New Bussa, Gbile; FHI 91497; 1972	Nigeria
	binderanum (Kotschy) Okafo	Ilorin, Oyo State; Oloranfemi & Oguntayo; FHI 88536; 1972	Nigeria
		Borgu G/R, Kwara; Child, D.S; FHI 30261; 1972	Nigeria
		Abuja; Onyeachusim & others; FHI 100679	Nigeria
7	*C. mooreanum* Exell	Borgu G/R, Kwara; Child, D.S; FHI 30259; 1972	Nigeria
		New Bussa, Gbile & others; FHI 91497; 1975	Nigeria
		Mokwa, Ngier State; FHI 95117	Nigeria
		Awum/Jebba FR; Onyeachusim & others; FHI 101459	Nigeria
8	*C. confertum* (Laws) Benth	Bendiga Ayuk, Ikom, C/R State; FHI 2817; 8/12/1950	Nigeria
		Akamkpa, C/R State; B.O. Daramola; FHI 56413; 19/10/1965	Nigeria
		Komgina, Cameroun; R.G. Lowe; FHI 18321; Dec. 1978	Cameroon
		Okobodo, Itu, C/R state; J.O. Ariwodo; FHI 88819; 1/11/1978	Nigeria
9	*C. constrictum* (Benth.) Laws	Edge of Orugi Creek, Kabba; Kogi; A.P.D. Jones; 630; 10/2/1943	Nigeria
		Oguta Lake, Imo State; Ekwuno & others; FHI 96294; 1/9/1981	Nigeria
		Taylor Creek, Bayelsa; FHI 16524; 10/5/1940	Nigeria
		Ibadan, Oyo; Ekwuno; P; FHI 96294	Nigeria
10	*C. cuspitatum*	Ile Boulay Island, Ivory Coast; G.J.H. Amoshff; FHI 14055; 14/11/1964	Ivory Coast
	Planch. ex Benth.	Abeokuta, Ogun State; C.F.A. Onochie; FHI 32443; 16/12/1952	Nigeria
		Benin, Bank of Abiala Creek, Edo; J.R. Charter; FHI 43263; 30/11/60	Nigeria
		Itu swamp, C/R State; L.G. Cooper; FHI 36729; 15/10/1957	Nigeria
11	*C. dolichopetalum*	Benin, Edo; Onochie; FHI 39274; Nov. 1956	Nigeria
	Engl. & Diels	Uyo, Etip Ediene, Akwa Ibom; Okafor & Latilo; FHI 57764; 23/1/1966	Nigeria
		Manu F/R, Awka, Enugu; E.T. Akagu; FHI 68056A; 7/3/1974	Nigeria
		Port Harcourt, Rivers; Jones; 6194; 6/1/1974	Nigeria
		Ntalakwu-Itu, Abia; Ariwodo & others; FHI 103536; 6/2/1982	Nigeria
12	*C. excelsum* Keay	Ogoja-Ikom, C/R State; Keay; FHI 28147; 7/12/1950	Nigeria
13	*C. fuscum* Planch.	Owena/Ondo, Olorumfemi & Daramola; FHI 71047; 19/7/1974	Nigeria
		Ubukpa/Nsuka, Enugu; Okafor & Emwiogbon; FHI 72267; 24/11/1973	Nigeria
		Oyo/Ibadan, Oyo; Keay & Jones; FHI 14625; 30/1/1946	Nigeria
		Awka/Onitsha, Anambara State; Latilo; FHI 27310; 14/8/1950	Nigeria
14	*C. ghasalense* Engl. & Diels.	Zaria, Kaduna; Peal; FHI 39645; 7/6/1957	Nigeria
		Damaturu, Yobe; Peal; FHI 23370; 24/6/1947	Nigeria
		Kano/Dangora; Latilo; FHI 27434; 24/4/1950	Nigeria
		Awum/Jebba FR; Onyeachusim & others; FHI 101455	Nigeria

Table 2. Continued: Information about the West African Voucher Specimens studied

S/N	*Species name*	Voucher information	Country
15	*C. glutinosum* Perr. Ex DC.	Zamfara, Zamfara State; Keay; FHI 70598; 29/6/1944.	Nigeria
		New Bussa; Gbile & others; FHI 91590; 1975.	Nigeria
		Awum/Jebba F/R, Onyeachusim & others; FHI 101398.	Nigeria
		Bauchi; Lely; FHI 2080.	Nigeria
16	*C. hispidum* Laws	Ibadan, Oyo; Samuel, *et al*.; FHI 32315; 25/1/1972.	Nigeria
		Ekiti 7 48N, 5 20E; Ekiti; Jones; FHI 77524; 20/1/1975.	Nigeria
		Ebonyi/Abakaliki, Ebonyi; Okafor & Emwiogbon; FHI 66030; 27/2/1973.	Nigeria
17	*C. insulare* Engl. & Diels.	Gambari F/R, Ibadan; Chizea, L.G.; 1975.	Nigeria
		Ibadan North F/R, Oyo State; Chizea; L.G.; FHI 23971; 23/02/50.	Nigeria
18	*C. miranthum* G. Don	Tregina Rd, Minna; Chizea, L.G.; FHI 100444; 1975.	Nigeria
		Ibadan, Oyo State; Lowe; J.; FHI100181.	Nigeria
		Minna, Niger; Onyeachusim & others; FHI 100655.	Nigeria
		Katsina, Kastina State; MacGregor W.D.; FHI 2085	Nigeria
19	*C. molle* R. Br. ex G. Don.	Adamawa, Adamawa; Latilo; FHI 28721; 19/11/1954	Nigeria
		Zaria, Kaduna; Horum; FHI 55671; 21/12/1964	Nigeria
		Gwari, Abuja; Onochie; FHI 35937; 27/5/1956	Nigeria
		Yankari game Reserve, Bauchi; C. Geerling; FHI 43609; 2/13/1970	Nigeria
20	*C. nigricans var. Elliotii* Engl. & Diels	Ilero/Oyo, Oyo; Latilo; FHI 58407; 23/3/1966	Nigeria
		Yankari game Reserve, Bauchi; C. Geerling; FHI 38395; 22/10/1970	Nigeria
		Pategi/Kwara; Eimujeze & Oguntayo; FHI 72829; 19/10/1974	Nigeria
		Lokoja, Kogi State; Gbeli *et al*; FHI 64202; 20/9/1971	Nigeria
21	*C. paniculatum* Vent.	Omo F/R, Ogun State; H.D. Onyeachusim; FHI 105622; Jan. 1977	Nigeria
		Manu F/R, Awka, Anambara State; J.A. Emwiogbon; FHI 64000; 17/3/1972	Nigeria
		Betem, Akamkpa, C/R state; J.O. Ariwodo; 28/01/1977	Nigeria
22	*C. platypterum* (Welw.) Hutch. & Diels.	Ikom, C/R State; Tunde & Oguntayo; FHI 86153; 1972	Nigeria
		Oshun-Ijesa-Ilumoba Rd; Olorunfemi; J.O.; FHI 91915; 1975	Nigeria
		Enugu-Nsuka Rd; Onyeachusim & others; FHI 100878	Nigeria
		Ikom, C/R State; Latilo; FHI 31852	Nigeria
23	*C. racemosum* P. Beauv.	Irewole; Tunde & Oguntayo; FHI 85465; 1972	Nigeria
		Ajibo, West Nigeria; Odewo & others; FHI 102508	Nigeria
		Udi Ngwo, Enugu; Jones; A.P.D; 260	Nigeria
		Abeokuta, Ogun; J.D. Kennedy; FHI 2090	Nigeria
24	*C. lamprocarpum* Diels.	Daddin, Kowa; Gombe; Wit; et al..; FHI 65054; 3/5/1975.	Nigeria
25	*C. zenkeri* Engl. & Diels	Ibadan, Oyo; Chizea; L.G.; FHI 99179; 1975	Nigeria
		Iwo, Oyo state; Olorunfemi & others; FHI 96534; 1975	Nigeria
		Abeokuta, Ogun; A.F. Ross; FHI 2097	Nigeria

3. Results

The trichome types, density and distribution among the 25 *Combretum* species studies are as follows:

3.1 Trichome Types

The types, density and distribution of trichomes found among the genus *Combretum* in parts of West Africa has been carried out. Generally, two major trichomes types (glandular and non-glandular) were identified in the genus *Combretum* studied. The glandular trichomes include: unicellular gland head with uniseriate stalk (UGHU), cylindrical uniseriate clavate trichome (CUCT), cylindrical uniseriae trichome (CUT), multicellular gland head with uniseriate stalk (MGU) and peltate gland head (PGH) while the non-glandular trichome comprised of the combretaceous conical trichome ECT (long and short types) (Figure 1 and Table 2).

3.1.1 Non-glandular or Eglandular Trichomes and Distribution

Non-glandular trichomes found in the species studied are presented in Figures 1A - 1C**.** It is represented by the conical trichome which is made up of the short type (Figure 1A) and long type (Figures 1B and C). The long and short trichomes were found in *C. zenkeri* while the long trichome type was found in *C. aculeatum*, *C. acutum*, *C.*

bauchiense, *C. bracteatum, C. collinum* Fresen. Subsp. *hypopilinum*, *C. collinum* subsp. *binderianum, C. confertum*, *C. constrictum*, *C. cuspitatum*, *C. dolichopetaluum, C. fuscum*, *C. ghasalense*, *C. hispidum*, *C. insulare*, *C. lamprocarpum, C. molle*, *C. mooreanum*, *C. nigricans* var. *elliotii, C. paniculatum*, *C. platypterum* and *C. racemosum* (Table 1).

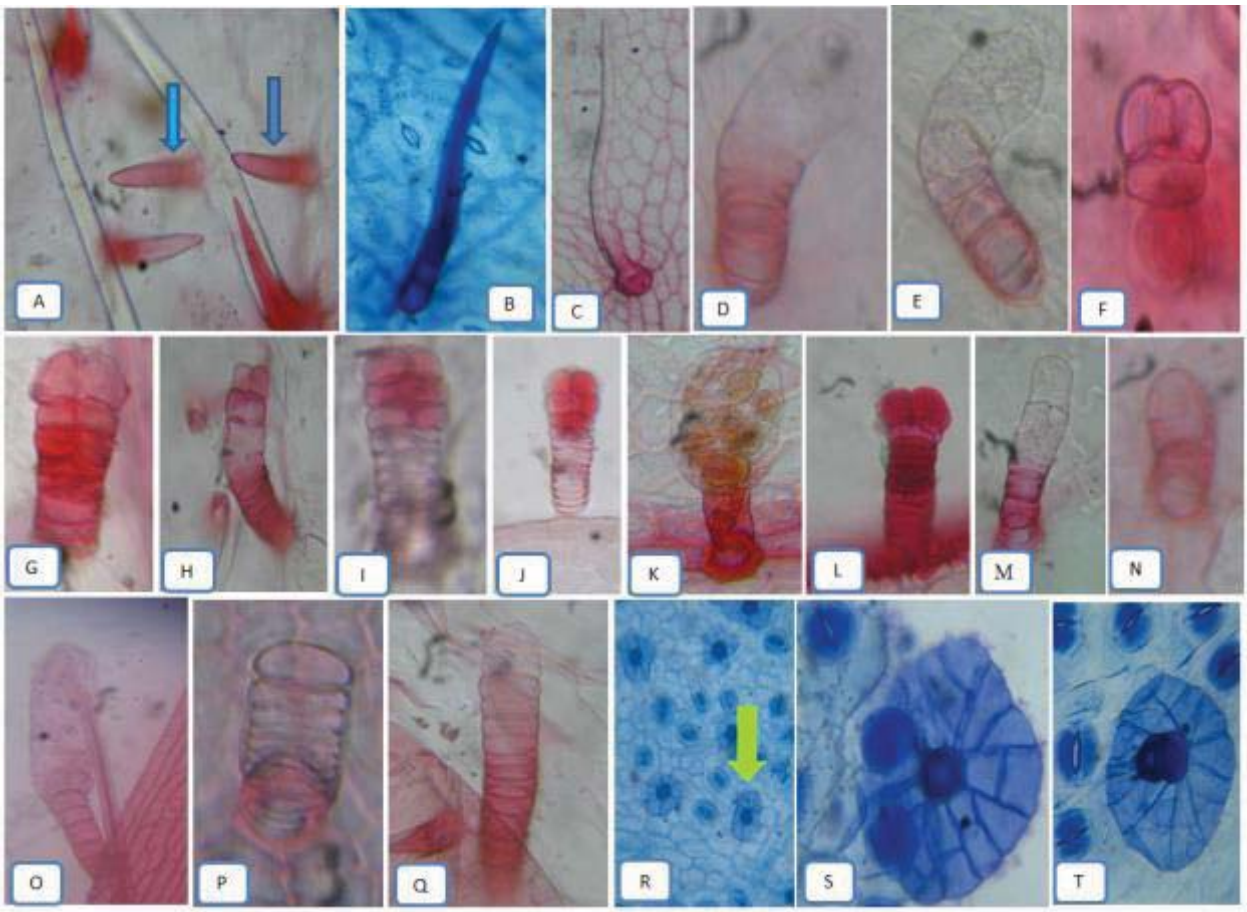

Figure 1. Types of trichomes in the *Combretum* species studied x1320: (A, B & C) Eglandular conical (arrows show short trichome), (D, E, F, H, I, J, K & L) Multicellular gland head/uniseriate stalk, (M & N) Cylindrical uniseriate clavate trichome, (O) Unicellular glandhead/uniseriate, (P & Q) Cylindrical uniseriate trichome and (R, S & T) Peltate trichome

3.1.2 Glandular Trichome Types and Distribution

Five glandular trichome types were identified among the *Combretum* species studied. These include multicellular gland head with uniseriate stalk, MGU trichome type (Figures 1D, E-L), cylindrical uniseriate clavate trichome type, CUCT (Figures 1M-N), unicellular gland with unisariate stalk, UGHU (Figure 1O), cylindrical uniseriate trichome type, CUT (Figures 1P-Q) and Paltate gland head type, PGH (Figures 1R-T). Among the glandular trichomes, multicellular gland head trichome with uniseriate stalk occurred in *C. bracteatum*, *C. collinum* subsp. *binderianum*, *C. collinum* subsp. *hypopilinum, C. constrictum, C. excelsum, C. hispidum, C. mooreanum, C. platypterum* and *C. racemosum* (Table 2). The unicellular gland trichome with unisariate stalk, paltate gland head trichome and cylindrical uniseriate trichome types occurred in 7 species each. Trichome with unicellular gland head and unisariate stalk occurred in *C. collinum* Fresen. subsp. *hypopilinum*, *C. collinum* subsp. *binderianum, C. cuspitatum, C. hispidum, C. paniculatum C. platypterum* and *C. zenkeri*. Paltate gland head trichome type occurred *C. acutum, C. bauchiense, C. fuscum, C. ghasalense, C. glutinosum, C. micranthum* and *C. molle* while the cylindrical uniseriate trichome type occurred in *C. aculeatum, C. bracteatum, C. collinum* Fresen. subsp. *hypopilinum, C. collinum* subsp. *binderianum, C. constrictum, C. hispidum* and *C. nigricans* var. *elliotii*. Unicellular gland head trichome with uniseriate stalk was found in *C. aculeatum, C. acutum, C. confertum, C. constrictum, C. dolichopetaluum, C. insulare, C. lamprocarpum* and *C. nigricans* var. *elliotii*) Table 1 and Figure 1.

Table 2. Trichome types, density and their distribution among the *Combretum* species studied

Species name	Ganldular Trichome					ECT[6]	Range	Mean ± STD	Remark
	CUT[1]	CUCT[2]	UGHU[3]	MGU[4]	PGH[5]				
C. aculeatum	+	-	+	-	-	+	40 – 90	60.95 ± 14.35[k]	Very densely hairy
C. acutum	-	-	+	-	+	+	11 – 28	19.85 ± 4.52[f]	Sparsely hairy
C. bauchiense	-	-	-	-	+	+	168 – 104	138.9 ± 15.97[q]	Very densely hairy
C. bracteatum	+	-	-	+	-	+	1 – 3	1.50 ± 0.61[a]	Glabrescent
C. collinum Fresen. subsp. *hypopilinum*	+	+	-	+	-	+	550 - 600	575.60 ± 18.07[s]	Very densely hairy
C. collinum subsp. *binderianum*	+	+	-	+	-	+	4 – 10	7.10 ± 2.02[d]	Glabrescent
C. confertum	-	-	+	-	-	+	30 – 106	58.05 ± 21.26[j]	Very densely hairy
C. constrictum	+	-	+	+	-	+	1 – 8	5.35 ± 2.03[c]	Glabrescent
C. cuspidatum	-	+	-	-	-	+	1 – 3	1.75 ± 0.72[a]	Glabrescent
C. dolichopetaluum	-	-	+	-	-	+	1 – 3	1.50 ± 0.61[a]	Glabrescent
C. excelsum	-	-	-	+	-	+	70 – 110	85.20 ± 14.02[l]	Very densely hairy
C. fuscum	-	-	-	-	+	+	80 – 150	115.2 ± 20.60[o]	Very densely hairy
C. ghasalense	-	-	-	-	+	+	104 – 190	136.95±21.44[p]	Very densely hairy
C. glutinosum	-	-	-	-	+	-	70 – 156	107.35±24.03[n]	Very densely hairy
C. hispidum	+	+	-	+	-	+	26 – 90	54.60 ± 20.01[i]	Very densely hairy
C. insulare	-	-	+	-	-	+	2 – 8	4.45 ± 1.90[b]	Glabrescent
C. lamprocarpum	-	-	+	-	-	+	3 – 9	6 .00 ± 1.81[c]	Glabrescent
C. micranthum	-	-	-	-	+	-	33 – 81	47.80 ± 14.60[g]	Densely hairy
C. molle	-	-	-	-	+	+	76 – 198	143.0 ± 37.16[r]	Very densely hairy
C. mooreanum	-	-	-	+	-	+	4 – 12	7.10 ± 0.02[d]	Glabrescent
C. nigricans var. elliotii	+	-	+	-	-	+	31 – 81	51.60 ± 14.37[h]	Very densely hairy
C. paniculatum	-	+	-	-	-	+	6 – 10	8.40 ± 1.27[e]	Glabrescent
C. platypterum	-	+	-	+	-	+	1 – 2	1.25 ± 0.44[a]	Glabrescent
C. racemosum	-	-	-	+	-	+	4 – 12	7.10 ± 2.02[d]	Glabrescent
C. zenkeri	-	+	-	-	-	+	42 – 163	90.70 ± 44.50[m]	Very densely hairy

[1]Cylindrical uniseriate trichome, [2]Cylindrical uniseriate clavate trichome, [3]Unicellular gland head/ uniseriate stalk, [4]Multicellular glandhead/ uniseriate stalk, [5]Peltate gland head, [6]Eglandular conical trichome, Note: + = Present, - = absent; values followed by the same letter in a column are not significantly different at 5% level using LSD.

3.2 Trichome Density and Leaf Surface

The trichome density in the *Combretum* species sampled varied from 1.25±0.44 trichomes per 100 cells for *C. platypterum* (glabrescent) to >500 trichomes per 100 cells for *C. collinum* subsp *hypopilinum* (very densely hairy). The leaf surface of most the species are glabrescent. The trichome densities of these species include: *C. platypterum,* 1.25±0.44; *C. bracteatum,* 1.50±0.61; *C. dolichopetaluum,* 1.50±0.61; *C. cuspitatum,* 1.75±0.72; *C. insulare,* 4.45±1.90; *C. constrictum,* 5.35±2.03; *C. lamprocarpum,* 6.00±1.81; *C. collinum* subsp. *binderianum,* 7.10±2.02; *C. mooreanum,* 7.10±2.02; *C. racemosum,* 7.10±2.02; *C. paniculatum,* 8.4±1.27 and *C. acutum,* 19.85±4.52. These species are sparsely hairy while *C. micranthum* is densely hairy with trichome density of 47.8±14.60. Other species of this genus studied are very densely hairy and their trichome densities are as follows: *C. nigricans* var. *elliotii,* 51.60±14.37; *C. confertum,* 58.05±21.26; *C. hispidum,* 54.6±20.01; *C. aculeatum,* 60.95±14.35; *C. excelsum,* 85.20±14.02; *C. zenkeri,* 90.70±44.50; *C. glutinosum,* 107.35±24.03; *C. fuscum,* 115.20±20.60; *C. ghasalense,* 136.95±21.44; *C. bauchiense*, 138.9±15.97 and *C. molle,* 143.0±37.16.

4. Discussion

The foliar trichome amongst members of the genus *Combretum* in West Africa is scarcely studied. In this work we surveyed the occurrence of different trichome types, the degree of hairiness on leaf surfaces/trichome densities of these species. The non-glandular trichome types were the most diversified and widely distributed trichome found in the species studied and could be used to distinguish members of this genus. For instance, among the species studied, this trichome type was not observed in two species namely; *C. glutinosum* and *C. micranthum.* This character therefore makes the two species distinct from the other ones and the species are further delimited based on their trichome densities (Table 2). *C. glutinosum* is very densely hairy with trichome of 70 – 156 (107.35±24.03) trichomes per 100 cells while *C. micranthum* is densely hairy with trichome density of 33 – 81 (47.80 ± 14.60) trichomes per 100 cells. This further explains the occurrence of these species in different ecological zones (Ekeke, 2013). This is in line with the work of Stace (1980) who noted that the length, size and density of trichomes could

be influenced by environmental conditions. Also, the presence of a particular type of trichome has been used in the taxonomy of *Combretum* (Stace 1980). Since environmental conditions can influence the length and density of trichome, it can be used in placing these species into different geographical or ecological zones.

Five glandular trichome types were identified among the *Combretum* species studied (Table 2). Among the glandular trichomes, CUT was the most dominant occurring in 11 species namely; *C. aculeatum, C. bracteatum, C. collinum* subsp. *binderianum, C. collinum* subsp. *hypopilinum, C. constrictum*, *C. capitatum, C. hispidum, C. nigricans*, *C. panuculatum, C. platypterum* and *C. zenkeri.* This is followed by multicellular gland head with uniseriate stalk (MGU) trichome type occurring in 9 species (*C. bracteatum, C. collinum* subsp. *binderianum, C. collinum* subsp. *hypopilinum, C. constrictum*, *C. excelsum*, *C. hispidum, C. mooreanum*, *C. platypterum* and *C. racemosum*) Table 2. This showed that these species are related however, variation in number gland heads and the morphology of the trichomes could be used to further distinguish them. For instance, among these *Combretun* species with uniseriate trichome, *C. collinum* Fresen. subsp. *hypopilinum*, *C. collinum* subsp. *binderianum* and *C. hispidum* have MGU and ECT but the trichome densities differed from one species to the other. *C. collinum* subsp. *binderianum* is glabrescent while *C. collinum* Fresen. subsp. *hypopilinum* and *C. hispidum* are very densely hairy. Furthermore, *C. collinum* Fresen. subsp. *hypopilinum* has more trichomes than *C. hispidum*. Also, *C. platypterum* and *C. paniculatum* have CUCT and are glabrescent however; the presence of MGU in *C. platypterum* distinguishes it from *C. paniculatum.* Similarly, *C. bracteatum* and *C. constrictum* have CUT, but *C. constrictum* has UGHU and MGU which are not found in *C. bracteatum*. In the same vein, *C. zenkeri* and *C. cuspidatum* could be distinguished base on the density of trichomes on the leaf surface (Table 2). Though these two species have CUCT, *C. zenkeri* has trichome density of 42 – 163 (90.70±44.50) trichomes per 100 cells while *C. cuspidatum* has trichome density of 1 – 3 (1.75 ± 0.72) trichomes per 100 cells. *C. mooreanum* and *C. racemosum* have only two trichome types (MGU and ECT). The analysis of variance of the trichome densities showed that there is significant difference in densities of the trichomes among the species studied (Table 2). This suggests that the variation in trichome density could be used in delimitating the genus and could complement the existing data on these species.

Trichomes have been reported to have contributed immensely to the taxonomy of the genus *Combretum* in particular and Combretaceae family at large. The unicellular combretaceous trichome type has been reported among the American species (Stace 1961, 1965) and glandular trichome with peltate head or without peltate head (stalk gland) (Solereder 1908; Stace 1969a, b, 1980; Metcalfe & Chalk 1979; Patricia 2002). Similarly, the trichomes recorded in this report are the same as those in the previous reports. Stace (1969) noted the value of the leaf epidermal characteristics and particularly the glandular trichomes in the identification and classification of the 37 species of *Combretum* in America. He used the wide range of trichome types found among the species to differentiate groups of species corresponding closely with the 11 sections recognized by Exell, rather than distinguishing individual species and suggested that these trichomes have great taxonomic value as that of any other organ in the genus. Also, Jordaan *et al.* (2011) reported peltate trichome in South African *Combretum* species as important taxonomic character. Trichome morphology, densities and types have been employed in distinguishing other genera other than *Combretum.* These have been employed to differentiate *Ajuga* in Turkey (Ilkay *et al.* 2014), *Croton* in Thailand (Chadaporn & Pranom 2010) and *Hibiscus* (Shaheen *et al.* 2009).

5. Conclusion

The findings in this study showed that trichomes in combination with other taxonomic characters can be used in differentiating the genus *Combretum* in West Africa and supports previous works on other members of this genus from other parts of the world.

Acknowledgement

The authors wish to appreciate and thank the staff of the Forestry Institute of Nigeria (FRIN) and Department of Plant Science and Biotechnology, University of Port Harcourt for their assistance in providing laboratory equipment and enabling environment for carrying out this research.

References

Agbagwa, I. O., & Bosa, B. E. (2006). Leaf Epidermal Micromorphology in the Systematics of *Abrus* (Papilionaceae) in Parts of Tropical West Africa. *Asian Journal of Plant Science, 5*(1), 41-49. https://doi.org/10.3923/ajps.2005.652.659

Airy-Shaw, H. K. (1985). *A dictionary of the flowering plant*. 8th Edn., Cambridge University Press, London.

Altaf, A. D., Bokhari, T. Z., Saeed, A. M., & Rubina, A. (2003). Epidermal Morphology of Some Members of Family Boraginaceae in Baluchistan. *Asian Journal of Plant Sciences, 2*(1), 42-47.

https://doi.org/10.3923/ajps.2003.42.47

Baranova, M. (1972). Systematic anatomy of the leaf epidermis in the Magnoliaceae and some related families. *Taxon, 21*, 447-467. *BIO: http://www.jse.ac.cn/wenzhang/aps06137.pdf*

Bhatia, R. C. (1984). Foliar Epidermal Studies of *Heliotropium supinum* L. Folia Geobot. *Phytotaxon, 19*, 381-385. https://doi.org/10.1007/BF02853177

Chadaporn, S., & Pranom, C. (2010). A morphological survey of foliar trichomes of *Croton* L. (Euphorbiaceae) in *Thailand. Thai For. Bull. (BOT.)*, *38*, 167-172. *http://www.tci-thaijo.org/index.php/ThaiForestBulletin/article/viewFile/24427/20792*

Cowan, J. L. (1950). The *Rhododendron* leaf; a study of the epidermal appendages. Oliver and Boyd, Edinburgh.

Cutler, D. F. (1978). *Applied Plant Anatomy*. Longman Inc, New York, USA.

Dilcher, D. L. (1974). Approaches to the identification of angiosperm leaf remains. *Bot. Rev*., *40*, 1-157. https://doi.org/10.1007/BF02860067

Ekeke, C. (2013). Taxonomic studies on the genus Combretum Loefl. In Nigeria. PhD. Thesis. University of Port Harcourt.

Elena, V., Juha-Pekka, S., Julia, K., & Kalevi, P. (2003). Comparative analysis of leaf trichome structure and composition of epicuticular flavonoids in Finish Birch Species. *Annals of Bot., 91*, 643-655. https://doi.org/10.1093/aob/mcg070

Ferhat, C., Ahmet, K., Zeynep, A., & Musa, D, (2011). Morphology, anatomy and trichome properties of *Lamium truncatum* Boiss. (Lamiaceae) and their systematic implications. *Australian Journal on Crop Science (AJCS), 5*(2), 147-153. http://www.cropj.com/celep_5_2_2011_147_153.pdf

Hutchinson, J., & Dalziel, J. M. (1954). *Flora of West Tropical Africa.* Revised by Keay, R. W. J. *Vol. I Part I.* Crown Agents for Oversea Governments and Administrations, London.

Ilkay, Ö. Ç., Arzu, C., & Cengiz, Y. (2014). Trichome morphology of *ajuga orientalis* l. (Lamiaceae) from Turkey. *Bangladesh J. Bot., 43*(1), 91-95. https://doi.org/10.3329/bjb.v44i1.22721

Jafari, A., Zokai, M., & Fathi, Z. (2002). A Biosystematical Investigation on *Silene* L. species in North East of Iran. *Asi. J. Pl. Sci., 7*(4), 394-398.

Jordaan, M., van Wyk, A. E., & Maurin, O. (2011). A conspectus of *Combretum* (Combretaceae) in southern Africa, with taxonomic and nomenclatural notes on species and sections. *Bothalia, 41*(1), 135-160. *http://www.abcjournal.org/index.php/ABC/article/viewFile/36/36*

Lawrence, G. H. M. (1951). Taxonomy of vascular plants. Macmillan Co., New York

Metcalfe, C. R., & Chalk, L. (1950). *Anatomy of dicotyledons, Vol. 1,* Oxford University Press, New York.

Metcalfe, C. R., & Chalk, L. (1979). *Anatomy of the dicotyledon, vol. 1: Systematic anatomy of the leaf and stem*. Oxford University Press, New York.

Okoli, B. E., & Ndukwu, B. C. (2002). Procedure for the Observation of Living tissues (Vital Observation) in *Field, Herbarium and Laboratory Techniques.* Edited by Okoli, B. E. Mbeyi and associates Nig. Ltd. Port Harcourt. 34-38.

Olowokudejo, J. D. (1990). Comparative morphology of leaf epidermis in the genus *Annona* (Annonaceae) in West Africa. *Phytomorph., 4*(3&4), 407-422.

Patricia, M. T. (2002). A contribution to the leaf and young stem anatomy of the Combretaceae. *Botanical Journal of the Linnean Society*, *138*, 168-196. *http://onlinelibrary.wiley.com/doi/10.1046/j.1095-8339.2002.138002163.x/pdf*

Rejdali, M. F. L. S. (1991). Leaf micro-morphology and anatomy of North African species of *Sideritis* L. (Lamiaceae). *Bot. J. Linn. Soc., 107*, 67-77

Saheed, S. F., & Liloh, H. C. (2010). A taxonomic study of some species of *Cassiinae* (Leguminosae) using leaf epidermal characters. *Not. Bot. Hort. Agrobot*, *38*, 21-27.

Shaheen, N., Ajab, M., Hayat, M. Q, & Yasmin, G. (2009). Diversity of Foliar trichomes and their systematic relevance in the genus *Hibiscus* (Malvaceae). *Int. J. Agric. Biol., 11*, 279-284. *https://www.fspublishers.org/published_papers/61916_..pdf*

Solereder, H. (1908). *Systematic anatomy of dicotyledons: a handbook for laboratories of pure and applied botany*.

Clarendon Press, Oxford.

Stace, C. A. (1961). Cuticular characters as an aid to the taxonomy of the South-West African species of *Combretum. Mitteilungen der Botanischen Staatssmmlung Munchen, 4*, 9-19.

Stace, C. A. (1965). The significance of leaf epidermis in the taxonomy. *Bull. Br. Mus. (Nat. Hist.) Bot.*, *4*(1), 1-78.

Stace, C. A. (1969a). The significance of leaf epidermis in the taxonomy of Combretaceae II: The genus of *Combretum* subsp *Combretum* in Africa. *Botanical Journal of the Linnean Society, 62*, 131-168.

Stace, C. A. (1969b). The significance of leaf epidermis in the taxonomy of Combretaceae III: The genus of *Combretum* in America. *Brittinia, 12*, 131-143.

Stace, C. A. (1973). The significance of leaf epidermis in the taxonomy of Combretaceae IV: The genus of *Combretum* in Asia. *Botanical Journal of the Linnean Society, 66*, 97-115.

Stace, C. A. (1980). The significance of leaf epidermis in the taxonomy of Combretaceae V: The genus of *Combretum* subsp. *Cacoucia* in Africa. *Botanical Journal of the Linnean Society, 81*, 185-203.

Journal of Plant Studies; Vol. 6, No. 2; 2017
ISSN 1927-0461 E-ISSN 1927-047X
Published by Canadian Center of Science and Education

Cellular Calcium Distribution Modulates the Growth of Callus and Protoplasts of Halophyte Mangrove Plant, *Avicennia Alba* - an X-ray Microanalysis

Manabu Hayatsu[1,2,3], Suechika Suzuki[1,2], Shinpei Tsuchiya[4] & Hamako Sasamoto[2,5]

[1]Department of Biological Sciences, Faculty of Science, Kanagawa University, Hiratsuka, Kanagawa 259-1293, Japan

[2]Research Institute for Integrated Science, Kanagawa University, Hiratsuka, Kanagawa 259-1293, Japan

[3]Division of Microscopic Anatomy, Graduate School of Medical and Dental Sciences, Niigata University, Niigata, 951-8510, Japan (present address)

[4]Graduate School of Environment and Information Sciences, Yokohama National University, Yokohama 240-8501, Japan

[5]Faculty of Environment and Information Sciences, Yokohama National University, Yokohama 240-8501, Japan

Correspondence: Hamako Sasamoto, Research Institute for Integrated Science, Kanagawa University, Hiratsuka, Kanagawa 259-1293, Japan. Tel: 81-463-59-4111. E-mail: sasamoto@ynu.ac.jp

Received: February 13, 2017 Accepted: March 11, 2017 Online Published: March 28, 2017

doi:10.5539/jps.v6n2p18 URL: https://doi.org/10.5539/jps.v6n2p18

Abstract

Two cultured cell lines were developed from cotyledons of a halophyte mangrove, *Avicennia alba.* In the high-Ca callus line, which was sub-cultured in a modified amino acid medium containing 3 mM $CaCl_2$, growth of calluses and their protoplasts were both inhibited by low concentrations of $CaCl_2$ in the culture medium. Removal of Ca^{2+} from the culture medium stimulated callus growth and the calluses could be sub-cultured without $CaCl_2$ (low-Ca callus line). The intra- (cytoplasmic matrix and vacuole) and extra- (cell wall) cellular concentrations of elements, i.e., [Ca], [K], [Cl], [Na], [Mg], [P] and [S] were investigated using quantitative X-ray microanalysis of cryosections of calluses from both cell lines. [Ca] was high in the cytoplasmic matrix and cell wall of the high-Ca line. [Ca] was lowered in the low-Ca line in all cell compartments, though still detected. Ca-containing electron-dense precipitates were accumulated in the middle lamella of cell walls in resin-embedded sections of the high-Ca line. $CaCl_2$ in the medium stimulated protoplast growth only in the low-Ca line. These results suggested that a low cellular [Ca] is needed for protoplasts growth of *A. alba.* The importance of cellular [Ca] for the growth of halophilic mangrove plant cells was discussed.

Keywords: Ca^{2+} ions, halophilism, mangrove plant cells, salts tolerance, x-ray microanalysis

1. Introduction

Mangrove plants grow in brackish waters in tropical and subtropical areas. More than 100 species of different families of trees and woody plants and ferns are included in mangrove plants (Tomlinson, 1986; Spalding, Kainuma, & Collins, 2010). Degree of salt tolerance differs considerably between species grown on the seaward side and those grown upstream. *Avicennia alba* and *Sonneratia alba* are halophyte mangrove species that can grow on the most seaward side of a mangrove forest. As it is difficult to grow young seedlings of mangrove species year round, cell cultures are excellent experimental systems to study the specific cellular mechanisms underlying the halophilism of mangrove plants (Kawana et al., 2007; Kawana, Sasamoto, & Ashihara, 2008). Callus cultures of mangrove species were first produced using the pistil of *S. alba* (Akatsu, Hosoi, Sasamoto, & Ashihara, 1996). Then suspension cultures were established using cotyledons of three *Sonneratia* mangroves species, *S. alba*, *S. caseolaris* and *S. ovata*, (Kawana et al., 2007; Yamamoto, Kawana, Minagawa, & Sasamoto, 2011; Hasegawa, Oyanagi, Minagawa, Fujii, & Sasamoto, 2014). Murashige and Skoog (MS) (Murashige & Skoog, 1962) basal medium, which is commonly used in cultures of plant tissues, was used in these studies. The latter two *Sonneratia* species are less tolerant to Na^+ salt (Hasegawa et al., 2014). By contrast, in *Avicennia* mangrove species, only *A. alba* could be sub-cultured as a suspension culture in the modified amino acid (mAA)

basal medium (Hayashi et al., 2009), in which the concentration of $CaCl_2$ (3 mM) is the same as the MS basal medium. Though the halophilic nature to Na^+ and Mg^{2+} was shown in leaf culture of another seaward side grown mangrove species, *A. marina* (Hayashi et al., 2009), callus growth in sub-culture has not been established in *Avicennia* species other than *A. alba*.

We investigated the halophilic and salts-tolerant nature using cotyledon-derived suspension cultures of *S. alba* (Kawana & Sasamoto, 2008) and *A. alba* (Hayashi et al., 2009) and their protoplast cultures (Hasegawa, Kurita, Hayashi, Fukumoto, & Sasamoto, 2013). The effects of adding high concentrations (10-200 mM) of Na^+, K^+, Mg^{2+}, Ca^{2+}, Cl^-, and SO_4^{2-} ions in the medium, on the growth of suspension cells and protoplasts were investigated. These ions are constituent ions in seawater and soil and the habitat of mangrove plants contain various amounts of each ion (Dagar, Singh, & Mongia, 1993). *A. alba* suspension cells showed tolerance or halophilism to Na^+, K^+, Mg^{2+}, Cl^-, and SO_4^{2-} ions; however, further addition of 10 mM of $CaCl_2$, was inhibitory to growth (Hayashi et al., 2009), while *S. alba* suspension cells showed halophilic nature to all of the salts investigated including Ca^{2+} (Kawana & Sasamoto, 2008). The protoplast cultures showed similar differences in Ca^{2+} effect between *S. alba* and *A. alba* (Hasegawa et al., 2013).

Previously, distribution of cellular elements, in cryosections of *S. alba* suspension cells was compared with that of glycophyte rice suspension cells (Hayatsu, Suzuki, Hasegawa, Tsuchiya, & Sasamoto, 2014). We found that decrease of cellular Ca concentration ([Ca]) in the cytoplasmic matrix and vacuole was related to the halophilic nature of *S. alba* to Na^+. This is likely through an increase of possible transport activities of Na^+ from cytoplasmic matrix into the vacuoles under the stress of additional 50 mM NaCl in the medium. This line of *S. alba* suspension culture was successfully sub-cultured in medium containing 50 mM NaCl.

Here, we investigated the inhibitory effects of lower concentrations of $CaCl_2$ on the growth of cotyledon-derived callus culture of *A. alba* which was newly induced in a mAA medium (Tsuchiya et al., 2013). Furthermore, a 'low-Ca callus line' was established by sub-culturing in the medium without Ca^{2+}. To determine the cellular mechanisms underlying Ca^{2+} inhibition in callus culture of *A. alba*, we studied the ultrastructural features of cells, and intra- (cytoplasmic matrix and vacuole) and extracellular (cell wall) [Ca] and concentrations of various elements, using electron probe X-ray microanalysis and compared the results with those of *S. alba* (Hayatsu, Ono, Hamamoto, & Suzuki, 2012; Hayatsu et al., 2014). Effects of deletion of $CaCl_2$ in the medium were also investigated on growth for their protoplast cultures. The mechanisms underlying the tolerance to salts and halophilic nature of mangrove cells were discussed.

2. Method

2.1 Callus Culture of Avicennia alba

Callus culture of *A. alba* was developed from cotyledons of crypto-viviparous seeds, collected in Thailand and stored in tap water as described previously (Tsuchiya et al., 2013). The calluses were sub-cultured at 4- to 8 -week intervals in 6-9 cm petri dishes. The culture medium was the modified amino acid (mAA) basal medium, containing various elements as the major salt components (26 mM Cl, 21.25 mM K, 0.2 mM Na, 1.5 mM Mg, 1.25 mM P, and 1.73 mM S, 3 mM Ca), 1 µM 2,4-dichlorophenoxyacetic acid (2,4-D), 1 µM thidiazuron and 3% sucrose solidified with 0.8% agar. Sub-culture was performed in the medium with 3 mM $CaCl_2$ (high-Ca line). About one year after induction of a high-Ca line, a low-Ca line was developed by sub-culture in the medium without $CaCl_2$ after checking the growth in 0-6 mM $CaCl_2$ containing media (see Figure 2 in setion *3.1*). Pure water (Milipore Elix or Direct Q UV, 18.2 MΩ) was used for all culture media preparation. The pH was adjusted to 6.2 with NaOH and then autoclaved at 120°C, 20 min. The petri dishes were kept at 30°C in the dark

2.2 Effect of $CaCl_2$ on Growth of High-Ca Callus Line of A. alba

Effects of $CaCl_2$ concentrations on growth of *A. alba* calluses were measured by using a 24-well culture plate containing 0.8 mL medium solidified with agarose (0.8%, Type VII, Sigma A-4018) in a well. Cultures were incubated at 30°C in a humid incubator (CO_2-incubator without the supply of CO_2 gas, APC-30DR, ASTEC Co. Ltd.). Photographs of callus in each well were taken with digital camera after 0 and 31 d of culture. By Image J (Rasband, 1997-2016) analysis (see Appendix), pixel area of callus was calculated as % of the initial area. Data were averaged from two wells with standard deviation. Fresh and dry weights were measured after three months of culture.

2.3 Protoplast Isolation and Culture of A. alba Callus

Protoplasts were isolated from the *A. alba* calluses in axenic condition as described previously, with 1% each of Cellulase RS and Driselase 20 in 0.6 M mannitol solution (Tsuchiya et al., 2013). Protoplasts were washed with mannitol solution by centrifugation at 1300 rpm for 5 min after purification on the density gradient on 0.6 M

sucrose. Protoplast culture was performed in each 50 μL liquid medium using a 96-well culture plate as described previously for suspension protoplasts of *A. alba* (Hasegawa et al., 2013), except for osmotic condition. Basal medium was mAA containing 3% sucrose, 0.1 μM or 1 μM each of 2,4-D and thidiazuron and 0.6 M mannitol with and without 3 mM of $CaCl_2$. Initial protoplast densities were 10^4/mL or $5x10^4$/mL. Numbers of enlarged (more than 50 μm diameter) protoplasts were counted in a well after 6 days of culture under an inverted microscope.

2.4 Conventional Transmission Electron Microscopy and X-ray Microanalysis

Two-week-old calluses of *A. alba* were mixed with agarose (Type VII, Sigma A-4018), which was dissolved (2%) with liquid medium at 60°C for 20 min, and solidified at room temperature. Calluses in agarose block were fixed with a 6% glutaraldehyde solution (0.1 M phosphate buffer, pH 7.2) for 12 h and post-fixed with a 2% osmium tetroxide solution overnight at 4°C. The fixed specimens were dehydrated with a graded acetone series and embedded in Quetol 812 epoxy resin (Nisshin EM Co. Ltd., Tokyo, Japan). The preparation of ultrathin sections, electron staining with uranyl acetate and lead citrate, and microscope observation were carried out as described previously (Hayatsu et al., 2012, 2014). X-ray microanalysis was performed as detailed in section *2.6* on the electron-dense precipitates at the middle lamella of cell wall in the resin-embedded sections without electron staining as described previously (Inoue et al., 2013).

2.5 Preparation of Cryosections

Calluses of *A. alba* were embedded in agarose as described in section *2.4*. The method used for the cryosection preparation, freeze-drying, and the quantitative X-ray microanalysis was essentially the same as in our earlier studies (Hayatsu et al., 2012, 2014). Briefly, samples in agarose blocks were high-pressure frozen (EM-PACT, Leica, Austria) and stored in liquid N_2. Cryosections prepared with cryoultramicrotome (Ultracut UCT/EM FCS, Leica, Austria) were freeze-dried (VDF300S, Vacuum Device, Inc., Mito, Japan) at 1.3×10^{-4} Pa and -80°C for 6 h, and were lightly evaporated in vacuo with carbon. X-ray microanalysis was performed as detailed in section *2.6*.

2.6 X-ray Microanalysis

Quantitative X-ray microanalysis of cryosections was performed as described previously (Hayatsu et al., 2012, 2014) using an analytical electron microscope (JEM 1230/MiniCup/EX-14033JTP: JEOL, Akishima, Tokyo, Japan) with a Be-stage holder or a cryotransfer holder (G626DH: Gatan, Tokyo, Japan), respectively. Elemental concentrations were calculated on the basis of the Peak/Background intensity ratio (*P*/*B* ratio) using the software NORAN System SIX (Thermo Electron Co., Middleton, WI, USA) and the concentrations were indicated in mmol /kg dry weight (DW). The experiments were repeated with independently prepared samples. Concentrations of each element from cryosections were averaged from ten values for each element, and the standard error was calculated from these values, respectively. The Student's *t* distribution was used to determine the significances of difference between the elemental concentrations of calluses that were cultured with and without 3 mM $CaCl_2$.

3. Results and Discussion

3.1 $CaCl_2$ Inhibition on the Growth of High-Ca Callus Line and the Development of Low-Ca Callus Line of A. alba

Figure 1 shows the effects of $CaCl_2$ on the growth of a callus of a high-Ca line sub-cultured on the mAA basal medium containing 3 mM $CaCl_2$ for about two years after induction, quantitated by using a 24-well culture plate. Callus grew in medium containing $CaCl_2$ at concentrations less than 1/10 of that in the sub-culture medium, but growth was inhibited at higher concentrations of $CaCl_2$.

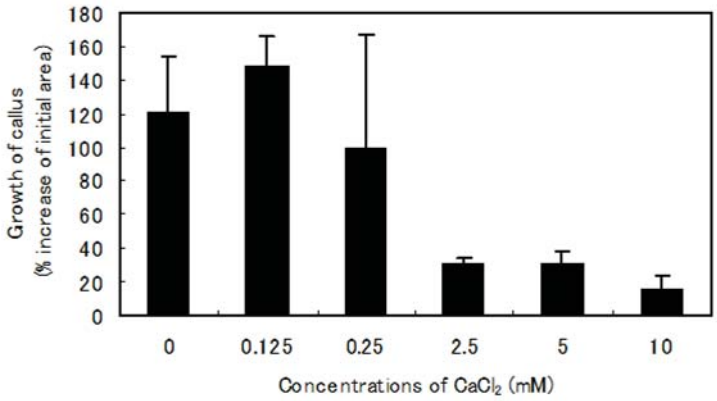

Figure 1. Effect of $CaCl_2$ on the callus growth of high-Ca line of *A. alba* cotyledon callus. Callus growth (% increase of initial area) after 31 days of culture was measured using Image J analysis. Callus was cultured in mAA basal medium without $CaCl_2$ containing 3% sucrose and 1 μM each of 2,4-D and thidiazuron

These findings are consistent with the fact that addition of 10 mM $CaCl_2$ inhibited the growth of cotyledon-origin suspension cells (Hayashi et al., 2009), when the packed cell volume was measured after culture of suspension cells using a 24-well culture plate. In the present study, growth of callus was measured as increased pixel area using Image-J software. Fresh and dry weights of callus were measured after three months of culture, and a similar decrease of growth was obtained depending on the $CaCl_2$ concentration (data not shown). Dry weight was about 5 % of the fresh weight.

The low-Ca callus line was developed from a one-year-old high-Ca line derived from *A. alba* cotyledons, and it was sub-cultured in 9 cm diameter petri dishes for more than three years. Although the addition of 3 and 6 mM of $CaCl_2$ inhibited the growth (brown color and smaller size) of *A. alba* callus in the second sub-culture (Figure 2), deletion of Ca^{2+} ions in the medium for a long period of sub-culture was challenging, because Ca^{2+} ions are thought to be indispensable for plants and are included in almost all plant tissue culture media (1-9 mM, Franklin & Dixon, 1994; Poothong & Reed, 2015).

Figure 2. Subculture of low-Ca line of *A. alba* cotyledon callus, without (a), with 3 mM (b) or 6 mM (c) of $CaCl_2$, cultured in 6 cmφ plastic dishes. $CaCl_2$ at 3 and 6 mM was inhibitory on the callus growth. Basal medium was the same as of Figure 1

3.2 Ultrastructures of A. alba Callus

The cotyledon-derived calluses of *A. alba*, sub-cultured for about two years with (high-Ca line, Figure 3a) and for about one year without (low-Ca line, Figure 3b) 3 mM $CaCl_2$, were observed by conventional electron microscopy. Diameters of cells sub-cultured with and without 3 mM $CaCl_2$, were ~25 μm and ~45 μm, respectively. These cells contained a well-developed central vacuole and the cytoplasmic matrix was located at the peripheral region of the cells and contained of organelles, e.g., nucleus, mitochondria, and amyloplasts. From the ultrastructural observation, no significant difference was observed between the high-Ca line and low-Ca line, except for the electron-dense precipitates in the cell wall (Figure 4). In resin-embedded sections of both callus lines, electron-dense precipitates were observed in the middle lamella of the cell wall, though these precipitates were observed more frequently in the high-Ca line (Figure 4a) than in the low-Ca line (Figure 4b).

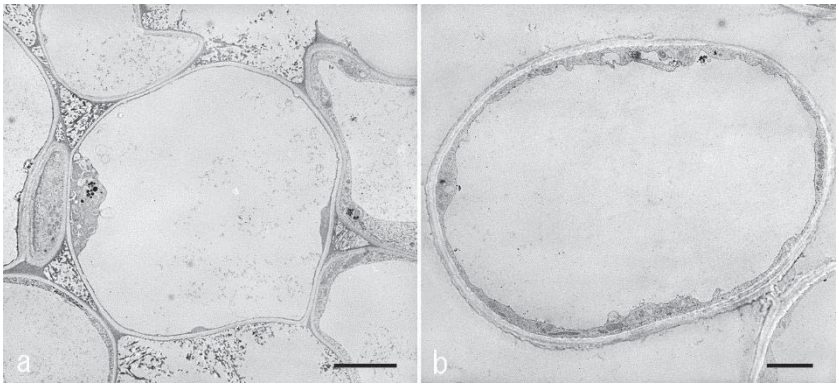

Figure 3. Electron microscope images from the chemically fixed and resin-embedded cell clusters of *A. alba* cotyledon callus. The high-Ca line (a) was cultured with 3 mM of $CaCl_2$, and low-Ca line (b) was cultured without $CaCl_2$. Scale bars, 5 μm

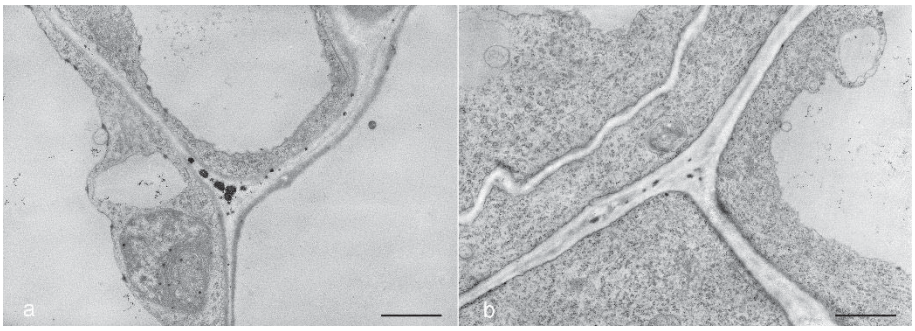

Figure 4. Electron-dense precipitates at the middle lamella of cell wall in *A. alba* cotyledon callus. The high-Ca line (a) was cultured with 3 mM of $CaCl_2$, and low-Ca line (b) was cultured without $CaCl_2$. Scale bars, 5 μm

3.3 Cellular Concentrations of Elements Detected by X-ray Microanalysis of Cryosections

A spot analysis was carried out at the cell wall, the cytoplasmic matrix, and the vacuolar lumen in the cryosections that were cut from the frozen cell clusters of *A. alba* callus sub-cultured with and without 3 mM $CaCl_2$. The results are summarized in Table 1 (high-Ca line) and Table 2 (low-Ca line). The given elements were those that were detected in X-ray spectra as a significant spectral peak and were included fundamentally in the MS basal medium, and mAA basal medium and are generally found in plant tissues and cells. Concerning the results of Student's *t* distribution, the differences between the mean values with $P < 0.01$ were considered significant.

Table 1. The concentrations of various elements in the cell wall, cytoplasmic matrix and vacuole in a high-Ca line of *A. alba* cotyledon callus

Element	Cell wall	(%)	Cytoplasmic matrix	(%)	Vacuole	(%)
Ca	36.5±7.1	(34)	51.2±11.2	(48)	18.1±3.1	(17)
K	126.3±24.4	(42)	87.1±7.3	(29)	87.5±14.5	(29)
Cl	73.8±12.6	(46)	52.4±5.5	(33)	34.9±6.4	(22)
Na	2.7±1.8	(32)	3.1±1.5	(37)	2.6±1.8	(31)
Mg	13.2±2.7	(28)	22.7±6.0	(49)	10.8±1.8	(23)
P	14.0±3.0	(17)	59.2±16.4	(73)	7.5±2.5	(9)
S	14.0±2.8	(26)	26.3±5.0	(49)	13.9±4.4	(26)

The values are mmol/kg DW (mean ±S.E.M., *N = 10*).

The values in parentheses are percentages of each component.

Table 2. The concentrations of various elements in the cell wall, cytoplasmic matrix and vacuole in a low-Ca line of *A. alba* cotyledon callus

Element	Cell wall (%)	Cytoplasmic matrix (%)	Vacuole (%)
Ca	4.6±1.4*[4] (52)	2.6±1.1*[4] (30)	1.6±0.7*[4] (18)
K	237.5±25.0*[4] (62)	78.4±9.8*[1] (21)	64.4±15.0*[1] (17)
Cl	122.6±10.4*[4] (62)	37.5±6.0*[2] (19)	36.8±7.7*[1] (19)
Na	3.6±2.0*[1] (63)	0*[2] (0)	1.9±1.0*[1] (37)
Mg	18.5±1.7*[1] (49)	9.9±2.4*[2] (26)	9.5±2.1*[1] (25)
P	33.8±6.8*[3] (41)	41.8±7.2*[1] (51)	6.7±1.3*[1] (8)
S	14.3±3.0*[1] (42)	13.8±2.7*[3] (40)	6.0±0.7*[1] (18)

The values are mmol/kg DW (mean ±S.E.M., *N = 10*). Significances of difference between the concentration of various elements in high-Ca line and low-Ca line are shown. *[1]$P > 0.1$, *[2]$P < 0.1$, *[3]$P < 0.05$, *[4]$P < 0.01$.

The values in parentheses are percentages of each component.

3.3.1 Ca Distribution in Cytoplasmic Matrix

[Ca] in the cytoplasmic matrix of the high-Ca line was 51.2 mmol /kg DW, 48%. The values are very high, compared with those in *S. alba* (20.5 mmol /kg DW, 17%) and those in rice suspension cells (11.9 mmol /kg DW, 34%) reported previously (Hayatsu et al., 2014). These results suggest that in the high-Ca line of *A. alba* transport ability of Ca^{2+} is low from the cytoplasmic matrix to the cell wall or to the vacuole, and the high [Ca] in the cytoplasmic matrix may be related to the lower growth rate of the high-Ca line in the medium containing high concentrations of $CaCl_2$ (Figure 1). Generally a trace amount of Ca is said to regulate various physiological phenomena of organisms (Plieth & Trewavas, 2002; Hayatsu & Suzuki, 2015). The intracellular [Ca] is kept nearly constant to avoid cytotoxic damage induced by increase of intracellular [Ca] (Gilroy, Blowers, & Trewavas, 1987; Belyavskaya, 1996). In the low-Ca line, [Ca] was reduced dramatically at all cell components, although the low amount of [Ca] was still detected (Table 2). Although pure water was used for medium preparation, the low-Ca line could be sub-cultured for more than three years. These results suggest that the trace amount of [Ca] might be carried by transfer of callus to fresh medium or that specific mechanism might be working in *A. alba* cells for accumulation of Ca from trace constituents of chemicals. Since the growth of *A. alba* callus was promoted by the very low concentrations of Ca^{2+} (Figure 1), a trace amount of Ca^{2+} was considered to stimulate the cell growth of *A. alba* callus.

3.3.2 Ca Distribution in Cell Wall

The quantitative X-ray microanalysis of the cell wall in *A. alba* callus observed in cryosections showed that [Ca] in the high-Ca line (36.5 mmol /kg DW, 34%) was approximately seven times that of the low-Ca line (4.6 mmol /kg DW, 52%). As reported previously, the quantitative X-ray microanalysis of cryosections of halophilic *S. alba* and glycophyte *O. sativa* cells cultured with 3 mM of $CaCl_2$ showed that a large amount of Ca (69.8 mmol /kg DW, 56%) distributes in the cell wall of *S. alba* and that low [Ca] (8.2-14.4 mmol /kg DW) were found in all cell components of *O. sativa* (Hayatsu et al., 2014). These results showed that high [Ca] in the cell wall of *A. alba* and *S. alba* cells indicate that halophyte mangrove plants have the ability to accumulate Ca in the cell wall.

3.3.3 K and Cl Distribution

The [Ca], [K] and [Cl] in the cell wall were different in the two callus lines of *A. alba*. In contrast, [Na], [Mg], [P] and [S] were similar in all components, suggesting that the cellular distributions of these elements were not affected by the deletion of Ca^{2+} in the medium. In the high-Ca line, [Ca], [Na], [Mg], [P] and [S], but not [K] and [Cl] were mainly high in the cytoplasmic matrix. In contrast, in the low-Ca line, [Ca], [K], [Cl], [Na] and [Mg], were mainly high in the cell wall. The concentrations of the elements were lower in the vacuole in both lines of *A. alba*. [K] and [Cl] in the cell wall of low-Ca line of *A. alba* were twice those of high-Ca line without any significant change of concentration in the cytoplasmic matrix and vacuole.

In higher plants, [Ca] makes the cell wall rigid and subsequently reduces the cell growth (Cooil & Bonner, 1957; Hayatsu & Suzuki, 2015). In the low-Ca line of *A. alba* callus, the increase of [K] and [Cl] in the cell wall may be caused by the decrease of [Ca] in the cell wall and reflect the supply of these ions from the mAA medium including K^+ and Cl^- in high concentrations. In *A. alba*, possible transport of [Ca], [K] and [Cl] from the cell wall to the cytoplasmic matrix at cell membrane must be reduced by the deletion of $CaCl_2$ in the medium. In contrast, in *S. alba* cells cultured with 3 mM of $CaCl_2$, [K] (55%) and [Cl] (64%) were high in the vacuole, suggesting the uniqueness of halophilic *S. alba* suspension cells having high possible transport activities of [K], [Cl] and [Na]

into the vacuole (Hayatsu et al., 2014).

3.4 Ca-containing Electron-dense Precipitates in the Cell Wall in the Resin-embedded Section

X-ray microanalysis was performed on the electron-dense precipitates at the middle lamella of the cell wall in the resin-embedded section. A spectral peak of Ca (Ca-Kα at 3690 eV) was clearly detected on the electron-dense precipitates in the middle lamella of the cell wall of both callus lines. Spectral peak intensities of Ca-Kα emissions detected from precipitates in the high-Ca line were several times higher than those in the low-Ca line. Our observations suggest that the electron-dense precipitates contain Ca, and that the heavy accumulation of Ca in the middle lamella of the cell wall of the high-Ca line (Figure 4a) might be related to the inhibition of growth by high Ca^{2+} concentrations in callus culture of high-Ca line of *A. alba* (Figure 1). The high [Ca] in the cell wall of high-Ca line (Table 1) might reflect accumulation of Ca-containing electron-dense precipitates (Figure 4), which was not observed in cryosections of *A. alba*.

Electron-dense structures of plant cells contain a high amount of Ca, such as gravitropic soybean cells, which was confirmed by X-ray microanalysis (Hayatsu et al., 2012). Heavy deposition of electron-dense precipitates in the middle lamella of cell wall (Figure 4a) has been reported in radish and corn roots treated with high concentrations of lead (Inoue et al., 2013) or lanthanum (Hayatsu, Ono, & Suzuki, unpublished). The existence of these heavy metals in the electron-dense precipitates in the cell wall was also confirmed by X-ray microanalysis, suggesting that it is related to the accumulation and tolerance to these heavy metals. On the other hand, heavy accumulation of electron-dense precipitates in the middle lamella of cell walls are observed neither in the cells of halophyte mangrove *S. alba* nor in those of glycophyte *O. sativa* cultured with 3 mM $CaCl_2$ (Hayatsu et al., 2014), which did not inhibit their growth.

3.5 Effects of $CaCl_2$ on Protoplast Cultures of A. alba

To determine the effect of removal of cell wall, we isolated protoplasts and cultured them in the media with and without 3 mM of $CaCl_2$. When isolated, diameters of protoplasts of two lines of *A. alba* were less than 50 μm in 0.6 M mannitol solution. Osmotic condition, 0.6 M, instead of 1.2 M sorbitol (Hasegawa et al., 2011, 2013) was used after optimization. Small protoplasts (20 μm diameter) were found in the high-Ca line, while only large protoplasts (30 to 40 μm) were found in the low-Ca line. This might reflect the diameter difference found by the conventional electron microscopy (Figure 3). In protoplast cultures for plant regeneration, CPW salts, which include high concentrations of Mg^{2+} and Ca^{2+} ions, are occasionally used for obtaining viable protoplasts (Franklin & Dixon, 1994). In the present study and in our protoplast research (Hasegawa et al., 2013), isolation and purification of protoplasts was performed in cell wall degrading enzymes without using buffer salts, and without addition of Mg^{2+} and Ca^{2+} ions. The procedure is necessary to know the direct effects of these ions in the culture medium.

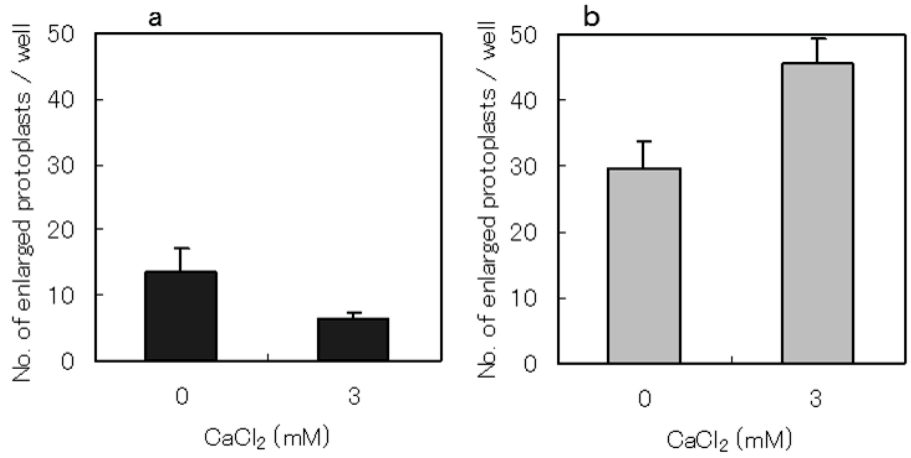

Figure 5. Effect of $CaCl_2$, on the growth of protoplasts of a high-Ca line (a) and low-Ca line (b) of *A. alba* cotyledon callus. The protoplasts were cultured in mAA basal medium containing 3% sucrose, 0.6 M mannitol and 1 μM each of 2,4-D and thidiazuron with and without 3 mM of $CaCl_2$

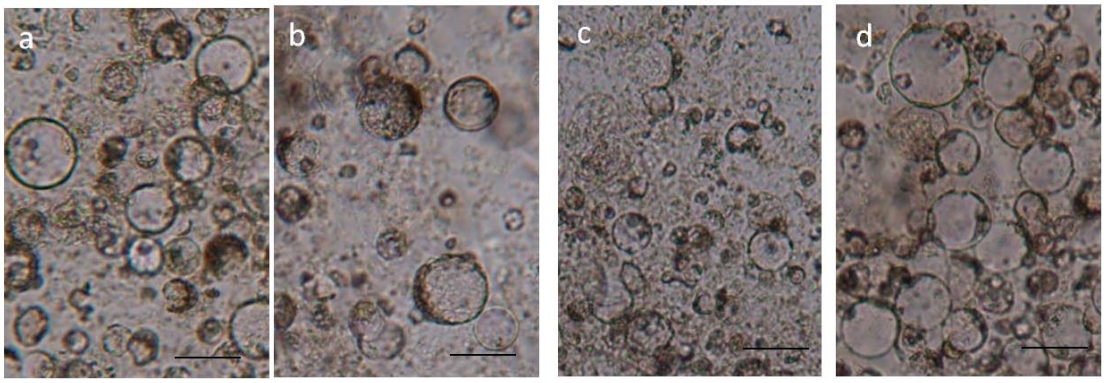

Figure 6. Effect of $CaCl_2$, on the growth of protoplasts in a high-Ca line (a, b) and low-Ca line (c, d) of *A. alba* cotyledon callus. The protoplasts were cultured in the same basal medium as of Figure 5 except for 0.1 μM each of 2,4-D and thidiazuron, with (b, d) and without (a, c) 3 mM of $CaCl_2$. Scale bars, 50 μm

Figure 5a shows the inhibitory effects of 3 mM $CaCl_2$ in the medium on the protoplast cultures of a high-Ca line of *A. alba* cotyledon-callus. Similar Ca^{2+} effects were obtained in different plant growth regulator conditions, i.e., 0.1 μM each of 2,4-D and thidiazuron (Figure 6a, b). These findings are consistent with the inhibition of growth of callus by 2.5 mM or more of $CaCl_2$ (Figure 1) and with that of protoplast culture of cotyledon-derived suspension culture (Hasegawa et al., 2013), though the optimal osmotic condition was 1.2 M sorbitol in the protoplast culture of suspension cells of *A. alba* (Hasegawa et al., 2011). Table 1 shows high [Ca] at the cell wall in the high-Ca line. Protoplast isolation must reduce the [Ca] distribution at the outer cell. However, a high cytoplasmic [Ca] and further application of Ca^{2+} ions in the medium might inhibit the growth of protoplasts (Figure 5a).

Figure 5b (low-Ca line) shows better growth than in Figure 5a, and the stimulatory effects of addition of 3 mM $CaCl_2$ in the medium. Addition of $CaCl_2$ increased cell enlargement of protoplasts. These are opposite the effects of Ca^{2+} on callus (Figure 1) and protoplast (Figure 5a) growth of the high-Ca line. Different hormonal conditions, 0.1 μM of 2,4-D and thidiazuron gave similar results (Figure 6c, d). In the protoplast isolation of low-Ca line, by removal of [Ca] at the cell wall, the amount of [Ca] in the cytoplasmic or vacuolar components might become lower than needed for culture. The overall results suggested that an appropriate, but very low amount of [Ca] at the cell wall is needed for cell growth in *A. alba*.

As Ca^{2+} is generally a prerequisite for culture of plant tissue and protoplasts, deletion of Ca^{2+} in medium is unusual. However, in this study, cotyledon-callus of halophyte *A. alba* could be sub-cultured for years in the absence of Ca^{2+} in the medium (low-Ca line), and a much lower cellular [Ca] was found using X-ray microanalysis. Very recently, we found that deletion of Ca^{2+} in cultures of cotyledons and hypocotyls of another seaward-side grown *Avicennia* mangrove, *A. marina,* caused much better growth than usual media (Sasamoto & Mochida, 2015). As Ca^{2+} in the culture media had similar inhibitory effects on growth in both *Avicennia* species, *Avicennia* species might have a specific cellular mechanism for accumulation of Ca in the cell wall and in the cytoplasmic matrix, but less transport activity of Ca into the vacuole. In another halophyte mangrove, *S. alba* (Hayatsu et al., 2014), in the usual medium (3 mM-$CaCl_2$), similarly, Ca accumulated in the cell wall, but the [Ca] in the cytoplasmic matrix was low. The [Ca] in the cytoplasmic matrix and vacuole was very low in the high Na^+ in the medium, which is optimum for cell growth of *S. alba*. Therefore, in cell cultures of halophilic mangrove species, decrease of cellular [Ca] might be the most important factor for their cellular growth. Cellular [Ca] was measured effectively by X-ray microanalysis of cryosections.

Acknowledgments

This study was partly supported by the research fund of the Research Institute for Integrated Science, Kanagawa University.

References

Akatsu, M., Hosoi, Y., Sasamoto, H., & Ashihara, H. (1996). Purine metabolism in cells of a mangrove plant, *Sonneratia alba*, in tissue culture. *Journal of Plant Physiology, 149*, 133-137. https://doi.org/10.1016/S0176-1617(96)80185-4

Belyavskaya, N. A. (1996). Free and membrane-bound calcium in microgravity and microgravity effects at the membrane level. *Advances in Space Research, 17*, 169-177. https://doi.org/10.1016/0273-1177(95)00631-N

Cooil, B., & Bonner, J. (1957). The nature of growth inhibition by calcium in the *Avena* coleoptile. *Planta, 48*, 696-723. https://doi.org/10.1007/BF01911596

Dagar, J. C., Singh, N. T., & Mongia, A. D. (1993). Characteristics of mangrove soils and vegetation of Bay Islands in India. In H. Lieth, & A. A. Masoom (Eds.), *Towards the rational use of high salinity tolerant plants. Vol.1. Deliberations about high salinity tolerant plants and ecosystems* (pp. 59-80). Kluwer Academic. https://doi.org/10.1007/978-94-011-1858-3_6

Franklin, C. I., & Dixon, R. A. (1994). Initiation and maintenance of callus and cell suspension cultures. In R. A. Dixon, & R. A .Gonzales (Eds.), *Plant Cell Culture. A Practical Approach* (pp. 1-25). Oxford: IRL Press.

Gilroy, S., Blowers, D. P., & Trewavas, A. J. (1987). Calcium: a regulation system emerges in plant cells. *Development, 100*, 181-184.

Hasegawa, A., Hayashi, S., Kurita, A., Kaai, F., Kawana, Y., Fukumoto, T., & Sasamoto, H. (2011). Stimulatory and inhibitory effects of abscisic acid on cell growth in protoplast cultures and the relation to its endogenous levels in Avicenniaceae mangrove cells. *Mangrove Science, 8,* 11-18.

Hasegawa, A., Kurita, A., Hayashi, S., Fukumoto, T., & Sasamoto, H. (2013). Halophilic and salts tolerant protoplast cultures of mangrove plants, *Sonneratia alba* and *Avicennia alba*. *Plant Biotechnology Reports, 7,* 205-209. https://doi.org/ 10.1007/s11816-012-0251-2

Hasegawa, A., Oyanagi, T., Minagawa, R., Fujii, Y., & Sasamoto, H. (2014). An inverse relationship between allelopathic activity and salt tolerance in suspension cultures of three mangrove species, *Sonneratia alba*, *S. caseolaris* and *S. ovata*: development of a bioassay method for allelopathy, the protoplast co-culture method. *Journal of Plant Research, 127,* 755-761. https://doi.org/10.1007/s10265-014-0651-1

Hayashi, S., Kuriyama, S., Kawana, Y., Hasegawa, A., Kurita, A., Minagawa, R., & Sasamoto, H. (2009). Stimulatory effects of sea salts on cell growth in liquid culture of Avicenniaceae mangrove. *Plant Biotechnology, 26,* 561-564. https://doi.org/10.5511/plantbiotechnology.26.561

Hayatsu, M., Ono, M., Hamamoto, C., & Suzuki, S. (2012). Cytochemical and electron probe X-ray microanalysis studies on the distribution change of intracellular calcium in columella cells of soybean roots under simulated microgravity. *Journal of Electron Microscopy, 61,* 57-69. https://dx.doi.org/10.1093/jmicro/dfr095

Hayatsu, M., Suzuki, S., Hasegawa, A., Tsuchiya, S., & Sasamoto, H. (2014). Effect of NaCl on ionic content and distribution in suspension-cultured cells of the halophyte *Sonneratia alba* versus the glycophyte *Oryza sativa*. *Journal of Plant Physiology, 171,* 1385-1391. https://doi.org/10.1016/j.jplph.2014.06.008

Hayatsu, M., & Suzuki, S. (2015). Electron probe X-ray microanalysis studies on the distribution change of intra- and extracellular calcium in the elongation zone of horizontally reoriented soybean roots. *Microscopy, 64*(5), 327-334. https://doi.org/10.1093/jmicro/dfv031

Inoue, H., Fukuoka, D., Tatai, Y., Kamachi, H., Hayatsu, M., Ono, M., & Suzuki, S. (2013). Properties of lead deposits in cell walls of radish (*Raphanus sativus*) roots. *Journal of Plant Research, 126*, 51-61. https://doi.org/10.1007/s10265-012-0494-6

Kawana, Y., & Sasamoto, H. (2008). Stimulation effects of salts on growth in suspension culture of a mangrove plant, *Sonneratia alba*, compared with another mangrove, *Bruguiera sexangula* and non-mangrove tobacco BY-2 cells. *Plant Biotechnology, 25*, 151-155. https://doi.org/10.5511/plantbiotechnology.25.151

Kawana, Y., Yamamoto, R., Mochida, Y., Suzuki, K., Baba, S., & Sasamoto, H. (2007). Generation and maintenance of suspension cultures from cotyledons and their organogenic potential of two mangrove species, *Sonneratia alba* and *S. caseolaris*. *Plant Biotechnology Reports, 1,* 219-226. https://doi.org/10.1007/s11816-007-0035-2

Kawana, Y., Sasamoto, H., & Ashihara, H. (2008). Mechanism of salt tolerance in mangrove plants. *Bulletin of the Society of Sea Water Science, Japan, 62*, 207-214. (in Japanese with English abstract) https://doi.org/10.11457/swsj1965.62.207

Murashige, T., & Skoog, F. (1962). A revised medium for rapid growth and bioassay with tobacco tissue cultures. *Physiologia Plantarum, 15*, 473-497. https://doi.org/10.1111/j.1399-3054.1962.tb08052.x

Plieth, C., & Trewavas, A. J. (2002). Reorientation of seedlings in the Earth's gravitational field induces

cytosolic calcium transients. *Plant Physiology, 129*, 786-796. https://doi.org/10.1104/pp.011007

Poothong, S., & Reed, B. M. (2015). Increased $CaCl_2$, $MgSO_4$, and KH_2PO_4 improve the growth of micropropagated red respberries. *In Vitro Cellular and Developmental Biology Plant, 51*, 648-658. https://doi.org/10.1007/s11627-015-9720-y

Rasband, W. S. (1997-2016). Image J. U. S. National Institute of Health, Bethesda, Maryland, USA, http://imagej.nih.gov/ij

Sasamoto, H., & Mochida, Y. (2015). Ca inhibits callus induction from seeds of a mangrove plant, *Avicennia marina* (in Japanese). *Abstracts of the 21st Annual Meeting of Japan Society for Mangroves*, p. 6.

Spalding, M. D., Kainuma, M., & Collins, L. (2010). *World Atlas of Mangroves*. London: Earthscan Publications.

Tomlinson, P. B. (1986). *The Botany of Mangroves*. London: Cambridge University Press.

Tsuchiya, S., Ogita, S., Kawana, Y., Oyanagi, T., Hasegawa, A., & Sasamoto, H. (2013). Relation between amino acids profiles and recalcitrancy of cell growth or salt tolerance in tissue and protoplast cultures of three mangrove species, *Avicennia alba, Bruguiera sexangula,* and *Sonneratia alba*. *American Journal of Plant Sciences, 4*, 1366-1374. https://doi.org/10.4236/ajps.2013.47167

Yamamoto, R., Kawana, Y., Minagawa, R., & Sasamoto, H. (2011). Effects of sea salts on induction of cell proliferation in liquid cultures of mangrove plants, *Sonneratia caseolaris* and *S. alba*. *American Journal of Plant Sciences, 2*, 35-42. https://doi.org/10.4236/ajps.2011.21004

Appendix

Image J Analysis of Callus Growth

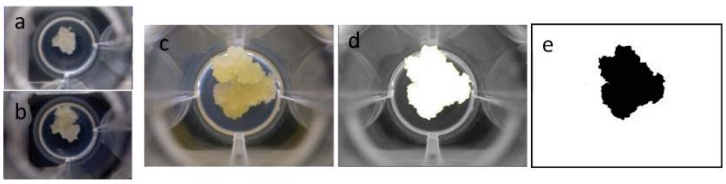

Figure 7. Digital images of calluses in each well of a 24 well culture plate (a, b, c), and steps of Image J analysis of an example of callus (c, d, e). The original view of callus (c) was cut with freehand selection and converted to binary image to demonstrate the transverse section (d), and then the section image was inverted from white to black (e). Area of transverse section (e) was measured in pixels. Images a (at 0 day) and b (at 22 day of culture) were derived from the same well

Journal of Plant Studies; Vol. 6, No. 2; 2017
ISSN 1927-0461 E-ISSN 1927-047X
Published by Canadian Center of Science and Education

Allometric Dynamics in Branch Growth of Crape Myrtle

Xiongwen Chen[1]

[1]Department of Biological & Environmental Sciences, 139 ARC, Alabama A & M University, Normal, AL, USA

Correspondence: Xiongwen Chen Department of Biological & Environmental Sciences, 139 ARC, Alabama A & M University, Normal, AL, USA. Tel: 256-372-4231. E-mail: xiongwen.chen@aamu.edu

Received: February 18, 2017 Accepted: March 21, 2017 Online Published: March 29, 2017

doi:10.5539/jps.v6n2p28 URL: https://doi.org/10.5539/jps.v6n2p28

Abstract

Tree branches provide multiple functions in tree growth. It is necessary to study the allometric patterns of branches in order to understand some quantitative perspectives in tree growth. In this study, branches of seven crape myrtle trees (*Lagerstroemia indica*) were studied to examine allometric relationships in different times. The results indicated that the total basal area of branches at one order was far more than it at the next lower order (branches far from trunks). The scaling exponents of frequency distribution in both branch length and diameter decreased from above 1.0 in May to 0.1 in November as branches grew. The entropy of branch length and diameter both decreased at the beginning and then increased for all trees during the growing season. The observed entropy was always less than the maximum entropy. The average slenderness of branches was close to 20 for all trees. There were higher fluctuations in the slenderness within small or short branches (diameter less than 10 mm or length less than 100 cm). The scaling exponents between branch radius and length were concentrated at 1.0 for most trees. The correlation between the branch diameters of 1st order and the number of branches at 2nd order was not significant. The general trend and deviations in allometric relationships may help to understand the complexity in tree branch development.

Keywords: Alabama, branch order, entropy, scaling exponent, slenderness

1. Introduction

Studying the patterns of branch growth is important to understand tree growth. Changes to tree morphology, such as changes with age and crowding, have been previously studied in forestry with an emphasis on timber (Raulier et al., 1996). Tree branches provide multiple functions during tree growth, such as light interception, canopy photosynthesis, water and nutrient transportation, space filling, and biomechanical tolerance of wind or rain (snow) loading (Küppers, 1989; Skatter & Kucera, 2000; Nishimura 2005). Tree branching is influenced by many biological and environmental processes in trees, such as photosynthesis and drought. Analysis of branch development is an essential procedure for improving our knowledge of tree survival and growth strategies. Multiple parameters including branch diameter, length, intensity, angle, and age have been incorporated into analyses of branch growth because they all affect branch growth and branching patterns (Remphrey & Powell, 1984; Remphrey & Davidson, 1992; Takenaka, 2000; Taugourdeau et al., 2012).

The quantitative relationship in tree branching, which means allometric patterns of branches, is one important aspect in studying tree branching because it can help to understand tree growth and make prediction in the similar species (or groups). For example, the sum of the cross sections of branches at next level (or branch order) is the same as that of the parent branches which are close to trunks (Richter, 1970); fractal geometry (Mandelbrot, 1978) could be used to describe iterative branching systems or the similarity of branching patterns. It was suggested that branches of each tree-shape organism (e.g., trees, heart systems and etc) follow a power law with an invariant exponent (e.g., 3/4) because all tree species share an optimal design of the vascular system which is related to plant physiology (Enquist et al., 1999, West et al., 1999). Sperry et al. (2008) indicated that tree crowns do not exhibit the most efficient hydraulic architecture due to the limitations of mechanical safety. Allometric relationships that describe branch growth are often studied through log–log relationship. There are three similar models that describe growth patterns in trees as power law functions ($L = aR^b$, here L is branch length, R is branch or stem radius). When the b values are close to 1.0, 0.67, or 0.5, the power function is called geometric similarity model, elastic similarity model and static stress similarity model, respectively (McMahon, 1975). Previous researchers have found different outcomes for allometric patterns in different tree species (e.g., McMahon, 1975; King, 1986; Niklas, 1995; Osunkoya et al., 2007). Chen & Burton (2010) found that loblolly

pines and sugar maples followed the same power law in individual trees and also at species level. Most of the red maple individuals did not follow a power law although they followed a power law at the species level. There is a suggestion that an allometric relationship might change from the elastic model to the stress similarity model due to species and other factors (Niklas & Spatz, 2000). Smaller branches fit a curvilinear pattern in *Quercus alba* L. and *Acer saccharinum* L. until they reach approximately 3,000 mm where they are best modeled with elastic similarity model (McMahon & Kronauer, 1976). Bertram (1989) found that slenderness (branch length/branch basal radius) increased in small branches (radius $\leq$10 mm) while decreased in large branches (radius $\geq$ 10 mm). Here a hypothesis could be derived that allometric relationships in branches may change with tree growth.

Furthermore, all the branches of a tree are formed as a self-organized network. The tree branch network should follow the principle of maximum entropy (MaxEnt), which means the probability distribution of branches best represents the current state and reaches the largest entropy (e.g., Jaynes, 1957). MaxEnt has been frequently used in ecology (Harte, 2011). It could be assumed that tree branches follow MaxEnt during their growth. It is hard to test these hypotheses on large trees due to the difficulty of accessing and measuring branches. However, it is possible to measure all branches on crape myrtle in the southern region due to its unique management. Crape myrtle is usually coppiced in winter, allowing easy access to its branches. It is possible to use crape myrtle trees as a case study to test the above hypotheses related to allometric patterns of tree branches. The specific objectives include (i) whether the distribution of branch length and diameter follows similar power laws for individual trees; whether the scaling exponents of these power laws are the same; (ii) whether branch slenderness stays the same during the growth of individual trees; (iii) whether MaxEnt exists in branch length or diameter during a growing period. The results of this study will provide better understanding of tree growth, especially on the quantitative relationships of tree growth.

2. Materials and Methods

Crape myrtle (*Lagerstroemia indica*) is a popular ornamental plant in the south because of their showy flowers and aesthetic display. The species is most often found as a multiple-trunked tree or shrub. Usually all branches on crape myrtle are cut (pruned) in winter or early spring and bloom on new growth from the stems (Fig. 1). This is a common tree management activity in the southern region. Due to this unique practice where all branches are cut in winter, it provides convenience for us to measure each branch multiple times during the growing period. In this study, seven trees of crape myrtle at the same location on the campus of Alabama A & M University were selected. The trees at the same location were chosen because we want to limit the influence from environmental factors related to locations. Seven trees were selected because of the considerable amount of measurements in branches with tree growth. All branches were cut in the winter of 2015. The trunks were approximately 1.3 m in height. The tree branches started to grow near the end of April in 2016. The measurements, which include the branch length (cm) and diameter at branch base (mm), were conducted in May, July and October, 2016. The branch order (1st, 2nd, 3rd) for each branch was determined in October. The 1st order branches are those directly growing from trunks.

Figure 1. Crape myrtle in early spring and summer

The lengths of all branches at each tree were sorted based on the length increase of every 20 cm. For example, branches with a maximal length of 120 cm have the following length categories: ≤ 20, ≤ 40, ≤ 60, …, ≤ 120. The number of branches within each length category was counted. For each tree, a table was made showing the cumulative percentage for the number of branches within each length based on a method provided by White et al. (2008). Finally, a figure with the logarithm of diameter and logarithm of accumulated frequency was used. Similar method was used for branch diameters.

The exponent of branch length and diameter ($L \propto D$) was estimated through $\log_{10}$-$\log_{10}$ transformation. A figure with the $\log_{10}$ of L and the $\log_{10}$ of D was produced for this study. To be consistent with current literature on the estimation of allometric relationships, a reduced major axis (RMA) of regression analysis Model Type II was used to determine scaling exponents (αRMA). ANOVA of SAS software (Cary, NC) was used to compare statistical difference at α=0.05 level.

The entropy (E) of branch length or diameter was calculated as the followings:

$$E = \sum p_i \log p_i$$

where p_i is the percentage of any one branch in the total length or diameter (branch length (diameter) of any one branch / total branch length (diameter)) for each tree at the measuring time i. It is also called information entropy. The MaxEnt was estimated with the assumption that all p_i values are the same.

3. Results

The first tree (Tree ID 1) grew fast and the last tree (Tree ID 7) grew slowly based on the total branch length and basal area (Fig. 2). The total basal area of branches at one level were far more than it at the next lower level, even at each trunk, such as for Tree 1 and 2 (Table 1). The pipe model was not followed.

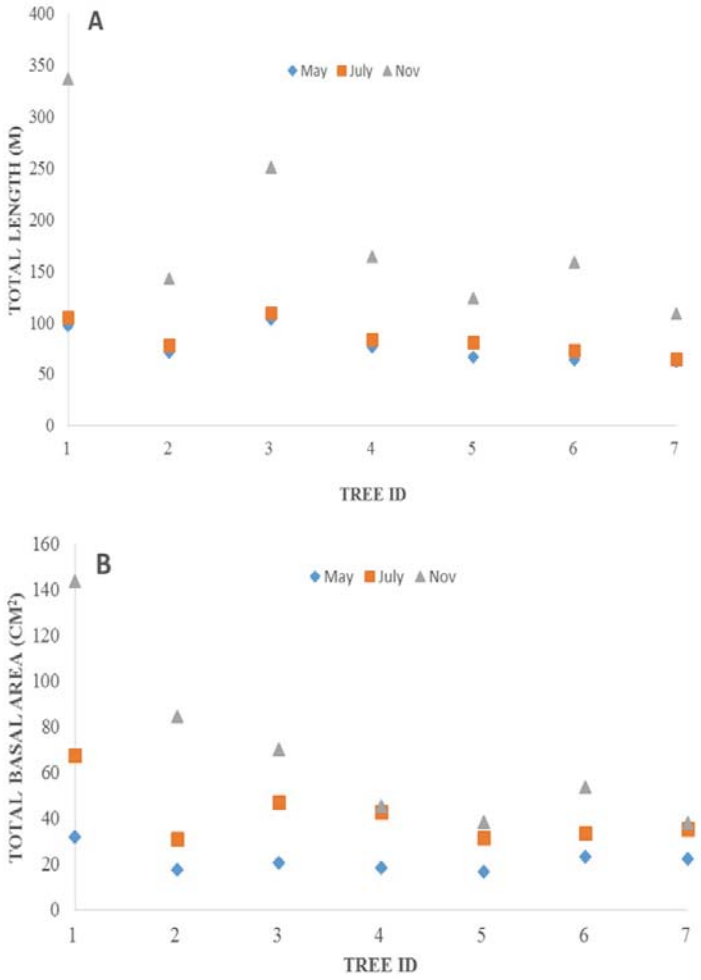

Figure 2. Dynamics of total branch length (A) and basal area (B) for each tree

Table 1. Total basal area (cm^2) of branches at different levels (orders) for some trees

Tree ID	Trunk #	Trunk section area	Level 1	Level 2	Level 3	Level 4
1	I	29.4	14.7	6.1	4.1	0.7
	II	24.0	9.6	3.6	1.2	0.1
	III	36.0	28.2	20.4	17.8	0.8
	IV	33.7	20.8	11.4	7.2	1.1
	V	28.8	13.3	6.9	4.6	0.8
2	I	21.2	10.6	4.1	1.8	0
	II	21.5	7.5	2.9	0.6	0
	III	25.3	12.0	5.8	1.9	0.5
	IV	15.7	7.0	1.3	0.4	0
	V	19.4	5.0	3.6	1.4	0

The scaling exponents of the frequency distribution for branch length in each tree decreased with branch growth from above 1.0 in May to 0.1 in November (Table 2). The scaling exponents of the frequency distribution for branch diameter decreased with branch growth for Tree 2 and 3 (Table 2), but some trees (Tree 1, 4, 5 and 6) the scaling exponents increased in July and then decreased in November.

Table 2. Scaling exponents of the frequency distribution for branch length and diameter at different times in seven trees

Tree ID	May		July		November	
	Length	Diameter	Length	Diameter	Length	Diameter
1	1.1066	1.0327	1.1045	1.1813	0.0891	0.0893
2	1.3045	0.9378	0.5960	0.4982	0.1378	0.1327
3	1.2697	1.0207	0.7273	0.8201	0.1215	0.1231
4	1.1520	0.4334	0.7741	0.7414	0.1956	0.6151
5	1.4699	0.7725	0.5224	1.3403	0.1285	0.6497
6	1.1277	0.8198	0.9408	1.0611	0.3434	0.4838
7	1.0570	1.0179	0.7129	0.6033	0.1677	0.7626

The entropy of branch length was very similar with the entropy of branch diameter for each tree (Table 3). Both entropy values decreased in July and increased in November for all trees. At each time the entropy values of branch length and diameter were less than the MaxEnt.

Table 3. Entropy of branch length and diameter at different times for seven trees

Tree ID	May, 2016			July, 2016			November, 2016		
	Length	Diameter	MaxEnt	Length	Diameter	MaxEnt	Length	Diameter	MaxEnt
1	2.36	2.37	2.41	1.99	2.00	2.07	2.94	2.99	3.20
2	2.22	2.22	2.26	2.04	2.03	2.14	2.43	2.46	2.67
3	2.39	2.30	2.34	1.92	1.94	2.04	2.69	2.41	2.93
4	2.26	2.25	2.44	2.11	1.97	2.04	2.56	2.60	2.71
5	2.17	2.17	2.20	1.80	1.85	1.91	2.42	2.45	2.68
6	2.19	2.08	2.24	1.97	1.99	2.05	1.89	1.92	2.06
7	2.21	2.15	2.26	1.99	2.00	2.09	2.34	2.41	2.56

The average slenderness of branches was always close to 20 with tree growth for each tree. There was no significant difference in average slenderness among trees due to variances (Fig. 3). Generally there were higher fluctuations in slenderness for the small branches (diameter less than 10 mm) than the bigger ones (Fig. 4A). Similar results were observed for the slenderness along branch length (Fig 4B). There were higher fluctuations in slenderness for the short branches (length less than 100 cm) in comparison to the longer branches.

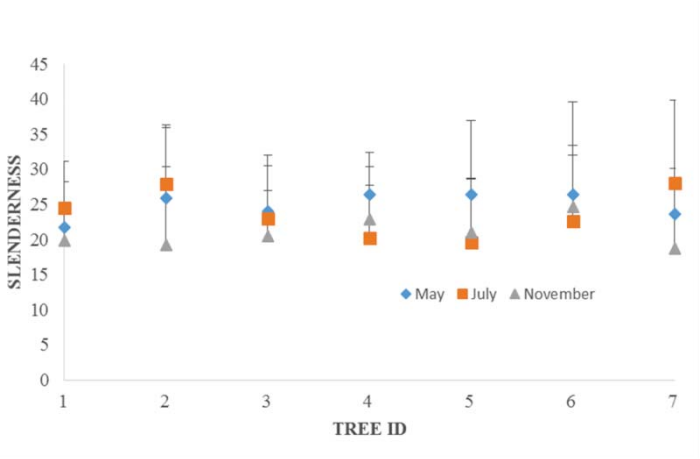

Figure 3. Dynamics of branch slenderness for each tree (vertical lines indicate standard deviation)

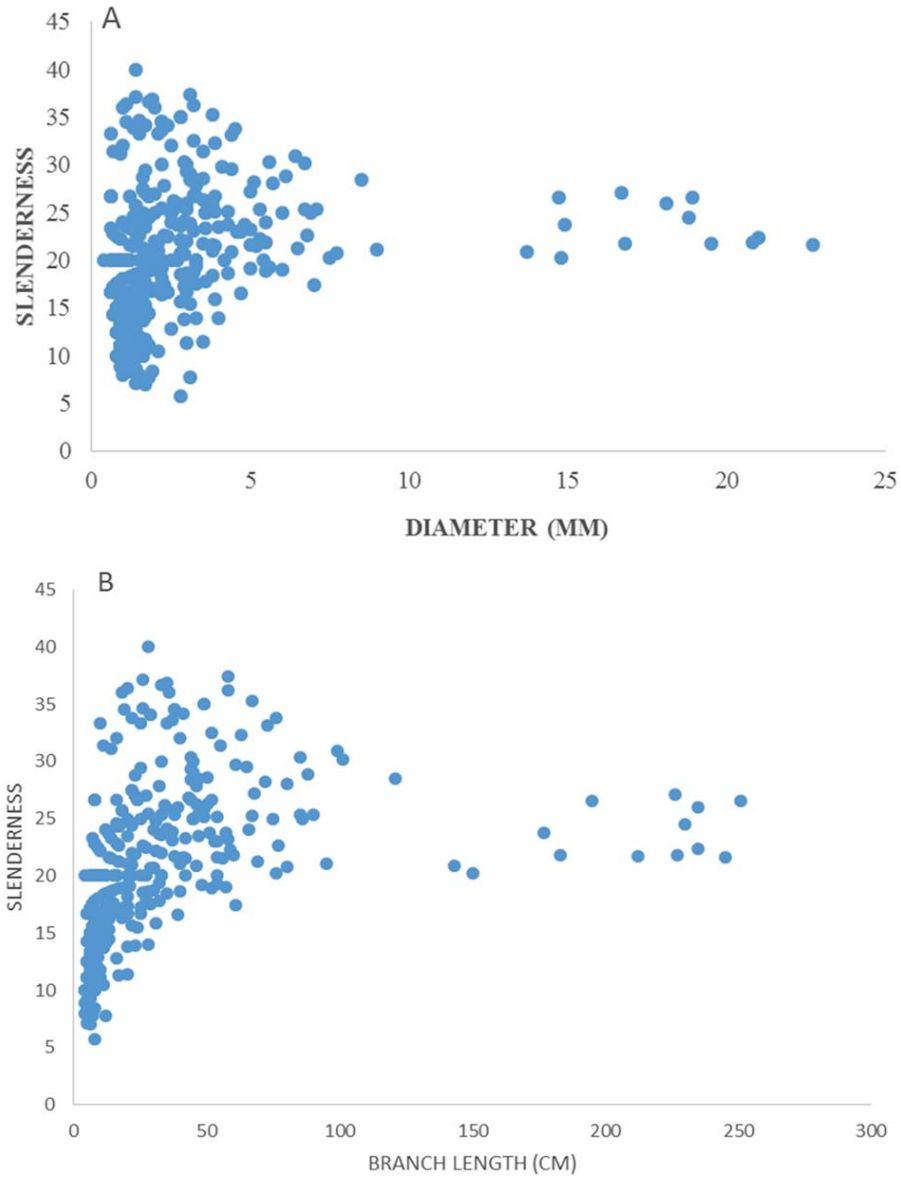

Figure 4. Slenderness changed with branch diameter (A) and length (B).

The scaling between branch radius and length (log$R$ – log$L$) indicated that the scaling exponents were concentrated around 1.0 (p<0.05) (Table 4), but for some trees (such as for Tree 2 and 5) the exponents changed significantly with branch growth (p<0.05).

Table 4. Scaling exponents between branch radius and length for each tree along time (The correlations were significant at α <0.05 for all except for the indicated ones by £)

Tree ID	May, 2016		July, 2016		November, 2016	
	Exponent	R^2	Exponent	R^2	Exponent	R^2
1	0.88	0.6693	1.01	0.8083	1.15	0.6984
2	0.73£	0.5863	1.02	0.8056	1.05	0.8278
3	1.01	0.7158	1.13	0.8202	1.09	0.8773
4	0.94	0.7793	1.05	0.7298	0.99	0.7957
5	0.77£	0.5405	0.98	0.6613	1.21	0.8553
6	0.82	0.6992	0.93	0.7412	1.12	0.8342
7	1.02	0.6335	0.92	0.7499	1.16	0.8387

The correlation between the branch diameters of 1st order and the branch number of 2nd order was not significant, such as for Tree 1 (Fig. 5A). Same as the correlation between the branch diameters of 1st order and the branch number at all next orders, such as for Tree 1 (Fig. 5B). The correlation between the branch length of the 1st order and the number of branches at all next orders was also not significant (Fig. 5C). This means that the large branches did not necessary have more branches at the next lower orders.

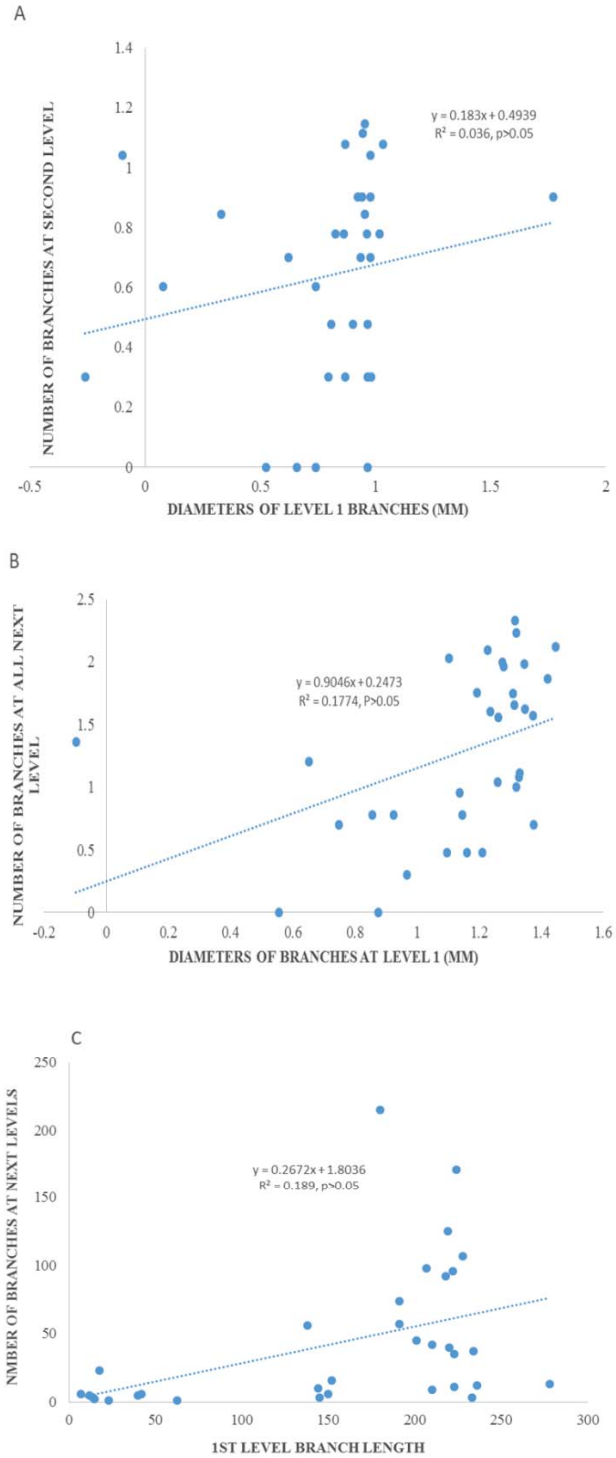

Figure 5. Correlation between the branch diameters of 1st level (order) and the branch number at 2nd level (A), and the branch number at all next levels (B); the correlation between the branch lengths of 1st level and the branch number at all next levels (C)

4. Discussion

The pipe model theory assumed that the cross-section areas in branches should be equal to stem areas of a tree (Shinozaki et al., 1964), which means the basal area of branches at one level (order) should be equal to the branch basal area at the next level (order). The results in this study did not support this assumption. Mäkelä

(2002) suggested that the pipe model theory should be modified to include the transitional, inactive sapwood zone because active pipes may not always be identified with the entire sapwood area. The dependence of pipe model may also be affected by numerous other factors such as site, stand closure, and social class of the tree position in the stand (Whitehead, 1978; Thompson, 1989).

It was expected that the distribution of branches in each individual tree would follow a similar power law because the branches are connected as a network. Tree branches, like other networks in nature, are considered to follow a similar power law with a fixed scaling exponent (e.g., 3/4) (Brown et al., 2002). It was found in this study that the scaling exponents of frequency distribution for both branch length and diameter changed with time in seven trees. Differences also existed among individual trees. The scaling exponents were not a fixed number. This was supported by the previous result (e.g., Chen & Burton, 2010). This study showed the dynamics of the scaling exponents within one growing season.

Entropy is used to reflect the information on branch length and diameter. The entropy was very consistent for branch length and diameter among trees. This means that these tree branches were very well organized networks. Also there were dynamics in entropy during tree growth. The decreased entropy in July might be related to quick growth during the summer time or some branches were broken down during measuring. The increased entropy in November indicated tree canopy is a self-organized network. However, at the end of the growing season of 2016, the entropy of neither branch length nor diameter reached the maximum entropy (MaxEnt). The MaxEnt could overestimate the information entropy in ecological systems (Chen et al., 2016). Previous studies found that MaxEnt is not correct when characterizing the size-density relationship and intraspecific distribution of body size (Xiao et al., 2015). It is possible that a tree's canopy may not reach the MaxEnt status in its branch distribution.

Slenderness could be used to characterize a branch's form. The change in slenderness reflected the relative growth rate of length to radius. In this study, the average slenderness for branches of seven trees was about 20, but some trees could reach a slenderness of 28 during their growth. There existed high variations within small branches which were less than 10 mm in diameter or less than 100 cm in length. These numbers may be unique to crape myrtle, because other tree species could reach a slenderness around 260 (Bertram, 1989). Dahle & Grabosky (2010) found that slenderness of *Acer platanoides* L. (Norway maple) peaked near 300 and appeared to shift at the branch length of 300 cm. These thresholds might mean that branches approach potential instability when they were transitioning from a primary role of flexible branch to a stiffer structural branch. Quantifying slenderness may be a useful tool in predicting branch form and instability.

For the scaling relationship between branch length and diameter, the results from this study showed that the scaling exponents were close to 0.67 for some individual trees (Tree 2, 5 and 6) in May, but the scaling exponents were close to 1.0 in July and November. This means that the branches of crape myrtle followed the geometric similarity model most of the time. McMahon & Kronauer (1976) studied several whole tree crowns and concluded that branch length scales as 0.67, as predicted by their elastic similarity model. The elastic similarity model simulates branch growth through the process of secondary growth, not primary growth (Niklas, 1994). The scaling exponents could change for individual trees at same location within a growing season. Although the scaling exponent has been assumed to be constant within an individual (Mäkelä, 1986) or even for different tree species (Enquist et al., 1999), it may vary to reflect the different stages in growth of branches (Bertram, 1989).

Allometric scaling was also related to the correlation between the diameters of 1st order branches and the number of branches at the 2nd order or next orders. The change in the relationship could affect energy investment in branch elongation. In this study the results indicated that the large branches of crape myrtle did not necessary have more branches at next lower orders. But for another species, Norway maple, a significant quadratic regression existed between the number of 2nd order and the 1st order branch length (Dahle & Grabosky, 2010). This indicates that when primary branch length slows, investment of photosynthetic product in elongation would likely turn towards the lateral branches.

In conclusion, after studying the allometric properties of branches in crape myrtle during one growing season, there were some general trends in dynamics (e.g., entropy and scaling exponents) but divergence also existed in allometric scaling relationships for each tree and among trees. Any fixed number in allometric scaling exponents may not reflect the real situation. The knowledge from this study may help to understand the dynamics of branch development in crape myrtles to form canopy in individual trees.

Acknowledgements

The author is thankful to Matthew Shaw, Lawson Quick, and Michael Brown for assisting in field work. This

study was supported by USDA National Institute of Food and Agriculture McIntire Stennis project (1008643).

References

Bertram, J. E. A. (1989). Size-dependent differential scaling in branches: the mechanics design of trees revisited. *Trees, 4*, 241-253. https://doi.org/10.1007/BF00225358

Brown, J. H., Gupta, V. K., Li, B. L., Milne, B. T., Restrepo, C., & West, G. B. (2002). The fractal nature of nature: power laws, ecological complexity and biodiversity. *Philosophical Transactions of the Royal Society of London B Biological Science, 357*, 619-626. https://doi.org/10.1098/rstb.2001.0993

Chen, X., & Burton, S. (2010). Power law relationships in the branches of loblolly pine, red maple and sugar maple trees. *Dendrobiology, 63*, 3-9.

Chen, X., Brockway, G. D., & Guo, Q. (2016). Entropy dynamics in cone production of logleaf pine forests in the southeastern United States. *Mathematical and Computational Forestry & Natural-Resource Sciences, 8*, 11-15.

Dahle, G. A., & Grabosky, J. C. (2010). Allometric patterns in Acer platanoides (Aceraceae) branches. *Trees, 24*, 321-326. https://doi.org/10.1007/s00468-009-0401-5

Enquist, B. J, West, G. B., Charnov, E. L., & Brown, J. H. (1999). Allometric scaling of production and life-history variation in vascular plants. *Nature*, 88, 907-911. https://doi.org/10. 1038/44819

Harte, J. (2011). *Maximum entropy and ecology: a theory of abundance, distribution, and energetics*. Oxford University Press, Oxford.

Jaynes, E. T. (1957). Information theory and statistical mechanics. *Physical Review, 106*, 620-630. https://doi.org/10.1103/PhysRev.106.620

King, D. A. (1986). Tree form, height growth, and susceptibility to wind damage in Acer saccharum. *Ecology, 67*, 980-990. https://doi.org/10.2307/1939821

Küppers, M. (1989). Ecological significance of above ground architectural patterns in woody plants: a question of cost-benefit relationships. *Trends in Ecology and Evolution, 4*, 375-379. https://doi.org/10.1016/0169-5347(89)90103-1

Mäkelä, A. (1986). Implications of the pipe model theory on dry matter partitioning and height growth in trees. *Journal of Theoretical Biology, 123*, 103-120. https://doi.org/10.1016/S0022-5193(86)80238-7

Mäkelä, A. (2002). Derivation of stem taper from the pipe theory in a carbon balance framework. *Tree Physiology, 22*, 891-905. https://doi.org/10.1093/treephys/22.13.891

Mandelbrot, B. B. (1978). The fractal geometry of trees and other natural phenomena. P. 235-249. *In*: Miles, R. E., J. Serra (eds). Geometrical probability and biological structures: Buffon's 200th anniversary. Springer, Berlin.

McMahon, T. A., & Kronauer, R. E. (1976). Tree structures: deducing the principle of mechanical design. *Journal of Theoretical Biology, 59*, 443-466. https://doi.org/10.1016/0022-5193(76)90182-X

Niklas, K. J. (1995). Size-dependent allometry of tree height, diameter and trunk-taper. *Annals of Botany, 75*, 217-227. https://doi.org/10.1006/anbo.1995.1015

Niklas, K. J., & Spatz, H. C. (2000). Wind-induced stresses in cherry trees: evidence against the hypothesis of constant stress levels. *Trees, 14*, 230-237. https://doi.org/10.1007/s004680050008

Nishimura, T. B. (2005). Tree characteristics related to stem breakage of *Picea glehnii* and *Abies sachalinensis*. *Forest Ecology and Management, 215*, 295-306. https://doi.org/10.1016/j.foreco.2005.05.018

Osunkoya, O. O., Omar-Ali, K., Amit, N., Dayan, J., Daud, D. S., & Sheng. T. K. (2007). Comparative height-crown allometry and mechanical design in 22 tree species of Kuala Belalong rainforest, Brunei, Borneo. *American Journal of Botany, 94*, 1951-1962. https://doi.org/10.3732/ajb.94.12.1951

Raulier, F., Ung, C-H., & Ouellet, D. (1996). Influence of social status on crown geometry and volume increment in regular and irregular black spruce stands. *Canadian Journal of Forest Research, 26*, 1742-1753. https://doi.org/10.1139/x26-198

Remphrey, W. R., & Davidson, C. G. (1992). Branch architecture and its relation to shoot-tip abortion in mature *Fraxinus pennsylvanica*. *Canadian Journal of Botany, 70*, 1147-1153. https://doi.org/10.1139/b92-142

Remphrey, W. R., & Powell, G. R. (1984). Crown architecture of *Larix laricina* saplings: quantitative analysis

and modelling of (nonsylleptic) order 1 branching in relation to development of the main stem. *Canadian Journal of Botany, 62*, 1904-1915. https://doi.org/10.1139/b84-260

Richter, J. P. (1970). *The notebooks of Leonardo da Vinci*. Dover Publications, Dover.

Shinozaki, K., Yoda, K., Hozumi, K., & Kira, T. (1964). A quantitative analysis of plant form. Pipe model theory. I. Basic analysis. *Japanese Journal of Ecology, 14*, 97-105.

Skatter, S., & Kucera, B. (2000). Tree breakage from torsional wind loading due to crown asymmetry. *Forest Ecology and Management, 135*, 97-103. https://doi.org/10.1016/S0378-1127(00)00301-7

Sperry, J. S., Meinzer, F. C., & McCulloh, K. A. (2008). Safety and efficiency conflicts in hydraulic architecture: scaling from tissues to trees. *Plant, Cell and Environment, 31*, 632-645. https://doi.org/10.1111/j.1365-3040.2007.01765.x

Takenaka, A. (2000). Responses to light microenvironment and correlative inhibition in the growth of shoots of tree seedlings under a forest canopy. *Tree Physiology, 20*, 987-991. https://doi.org/10.1093/treephys/20.14.987

Taugourdeau, O., Dauzat, J., Griffon, S., Sabatier, S., Caraglio, Y., & Barthe´le´my, D. (2012). Retrospective analysis of tree architecture in silver fir (*Abies alba* Mill.): ontogenetic trends and responses to environmental variability. *Annals of Forest Science, 69*, 713-721. https://doi.org/10.1007/s13595-012-0188-1

Thompson, D. C. (1989). The effect of stand structure and stand density on the leaf area - sapwood area relationship of lodge pole pine. *Canadian Journal of Forest Research, 19*, 392-396. https://doi.org/10.1139/x89-061

West, G. B., Brown, J. H., & Enquist, B. J. (1999). A general model for the structure and allometry of plant vascular systems. *Nature, 400*, 664-667. https://doi.org/10.1038/23251

White, E. P., Enquist, B. J., & Green, J. L. (2008). On estimating the exponent of power-law frequency distributions. *Ecology, 89*, 905-912. https://doi.org/10.1890/07-1288.1

Whitehead, D. (1978). The estimation of foliage area from sapwood basal area in Scots pine. *Forestry, 51*, 137-149. https://doi.org/10.1093/forestry/51.2.137

Xiao, X., McGlinn D. J., & White, E. P. (2015). A strong test of the maximum entropy theory of ecology. *American Naturalist, 185*, E70-E80. https://doi.org/10.1086/679576

Journal of Plant Studies; Vol. 6, No. 2; 2017
ISSN 1927-0461 E-ISSN 1927-047X
Published by Canadian Center of Science and Education

Establishment of Callus Induction and Cell Suspension Cultures of *Dendrathema Indicum* var. *Aromaticum* a Scented Chrysanthemum

Liyan Jin[1,*], Yang Yang[1,*], Wenjie Gao[1], Mingxue Gong[1], Jijia Wang[1], Neil O. Anderson[2] & Miao He[1,2]

[1]Department of Landscape Architecture of Northeast Forestry University, 26 Hexing Road, Harbin, Heilongjiang 150040, China

[2]Department of Horticulture, University of Minnesota, Saint Paul, MN 55108, USA

*Both authors contributed equally to this work.

Correspondence: Miao He, Department of Landscape Architecture of Northeast Forestry University, 26 Hexing Road, Harbin, Heilongjiang 150040, China.Tel: 1-361-364-9547. E-mail: hemiao_xu@126.com

Received: February 9, 2017 Accepted: March 18, 2017 Online Published: April 24, 2017

doi:10.5539/jps.v6n2p38 URL: https://doi.org/10.5539/jps.v6n2p38

Abstract

Dendranthema indicum var. *aromaticum* is an important aroma plant in genus *Dendrathema*, and the establishment of callus cultures and cell suspension cultures is the basement of further protoplast fusion studies, which make it possible to breed new fragrant chrysanthemum. In this study, the effects of different plant growth regulating substances in different concentrations on callus induction were investigated with stem segments, leaves, petioles as explants. The results showed that the optimal explants were lower stem segments according to the percentage of callus formation, callus hardness, growth potential and shoot differentiation. The optimal induction mediums were MS supplemented with 1.0 mg· l^{-1}2.4 D and 0.2 mg· l^{-1} 6-BA. The cell suspension culture system was established by using the subculture calli. The results showed that the suitable inoculum size was 2g and the suitable cell suspension culture medium was MS supplemented with 0.2 mg· l^{-1} 6-BA and 0.5 mg· l^{-1} 2,4-D. The time course of cell growth showed that the greatest cell fresh weight appeared on day 14 and the highest cell viability on day 3.

Keywords: scented *Chrysanthemum*, in vitro, explants, callus formation, cell culture

1. Introduction

1.1 Introduce the Problem

Chrysanthemum *(Dendrathema×grandiflora)*, one of the famous traditional flowers in China, is widely cultivated in the world. Flowers of Chrysanthemum with brightly colored flowers and varied flower types are not fragrant or with a slightly scent. Thus, the improvement of Chrysanthemum's aroma is an important topic in chrysanthemum breeding.

Dendranthema indicum var. *aromaticum* is an herbaceous perennial plant characterized by special scent, which is the important aroma resource in genus *Dendrathema* and found in Shennongjia, Hu Bei province, P. R. China (Liu, Jia, & Yang, 1983). Previous research has proved that *Dendranthema indicum* var. *aromaticum* was diploid (2n=2x=18) and *Dendrathema* × *grandiflora* was polypoild (2n=6x=54) (Zhu, Liu, & Dai, 2011) .As we know that it is difficult to cross breed if one species is diploid while the other is a higher ploidy level. In order to breed scented chrysanthemum, somatic hybridization will be applied. Somatic hybridization is to hybrid plants through the fusion of somatic protoplasts of two different plant species/varieties, with which some interspecific hybrids have been obtained in family *Compositae*, for example the hybrids between *Helianthus annuas* and *H. giganteus* (Henn, Wingender, & Schnabl, 1998; Krasnyanski, & Menczel, 1995), *Tanacetum vulgare* and *T. cinerariifolium* (Keskitalo, Angers, Earle, & Pehu,1999), *Dendrathema×grandiflorum* and *Artemsia sieversiana*(Lee, Paek, & Hwang, 1995),ect.

The objective of this project was to establish callus cultures and cell suspension cultures of *D. indicum* var. *aromaticum* for further protoplast fusion studies, which make it possible to breed new fragrant chrysanthemum.

2. Materials and Methods

2.1 Plant Material and Callus Induction

Seedlings of *D. indicum* var. *aromaticum* were obtained in 2008 from Shennongjia in the Hu Bei province, P. R. China and were maintained in the garden nursery, College of Landscape Architecture and Horticulture, Northeast Forestry University, Harbin, P. R. China. Shoots were surface sterilized first by washing under running tap water and laundry bleach for 10 min, then disinfected in 2% or 5% sodium hypochlorite for 10 min and rinsed with sterile distilled water 6-8 times. Surface sterilized shoots were trimmed, prior to inoculation on the basal medium under sterile conditions. The subcultures were done at regular intervals incubated at 25±2℃ with a 16-h photoperiod and illumination of 2000 lx. Basal nutrient medium contained MS(Murashige & Skoog,1962) salts and vitamins and sucrose (30 g· l^{-1}).Nutrient medium pH was adjusted to 5.8 prior to addition of 8 g· l^{-1} Agar and the autoclaved 121℃ for 20min.Fresh and healthy leaves(2×2mm from the central plate),stem segments(4mm in length) and petioles were obtained from in vitro grown plants, then transferred on MS basal medium supplemented with different concentrations of 2,4-D(0.0,0.5,1.0,1.5,2.0,2.5,3.0 mg· l^{-1}), BA(0.2 mg· l^{-1}), sucrose(30 g· l^{-1}) and agar(8 g· l^{-1}).The pH of medium was adjusted to 5.8±0.1.Each treatment combination consisted of three replications and maintained in the presence or absence of light.

2.2 Cell Suspension Cultures and Cell Growth Determination

Suspension cultures were established from friable calli. 1-4g fresh weight friable calli was transferred to 100 ml Erlenmeyer flasks containing 50 ml MS basal medium with BA 0.2 mg· l^{-1}, 2,4-D 0.5 mg· l^{-1}， 30 g· l^{-1} sugar in order to optimize the suitable inoculum size. The research of effect of exogenous plant growth regulators on cell suspension cultures were carried out by using 2 g fresh weight friable calli, the best inoculum size, with different concentrations of 2,4-D,6-BA and NAA, which was designed by orthogonal design L9 (3^3).All the cell suspension cultures were placed on a rotary shaker with a speed of 90 rpm at 25 ± 2℃ under a 16-h photoperiod and illumination of 1000 lx. The FWt was measured after 18 days of culture. Five flasks were used per treatment and each experiment was repeated third. Anovas and Duncan comparison tests for each evaluated factor were carried out using the SPSS 12.0 software.

3. Results and Discussion

3.1 Effect of 2, 4-D and the Types of Explants on Callus Induction

Different types of explants were placed on MS basal medium supplemented with different concentrations of 2,4-D and 0.2 mg· l^{-1} BA for 60 days of cultivation. The percentage of callus formation, growth potential, callus hardness and shoots per callus were evaluated according to the method of Fadi Chen (Chen, Jiang, & Guo, 2003).

Some related research indicated that 2, 4-D played a more important role in callus formation from leaf and stem explants compared to BA (Satyavani, Ramanathan, & Gurudeeban, 2011).But in this experiment, Calli were successfully generated in all treatments regardless of 2, 4-D concentration and different types of explants (Table 1).These results showed that leaf and stem explants were suitable for callus induction. Similar results were reported in callus induction of *Corydalis saxicola and Orthosiphon stamineus*, in which it were described that callus could be induced successfully from leaf, petiole, stem (Cheng, Yu, Hu, Chen, & Sun, 2006).

The callus hardness was classified into level 1 to level 5 according to the visual observation. The higher hardness level showed the callus was more hardness, which was bad to cell suspension culture. The callus potential growth was also classified into level 1 to level 4 according to the growth from slow to fast. The percentage of callus formation was the highest with the leaf as exlants (Table 1), but the callus was more hardness and the potential growth was lower. As for further cell suspensions, the friable calli were better than the compact calli. Thus we thought that lower stem segments were the best explants because the induced calli hardness was smaller and the growth potential was the biggest although the percentage of callus formation was not the highest. And the optimum medium was MS containing 0.2 mg· l^{-1}6-BA and 1.0 mg· l^{-1} 2,4-D.

3.2 Effects of Inoculum Size on Cell Suspension Cultures

Suspension cultures were initiated by transferring 1-4 g fresh friable calli into 50 ml MS medium in 100 ml flasks. The inoculum size had a positive effect on biomass. Cell fresh weight reached the lowest value of 1.71g at the inoculum size of 1g, and increased to the highest value of 5.88g at 4g. But the highest proliferation ratio and the best cell growth status were observed at the inoculum size of 2g（88.5）(Table 2), and its cell cluster was small round and well dispersed, cell suspension liquid was clear.

3.3 Effects of Exogenous Plant Growth Regulators on Cell Suspension Cultures

The effect of these plant growth regulators on cell suspension culture was presented in Table 3. There existed significant differences among all the treatments which were designed by orthogonal design L9 (3^3) (α=0.05).In case of Treatment 4 and 7 the cell fresh weights (Fwt) were significantly higher than other treatments, and cell suspension liquids were clear the cell cluster was small and high dispersion. Therefore, the most suitable cell suspension culture medium for cell growth in *D. indicum* var. *aromaticum* was MS+0.2 mg·l^{-1} 6-BA+0.5 mg·l^{-1} 2, 4-D.

3.4 Time Course of Cell Growth

The time course of cell growth has been studied by growing suspension cells in 100 ml flasks, containing 40ml liquid MS medium with 0.2 mg· l^{-1} 6-BA , 0.5 mg· l^{-1} 2,4-D and 30 g· l^{-1} sugar. As shown in Fig. 1, cell growth was slow during initial 6 d of cultivation. From day 6, biomass accumulated rapidly and reached the greatest value on day 14. Then a slow decrease of biomass was observed in the later stage of cultivation. These results showed that some cells which couldn't adapt to the change from solid to liquid medium and gradually went to death. After that, biomass increased rapidly and reached the highest value. Similar results were reported in *Cleistocalyx operculatus* (Zhou, Wang, & Xiao, 2007), *Dendrathema grandiflora* (Jiang, 2002), *Morus alba* (Li Yong et al., 2007) .Cell viability was measured by TTC method（Steponkus & Lanphear, 1967） using a Unic spectrophotometer, model UV-2102C, at 485 nm wavelength. The bigger OD value indicates the greater cell viability. The TTC test results showed cell viability increased in the initial 3 d followed by a gradual decrease. The growth patterns of cultures showed that cell viability was lower in its rapid growth, and higher in its slow growth stage, which was the same with *Xanthoceras sorbifolia* (Liu,2009)and *Taxus cuspidata*(Liu,2002).

In conclusion, the friable callus of *D. indicum* var. *aromaticum* could be efficiently introduced with lower stem segments as explants on MS medium supplemented with 1.0 mg· l^{-1}2.4 D and 0.2 mg· l^{-1} 6-BA. 2 g fresh weight friable calli were the best inoculum size. The most suitable cell suspension culture medium was MS+0.2 mg· l^{-1} 6-BA+0.5 mg· l^{-1} 2,4-D. The growth patterns of cell cultures showed S-curve and the greatest cell fresh weight appeared on day 14, the highest cell viability on day 3.

Table 1. Effect of 2,4-D and different types of explants on the callus induction

Treat-ment code	2,4-D	Explants' types	Percentage of Callus formation	Callus potential growth classification	callus hardiness classification	Shoots per callus
T1	0	leaves	100±0.00	0.80±0.18	5.00±0.00	0.90±0.00
T2	0	peridol	73.3±2.40	1.20±0.00	5.00±0.00	1.19±0.01
T3	0	Upper stem	100±0.00	1.00±0.14	5.00±0.00	1.62±0.02
T4	0	Lower stem	86.7±2.40	1.80±0.13	5.00±0.00	1.19±0.01
T5	0.5	leaves	100±0.00	1.80±0.16	3.50±0.11	1.70±0.12
T6	0.5	peridol	83.3±1.40	2.00±0.14	4.30±0.15	1.10±0.11
T7	0.5	Upper stem	76.7±2.40	1.80±0.28	3.20±0.10	1.30±0.01
T8	0.5	Lower stem	100±0.00	3.60±0.22	1.50±0.08	1.10±0.16
T9	1	leaves	100±0.00	2.20±0.15	4.00±0.10	0.80±0.11
T10	1	peridol	76.7±2.40	1.20±0.31	3.90±0.12	0.56±0.06
T11	1	Upper stem	70.0±3.30	2.60±0.11	2.10±0.10	0.26±0.01
T12	1	Lower stem	96.7±2.40	3.80±0.15	1.00±0.00	0.79±0.01
T13	1.5	leaves	100±0.00	1.60±0.21	4.00±0.14	0.32±0.08
T14	1.5	peridol	93.3±2.53	2.40±0.14	4.10±0.23	0.60±0.01
T15	1.5	Upper stem	63.3±2.33	1.80±0.14	3.10±0.11	0.12±0.01
T16	1.5	Lower stem	90±1.33	2.80±0.13	1.50±0.11	0.60±0.01
T17	2	leaves	96.7±2.40	2.20±0.23	3.50±0.15	0.42±0.02
T18	2	peridol	100±0.00	2.60±0.14	2.90±0.07	0.16±0.02
T19	2	Upper stem	83.3±2.33	2.80±0.18	2.90±0.21	0.00±0.00
T20	2	Lower stem	93.3±2.53	2.20±0.28	2.00±0.24	0.54±0.04
T21	2.5	leaves	100±0.00	2.80±0.18	3.50±0.11	0.30±0.01
T22	2.5	peridol	80±2.73	2.20±0.14	2.20±0.18	0.30±0.02
T23	2.5	Upper stem	73.3±4.40	2.20±0.13	1.80±0.22	0.30±0.01
T24	2.5	Lower stem	96.7±2.40	3.20±0.14	1.00±0.14	0.86±0.01
T25	3	leaves	100±0.07	2.00±0.07	3.50±0.07	0.80±0.07
T26	3	peridol	60±0.08	1.60±0.08	3.20±0.08	0.10±0.08
T27	3	Upper stem	100.0±0.00	1.00±0.00	3.80±0.00	0.00±0.00
T28	3	Lower stem	90±0.02	2.20±0.02	2.00±0.02	0.28±0.02

Table 2. Effect of inoculum size on cell growth in *Dendranthema indicum* var. *aromaticum* suspension cultures

Inoculum mass(g)	Cell fresh weight(g)	proliferation ratio	Cell Growth status
1	1.71±0.48	71.0 B	Good dispersion, cell cluster small and pale yellow, medium clear
2	3.77±0.53	88.5 A	Excellent dispersion, cell cluster small and pale yellow, clear
3	4.59±0.78	53.0 C	Bad dispersion, cell cluster big and dark yellow, a little turbidity
4	5.88±0.49	47.0 D	Bad dispersion, cell cluster big and dark yellow, turbidity

The suspension cultures were cultivated in MS medium containing 0.5 mg·l^{-1} 2,4-D and 0.2 mg·l^{-1} BA on a rotary shaker. Data are expressed as means e S.D. (n = 3).

Note: A~D is the variance analysis of LSD letter notation, α=0.01, All values are T statistical data after 18 d culture.

Table 3. Effects of exogenous plant growth regulators on cell suspension cultures in *Dendranthema indicum* var. *aromaticum*

Treatment Code	exogenous plant growth regulators (mg. l-1)			FWt (g)
	2,4-D	NAA	6-BA	
1	0.0	0.0	0.0	1.30±0.52 bc
2	0.0	0.2	0.2	1.33±0.32 bc
3	0.0	0.5	0.5	0.90±0.27 c
4	0.5	0.0	0.2	2.19±0.35 a
5	0.5	0.2	0.5	1.54±0.33 b
6	0.5	0.5	0.0	1.62±0.40 b
7	1.0	0.0	0.5	2.06±0.41 a
8	1.0	0.2	0.0	0.99±0.41 c
9	1.0	0.5	0.2	1.12±0.33 c

The suspension cultures were cultivated on a rotary shaker and collected on day 18 of cultivation. Data indicate means of three independent experiments (means e S.D.)

Note: a~c is the variance analysis of LSD letter notation, α=0.05, All values are T statistical data after 18 d culture.

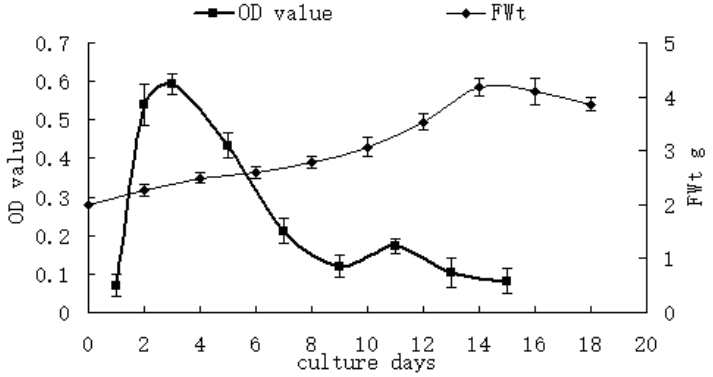

Figure 1. Time course of cell growth and viability in *D. indicum* var. *aromaticum* suspension culture

The suspension cells were grown in liquid MS medium containing 0.5 mg· l^{-1} 2,4-D and 0.2 mg· l^{-1} BA and incubated on a rotary shaker at (25±2)℃ under a 16-h photoperiod and illumination of 1000 lx. Data indicate means of three independent experiments (means e S.D.).

Abbreviations: MS, Murashige and Skoog medium; 6-BA, 6-Benzylaminopurine;2,4D,2,4-Diclorophenoxyacetic acid; 2,3,5-triphenyltetrazolium chloride. I am deeply grateful to Dr. Shunsuke Naruto for his invaluable guidance and advice.

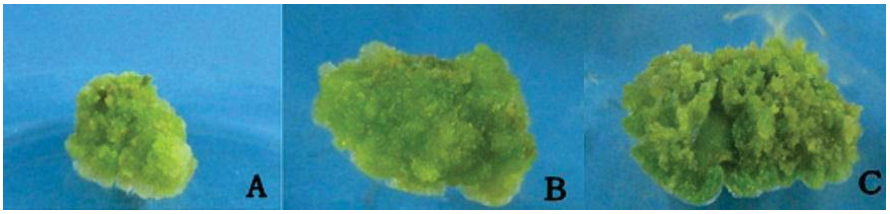

Figure 2. Different types of explants of *D. indicum* var. *aromaticum* on the callus induction

A.The callus induction of stem segments.B.The callus induction of leaves .C.The callus induction of petioles.

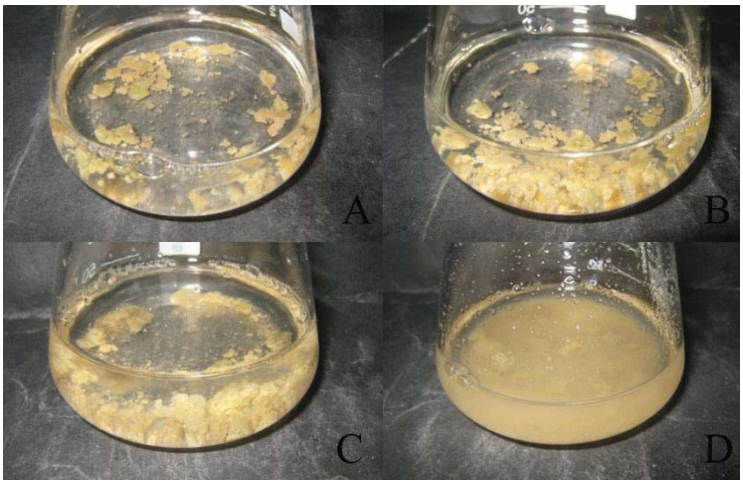

Figure 3. Cells suspension culture growth in different initial quantity of *Dendranthema indicum* var. *aromaticum*

A. The initial quantity is 1g.B. The initial quantity is 2g.C. The initial quantity is 3g.D. The initial quantity is 4g.

Acknowledgments

This research was supported by the National Natural Science Foundation of China (31400590). I am deeply grateful to my teacher for her invaluable guidance and advice.

References

Chen, F. D., Jiang J. F., & Guo, W. M. (2003). Study on irradiation breeding of suspension cell of Dendranthema morifolium with small inflorescence Ⅰ. Selection of genotype, explant and callus induction media. *Journal of Nanjing Agricultural University*, *4*, 006.
Retrieved from http://en.cnki.com.cn/Article_en/CJFDTOTAL-NJNY200304006.htm

Cheng, H., Yu, L. J., Hu, Q. Y., Chen, S. C., & Sun, Y. P. (2006). Establishment of callus and cell suspension cultures of Corydalis saxicola Bunting, a rare medicinal plant. *Zeitschrift für Naturforschung C*, *61*(3-4), 251-256. https://doi.org/10.1515/znc-2006-3-416

Henn, H. J., Wingender, R., & Schnabl, H. (1998). Regeneration of fertile interspecific hybrids from protoplast fusions between Helianthus annuus L. and wild Helianthus species. *Plant cell reports*, *18*(3), 220-224. https://dx.doi.org/10.1007/s002990050560

Jiang Jiafu. (2002).Studies on the performance of some traits of F1 generation, cell suspension culture and plant regeration of *Dendratehma grandiflora*.(Master's thesis, Nanjing Agricultural University). Retrieved from http://kns.cnki.net/KCMS/detail/detail.aspx?dbcode=CMFD&dbname=CMFD9904&filename=2002124433.nh&uid=WEEvREcwSlJHSldRa1FhdkJkcGkzcUJoU2ZEWFBSM1RMZHU2bGFheFJ0QT0=$9A4hF_YAuvQ5obgVAqNKPCYcEjKensW4ggI8Fm4gTkoUKaID8j8gFw!!&v=MzI1MjZLNkd0WFBySkViUElSOGVYMUx1eFlTN0RoMVQzcVRyV00xRnJDVVJMMmZaT2RvRnlEblVyL0lWMTI3SEw=

Keskitalo, M., Angers, P., Earle, E., & Pehu, E. (1999). Chemical and genetic characterization of calli derived from somatic hybridization between tansy (Tanacetum vulgare L.) and pyrethrum (Tanacetum cinerariifolium (Trevir.) Schultz-Bip.). *Theoretical and applied genetics*, *98*(8), 1335-1343. https://dx.doi.org/10.1007/s001220051200

Krasnyanski, S., & Menczel, L. (1995). Production of fertile somatic hybrid plants of sunflower and Helianthus giganteus L. by protoplast fusion. *Plant cell reports*, *14*(4), 232-235. https://dx.doi.org/ 10.1007/BF0023363

Lee, C. H., Paek, K. Y., & Hwang, J. K. (1995). Somatic hybridization between Dendranthema grandiflorum and Salpiglossis sinuata via protoplast fusion. *Korean Journal of Breeding (Korea Republic), 27*(3), 290-297. http://lib.rda.go.kr/newlib/adlib_en/index.html

Li Yong et al., (2007).Research on the growth regularity and physiological characteristics of Mulberry suspension cells. *Science of Sericulture, 33*(1), 91-94.
Retrieved from http://en.cnki.com.cn/Article_en/CJFDTOTAL-CYKE200701016.htm

Liu Hua. (2002). The relationship of the growth of *Taxus chinensis* cell in suspension culture to the viability and subsistence rate. *Journal of Biology, 18*(1), 19-20. Retrieved from http://en.cnki.com.cn/Article_en/CJFDTOTAL-SWXZ200201006.htm

Liu Lei. (2009).Establishment of suspension culture and isolation of protoplasts in *xanthoceras sorbifolia* Bunge. (Master's thesis, Agricultural university of Hebei, Baoding). Retrieved from http://kns.cnki.net/KCMS/detail/detail.aspx?dbcode=CMFD&dbname=CMFD2009&filename=2009132005.nh&v=MTEyMjZLN0hOSE1xcEViUElSOGVYMUx1eFlTN0RoMVQzcVRyV00xRnJDVVJMMmZaT2RvRkNua1ViM09WMTI3Rjc=

Liu, Q., Jia, W., & Yang, D. (1983). The investigation on geographical distribution, ecological habit and storage quantity on a new resource plant of Hubei, *Dendrathma indicum* (L.) Des Monl.Var.aromaticum. *Journal of Wuhan Botanical Research, 1*(2), 239-246. Retrieved from http://xueshu.baidu.com/s?wd=paperuri%3A%287d3a9ac53b232d4ab4bb3503a3101f2a%29&filter=sc_long_sign&tn=SE_xueshusource_2kduw22v&sc_vurl=http%3A%2F%2Fen.cnki.com.cn%2FArticle_en%2FCJFDTotal-WZXY198302014.htm&ie=utf-8&sc_us=8046499129164148898

Murashige, T., & Skoog, F. (1962). A revised medium for rapid growth and bio assays with tobacco tissue cultures. *Physiologia plantarum*, *15*(3), 473-497. https://dx.doi.org/10.1111/j.1399-3054.1962.tb08052

Satyavani, K., Ramanathan, T., & Gurudeeban, S. (2011). Effect of plant growth regulators on callus induction and plantlet regeneration of bitter apple (Citrullus colocynthis) from stem explant. *Asian Journal of Biotechnology*, *3*, 246-253. https://doi.org/10.3923/ajbkr.2011.246.253

Steponkus, P. L., & Lanphear, F. O. (1967). Refinement of the triphenyl tetrazolium chloride method of determining cold injury. *Plant Physiology*, *42*(10), 1423-1426. https://dx.doi.org/10.1104/pp.42.10.1423

Zhou, Y. B., Wang, R., & Xiao, D. G. (2007). Establishment of Cleistocalyx-operculatus' Suspension Cell Lines and Study on Its Vegetative Character on Suspension Culture. *Biotechnology*. Retrieved from http://en.cnki.com.cn/Article_en/CJFDTOTAL-SWJS200701023.htm

Zhu, M. L., Liu, Q. Q., & Dai, S. L. (2011). Karyotype analysis of 38 large-flowered chrysanthemum cultivars from China. *Chinese Bulletin of Botany, 46*(4), 447-455. https://doi.org/10.3724/SP.J.1259.2011.00447

Journal of Plant Studies; Vol. 6, No. 2; 2017
ISSN 1927-0461 E-ISSN 1927-047X
Published by Canadian Center of Science and Education

Genetic Stability and Disease Resistance Analysis of *Hrpzpsta* Gene in Transgenic Soybean Lines

Miao Yu[1], Peiwu Wang[1], Yang Song[1],Yong Qi Feng[1], Jing Qu[1] ,Jie Rong[1], Mo Zhang[1] & Zhuo Zhang[1]

[1]Center for Plant Biotechnology, Jilin Agricultural University, Changchun, Jilin, China

Correspondence: Peiwu Wang, Center for Plant Biotechnology, Jilin Agricultural University, Changchun, Jilin, China. Tel: 0431-8453-2908. E-mail: peiwuw@163.com

Received: February 19, 2017 Accepted: April 19, 2017 Online Published: May 29, 2017

doi:10.5539/jps.v6n2p45 URL: https://doi.org/10.5539/jps.v6n2p45

Abstract

This experiment was carried out to evaluate genetic stability and disease resistance in transformed soybean lines with *hrpZpsta* gene using PCR analysis, southern blotting, real-time quantitative PCR (qRT-PCR) and to analyze the resistance against *Phytophthora sojae* (*P. sojae*) and *Cercospora sojina* (*C. sojina*) after inoculation. The results obtained using PCR and southern blotting analytical methods showed that exogenous gene functional elements were stably inherited in transgenic soybean and *hrpZpsta* gene was successfully integrated into the soybean genome in a single copy. Results at high-generation (T_7, T_8) transgenic lines of *hrpZpsta* revealed that their relative expression of *hrpZpsta* gene was the highest in leaves followed by roots, and much lower in stems, flowers, and seeds. Activity change rates of peroxidase (POD), polyphenol oxidase (PPO) and phenylalanine ammonia lyase (PAL) showed that transgenic lines significantly enhanced receptor species. The resistance of transgenic strains T_7 and T_8 generations against *P. sojae* was significantly increased with artificial inoculation methods, and the resistance against *C. sojina* was increased from susceptibility to the level of resistance. Under natural conditions in the field, the response of T_8 transgenic lines to *C. sojina* reached disease resistance level. There were no significant differences in transgenic lines and recipient variety in maturing stage, leaf shape, flower color, plant height, 100-grain weight and quality content, and the two years average yield of plots increased to 11.59% and 8.19%, which significantly higher than recipient cultivar. The current results provide data support for the release of transgenic lines.

Keywords: disease resistance, *hrpZpsta* gene, genetic transformation, soybean

1. Introduction

Soybean (*Glycine max* L.) is a major food and oilseed crop worldwide and provides the largest source of vegetable oil and protein for humans and animals (Li, Zhang, Hao, Hua, Duan, Zhang, & Li, (2013). Its fungal disease is currently a major hurdle restricting the quality of soybean and causes damage to the crop's yield (Li, Luan, & Liu, 2015). However, the complex physiology of pathogenic bacteria makes it difficult to breed a resistant plant to break through the problem (Dorrance, Jia, & Abney, 2004; Kim, et al., 2013), and conventional breeding methods have limitations which make it difficult to fulfill the production needs (Molinar, 2012). Therefore, a combination of biotechnology and traditional breeding methods provides a new way to breed for disease resistant varieties and the renewal of germ plasm resources (Kamthan, Chaudhuri, Kamthan, & Datta, 2016).

Harpin protein is a class of nonspecific protein elicitors encoded by the *hrp* gene in gram-negative plant pathogenic bacteria which can: excite hypersensitive reaction (HR) in plants; make plants gain broad spectrum disease resistance (Alfano, & Collmer, 1997; Strobel, Ji, Goplan, Kuc, & He, 1996); can be induced by different signaling pathways to produce disease, insect and drought resistance and promote plant growth and other beneficial effects (He, Huang, Collmer, 1993; Pandey et al., 2005). Furthermore, it has important theoretical and practical values in the production of better application prospects. The gene encoding harpin protein was transferred into rapeseed (Ma et al., 2008), rice (Cheng & Xu, 2008), and wheat (Fu et al., 2014), all of which showed significant disease resistance. Studies have shown that harpin protein can induce resistance to 60 kinds of diseases in more than 40 kinds of crops. In addition, the physiological and biochemical mechanisms of resistance in harpin protein shows that it could induce the expression of POD, PPO, PAL and other protective enzymes in tomato, cucumber and eggplant, (Yuan & Meng, 2008), and as a consequence, induce plant defense

response and enhance plant resistance to diseases. In transgenic tobacco, hpa1Xoo can increase the POD, PPO, PAL and other defense enzymes, and enhance resistance to tobacco mosaic virus (Han & Chang, 2013).

The *hrpZpsta* gene derived from tobacco wildfire pathogen, is a broad-spectrum resistance gene which encodes the harpin protein and effectively stimulates the soybean plant to produce disease defense response so as to effectively improve its disease resistance and reduce yield loss caused by soybean diseases (Dorrance, Jia, & Abney, 2004; Wu, Zhang, Zhang, Gu, & Gao, 2017). Bioinformatics analysis showed that the gene and its encoded protein are not toxic for humans and animals. In this study, high-generation (T_7, T_8) transgenic lines of *hrpZpsta* were used to test the genetic stability of transformed *hrpZpsta* gene and the resistance of the transgenic lines was analyzed. In order to improve the ability of soybean to resist gray leaf spot and *phytophthora* root rot, it aims to reduce the disease to improve the yield of soybean.

2. Materials and Methods

2.1 Materials and Experimental Design

2.1.1 Plant Materials and Strain

Transformed *hrpZpsta* gene stable lines JL30-187 and JL30-80 at T_7 to T_8, receptor cultivar named JL30 were provided by the Plant Biotechnology Center, Jilin Agricultural University, (Changchun, China). *P. sojae* PmC-1 and *C. sojae* CSJ-1 were provided by the Jilin Academy of Agricultural Sciences, (changchun, China).

2.1.2 Test Design

Plant material were planted the randomized block design (three replications) was used in the field trial, used for genetic stability analysis and field surveys. The experimental site is Jilin Agricultural University transgenic crop test base (Changchun, China). It is located in 125.13 degrees east longitude, Latitude 43 degrees 53 minutes north, 236.8 meters above sea level, The annual average temperature of 4.8℃, frost-free period of 148 days, accumulated temperature of more than 10℃ is 2921.8℃, Sunshine 2300-3000 hours per square centimeter annual radiation 120-130 kcal, Annual rainfall of 567 mm, The precipitation in the four seasons is the percentage of the year: the spring (3-5) is 11.4%; the summer (6-8) is 69.5%; the autumn (9-11) is 17.0%, the winter (12-2) is 2%. April average temperature of 7.2℃, July average temperature of 26.1℃, September 8.4 ℃, is a continental monsoon climate.

2.2 Genetic Stability Analysis of Target Genes

Transgenic plants at T_7 to T_8 were detected by PCR, Soybean Fresh leaves genome were collected from each of the transformed plants at 60 days after planting and DNA was extracted according to the manufacturer's instruction of NuClean Plant Genomic DNA kit (CWBIO, Beijing, China). Specific primers were designed to target these three genes *hrpZpsta*, *badh* and *35s-hrpZpsta-NOS was* designed with Primer 5.0 soft ware, and two pairs primers named QhrpZpsta, QActin were designed using the Primer 5.0 software to amplify *hrpZpsta* and *TUB4*(reference gene) for real-time quantitative PCR, respectively(Table 1).

PCR amplification system was 2.5uL loading buffer, 2.5 uL $MgCl_2$, 0.5uLdNTP, 1uL forward primer, 1uL reverse, 1uLDNA and 0.3uL Taq, add DDH_2O to 25uL. *hrpZpsta* PCR reaction conditions were pre-denaturation at 94℃for 3 min, followed by 36 cycles of 94℃for 40s, 54℃for 40s, 72℃for 40s, and 72℃for 8 min. PCR conditions for the *badh* were pre-denaturation at 94℃for 3 minutes, followed by 40 cycles of 94℃for 50s, 54℃ for 50s, 72℃for 50s, and 72℃for 8 min. and *35s-hrpZpsta-NOS* genes were similar to those of *hrpZpsta* except that 56℃annealing temperatures were used.

Table1. Primer sequence of PCR and qRT-PCR

Primer name	Forward Primer sequence（from 5′ to 3′）	Reverse Primer sequence（3′ to 5′）
hrpZpsta	ATGCAGAGTCTCAGCTTAAC	TCACCATTGGAATTGCTGTTG
35S-hrpZpsta-NOS	TTCAGAAAGAATGCTAACCCACAG	TGCGGGACTCTAATCATAAAAACC
BADH	TGTCGATCCCTATACCTTC	TTAAGGAGACTTGTACCAC
QhrpZpsta	GACTTGATGACACAGGTG	ACCATTGGAATTGCTGTT
QTUB4	GGCGTCCACATTCATTGGA	CCGGTGTACCAATGCAAGAA

According to the experimental PCR results, from the genome extracted from T_7 to T_8 soybean leaves, the target gene and the marker probe were labeled according to DIG High Prime DNA Labeling and Detection Starter Kit (Roche, America). The genomic DNA was digested with restriction endonuclease for 20 hours. The recombinant

plasmid digest was separated on 0.8% agarose gel electrophoresis. The digest was then denatured to enable transfer onto a membrane for further analysis.

RNA was extracted from different tissues (roots, stems, leaves, flowers and seeds) of the plant at anthesis using RNAiso Plus kit (Takara), with three replicates. Using the above RNA as a template, reverse transcription into cDNA was made, and the specific primers were designed with primer 5.0 for the *hrpZpsta* gene sequence and soybean TUB4 (GeneBank No.EV263740) as shown in Table 1. The relative expression was analyzed using Mx3000P instrument (America), according to manufacturer's instructions for which each sample mRNA were detected three times. The relative quantitative calculation was performed by $2^{-\Delta CT}$ method. CDNA reverse transcription and real-time PCR analysis were performed according to the instructions of All-in-One TM First-strand cDNA Synthesis Kit (GeneCopoeia, beijing China) and All-in-One TM qPCR Mix (GeneCopoeia, beijing China).

2.3 Enzyme Activity Determination for Resistance against P. Sojae

In order to eliminate the effects of temperature and humidity on enzyme activity, two sets of parallel experiments were conducted, transgenic lines at T_7 generation and non-transgenic receptors were planted at pots, three strains were planted per barrel, each treated three timesa total. After the opposite leaf of soybean plant was completely grown, the hypocotyls were used to induce the test material. one group was inoculated and the other group was not. Leaves were taken at 0h, 24h, 48h, 72h, 96h and 120h after inoculation. Samples were frozen using liquid nitrogen and placed in -80 ℃ refrigerator for preservation.

Leaves picked at different times to weigh 0.2g, and 5 ml of sample extract (boric acid buffer pH 8.8, 5 mmol/L mercaptoethanol, 1 mmol/L EDTA and 5% glycerol) was added to make the homogenate at 6×104r/min, 4 ℃ and centrifuged for 20 min. The supernatant was extracted for enzyme solution and placed in 4 ℃refrigerator and then centrifuged again for 20 min. POD, PPO and PAL activities were determined as previously described (Cheng & Xu 2013; Xu & Chang, 2014; Zhang, Xu, Wu, & Chen, 2008). In order to eliminate the background enzyme activity of each strain, the change rate of enzyme activity was taken as the standard.

Change rate of enzyme activity % = (A1-A0 / A0) * 100

where A_1: vaccinated leaves activity.

A_0: unvaccinated leaves activity.

2.4 Disease Resistance Analysis against P. Sojae and C. Sojae

T_7 and T_8 soybeans were tested for *P. sojae* PmC-1, the pathogenic strain of *P. sojae*, by hypocotyl staining method after the soybean leaves were completely grown. After inoculation, keep the wound humidity, shed temperature control in 20-25 ℃, humidity maintained at 90% or more. Investigation and statistics of transgenic lines and control receptor varieties Vaccination rate of *Phytophthora* infestans at five days after inoculation. Resistance evaluation criteria were: resistant (R)- plant mortality less than 30 %; moderately resistant (MR)-mortality rate from 31 % to 69 %; susceptible (S)- plant mortality rate of 70 % or more.

In the flowering stage of soybean to the early flowering stage of inoculation, the foliar leaching method was used to test the inoculation test of T_7 transgenic lines and acceptor varieties。After the inoculation, the humidity was 80% -100%, the control temperature was about 25-27℃, and the disease was investigated after 15 days. The incidence and incidence of the whole soybean were counted. To evaluate the resistance to gray leaf spot at field natural environment, soybean plants at the T8generation at flowering stages were Investigation, using the diagonal 5 points sampling, each investigation 100 cases. Soybean resistance to gray spot disease identification of disease levels, the use of 1-9 ratio assessment, 1 represents no disease spots, 9 on behalf of the leaves there are many lesion area of more than 50%. Specific resistance evaluation criteria are: immune (IM), the disease index was 0; high resistance (HR), disease index of 2 and below; disease resistance (R), disease index was 2.1~15.0; moderately resistant (MR), disease index was 15.1~40.0; moderately susceptible (MS), disease index was 40.1~60; susceptible (S), disease index was 60.1~80; highly susceptible (HS), disease index of 80 or more.

2.5 Analysis of Agronomic Traits

During anthesis, the phenotypic characters of the plant material at T_7 to T_8 were investigated. After maturation, 10 plants were randomly selected from each plot to investigate the agronomic traits of yield, including growth period, leaf shape, color, coat color, plant height，node，100-see weight，branches, Pods，seed weight，plot yield. NIRS DS2500 (Denmark) was used to analyze the quality of plant material at T_8 generation. The yield of the plot was measured and the data were statistically analyzed by MS Exceland DPS data processing system.

3. Results and Analysis

3.1 Genetic Stability Analysis of Target Genes

The results of PCR detection of the target gene are shown in Fig. 1a. Target gene *hrpZpsta, 35S-hrpZpsta-NOS* expression full-length sequence screening marker, and gene *BADH* were detected in the T_7 and T_8 generation in transgenic soybean lines. The effect of exogenous inserts of different generations in transgenic soybeans was genetically stable.

The results of Southern blot analysis of *hrpZpsta* gene are shown in Fig. 1b. Hybridization bands were detected in T_7 and T_8 transgenic soybean lines, while the receptor was not detected in the control sample. The target gene *hrpZpsta* was integrated at different sites into the recipient genome in a single copy, andwas stably inherited in the transgenic lines.

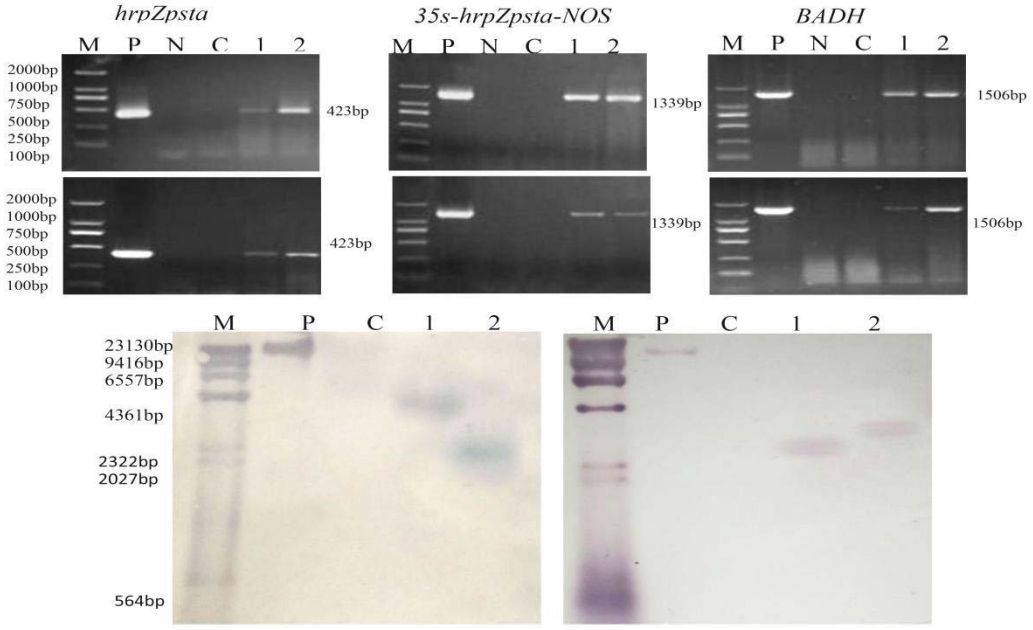

Figure 1. Genetic stability analysis of target genes

Note: (a): PCR analysis of T7 and T8 positive transgenic lines using *hrpZpsta*, 35s-*hrpZpsta*-NOS, and badh primer, respectively. (Note: M= DL2000 DNA marker, P= Positive control, N= Negative control, C= CK Jilin30, 1= Transformed Line JL30-187, 2= Transformed Line JL30-80). (b): Southern blot analysis of T7 and T8 transgenic plants (M=Southern DNA marker, P=Positive control, C= CKJilin30, 1-2= transgenic soybean plants).

The results showed that the target gene *hrpZpsta* was expressed in the roots, stems, leaves, flowers and grains of soybean (Fig. 1). The relative expression level of *hrpZpsta* gene in T7 generation transgenic soybean lines was the highest while the relative expression average of JL30-187 and JL30-80 were 8.477 and 6.971, respectively. In the roots, the average relative expression of JL30-187 and JL30-80 were 4.903 and 5.816, respectively. The expression levels of JL30-187 in stems, flowers and grains were lower at 1.423, 1.467 and 0.756, respectively, while the average expression levels were 0.686, 0.757 and 0.683, respectively for JL30-80. The relative expression level of *hrpZpsta* gene in T8 generation transgenic soybean lines was the highest with a relative expression average of 9.237 in JL30-187 and of 6.67 for JL30-80. In the roots, the average relative expression of JL30-187 and JL30-80 were 5.495 and 4.754, respectively. The expression levels in stems, flowers and grains were low. The results showed that the expression level of the target gene in different tissues was different. The gene of *hrpZpsta* and the transgenic materials could be stably expressed in different generations.

3.2 Enzyme Activity Determination against P. Sojae

The changes in enzyme activities of the transgenic line JL30-187 and receptor cultivar JL30 after inoculation with *P. sojae* are shown in Fig. 2. The change rates of POD, PPO and PAL activities in the leaves of the transgenic line showed no significant changes ($P < 0.01$) after 0 h and 120 h inoculation. However, 24 h inoculation resulted in a change rate in POD activity in the transgenic line, being181.39 % higher than in the recipient cultivar. After 48h inoculation, the rate of change in POD and PAL activities in the transgenic lines for the receptor species increased by 273.95 % and 464.99 %, respectively. After 72h inoculation, POD, PPO and

PAL activities in the leaves (transgenic lines) of receptor species increased to 156.52 %, 127.91 % and 106.99 %, respectively. The activity change rate in POD, PPO and PAL in transgenic lines increased to 163.76 %, 60.58 % and 27.51 %, respectively compared with the recipient cultivars after 96 h inoculation. The results showed that the activity of disease-resistant enzymes increased in the transgenic lines, which could be one of the causes of the resistance of the transgenic plants to infection by pathogenic fungi.

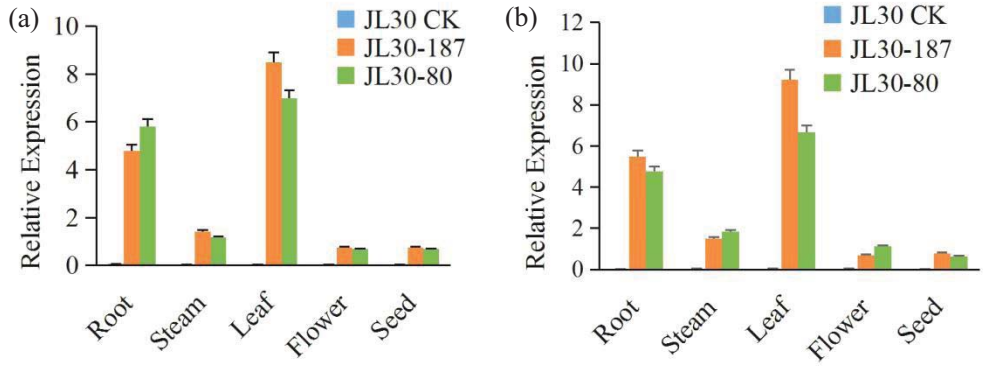

Figure 2. Analysis of target gene expression stability

Note: (a): T7 generation expression of *hrpZpsta* gene in different parts of plants. (b): T8 generation expression of *hrpZpsta* gene in different parts of plants.

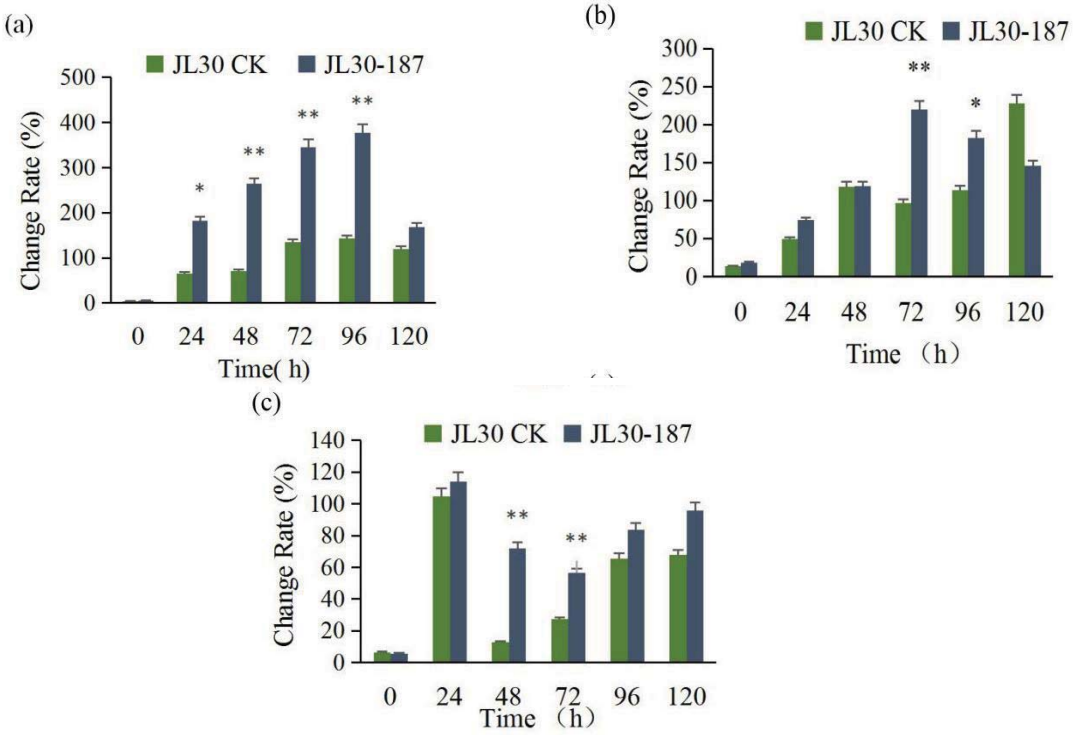

Figure 3. Changes in enzyme activity of leaves after inoculation with *P. sojae*

(a): POD activity change rate. (b): PPO activity change rate. (c): PAL activity change rate. * Indicates that the difference in treatment level was significant at 0.05 level ($p < 0.05$). ** Indicates that the difference in treatment level was significant at 0.01 level ($p < 0.01$).

3.3 Disease Resistance Analysis of P. Sojae and C. Sojina

Identification vaccination of *P. sojae* results are shown in Table 2 and Fig. 3. During the continuous 2-year comprehensive evaluation, JL30-187 and JL30-80 inoculation mortality rates were 6.94 % and 19.44 %, respectively, as all showed R. In the recipient variety, JL 30 inoculation mortality rate was 50.00 %, the performance of the MR. The resistance of the transgenic lines to *Phytophthora* root rot was evaluated from the MR to the R level.

Table 2. Identification vaccination *P. sojae*

Generation	Cultivar and lines	Detected No.	Alive No.	Death No.	Death rate (%)	Resistance reaction
	JL30 CK	18	9	9	50	MR
T_7	JL30-187	18	17	1	5.55	R
	JL30-80	18	15	3	16.67	R
	JL30 CK	36	15	15	50	MR
T_8	JL30-187	36	33	3	8.33	R
	JL30-80	36	28	8	22.22	R

Identification results of *C. sojina* are shown in Table 3. From Fig. 4, it can be seen that the lesion is obvious on the leaves of the recipient plant and the spots on the leaves of transgenic progeny are relatively few. Artificial inoculation results showed that T_7 transgenic lines JL30-187 and JL30-80 disease index was 16.94 % of which 16.42 % showed MR; receptor species JL30 disease index was 61.59 %, expressed as S. The resistance of the transgenic lines to gray leaf spot was improved from S to MR.

The results of field investigation showed that the disease index of JL30-187 was 13.93 % and JL30-80 was 14.60%, which indicated R. The disease index of JL30 was 60.29 % thus indicating S. Resistance evaluation of transgenic lines to gray leaf spot was improved from S to R level.

Table 3. Identification of Resistance to *C.sojina*

Method	Cultivar and line	Death rate (%)	Disease index	Resistance evaluation
Artificial vaccination (T7)	JL30-CK	96.67	61.59±2.35 A	S
	JL30-187	78.33	16.42±1.35 AB	MR
	JL30-80	76.67	17.33±2.15 AB	MR
Field investigation (T8)	JL30-CK	90.67	60.29±2.45 A	S
	JL30-187	49.67	13.93±1.65 AB	R
	JL30-80	50.33	14.60±3.25 AB	R

Note:The data in the table are mean ± standard deviation, Different lowercase letters indicate that the difference in treatment level is significant ($p < 0.01$).

3.4 Investigation of Agronomic Traits

The results of agronomic traits at T_7 and T_8 are shown in Table 4. The growth period of the transgenic lines were 132 days with the sharp leaves, gray hairs, white flowers and podding habits sub-limited and yellow-hued indicative of no significant differences from the recipient cultivar. Pod numbers and total grain weight were significantly different from those of recipients ($p < 0.5$). The yield of JL30-187 and JL30-80 increased 9.47% and 4.54%, respectively, compared to the control plot in 2015, and the yield of the plot increased by 13.46% and 11.83% in 2016.

2016 seed quality test results are shown in Table 5. Seed protein content of JL30-187 and JL30-80 were reduced by 3.59 % and 0.52 %, respectively, compared with JL30 and fat content decreased by 2.08 % and 3.45 %. There were no significant differences in the contents of amino acids and fatty acids between transgenic lines and recipient cultivar.

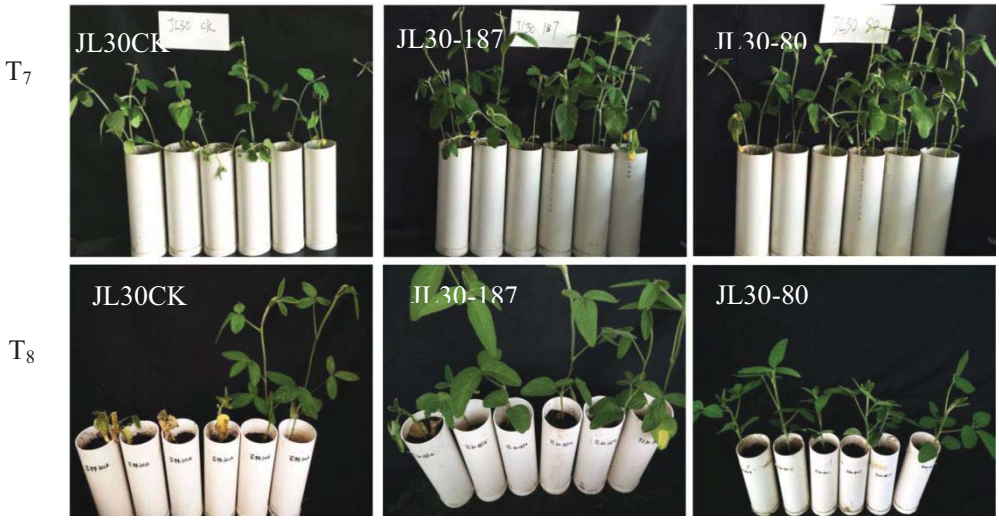

Figure 4. Identification of resistance against *P. Sojae*

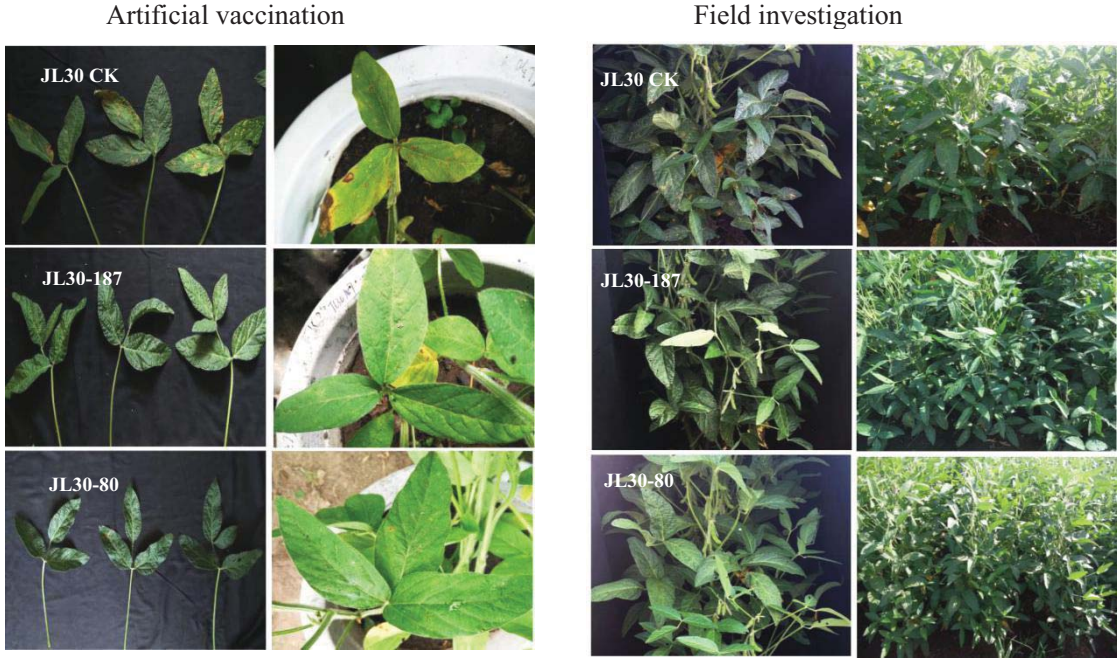

Figure 5. Identification of Resistance to *C.sojina*

Table 4. Investigation on Field Phenotypic Traits of transgenic lines

generation	Material	Plant height	Node	100-seed weight	Branches	Pods	Seed weight	Yield (m^2)	Increasing rate（%）
	JL30 CK	98.37±0.85a	17.6±0.08a	17.21±0.15a	1.90±0.21a	62.37±5.37a	29.35±2.61a	0.404±0.24a	
T_7	JL30-187	101.67±0.12a	17.67±0.12a	17.31±0.35a	2.23±0.40a	69.10±2.84a	32.71±0.98a	0.475±0.37a	9.71
	JL30-80	101.30±0.57a	17.87±0.05a	17.57±0.17a	2.5±0.08a	64.77±1.61a	31.13±0.98a	0.408±0.19a	4.54
	JL30 CK	89.57±0.26a	16.37±0.32a	19.36±0.05a	0.37±0.05a	29.7±1.65a	11.77±0.13a	0.362±0.63a	
T_8	JL30-187	92.03±0.37a	16.63±0.05a	19.31±0.06a	0.50±0.08a	40.60±1.13b	16.84±0.17b	0.418±0.56b	13.46
	JL30-80	93.10±0.45a	16.67±0.12a	19.84±0.03a	0.53±0.05a	37.90±2.11b	17.31±1.40b	0.412±0.49b	11.83

Note: The data in the table are mean ± standard deviation, Different lowercase letters indicate that the difference in treatment level is significant ($p < 0.05$).

Table 5. Seed quality analysis of T_8 transgenic lines

Quality / Cultivar	Protein	Fat	CYS	ARG	MET	PHE	C160	C180	C181	C182	C183
JL30 CK	40.08±0.31	21.13±0.33	0.53±0.00	3.01±0.05	0.45±0.00	2.08±0.02	9.34±0.11	3.25±0.13	12.63±0.33	62.21±0.27	4.33±0.21
JL30-187	38.64±0.72	20.69±0.11	0.52±0.00	2.88±0.08	0.42±0.03	2.05±0.03	9.18±0.13	3.35±0.21	12.86±0.79	61.60±0.53	4.36±0.27
JL30-80	39.87±0.40	20.4±0.16	0.53±0.00	2.97±0.02	0.44±0.01	2.09±0.00	9.04±0.11	3.28±0.11	12.32±0.51	62.39±0.21	4.10±0.16

Note: The data in the table are mean ± standard deviation.

4. Results and Discussion

The preliminary work of this experiment proved that T_1-T_6 generations of transgenic lines of the target gene can be stable (Zhang & Qu2011; Yin, Wang, Zhang, & Ma, 2013; Gu, Liu, & Wang, 2015). This study analyzes the genetic stability of target genes in T7, T8 transgenic lines; whether the presence of the primary PCR, the number of copies verified by Southern blotting or the expression of the transcriptional level detected by qRT-PCR confirmed that the transformed *hrpZpsta* gene was stably inherited and expressed in the recipient cultivar.

In recent years, a number of genetically modified soybean germ plasm have been obtained by genetic engineering. Zhou et al (2014) transferred *GmAKT2* gene into Williams82 to obtain transgenic material resistant to soybean mosaic virus disease. Fan et al (2012; 2015) cloned resistance genes SDR1 and Glym4l from anti-*Phytophthora sojae* variety Suinong 10, and transferred them into the susceptible cultivar Dongnong 50 to significantly increased its *Phytophthora* root rot capacity. Zhang, (2011) transferred *BnERF104* gene into Dongnong 50 and obtained significantly reduced lesion area of genetically modified soybean material. In this study, *hrpZpsta* gene was a broad-spectrum disease resistance gene, and its progenies were significantly improved in resistance to *Phytophthora* root rot and soybean gray leaf spot under indoor artificial inoculation conditions. The natural disease incidence of gray leaf spot disease in the field showed that the resistant ability of the transgenic lines reached the R level, which further proved the general resistance of the *hrpZpsta* gene.

Plant disease severity and disease resistance and plant defense enzyme activity changes are closely related (Qin, Sun, Zhao, Zhao, & Zhao,.2014; Liu et al., 2011). The results showed that the activities of POD, PPO and PAL in the transgenic lines increased rapidly after inoculation with *P. sojae.* The activity level was significantly higher than non-transgenic varieties, but the activity change rates of PAL, PPO and POD in the transgenic line was not significantly higher than in the untransformed variety which indicated that transformed *hrpZpsta* gene soybean had the ability to respond quickly to pathogen infection. This is consistent with reports of other plants on enzyme activity (Shi et al., 2014; Lei et al., 2010).

The results showed that there were no significant changes in the growth period, leaf shape, coat color, flower color, podding habit, hilum color, protein content and fat content of the transgenic lines.However, the number of pods per plant and plot yield were higher than that of the receptor control which may be associated with the insertion of the disease-resistance *hrpZpsta* gene as it reduces the risk of pathogens. Similar results have also been reported on other transgenic crops (Zhao, Zhu, Cai, Bai, & Ji, 2012; Guo, Zhu, Li, Bai, & Cai, 2008).

5. Conclusion

Molecular biology test, disease resistance analysis and agronomic traits of transgenic high-generation lines showed that transformed *hrpZpsta* gene has stable inheritance, and this significantly enhanced soybean root rot and gray leaf spot resistance. The main agronomic traits of the transgenic lines were not significantly different from recipient variety, but the number of pods per plant and plot yield were significantly higher than in the recipient variety. High-generation transgenic soybean lines showing resistance to *Phytophthora* root rot and *C. sojina* were obtained, which provides data support and theoretical basis for environmental release of transgenic lines.

Acknowledgments

We thank the Jilin Academy of Agricultural Sciences for providing the pathogenic bacteria of PmC-1 and Cjs-1 and the Jilin Agricultural University Professor Gao Jie for providing the *hrpZpsta* gene. This research was funded by Grants from the National Science and Technology Major Project (2016ZX08004004-003).

References

Alfano, J. R., & Collmer, A. (1997). The type Ⅲ (Hrp) secretion pathway of plant pathogenic bacteria:Trafficking harpins, Avr proteins, and death. *Journal of Bacteriology, 179*(18), 5655-5662. https://doi.org/10.1128/jb.179.18.5655-5662.1997

Chen, L., Zhang, S., Qu, S., Long, J., Yin, Q., Qian, J., Sun, F., & Zhang, S. (2008). A selected fragment of HpaGXooc, a harpin protein from Xanthomonas oryzae pv. oryzicola, affects disease reduction and grain yield of rice in extensive grower plantings. *Phytopathology, 98*, 792-802. https://doi.org/10.1094/PHYTO-98-7-0792

Cheng, P., & Xu, P. F. (2013). The activity of wild soybean after inoculation of Phytophthora root rot fungus peroxidase (POD). *Soybean Science, 02*, 197-201.

Dong, H., Peng, J., Bao, Z., Meng, X., Bonasera, J. M., Chen, G., & Beer, S. V. (2004).Downstream divergence of the ethylene signaling pathway for harpin-stimulated Arabidopsis growth and insect defense. *Plant Physiol, 136*, 3628-3638. https://doi.org/10.1104/pp.104.048900

Dorrance, A. E., Jia, H., & Abney, T., S. (2004). Evaluation of soybean differentials for their interaction with Phytophthora sojae. *Plant Health Prog*. https://doi.org/10.1094/PHP-2004-0309-01-RS

Fan, S. J. (2012). Cloning and Functional Analysis of SDR1 Gene Related to Phytophthora Root Rot Resistance in Soybean. *Chinese Journal of Agricultural Science, 45*(11), 2139-2146.

Fan, S., Jiang, L., Wu, J., Dong, L., Cheng, Q., Xu, P., & Zhang, S. (2015). A Novel Pathogenesis-Related Class 10 Protein Gly m 4l, Increases Resistance upon Phytophthora sojae Infection in Soybean (Glycine max [L.] Merr.). *PLoS One, 10*(10). https://doi.org/10.1371/journal.pone.0140364

Fu, M., Xu, M., Zhou, T., Wang, D., Tian, S., Han, L., ... Zhang, C. (2014). Transgenic expression of a functional fragment of harpin protein Hpa1 in wheat induces the phloem-based defence against English grain aphid. *J Exp Bot, 65*(6), 1439-53. https://doi.org/ 10.1093/jxb/ert488

Gu, X. N., Liu, Z., K., & Wang, P., W. (2015). Study on the realationship between the hrpZpsta resistance gene expression in transgenic soybean and resistance to gary leaf spot disease. Atlantis Press, International Coference on Applied Science an Engineering Innovation (ASEI 2015, China), 1195-1203.

Guo, Y. S., Zhu, Y. M., Li, J., Bai, X., & Cai, H. (2008). Study and Analysis on Main Agronomic Characters of Transgenic Bifurcated Antifungal Genes. *Journal of Northeast Agricultural University, 01*, 10-12.

Han, Y. Y., & Chang Y. W. (2013). The Defense Enzyme Activity in Transgenic Truncated hpa1_(Xoo) Gene Tobacco. *Anhui Agricultural Sciences, 41*(22), 9197-9199.

He, S. Y., Huang, H. C., & Collmer, A. (1993). Pseudomonas syringae pv. Syringae harpinPss:A protein that is secreted via the Hrp pathway and elicits thehypersensitive response in plants. *Cell, 73*, 1255-1266. https://doi.org/10.1016/0092-8674(93)90354-S

Kamthan, A., Chaudhuri, A., Kamthan, M., & Datta, A. (2016). Genetically modified (GM) crops: milestones and newadvances in crop improvement. *Theor Appl Genet, 129*(9), 1639-55. https://doi.org/10.1007/s00122-016-2747-6.

Kim, H., Newell, A. D., Cota-Sieckmeyer, R. G., Rupe, J. C., Fakhoury, A. M., & Bluhm, B. H. (2013) Mating-type distribution andgenetic diversity of Cercospora sojina populations on soybean from Arkansas: evidence for potential sexual reproduction. *Phytopathology, 103*, 1045-1051. https://doi.org/10.1094/PHYTO-09-12-0229-R

Lei, J. R., Wang, D. M., Li, J. P., Huang, L. P., & Li, X. R. (2010). Analysis on the Defense Enzyme Activity in Transgenic Cotton Transferring SNC1 Gene Inoculated with Fusarium oxysporum f. sp. Disinfectant. *Acta Agriculturae Boreali-Sinica, 24*, 9-13.

Li, J. B., & Luan, Y. S., & Liu, Z. (2015). SpWRKY1 mediates resistance to Phytophthora infestans and tolerance to salt and drought stress by modulating reactive oxygen species homeostasis and expression ofdefense related genes in tomato. *Plant Cell Tissue and Organ Culture, 123*, 67-81. https://doi.org/10.1007/s11240-015-0815-2

Li, Y., Zhang, J., Hao, L., Hua, J., Duan, L., Zhang, M., & Li, Z. (2013). Expression of an Arabidopsis molybdenum cofactor Sulphura-segene in soybean enhances drought tolerance and increases yield under field conditions. *Plant Biotechnology Journal, 11*, 747-758. https://doi.org/ 10.111/pbi.12066

Liu, H., Zhou, X., Dong, N., Liu, X., Zhang, H., & Zhang, Z. (2011). Expression of a wheat MYB gene in transgenic tobacco enhances resistance to Ralstonia solanacearum, and to drought and salt stresses. *Funct Integr Genomics, 11*, 431. https://doi.org/ 10.1007/s10142-011-0228-1

Ma, L. L., Huo R., Gao W., He D., Shao M., & Wang Q.(2008). Transgenic Rape with hrf2 Gene Encoding Harpinxooc Resistant to Sclerotinia sclerotinorium. *Agricultural Sciences in China, 04*, 455-461.

https://doi.org/10.1016/S1671-2927(08)60089-9

Molinar, R. (2012).Traditional plant breeding vs. genetic engineering a primer.IOP Publishing Western Farm Press Web. http://westernfarmpress.com/management.

Pandey, A. K., Ger, M. J., Huang, H. E., Yip, M. K., Zeng, J., & Feng, T. Y. (2005). Expression of the Hypersensitive Response-assisting Protein in Arabidopsis Results in Harpin-dependent Hypersensitive Cell Death in Response to Erwinia carotovora. *Plant Mol Biol., 59*, 771-80. https://doi.org/10.1007/s11103-005-1002-3

Qin, L. J., Sun, H. R., Zhao, D., Zhao, J. H., & Zhao, D. G. (2014). Overexpression of NrCN gene improved the TMV resistance in Nicotiana tabacum L. *Journal of Plant Physiology, 04*, 439-446.

Shi, W., Hao, L., Li, J., Liu, D., Huo, X., & Li, H. (2014). The Gossypium hirsutum WRKY gene GhWRKY39-1promotes pathogen infection defense responses and mediates salt stress tolerance in transgenic Nicotiana benthamiana. *Plant Cell Rep, 33*, 483. https://doi.org/ 10.1007/s00299-013-1548-5

Strobel, N. E., Ji, C., Goplan, S., Kuc, J. A., & He, S. Y. (1996). Induction of systemic acquired resistance in cucumber by Pseudomonas syringae pv. Syringae 61 HrpZPss protein. *The Plant Journal, 9*(4), 431-439.

Wu, H., Zhang, Y., Zhang, H., Gu, Q., & Gao, X. (2017). Identification of functional regions of the HrpZPsg protein from Pseudomonas savastanoi pv. glycinea that induce disease resistance and enhance growth in plants. *Eur J Plant Pathol, 147*, 55. https://doi.org/10.1007/s10658-016-0979-6

Xu, P. F., & Chang J. L. (2012). Polyphenol oxidase (PPO) activity of wild soybean inoculated with Phytophthora sojae. *Soybean Science, 01*, 99-102. https://doi.org/ 10.1007/s10681-016-1749-4

Yin, J. Q., Wang, P. W., Zhang, Z., & Ma, J. (2013). Study on the relationship between the hrpZpsta resistance gene expression in transgenic soybean and resistance to gray leaf spot disease. *Soybean Science, 02*, 238-241.

Yuan, R. L., & Meng, X. L. (2008). Effect of HrpZ Excitation on Activities of Defense-related Enzymes in Several plants. *Journal of Anhui Agricultural Sciences, 36*(32), 13951-13953

Zhang, S. Zh., Xu, P. F., Wu, J., & Chen, W. (2008). Change of Phenylalanine Ammonia-lyase (PAL) Activities among Different Resistance Soybean Varieties Treated with Pathotoxin from *Phytophthora* sojae. *Crops, 01*, 47-420.

Zhang, B. (2011). Study on Resistance Identification of Cercospora sojina and Resistance to Gray Leaf Spot in BnERF104 Soybean. Chinese Society of Plant Pathology.Chinese Society of Plant Pathology 2011 Annual Conference Proceedings. *Chinese Plant Pathology Society, 1*.

Zhang, Y. Y., & Qu, J. (2011). Studies on transgenic soybean with hrpZpsta resistance. *Journal of Northwest A & F University (Natural Science Edition), 09*, 86-92

Zhao, Y., Zhu, Y. M., Cai, H., Bai, X., & Ji, W. (2012). Research and Analysis on the Agronomic Traits of Salt Tolerant OsCDPK7 and OsMAPK4 Rice. *Crop, 05*, 22-25.

Zhou, L., He, H. Liu, R., Han, Q., Shou, H., & Liu, B. (2014). Overexpression of GmAKT2 potassium channel enhances resistance to soybean mosaic virus. *BMC Plant Biol, 14*(154), 1-11. https://doi.org/10.1186/1471-2229-14-154

Journal of Plant Studies; Vol. 6, No. 2; 2017
ISSN 1927-0461 E-ISSN 1927-047X
Published by Canadian Center of Science and Education

Stress, Strain-Rate Analysis of Sub-Surface Driveway Plants

Peter R. Greene[1] & Virginia A. Greene[2]

[1]B.G.K.T. Consulting Ltd. Bioengineering, Huntington, 11743, New York, USA

[2]VGA, Architect, PC, Chicago, IL 60604-2001, USA

Correspondence: Peter R. Greene, B.G.K.T. Consulting Ltd. Bioengineering, Huntington, New York. Tel: 1-631-935-5666. E-mail: prgreeneBGKT@gmail.com

Received: May 9, 2016 Accepted: May 1, 2017 Online Published: June 25, 2017

doi:10.5539/jps.v6n2p55 URL: https://doi.org/10.5539/jps.v6n2p55

Abstract

Sub-surface driveway plants are strong enough to penetrate a macadam surface of thickness 7 – 9 cm. The mechanics of how the *Taraxacum officinale* accomplishes this feat remain a mystery. Using the Maxwell model for pavement yielding over time, data are presented which may shed some light on this phenomenon. The post-buckling behavior of the plant stalk is quantified. Euler bending and buckling theory enables calculation of the cellular stress field, compared to turgor pressure, indicating impending cell buckling. Post-buckling plastic strain of the plant stem is 19%. At the cell wall, the stress concentration factor is 3-times greater than the applied external field, so the cell's *internal turgor pressure* is overwhelmed by imposed external stress. An Impulse Integral is developed for the surface whereby the product of applied FORCE times TIME is CONSTANT, in order to produce a given amount of surface deflection. *Taraxacum officinale* stems and leaf stalks are strong enough, in buckling mode, to lift and push apart the fractured macadam crater through which they erupt, but not strong enough to initially crack the surface. The purpose of this work is to determine the mechanisms underlying this unusual plant survival phenomenon, backed by quantified data.

Keywords: bending-buckling, Young's modulus, stress-strain, cell turgor, plant mechanics, mechanosensing, viscoelasticity, enhanced growth rates, *Taraxacum officinale*

1. Introduction

This paper deals with the interesting topic of how *Taraxacum officinale* plants manage to grow through apparently impenetrable materials such as asphalt-macadam, Figure 1. Commercial products from this plant include latex, and various pharmaceuticals (Kristo et al., 2003). Studying plant biomechanical properties, it is possible to make some important conclusions about plant and perhaps animal "mechanosensing" at the cellular level, based on the imposed external *uni-axial stress field* caused by buckling and bending the flower and leaf stems, compared to the cell's *turgor pressure* (Baskin & Jensen 2013; Dumais 2013). The fact that a plant can push through a solid surface suggests impressive biomechanical capabilities worthy of study.

1.1 Literature Review

Niklas & Paolillo (1998) report measurements of *Taraxacum* stems under tension, comparable to the compressive experiments reported here. Cao et al. (2015) report that collagen materials grow in response to an increase in hydrostatic pressure. Niklas et al. (2009) discuss the mechanical bending moment of various types of tree leaves, relevant to the "robust" stress-enhanced leaf stems reported here. Ennos et al. (1993; 2003) measure the mechanical properties of stems from sedge and sunflowers. Lintilhac (2014) reviews cell growth response to mechanical stress. Greene & Greene (2015, 2016) report measurements of plant mechanics cracking a macadam surface. They observe that the surface is visco-elastically bent upwards into a dome, then the partially cured macadam cracks, usually into 8 pie-shaped segments, over a circular area approximately 3-inches (7 - 9 cm) in diameter. Subsequently the developing *Taraxacum* stems and leaf stalks lift and push aside the 8 segments. It is likely the *Taraxacum* tap root is responsible for this initial penetration, constantly pushing upwards, visco-elastically bending the surface upwards, and in some cases cracking the asphalt-macadam. Roots can exert a pressure ahead of the tip, as great as the *cell turgor pressure* (25 to 80 p.s.i.). De Langre (2012) investigates plant response to wind loads. Silverberg et al. (2012) present experimental and theoretical results on root buckling in plants. Latz et al. (2008) and Kutschera & Niklas (2013) report cell "mechanosensing" in response to external stresses.

2. Materials & Methods

2.1 Bending, Buckling, Post-buckling

The hypothesis is that a slow and steady vertical force will cause bending, yielding, and cracking of the macadam surface over a time scale of 6 months. Thus, experiments presented here are divided into two parts – those on the plants, and those on the driveway surface. The *Taraxacum* buckling and bending procedures for flower stems and leaf stalks are described in Greene & Greene (2015). Experimental results for stem and leaf buckling are shown in Figure 2. The inset schematic in Figure 2 shows buckling of a column of length L with axial force F. The "post-buckling" phase of plant stems is shown in Figure 7, 8. Buckling and bending experiments on the *Taraxacum* and *Hypochaeris* are done *in vitro*.

2.2 Asphalt-macadam Deflection Experiments

The experiments on the driveway material measure the force and integrated pressure required to break the 3-inch thick (7-9 cm) macadam. This is calculated from 2 vertical deflection experiments, Figure 3, during the month of October 2014, 6 months after the driveway dandelions first appeared in April 2014.

2.3 Exp. 1

The load-deflection test is performed on the 8 cm thick partially cured macadam surface, 1 year after the macadam is steam rolled into place in compression, Oct. 2014. In order to determine its properties, a 200 lbf (880 N.) weight is arranged to push downward over a 4 sq. in. area (25 cm^2) measuring 2" x 2" (5 cm x 5 cm) which subsequently results in a 1" (2.5 cm) plastic depression downward, as shown in Fig. 3. This deflection occurs slowly and steadily over 30 days. The imposed vertical surface pressure is 50 p.s.i. (350 kPa). In engineering terms, this is a normalized *plastic strain-rate* **ε'/σ = (1/σ) [dε / dt] = 8% / yr / psi.** *Exp. 2* - A second similar load-deflection creep rate test is performed, using much greater weights over a larger surface. A 2,000 lbf weight (8,800 N) is loaded over a 5" x 5" (13 cm x 13 cm) area of 25 sq. in. (170 cm^2) resulting in a 1/2-inch depression (1.3 cm) in the surface during the ensuing 7 days. This amounts to a normal surface pressure of 80 p.s.i. (560 kPa). The *plastic strain-rate* is given by the normalized equation **ε'/σ = (1/σ)** x **[dε / dt] = 9% / yr / psi**. From these measurements, the plastic strain-rate *constituitive relation* for partially cured macadam results*:*

$$\varepsilon\,(t) = dz/d0 = -\,8.5\%\ [\text{ per yr. per p.s.i. }] \times \sigma\ [\text{p.s.i.}] \times t\ [\text{yr}] / (\ d0 / 3\text{"}\ )^{3} \qquad \text{Eq. 1}$$

For a surface of thickness **d0 [in.]** , the vertical deflection **z (t)** over time is given by:

$$z(t)\ [\text{in.}] = -\,8.5\% \times d0\ [\text{in.}] \times \sigma\ [\text{ p.s.i. }] \times t\ [\text{yr}] / (\ d0 / 3\text{"}\ )^{3} \qquad \text{Eq. 2}$$

2.4 Thickness Variations

The difference between a 2.5" and 3.5" (6 to 9 cm) surface (this degree of variability one locale to the next is typical for a 3" (8 cm) paving) is given by the dimensionless term **(do/3")^3** in Eq. 2, showing that the expected deflection can vary by a factor of 0.58 to 1.59 compared to the deflection of a standard 3" (8 cm) driveway surface. Thus, 1/2 inch (1.3 cm) one way or another can make a +/- 50% difference in the surface strain-rate. *It is important to quantify the surface properties because these are a direct indication of the forces generated by the sub-surface plants.*

3. Results

3.1 Taraxacum and Hypochaeris Plants

As shown in Figure1 below, buckling and bending measurements on the flower stalk and leaf stems reveal that a typical 8-leaved 2-stem dandelion plant can vertically lift a total of 3 lbf. (1.4 Kg). A more robust plant, the *Hypochaeris,* also fractures the surface, with 3 flower stems, capable of lifting overhead a remarkable total of 18 lbf. (8.2 Kg). The displaced 3-inch diameter (7-8 cm) area of macadam weighs approximately 2 to 3 newtons (0.7 to 1.0 lbf) so either plant is strong enough to lift and push aside the macadam segments, but neither is strong enough to visco-elastically bend and then crack the surface in the first place. Only the plant's tap root, essentially a wooden cylinder measuring 1/2-inch to 5/8-inch in diameter (1-2 cm), 3" to 4" long (8-10 cm), might puncture the surface. Each year, the tap root survives the Winter, then during the Spring, the perennial dandelion stalks and stems return, radiating from the top of the tap root surface, branching out of the upper 20%-30% of the tap root cylinder.

3.2 Thermal Cure Rate

In May of 2014, 21 dandelion plants are observed to penetrate a 3" (8 cm) macadam surface, Figure 1. At this point in time, the surface is 6-months old. Colleagues in Germany and the U.K. (countries with colder average temperatures) report observing similar sub-surface phenomena, for several different types of plants. Figure 1 below shows the *Taraxacum officinale* plant, having just penetrated the macadam surface, with the characteristic 8-segment volcano-like crater created by the plant, and the plant's "robust" (un-serrated) vertical leaves.

Figure 1. The plant is strong enough to penetrated a 3-inch (6-8 cm) thickness of macadam. A +2.00 diopt. "portrait lens" is used to photograph the "robust" *Taraxacum officinale* plant at a distance of 16-inches.

3.3 Stem Buckling Load

Experimental results for stem buckling (diamond symbols) are shown in Figure 2 below. The inset schematic in Figure 2 shows buckling of a column of length L with axial force F. Buckling and bending experiments on the *Taraxacum* and *Hypochaeris* are done *in vitro*. Theoretical buckling results (App. I) from the *Taraxacum* are shown in Figure 2 below (solid line). Measured values of stress allow calculation of the matrix force field surrounding cells in the plant tube wall, due to bending and buckling deflection at the inner and outer periphery of the flower and leaf stalks.

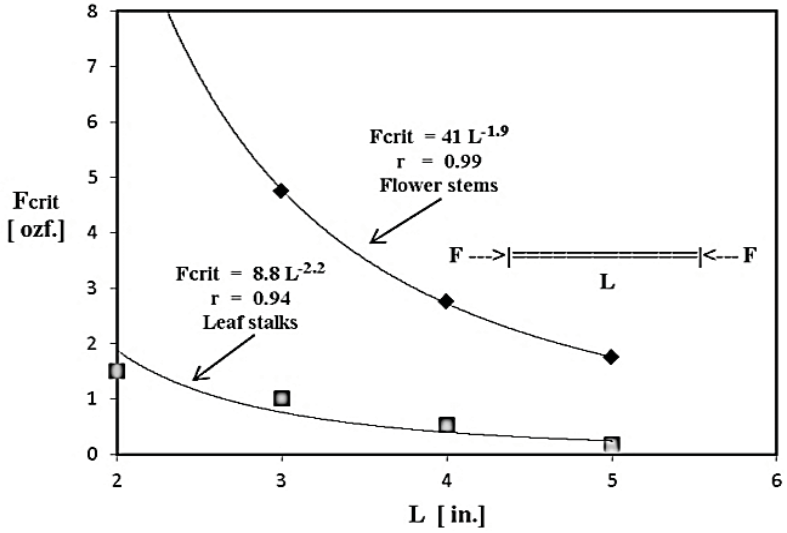

Figure 2. Stem buckling and leaf buckling data, confirming the Euler buckling exponent as -1.95, compared with -1.96, using the logarithm technique. Theory predicts the exponent should be -2.0. Inset shows buckling load F applied to a column of length L

3.4 Leaf Buckling Load

Figure 2 above shows *Taraxacum* leaf buckling data (square symbols). Niklas et al. (2009) discuss the mechanical bending moment of various types of tree leaves. Theory predicts the exponent should be -2.0 for both the flower stalks and the leaf stems. -1.95 to -2.23 exponents are observed experimentally here.

3.5 Experimental Strain-rate

Figure 3 below shows a 5 cm x 5 cm (2-inch by 2-inch) crater or miniature pothole, 2.5 cm (1-inch) deep is formed during the month of October 2014, resulting from a 880 N. (200 lbf) load applied over a 30-day period. At this point in time, the macadam surface has been in place for approximately 1 year. The surface was observed slowly deflecting downward at a constant rate over an interval of 4 weeks.

Figure 3. A 5 cm x 5 cm (2-inch by 2-inch) crater or miniature pothole, 2.5 cm (1-inch) deep is formed during the month of October 2014, resulting from a 880 N. (200 lbf) load applied over a 30-day period

3.6 Maxwell Strain-rate model

The 2-element viscoelastic Maxwell model used to describe the strain-rate response of partially cured macadam is shown in Figure 4 below. Using this model, only 1-parameter is needed to describe the surface strain-rate, the dashpot viscosity coefficient, with units of [% strain / yr / p.s.i.]

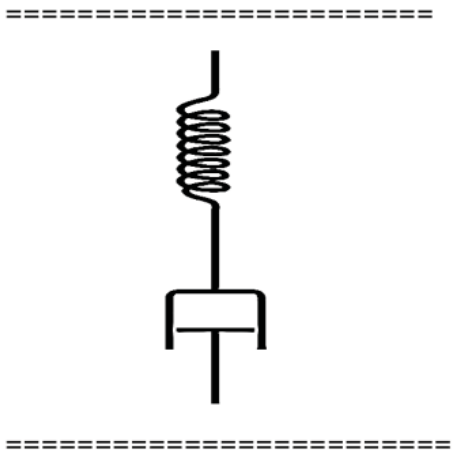

Figure 4. The 2-element viscoelastic Maxwell model is used to describe the strain-rate response of partially-cured macadam. 1-parameter describes the surface strain-rate, the dashpot viscosity coefficient [%/yr/p.s.i.]

3.7 Plant Young's Modulus

The *Hypochaeris radicata* (*catsear)*, a wild dandelion plant with *much* stronger flower stalks, essentially 3/16" (5 mm) diameter balsa wood dowels, easily manages to penetrate the 8 cm thick macadam surface, capable of

lifting 17-18 lbf. (70-80 N) *in vitro*. The original plants *in situ* are capable of greater forces *in vivo*. Buckling and bending experiments on the *Hypochaeris* stems *in vitro* determine Young's modulus at E = 1600 to 1700 MPa respectively in compression, compared with 3 to 14 MPa for the *Taraxacum* tube wall. The Euler equations for buckling and bending of tubes and rods are evaluated (Appendix I). The *Taraxacum* compression values measured for the stems are within a factor of 3 of those reported by Niklas & Paolillo (1998) for inflated *Taraxacum* flower stems in tension.

3.8 Cellular Transmural Pressure

Figure 5 below is a schematic of transmural pressures encountered by a cell in a uni-axial stress field. The transverse radial strain arises from the Poisson effect, where v ~ 0.5 for incompressible materials, v ~ 0.3 for wood.

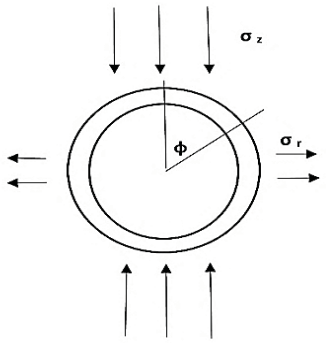

Figure 5. Schematic of transmural stresses encountered by a cell in a 2D uni-axial stress field. Transverse radial stress-strain arises from the Poisson effect. Stress concentration factor is 3.0 at $\phi = 90^0$.

3.9 Stress and Pressure Distribution

Figure 6 below is a polar plot of compressive stress around the cell periphery, showing a maximum of 3x amplification at the equator, and a minimum of -1x at the poles. The stress field is caused by far-field anisotropic forces arising from buckling and bending of the plant stem. The local hydrostatic pressure increase is an average of the 3 principle stresses, causing the cell *transmural pressure* to reverse sign over some regions of the cell surface. The extent this influences various *ion fluxes* across the cell membrane is yet to be determined. Cao et al. (2015) report that collagen materials grow in response to an increase in hydrostatic pressure. The +3x stress concentration factor greatly increases the possibility that the cell's turgor pressure will be overwhelmed by the external +1x external uni-axial stress field.

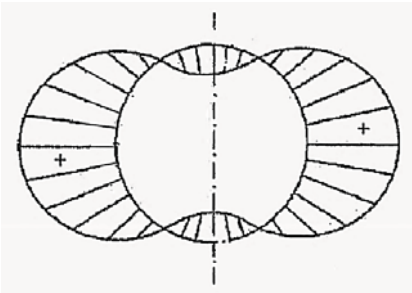

Figure 6. Polar plot of compressive stress around the cell periphery, showing a maximum stress concentration factor of +3x at the equator, and a minimum of -1x at the poles. Stress field is caused by far-field anisotropic forces arising from buckling and bending of the plant stem, Figure 5. Local hydrostatic pressure increase is an average of the principle stresses, causing the cell's transmural pressure to reverse in some geographical areas.

3.10 Stalk Buckling

Figure 7 below shows the characteristic S-shaped post-buckling configuration of the *Taraxacum* flower stalk after penetrating the surface, indicating the stalk was buckled under axial load during growth while penetrating the macadam.

Figure 7. S-shaped "post-buckling" configuration of the *Taraxacum* flower stalk after clearing the surface indicates the stalk buckled, under axial load during growth, while pushing aside the macadam. This second-order buckling configuration is 4-times stronger than the first-order mode

3.11 Stem Post-buckling

Once buckled, the stem remains in the sigmoidal configuration, after the overhead load is removed. Post-buckling plastic strain is estimated at 19%, Figure 7 above, based on radius of curvature and tube outer diameter (Greene, 1985). The plant cells are embedded in a cellulose matrix, so that when plastic failure of the stem occurs, at the inner radius, the cells are compressed, considerably more than 19%, according to their relative volume fraction in the matrix. By comparison metals and polymers yield plastically at 4% to 10% axial strain.

3.12 Enhanced Growth Rates

Figure 8 below shows that during Year II, May of 2015, the *Taraxacum* returns to last year's craters, considerably more prolific. Figure 8 shows a 15 to 16 stem plant, stemming from last year's tap root at this site, which produced only a 2 stem plant in 2014. Another plant produces 8-9 stems from a tap root which last year had only 3 flowers.

Figure 8. The *Taraxacum* regrows from last year's craters. Here, a 15 to 16 stalk plant is observed, stemming from last year's tap root at this site, which produced a 2 stem plant the year before. Inset shows wide un-serrated "robust" leaves of the *Taraxacum* plant in background

3.14 Crater Vent Segments

Experimentally, these driveway plants crack a partially cured surface in 0.1 to 0.3 yr., when the plate is bent upwards by just 1/3 of its thickness. During the period Nov.-Dec. 2014, after the first frost, the plants die and wither. Subsequently, the 8 pie-shaped segments of the volcano-like crater fold downward, partially closing the vent. These 8 segments are closed further by winter snow loading.

3.15 Robust Plant Development

During the 2nd year, puncturing the surface is mechanically easier for the plant, because the surface was pre-cracked the year before. Like human weight-lifters, it seems that plants "bulk-up" in response to stress, as shown in Figs. 1, 4, and 8. *In particular, the original serrated leaves instead develop a stronger full-leaved configuration under stress, without serrations, Figure 1 and 8.*

4. Discussion

4.1 Cell Mechanics

The phenomenon of "mechanosensing", whereby cells and fibers grow preferentially in response to stress, is discussed by Borau et al. (2014), Coutand et al. (2010), and Reilly & Engler (2010). In order to meet the weight-lifting challenge posed by the surface, the leaves and stems appear to strengthen their tube walls, to meet the demands of the situation, increasing stem diameter and wall thickness, possibly increasing cell turgidity pressure, perhaps increasing the cell reproduction, (Pickett-Heaps & Klein, 1998; Iddles, 2003).

4.2 Light and Temperature Cues

Buried under the macadam, the plants have no light-cues from above, only temperature-cues, so the plant may be deceived, (because it is warmer under the macadam due to absorbed radiant energy from sunlight and the heat capacity of the surface) that Spring is arriving in February or March, instead of April. This factor gives the plant extra growth time, necessary to visco-elastically buckle the driveway upwards, ultimately cracking the surface.

4.3 Stress Concentration Factor

At the cell wall, the compressive stress due to the external field is magnified 3-times, i.e. there is a "stress concentration factor" of 3.0. In practical terms, this means that the measured axial compressive stress in the celluslose matrix of 23 p.s.i. (at maximum buckling load) is augmented to 70 p.s.i. at the cell wall, comparable to the 40 – 80 p.s.i. internal cellular turgor pressure reported by Schopfer (2006) typical for plant cells. Dumais (2013) discusses the effect of such stress fields on cell deformation. Baskin & Jensen (2013) report the effects of anisotropic stress (i.e. uni-directional stress) on cell growth in stems.

4.4 Stem Buckling

It is likely that *macroscopic stem-buckling*, as shown in Fig. 4, is simultaneously a direct consequence of *microscopic cell buckling*, or even cell rupture. Measurements and calculations presented here indicate that the external *uni-axial stress field*, imposed during the post-buckling phase, is sufficient to overwhelm the cell's internal turgor pressure, reversing the cell membrane *transmural pressure*, causing impending ***cellular buckling***. The post-buckling stem configuration indicates that irreversible compression has done damage to the plant tube wall. The post-buckling plastic strain is estimated at 19%, an average value throughout the cellulose matrix, probably much greater locally at the cellular level, after compensating for matrix stiffness effects, (Kutschera & Niklas, 2013).

4.5 Mechanosensing

The physical stress, an *anisotropic* (one dimensional) stress field, imposed on the tube wall is significant. The annular area of a 6.4 mm O.D. (outside diam.) stalk, with I.D. = 4.8 mm (inside diam.) supports the axial load. At a maximum buckling load of 2.2 N. for the shortest columns measured, this amounts to a wall stress of $\boldsymbol{s}$ = 163 kPa, (23 p.s.i.), approximately 1.5 atmospheres, resulting in $\boldsymbol{e}$ = 5.8% compressive strain. Comparably, Arnoldi et al. (2000), report *cell turgor pressure* in the same range, 85 to 150 k Pa, (15 to 20 p.s.i.) measured in bacteria cells.

4.6 Plant-cell Turgor

Internal cell pressure (turgor) for plants is generally higher, in the range 300 – 600 k Pa (40 to 80 p.s.i.), Schopfer (2006). This remarkable plant wall stress level, caused by the overhead loading, is unusual. Internal stress at peak buckling load is calculated as $\boldsymbol{s}$ > 1.4 M Pa, *more than 10 atmospheres (Hypochaeris).* Compressive wall stress can be greater than the *cell turgor pressure*, typically 100 to 200 kPa (15 to 30 p.s.i.) for animal cells; Schopfer (2006) reports 300 – 600 kPa (40 to 80 p.s.i.) for peas; Kutschera & Niklas (2013) report

500 kPa (70 p.s.i.) for sunflowers. This level of stress will compress the plant cells longitudinally, Figure 5, 6.

4.7 Cell Compression

According to our measurements, the *axial tube-wall stresses* caused by bending and flexing during buckling are comparable to *cell turgor pressure.* This is particularly important, after compensating for the 3-fold *stress concentration factor* at the cell wall. In other words, the environment can, on occasion, "put the squeeze" on the cells, causing the *cell transmural pressure* to *reverse sign regionally* over the surface of the cell, as shown in Figure 6, overwhelming the cell walls with external compressive stress greater than their turgor pressure. Dumais (2013) discusses the effect of such stress fields on cell deformation. Baskin & Jensen (2013) report the effects of anisotropic stress (i.e. uni-directional) on cell growth in stems.

4.8 Transmural Pressure

Local *hydrostatic pressure*, external to the cell, is the average of the 3 orthogonal stresses. Cao et al. (2015) measure collagen materials growing in response to an increase in hydrostatic pressure. Linilhac (2014) discusses the mechanics of cell growth and mechanosensing. The extent to which the local reversal of transmural-pressure influences differential *ion flux*es across the cell membrane is fundamentally important.

4.9 Driveway Surface Mechanics

Most plants, even the remarkably strong *Hypochaeris* (Greene, 2016), simply cannot, on their own, produce enough vertical force to crack the 3-inch surface, so other factors must come into play during the winter months. Reasonable possibilities include *frost heave* of the surface, *thermal expansion* during the day from sunlight, thermal cycling (*freezing and thawing*) during the 24-hour day, and *impending vertical buckling* of the surface, due to accumulated in-plane compressive stress. Highways are known to buckle as a result of thermal expansion effects, so this phenomenon has some precedence in the literature.

5. Conclusions

5.1 Maximum Vertical Plant Force

Some driveway plants, during the growth phase, are remarkably strong, and this effect, coupled with the weaker than expected viscoelastic properties of a partially cured surface, may partially explain the ability of some plants to penetrate the driveway surfacing. Initial measurements suggested only a matter of grams (or ounces) as the vertical force generated by the plant, but experimental measurements presented here show the plants are capable of kilograms (or several pounds) of vertical force. Likewise, during steam rolling, the vertical surface forces were a matter of tons (or metric tons), but as measured here, just several kilograms (or tens of pounds) are required to fracture the surface, including the sustained time element.

5.1 Required Rupture Force

According to measurements reported here, there is *a factor of 10x discrepancy,* i.e. a shortfall, between what the plant is capable of, and what is required to rupture the surface. Thus, it is important to quantify, to calibrate, the surface, because it is basically the "force-platform" against which the sub-surface plant pushes.

5.2 Maxwell Strain-rate (Creep-rate)

The prime result of the *Maxwell dashpot model,* Figure 4, and mechanical measurements of the driveway surface, is that 3 lbf. (1.4 Kg) of vertical force (available from one *Taraxacum* plant, as measured) over a time scale of 10-months will produce the same plastic deflection as 30 lbf. (14 Kg) (available from 3 *Hypochaeris* stems as measured) exerted over 1-month, approximately 1/8-inch (3 mm). On a timescale of 24 hours, for this particular surface, approximately 1,000 lbf (454 Kg) is required to deflect the surface by 1/8-inch.

5.3 Force-time Impulse Integral

From these measurements, a useful "Impulse Integral" results, namely, that the product of applied FORCE times TIME is CONSTANT, (other things being equal, temperature, surface properties, etc.) in order to produce a given amount of surface deflection. McMahon & Greene (1979) measure elastic surface stiffness, the compliance element in Figure 4, of various surfaces (athletic and otherwise), reporting values in the range 50,000 lbf/ft. to 100,000 lbf/ft. (670 kN/m to 1,400 kN/m). The Maxwell strain-rate constant and creep hardening rates will vary according to regional temperature throughout the year. The sustained time element may be the key to explaining this unique plant survival phenomenon.

How exactly the Taraxacum plant manages to accomplish its escape, buried under 3" (8 cm) of macadam, is still unknown. So, the secrets of these remarkably strong plants remain a mystery for the time being.

References

Arnoldi, M., Fritz, M., Bäuerlein, E., Radmacher, M., Sackmann, E., & Boulbitch, A. (2000). Bacterial turgor pressure can be measured by atomic force microscopy. *Phys Rev E. Jul, 62*(1 Pt B), 1034-44. https://doi.org/10.1103/PhysRevE.62.1034

Baskin, T. I., & Jensen, O. E. (2013). On the role of stress anisotropy in the growth of stems. *J Exp Bot., 64*(15), 4697-707. https://doi.org/10.1093/jxb/ert176

Beisman, H., Wilhelmi, H., Bailieres, H., Spatz, H. C., Bogenrieder, A., & Speck, T. (2000). Brittleness of Twig Bases in the Genus Salix: Fracture Mechnaics and Ecological Relevance. *Jour. Exp. Bot. 51*(344), 617-633. https://doi.org/10.1093/jexbot/51.344.617

Borau, C., Kamm, R. D., García-Aznar, J. M. (2014). A time-dependent phenomenological model for cell mechano-sensing. *Biomech Model Mechanobiol, 13*(2), 451-62. https://doi.org/10.1007/s10237-013-0508-x

Cao, X., Xia, H., Li, N., Xiong, K., Wang, Z., & Wu, S. (2015). Mechanical Refractory Period Of Chondrocytes After Dynamic Hydrostatic Pressure. *Connect Tissue Res., 56*(3), 212-8. https://doi.org/10.3109/03008207.2014.1001383

Coutand, C., Chevolot, M., Lacointe, A., Rowe, N., & Scotti, I. (2010). Mechanosensing of stem bending and its interspecific variability in five neotropical rainforest species. *Ann Bot., 105*(2), 341-7. https://doi.org/10.1093/aob/mcp286

Dumais, J. (2013). Modes of deformation of walled cells. *J Exp Bot., 64*(15), 4681-95. https://doi.org/10.1093/jxb/ert268

Ennos, A. R. (1993). The Mechanics of Flower Stems of the Sedge *Carex acutiformis. Ann. Botany, 72*, 123-127. https://doi.org/10.1006/anbo.1993.1089

Fournier, M., Dlouhá, J., Jaouen, G., & Almeras, T. (2013). Integrative biomechanics for tree ecology: beyond wood density and strength. *J Exp Bot., 64*(15), 4793-815. https://doi.org/10.1093/jxb/ert279

Greene, P. R. (1985). Stress-strain behavior for curved exponential strips. *Bull Math Biol., 47*(6), 757-64. https://doi.org/10.1007/BF02469302

Greene, P. R. (2016). Vertical-Lift Potential of the Trapped Hypochaeris radicata (Catsear), a Phototropic Sub-Pavement Plant, *Res Rev J Botanical Sci., 5*(4), https://www.rroij.com/open-access/verticallift-potential-of-the-trapped-hypochaeris-radicata-catseara-phototropic-subpavement-plant-.php?aid=83488

Greene, P. R., & Greene, V. A. (2015). Buckling, Bending, and Penetration Response of *Taraxacum officinalae* (Dandelions) to Macadam Loading. *Australian J. Botany, 63*(6), 512-516. https://doi.org/10.1071/BT15083

Iddles, T. L., Read, J., & Sanson, G. D. (2003). Potential Contribution of Biomechanical Properties to Anti-herbivore Defense in Seedlings of Six Australian Rainforest Trees. *Austr. J. Botany, 51*, 119-128. https://doi.org/10.1071/BT02060

Kristo, T. S., Szoke, E., Kery, A., Terdy, P. P., Selmeczi, L. K., & Simandi, B. (2003). Production and Characterization of Taraxacum Officinale Extracts Prepared by Supercritical Fluid and Solvent Extractions. Acta Horticulturae, *Int'l. Soc. Hort. Sci., 597*(1), 1.

Kutschera, U., & Niklas, K. J. (2013). Cell division and turgor-driven stem elongation in juvenile plants: a synthesis. *Plant Sci., 207*, 45-56. https://doi.org/10.1016/j.plantsci.2013.02.004

Langre, E. (2012). Methodological advances in predicting flow-induced dynamics of plants using mechanical-engineering theory. *J Exp Biol., 215*(Pt 6), 914-21. https://doi.org/10.1242/jeb.058933

Latz, M. I., Bovard, M., VanDelinder, V., Segre, E., Rohr, J., & Groisman, A. (2008). Bioluminescent response of individual dinoflagellate cells to hydrodynamic stress measured with millisecond resolution in a microfluidic device. *J Exp Biol., 211*(Pt 17), 2865-75. https://doi.org/10.1242/jeb.011890

Lintilhac, P. M. (2014). The problem of morphogenesis: unscripted biophysical control systems in plants. *Protoplasma, 251*(1), 25-36. https://doi.org/10.1007/s00709-013-0522-y

McMahon, T. A., & Greene, P. R. (1979). The influence of track compliance on running. *J Biomech., 12*(12), 893-904. https://doi.org/10.1016/0021-9290(79)90057-5

Niklas, K. J., & Paolillo, D. J. (1998). Preferential States of Longitudinal Tension in the Outer Tissues of Taraxacum officinale (Asteraceae) Peduncles. *Am. J. Bot.,* 85(9), 1068-1081.

https://doi.org/10.2307/2446340

Niklas, K. J., Cobb, E. D., & Spatz, H. C. (2009). Predicting the allometry of leaf surface area and dry mass. *Am J Bot., 96*(2), 531-6. https://doi.org/10.3732/ajb.0800250

Pickett-Heaps, J. D., & Klein, A. G. (1998). Tip Growth in Plant Cells May be Amoeboid and Not Generated by Turgor Pressure. *Proc. Roy. Soc. B, 265*(1404), 1453-1459. https://doi.org/10.1098/rspb.1998.0457

Schopfer, P. (2006). Biomechanics of plant growth. *Am J Bot., 93*(10), 1415-25. https://doi.org/10.3732/ajb.93.10.1415

Silverberg, J. L., Noar, R. D., Packer, M. S., Harrison, M. J., Henley, C. L., Cohen, I., & Gerbode, S. J. (2012). 3D imaging and mechanical modeling of helical buckling in Medicago truncatula plant roots. *Proc Natl Acad Sci USA, 109*(42), 16794-9. https://doi.org/10.1073/pnas.1209287109

Smith, V. C., & Ennos, A. R. (2003). The effects of air flow and stem flexure on the mechanical and hydraulic properties of the stems of sunflowers Helianthus annuus L. *J Exp Bot., 54*(383), 845-9. https://doi.org/10.1093/jxb/erg068

Waghorn, M. J., & Watt, M. S. (2013). Stand variation in Pinus radiata and its relationship with allometric scaling and critical buckling height. *Ann Bot., 111*(4), 675-80. https://doi.org/10.1093/aob/mct015

Appendix I. Euler Equations for Buckling and Bending of Columns and Beams

[1] *Critical buckling load* **Fcrit** is given by: (unclamped)

Eq. (1) F crit = π ^2 x **EI / (L^2)**

where F crit = axial buckling force, E = Young's modulus of elasticity, I = moment of inertia, L = column length.

[2] *Beam bending deflection* **d** is given by: (cantilevered)

Eq. (2) d = F x **L^3 / 3 (EI)**

where d = lateral tip deflection, F = applied lateral force , L = beam length, (E and I as in Eq. 1)

Example: A practical example of plate strain-rate (using the Maxwell model, Figure 4) serves to illustrate: The *Hypochaeris* plant imposes an upwards vertical force of 18 lbf (80 N), as measured, over a surface area of 1/2 in^2 (1.5 cm^2). This is a normal surface stress of 36 p.s.i. We would like to know how long it takes the *Hypochaeris* plant to crack the driveway, a 3" (8 cm) thick macadam surface. Vertical strain-rate (Eqs. 1, 2) is calculated as 8.5% x 3" x 36 psi x 1 yr. = 9.2 in / yr. (23 cm/yr). Thus, this plant will take 0.3 yrs. to fully crack the surface, as observed.

[3] *Moment of inertia* ***I*** *of a tube* column or beam is given by: (neutral axis)

Eq. (3) I = π x **(R^3) ΔR**

where I = moment of inertia of the tube, R = average tube radius, ΔR = tube wall thickness

[4] *Moment of inertia* ***I*** *of a solid rod* column or beam is given by: (neutral axis)

Eq. (4) I = π x **R^4 / 4**

where I = moment of inertia for a solid rod, R = radius of the solid rod

[5] *The moment of inertia* ***I*** *of a rectangular beam* (plate) is given by:

Eq. (5) I = (1/12) x **W** x **d^3**

where W = width, d = thickness.

Journal of Plant Studies; Vol. 6, No. 2; 2017
ISSN 1927-0461 E-ISSN 1927-047X
Published by Canadian Center of Science and Education

Response of Assorted Maize Germplasm to the Maize Lethal Necrosis Disease in Kenya

Sitta, J.[1], Nzuve, F. M.[2], Olubayo, F. M.[2], Mutinda, C.[3], Muiru, W. M.[2], Miano, D. W.[2], Muthomi, J. W.[2] & Leley, P. K.[3]

[1]Chollima Agro-Scientific Research Centre, P. O. Box 1892, Morogoro, Tanzania

[2]Department of plant science and Crop Protection, University of Nairobi, P O Box 29053-00625, Nairobi, Kenya

[3]Kenya Agricultural and Livestock Research Organization, P O Box 57811-00200, Kenya

Correspondence: Felister Nzuve, University of Nairobi, Kenya. E-mail: fmbute@yahoo.com

Received: February 25, 2017 Accepted: May 9, 2017 Online Published: July 16, 2017

doi:10.5539/jps.v6n2p65 URL: https://doi.org/10.5539/jps.v6n2p65

Abstract

Maize (*Zea mays* L.) is the most widely grown staple food crop in Sub Saharan Africa (SSA) and occupies more than 33 million hectares each year. The recent outbreak and rapid spread of the Maize Lethal Necrosis (MLN) disease has emerged as a great challenge to maize production, threatening food security for the majority of households in the Eastern Africa region with yield loss estimated to be 50-90%. The disease is a result of synergistic interaction between two viruses, *Sugarcane mosaic virus* (SCMV) and *Maize chlorotic mottle virus* (MCMV). The objective of this study was to identify maize genotypes with resistance to MLN. In season one, 73 maize genotypes comprising 25 inbred lines from research institutes, 30 lines from the International Maize and Wheat Improvement Centre (CIMMYT) and 18 farmer varieties were screened for resistance to MLN. In season 2, only 48 genotypes were screened after some of the inbred lines showed complete susceptibility to MLN. These genotypes were grown in three replications in a completely randomized design in polythene bags in the greenhouse at the University of Nairobi. The plants were artificially inoculated using a mixture of SCMV and MCMV. .Weekly MLN disease severity scores using a scale of 1 to 5 (1 = highly resistant and 5 = highly susceptible) and % MLN incidence were recorded and eventually converted into Area under Disease Progress Curve (AUDPC) to give an indication of the disease intensity over time. The plants were allowed to grow to flowering stage to observe the effect of the MLN on the maize productivity. Analysis of Variance revealed wide genetic variation among the genotypes ranging from resistant to highly susceptible. In season 1, three farmer varieties namely MLR2, MLR11 and MLR13 showed resistance to MLN with a mean severity score of 2. In season 2, MLN12, MLN17, MLN18, MLN19, and MLR4 showed low MLN severity ranging from 2-3. The genotypes MLR6, MLR9, MLR16 and MLR18 showed MLN severity of 3 and early maturity traits. This study also validated the presence of MLN resistance among some CIMMYT lines depicted to show resistance in previous studies. These resistant genotypes could serve as donors in the introgression of the resistance into the adapted Kenyan maize backgrounds. This will go a long way in ensuring sustainable maize productivity while improving the livelihoods of the small-scale farmers who form the bulk of the major maize producers in Kenya.

Keywords: maize lethal necrosis disease, MLN severity, maize genotypes

1. Introduction

In Kenya, food security is synonymous with maize availability since it is a key staple food to over 90% of her population with about 42 dietary energy intakes (Keya and Rubaihayo, 2013). The recent outbreak and rapid spread of the Maize Lethal Necrosis (MLN) disease has emerged as a great challenge to maize production, threatening food security for the majority of households in the region. Maize lethal necrosis is a serious disease of maize, and since its first appearance in Kenya in 2011 (Wangai *et al*., 2012), the disease has spread to many countries in the East Africa region where maize is grown including Tanzania, Uganda, South Sudan and Rwanda (IITA, 2014). The disease has been identified as the most devastating foliar disease responsible for highest yield loss in maize because it causes the yield loss of up to 100% because of its ability to kill infected plant and cells (Mbega *et al*., 2016).

MLN is caused by a mixed or synergistic infection between *Maize chlorotic mottle virus* (MCMV, genus Machlomovirus) and potyviruses infecting maize which includes either *Sugarcane mosaic virus* (SCMV) or

Maize dwarf mosaic virus (MDMV) and *Wheat streak mosaic virus* (WSMV). The synergism between viruses refers to situations where co-infection with two viruses leads to more virulence as opposed to singular infections. It is also a state where multiplication of at least one of the viruses is enhanced by the other (Shi *et al*., 1997; Karyeija *et al*., 2000). The MCMV belongs to the genus Machlomovirus of the family Tombusviridae. It was first identified in maize in Peru in 1974 and USA in 1978 and 1980 (Wu *et al*., 2013). It is most common in the graminae family. The SCMV causes mosaic diseases and consists of four distinct Potyviruses including strains of *Johnsongrass mosaic virus* (JGMV), MDMV, *Sorghum mosaic virus* (SrMV) and SCMV (Yang and Mirkov, 1997). The MCMV causes mild mosaic, severe stunting, leaf necrosis, premature plant death, shortened male inflorescences with few spikes, and shortened, malformed and partially filled ears (Wu *et al*., 2013). *Sugarcane mosaic virus* and MDMV are two important pathogens of maize and related crops, causing yield losses, chlorosis and stunting (Xu *et al*., 2000). The infected maize plants are frequently barren, the ears formed are small, deformed and set little or no seeds, drastically reducing the yield. This greatly affects the physiological processes like photosynthesis and chlorophyll formation (Wangai *et al*., 2012), causing failure of tasseling or sterility in male plants. These could also lead to deformed or no ears or even rotting of the cobs (Adams *et al*., 2013).The MLN disease also predisposes the plants to secondary fungal infections (FSNWG, 2012; Wu *et al*., 2013). The type of virus, plant phenology, time of infection, host plant growth conditions and genotype all influence the extent of disease spread and distribution (Melchinger *et al*., 1998). The disease is also aggravated by drought conditions and poor soil fertility (http://www.fao.org/2012). Other predisposing factors include the growing of host crops like sugarcane and millet that contributes towards increased inoculum loads. Insect vectors also aid in the transmission of viruses e.g. maize thrips and beetles have been associated with the transmission of MCMV while aphids transmit SCMV (Cabanas *et al*., 2013; Wu *et al*., 2013). Other forms of transmission include either mechanical or through the seed (Miano and Kabaki, 2013; Wu *et al*., 2013).

The MLN challenge is compounded by the fact that the viruses inhabit leaves, pollen, female and male inflorescences, ear husks, cotyledons and seeds (Nelson *et al*., 2011) further complicating MLN disease management. A gene GRMZM2G018943 was reported to function as the translation initiation factor eIF-2B and this was associated with the mutation of plant proteins which aims at countering the viral attack (Ingvardsen *et al*., 2010). However, this seems not to be the case especially among the currently grown maize varieties in Kenya which have shown high susceptibility to MLN. The nature of entry and replication of the SCMV virus into the plants also aggravates the MLN menace (Ingvardsen *et al*., 2010; Gowda et al., 2015). Knowledge of the virus dynamics could offer a more reliable approach towards management of the MLN epidemics (Redinbaugh *et al*., 2000). The management of MLN disease could be achieved through integrating cultural methods, chemical method such as seed dressing and foliar spray with host resistance breeding. In Kenya, poor agricultural practices like leaving infected maize crop residues in the field and maize monoculture do not aid in breaking the disease transmission cycle. This implies that insect vectors transmit the viruses through crops and seasons. Lack of proper weed management practices has also aided in offering alternative hosts to these vectors since these weeds are susceptible to the MCMV. The use of chemicals is uneconomical and environmentally unfriendly especially among the resource constrained small-scale maize farmers. These chemicals are rendered ineffective due to the non-persistent transmission of the viruses (Melchinger *et al*., 1998).

Host breeding for resistance is the most ecologically safe and economical approach towards combating the MLN disease menace. Previous breeding efforts by the International Maize and Wheat Improvement Centre (CIMMYT) and Kenya Agricultural and Livestock Research Organization (KALRO) have reported very high susceptibility of around 90% to MLN disease among the pre-commercial and commercial maize germplasm (Gowda *et al*., 2015). This implies that reduction in maize production due to the impact of MLN disease will and has already adversely affected the Kenyan livelihoods and the overall market prices of maize (Wangai *et al*., 2012). The areas affected constitute major maize production acreage and given the recorded loss of up to 100%, it has become an important food security issue in Kenya. The impact of the disease has been felt in the whole maize value chain.

Efforts put in breeding to improve maize productivity are aimed at developing many varieties which are resistant to both biotic and abiotic stresses. CIMMYT has undertaken discovery studies to identify genomic regions associated with MLN disease resistance where two mapping panels and six bi-parental populations have revealed three major QTLs on chromosomes and a few minor QTLs across other chromosomes (Olsen *et al*., 2016). These QTLs are aimed for introgression into adapted maize genotypes. The identification of new sources of resistance could contribute valuable alleles which may supplement the ones in use. The objective of this study was to determine the response of assorted maize genotypes to MLN infection and identify any heterotic parents which could be utilized in maize breeding programs to improve maize productivity in the region.

2. Materials and Methods

2.1 Germplasms

The maize genotypes were assembled from diverse sources namely CIMMYT, KALRO and farmers' varieties (landraces) (Table 1).

2.2 Experiment Site Description

The experiments were done in the greenhouse located at the University of Nairobi Field Station (Kabete) for two seasons. Kabete is situated at Latitude of 1° 15′S and Longitude 36° 44′E, and at an altitude 1930 m above sea level. Soils are usually humic nitisol, well drained, deep (>180cm), dark red to darkish brown. Kabete has a bimodal distribution of rainfall, with long rains from early March to late May and the short rains from October to December. The mean annual temperature is 18° C and the mean annual rainfall is 1006 mm (Onyango *et al*., 2012).

2.2.1 Experiment Design and Layout

The experiment was set up in a completely randomized design in three replications. The genotypes were grown in polythene bags measuring 20 cm in diameter in the greenhouse. Previous studies have validated the use of greenhouse due to the fact that the plants are tender leading to efficacy in inoculations and clear genotype diagnosis (Melchinger *et al*., 1998). All the agronomic practices were observed namely; hand weeding, irrigation, fertilizer application whereby DAP was used during planting at the rate of 10 g/hill while urea was used as a top dressing fertilizer. After 14 days post germination, the genotypes were artificially inoculated using a combination of both viruses namely MCMV and SCMV through hand rubbing.

2.2.2 Isolation of the Pathogen

The MLN causal viruses namely MCMV SCMV were isolated from diseased tissue of maize leaves showing clear virus symptoms at KALRO where the two viruses are maintained at the Biosafety Greenhouse (BGH).

2.2.3 Preparation of Inocula and Inoculation

The leaves were cut into small pieces and stored in the freezer at a temperature of -20^0 C. Phosphate buffer 0.1 M was made by mixing potassium phosphate Dibasic (Anhydrous) and Potassium dihydrogen orthophosphate (Potassium phosphate monobasic) to a pH of 7.0 using the following ratios; KH_2PO4 = 10.8g, K_2HPO4 = 4.8g and Na_2SO3 = 1.26 and Carborandum (SiCO3) = 1g/l. Then 2g of leaves with MCMV and 10g of leaves with SCMV at a ratio of 1:5 were weighed and ground using sterile mortar and pestle to obtain homogenate solution or extract. The extract was added to the buffer to make 120 ml. The combination of MCMV and SCMV inoculums was then rubbed onto two week old young leaves of the maize seedlings in the greenhouse. The Carborandum powder ($SiCO_3$) which is an abrasive agent was used to cause microscopic injury of the leaves for easy penetration of the virus into the plant cells (Orawu *et al*., 2013). A second inoculation was done at the interval of one week from the first inoculation to ensure effective viral dissemination and spread among the genotypes and that there were no diseases escapes.

Table 1. List of the genotypes used for screening and their sources

UoN Designation	Genotype	Origin	Season 1	Season 2
UoN-2015-51	KAT25-1	KALRO	1	-
UoN-2015-52	KAT25-2	KALRO	1	-
UoN-2015-53	KAT25-3	KALRO	1	-
UoN-2015-54	KAT25-4	KALRO	1	-
UoN-2015-55	KAT25-5	KALRO	1	-
UoN-2015-56	KAT25-6	KALRO	1	-
UoN-2015-57	KAT25-7	KALRO	1	-
UoN-2015-58	KAT25-8	KALRO	1	-
UoN-2015-59	KAT25-9	KALRO	1	-
UoN-2015-60	KAT25-10	KALRO	1	-
UoN-2015-61	KAT25-11	KALRO	1	-
UoN-2015-62	KAT25-12	KALRO	1	-
UoN-2015-63	KAT25-13	KALRO	1	-
UoN-2015-64	KAT25-14	KALRO	1	-
UoN-2015-65	KAT25-15	KALRO	1	-
UoN-2015-66	KAT25-16	KALRO	1	-
UoN-2015-67	KAT25-17	KALRO	1	-
UoN-2015-68	KAT25-18	KALRO	1	-
UoN-2015-69	KAT25-19	KALRO	1	-
UoN-2015-70	KAT25-20	KALRO	1	-

UoN Designation	Genotype	Origin	Season 1	Season 2
UoN-2015-71	KAT25-21	KALRO	1	-
UoN-2015-72	KAT25-22	KALRO	1	-
UoN-2015-73	KAT25-23	KALRO	1	-
UoN-2015-74	KAT25-24	KALRO	1	-
UoN-2015-75	KAT25-25	KALRO	1	-
UoN-2015-76	MLN1	CIMMYT	1	2
UoN-2015-77	MLN2	CIMMYT	1	2
UoN-2015-78	MLN3	CIMMYT	1	2
UoN-2015-79	MLN4	CIMMYT	1	2
UoN-2015-80	MLN5	CIMMYT	1	2
UoN-2015-81	MLN6	CIMMYT	1	2
UoN-2015-82	MLN7	CIMMYT	1	2
UoN-2015-83	MLN8	CIMMYT	1	2
UoN-2015-84	MLN9	CIMMYT	1	2
UoN-2015-85	MLN10	CIMMYT	1	2
UoN-2015-86	MLN11	CIMMYT	1	2
UoN-2015-87	MLN12	CIMMYT	1	2
UoN-2015-88	MLN13	CIMMYT	1	2
UoN-2015-89	MLN14	CIMMYT	1	2
UoN-2015-90	MLN15	CIMMYT	1	2
UoN-2015-91	MLN16	CIMMYT	1	2
UoN-2015-92	MLN17	CIMMYT	1	2
UoN-2015-93	MLN18	CIMMYT	1	2
UoN-2015-94	MLN19	CIMMYT	1	2
UoN-2015-95	MLN20	CIMMYT	1	2
UoN-2015-96	MLN21	CIMMYT	1	2
UoN-2015-97	MLN22	CIMMYT	1	2
UoN-2015-98	MLN23	CIMMYT	1	2
UoN-2015-99	MLN24	CIMMYT	1	2
UoN-2015-100	MLN25	CIMMYT	1	2
UoN-2015-101	MLN26	CIMMYT	1	2
UoN-2015-102	MLN27	CIMMYT	1	2
UoN-2015-103	MLN28	CIMMYT	1	2
UoN-2015-104	MLN29	CIMMYT	1	2
UoN-2015-105	MLN30	CIMMYT	1	2
UoN-2015-106	MLR1	Farmer varieties	1	2
UoN-2015-107	MLR2	Farmer varieties	1	2
UoN-2015-108	MLR3	Farmer varieties	1	2
UoN-2015-109	MLR4	Farmer varieties	1	2
UoN-2015-110	MLR5	Farmer varieties	1	2
UoN-2015-111	MLR6	Farmer varieties	1	2
UoN-2015-112	MLR7	Farmer varieties	1	2
UoN-2015-113	MLR8	Farmer varieties	1	2
UoN-2015-114	MLR9	Farmer varieties	1	2
UoN-2015-115	MLR10	Farmer varieties	1	2
UoN-2015-116	MLR11	Farmer varieties	1	2
UoN-2015-117	MLR12	Farmer varieties	1	2
UoN-2015-118	MLR13	Farmer varieties	1	2
UoN-2015-119	MLR14	Farmer varieties	1	2
UoN-2015-120	MLR15	Farmer varieties	1	2
UoN-2015-121	MLR16	Farmer varieties	1	2
UoN-2015-122	MLR17	Farmer varieties	1	2

UoN= University of Nairobi; KALRO=Kenya Agricultural and Livestock Research Organization; CIMMYT=International Maize and Wheat Improvement Centre; - = not evaluated in season two

2.3 Data Collection

The MLN symptoms were assessed for disease severity based on the CIMMYT scale (Table 2) and percent MLN incidence. Disease severity scoring began one week after the repeat inoculation and this was done weekly for eight weeks. The delayed scoring for the presence of MLN was to detect late developing infections (Zambrano *et al*., 2013). The plants were allowed to grow to physiological maturity to enable one to get an indication of the effect of MLN on maturity and yielding potential. The percentage MLN incidence was measured as the percentage of the number of leaves with MLN infection.

Table 1. CIMMYT scale used in assessment of the MLN disease

Score	Symptoms
1	No MLN symptoms
2	Fine chlorotic streaks
3	Chlorotic mottling
4	Excessive chlorotic mottling and some necrosis
5	Dead heart symptoms/ complete plant death

Source (CIMMYT).

2.4 Data Analysis

The disease severity scores were converted into the Area Under Disease Progress Curve (AUDPC) values based on Wilcoxson *et al*. (1975). AUDPC is simply the intensity of disease integrated between two times. It is a crucial quantitative summary of the disease intensity over time for comparison across years, locations as well as management tactics. The AUDPC expresses the dynamics of an epidemic as a single value and different epidemics can be compared by normalizing the different AUDPC value of each epidemic by calculating the relative area under disease progress curve (AUDPC) (Equation (1) (Wilcoxson *et al*., 1975).

$$\text{AUDPC} = \sum_{i=1}^{n-1}\left(\frac{y_1+y_{1+1}}{2}\right)(ti+1-ti) \qquad \text{Equation 1} \qquad (1)$$

Whereby,

n= total number of observations, y_i= injury intensity (usually incidence in crop health data) at the *i*th observation, *t* = time at the *i*th observation.

2.4.1 Analysis of Variance

The AUDPC values, the weekly MLN severity scores, % MLN incidence and other agronomic traits were subjected to the analysis of variance (ANOVA). The genotype means were separated using Fisher's protected least significant differences (LSD) test at 5% significance level.

2.4.2 Correlation among the Different Traits

A Pearson's Correlation Coefficient to establish the phenotypic relationship among the different disease parameters assessed was done following the formula by Pearson (1896) shown on Equation (2).

$$r = \frac{\sum(X-\bar{X})(Y-\bar{Y})}{\sqrt{\quad}\sqrt{\quad}} \qquad (2)$$

Where,

$\bar{X}$= mean of X variable; $\bar{Y}$= mean of Y variable

3. Results

3.1 Analysis of Variance

The findings revealed that there were significant differences among the genotypes for the different MLN disease parameters at P<0.05. The replications were not significantly different implying that these findings were repeatable and reproducible through seasons (Table 3 and Table 4).

3.2 Mean Performance of the Assorted Maize Germplasm across Two Seasons

The mean performance of the maize genotypes under MLN artificial infection varied significantly across the two seasons (Table 5). During season 1, 73 genotypes were screened for resistance to MLN whereas in season 2, 50 genotypes were assessed for MLN resistance. The response of the genotypes to the MLN was assessed based on the parameters AUDPC, final disease severity (FS) and MLN disease incidence. To obtain absolute values, there was the use of the relative Final MLN severity (rFS) scores and relative Area Under Disease Progress Curve (rAUDPC).

The genotypes assembled from CIMMYT showed good resistance to the MLN especially during season 2 despite the heavy MLN disease pressure. The genotypes were also divergent with respect to either earliness or lateness in maturity with most of the KALRO and farmer varieties showing the earliness trait. Most of the CIMMYT derived genotypes showed lateness trait.

In season 1, the MLN severity scores ranged from 1 to 5 among the genotypes. The AUDPC had a range of 76 to 148 while the % MLN incidence had a range of 5 to 100%. During season 2, the MLN severity scores ranged from 2 to 5 among the genotypes. The AUDPC had a range of 109 to 246 while the % MLN incidence had a

range of 26 to 100%.

In season one, twenty of the genotypes which showed high MLN resistance also had earliness trait namely KAT25-10, KAT25-16, MLN1, MLN15, MLN16, MLR-10, MLR-13 and MLR-17 with MLN scores ranging from 1 to 2 (Table 4). In season 2, MLN17, MLN19, MLR4, MLN18 and MLN12 combined good MLN disease parameters with MLN severity ranging from 2-3 and also statistically low AUDPC, rAUDPC and % MLN incidence values. These genotypes also exhibited lateness in flowering with statistically many days to 50% tasseling and silking. The genotypes MLR6, MLR9, MLR16 and MLR18 showed MLN severity of 3 and early maturity with statistically few number of days to both 50% tasseling and silking.

3.3 Correlations among Traits in Season across the Two Seasons

The MLN disease parameters namely AUDPC, FS and % DI showed positive and highly significant correlation coefficient values validating their use in estimating the most susceptible and most MLN resistant genotype (Table 7). The weekly MLN progressions also showed positive and highly significant correlation coefficients implying that the period of MLN evaluation was sufficient. However, no distinct relationship was established between the maturity indicators namely days to 50% pollen shed and silking and the MLN assessment parameters.

Table 3. Mean Squares for the MLN disease parameters during season 1

Source of variation	df	% incidence	MLN severity	AUDPC	rAUDPC	rFS
Replications	2	4444.90	3.90	2316.70	882.70	3.90
Genotypes	71	1879.4*	1.5*	993.3*	378.5*	1.5*
Residual	124	846.90	0.50	380.60	145.00	0.50
Total	197					

Table 4. Mean squares for the MLN disease parameters during season 2

Source of variation	**df**	**% MLN incidence**	**MLN severity**	**AUDPC**	**rAUDPC**	**rFS**
Replications	2	24240.80	8.27	46273.00	5210.70	17.33
Entry	46	10562.7*	5.43*	21743*	2448.4*	6.3*
Residual	68	526.90	0.49	1165.00	131.20	0.58
Total	116					

*=Significant difference at 5%; MLN Severity: was assessed based on CIMMYT scale (1-5) where 1 = No MLN symptoms and 5 = Dead heart symptoms/ complete plant death; AUDPC: area under the disease progress curve calculated from the weekly MLN severity scores based on Wilcoxson *et al*. (1975) equation; rAUDPC: relative Area Under Disease Progress Curve was calculated to obtain absolute values where the most MLN susceptible genotype was used for computation; % MLN incidence: percentage of the number of leaves with MLN infection

Table 5. Weekly MLN disease progression in season 1 and MLN disease parameters

Entry	**Genotypes**	**Weekly MLN severity scores (1 – 5)**								**AUDPC**	**rAUDPC**	**% MLN incidence**	**rFS**	**DTS**	**DTP**
		week1	**week2**	**week3**	**week4**	**week5**	**week6**	**week7**	**week8**						
1	KAT25-1	1.67	2.00	2.33	3.00	3.33	3.67	3.67	4.67	146.00	90.12	100.00	4.67	58.08	64.53
2	KAT25-2	1.33	2.00	2.67	3.00	3.67	3.67	3.67	4.33	148.20	91.46	100.00	4.33	62.59	70.53
3	KAT25-3	0.67	1.67	2.67	2.33	3.00	3.00	3.00	3.00	120.30	74.28	100.00	3.00	59.08	60.33
4	KAT25-4	0.67	2.00	3.00	3.00	3.33	3.00	3.00	3.33	132.80	82.00	86.70	3.33	61.81	67.00
5	KAT25-5	1.00	1.67	2.33	2.33	2.67	2.33	2.33	3.33	108.80	67.18	79.20	3.33	71.77	70.53
6	KAT25-6	1.67	2.00	2.33	2.67	2.33	2.67	2.67	3.00	116.80	72.12	76.80	3.00	62.59	71.19
7	KAT25-7	1.67	2.00	2.00	2.00	2.33	2.00	2.33	2.67	101.80	62.86	66.10	2.67	63.67	55.67
8	KAT25-8	0.94	1.94	1.44	1.44	1.44	1.94	1.44	1.94	75.60	46.68	15.20	1.87	63.31	51.78
9	KAT25-9	0.67	1.67	1.33	1.67	2.33	2.33	3.00	2.67	96.50	59.57	69.40	2.67	66.77	64.00
10	KAT25-10	2.04	2.04	1.04	2.04	2.54	2.54	2.04	2.54	100.60	62.10	67.20	2.57	55.61	51.00
11	KAT25-11	1.33	1.67	2.00	2.67	2.67	2.33	2.00	2.33	104.30	64.40	44.20	2.33	70.83	67.33
12	KAT25-12	0.67	2.00	2.00	2.33	2.00	1.67	1.00	1.00	80.80	49.90	4.80	1.00	62.59	71.00
13	KAT25-13	1.33	1.33	2.00	2.33	2.00	2.00	1.33	1.33	84.70	52.26	6.70	1.33	62.59	71.19
14	KAT25-14	1.02	1.52	1.52	2.02	2.52	2.02	2.02	2.02	90.30	55.73	51.50	2.06	65.67	54.67
15	KAT25-15	1.67	2.33	2.00	2.67	2.67	3.00	3.00	3.00	123.80	76.44	93.60	3.00	59.58	53.03
16	KAT25-16	1.04	2.04	2.04	2.04	2.54	2.54	2.04	2.04	101.80	62.87	41.80	2.07	58.33	60.00
17	KAT25-17	1.33	2.00	2.67	2.67	3.00	3.00	3.00	3.00	127.20	78.50	88.90	3.00	63.31	53.78
18	KAT25-18	1.00	2.00	1.67	2.67	2.67	2.67	2.67	3.00	112.50	69.44	96.70	3.00	58.00	76.00
19	KAT25-19	1.67	1.33	1.67	2.00	2.33	2.00	1.67	1.67	87.20	53.81	17.40	1.67	63.11	51.69
20	KAT25-20	1.02	2.02	2.52	2.52	3.02	4.02	3.91	4.90	139.50	86.12	93.80	4.85	70.61	60.69
21	KAT25-21	1.67	2.00	2.00	2.67	2.67	2.67	2.67	2.67	115.80	71.50	70.40	2.67	65.81	71.00

Entry	Genotypes	Weekly MLN severity scores (1 – 5)								AUDPC	rAUDPC	% MLN incidence	rFS	DTS	DTP
		week1	week2	week3	week4	week5	week6	week7	week8						
22	KAT25-22	1.67	2.00	3.00	3.00	3.33	3.33	3.33	4.33	144.50	89.20	100.00	4.33	62.59	70.60
23	KAT25-23	1.67	2.00	2.00	2.33	2.67	2.33	2.00	2.33	105.30	65.02	68.30	2.33	62.59	70.43
24	KAT25-24	1.00	2.00	2.00	2.00	2.00	2.33	2.33	2.67	99.50	61.42	54.20	2.67	62.59	71.92
25	KAT25-25	0.67	2.00	2.33	3.00	2.67	2.67	2.67	2.67	116.80	72.12	60.70	2.67	65.81	58.00
26	MLN1	1.02	2.02	1.52	1.52	2.02	2.52	2.02	2.02	90.00	55.58	18.90	2.06	54.85	60.78
27	MLN2	1.67	1.33	1.67	2.00	2.67	2.67	2.67	2.33	103.50	63.89	61.10	2.33	59.84	77.90
28	MLN3	1.33	1.67	2.00	2.00	2.00	2.00	2.00	2.33	90.30	55.76	56.80	2.33	71.77	67.28
29	MLN4	0.67	2.00	2.00	2.00	2.67	2.67	2.33	2.33	104.20	64.30	66.20	2.33	65.38	63.69
30	MLN5	1.00	1.67	1.00	1.67	2.33	2.00	2.00	3.00	87.30	53.91	69.10	3.00	62.59	67.92
31	MLN6	1.44	1.94	2.44	1.94	2.94	2.44	2.44	2.44	110.10	67.98	53.30	2.37	67.08	56.53
32	MLN7	1.67	1.67	1.00	1.33	2.33	2.33	2.67	3.00	94.30	58.23	100.00	3.00	54.85	74.91
33	MLN8	1.54	2.04	2.54	2.54	3.04	3.04	3.04	3.04	127.80	78.92	89.30	3.07	61.00	66.00
34	MLN9	1.33	1.67	1.00	1.33	2.00	2.00	1.67	1.33	75.70	46.71	9.10	1.33	70.83	64.78
35	MLN10	1.33	2.33	2.00	2.33	2.67	2.67	2.67	2.67	114.50	70.68	63.30	2.67	70.83	65.78
36	MLN11	0.67	1.67	2.00	2.33	3.00	3.33	3.00	3.00	118.30	73.05	77.80	3.00	59.00	71.33
37	MLN12	1.33	1.67	1.33	2.00	2.00	2.00	2.00	2.00	87.20	53.81	13.70	2.00	62.59	64.85
38	MLN13	1.33	2.00	1.67	2.00	2.33	2.00	2.00	2.33	95.00	58.64	55.50	2.33	65.84	70.43
39	MLN14	1.54	2.04	2.54	3.04	3.04	2.54	3.54	4.04	134.80	83.24	95.30	4.07	57.61	66.00
40	MLN15	1.23	1.82	1.92	2.24	2.58	2.56	2.51	2.66	107.10	66.13	63.20	2.66	59.33	50.00
41	MLN16	1.00	1.00	1.00	1.67	1.67	2.00	2.00	2.33	76.00	46.91	53.40	2.33	56.61	63.69
42	MLN17	1.33	1.33	1.67	1.67	2.00	2.33	2.33	2.33	90.70	55.97	52.40	2.33	54.85	72.78
43	MLN18	0.67	1.33	1.33	2.00	2.33	2.33	2.33	2.33	90.80	56.07	50.40	2.33	55.79	74.28
44	MLN19	1.33	1.33	1.67	1.33	2.33	2.67	2.33	2.00	91.80	56.69	51.10	2.00	62.59	69.19
45	MLN20	1.00	2.33	1.33	2.00	2.00	2.33	2.00	2.00	92.70	57.20	31.20	2.00	59.39	70.33
46	MLN21	1.00	2.00	2.00	1.67	3.33	2.67	3.00	3.00	114.70	70.78	62.10	3.00	64.58	66.33
47	MLN22	1.04	2.04	1.54	2.54	2.54	2.54	2.04	2.04	102.10	63.02	48.00	2.07	60.00	67.00
48	MLN23	1.67	2.00	2.00	2.67	3.00	3.00	3.00	3.00	124.00	76.54	89.80	3.00	55.79	73.60
49	MLN24	1.33	2.00	2.33	2.00	2.33	2.67	2.67	2.67	109.80	67.80	62.80	2.67	70.37	68.53
50	MLN25	1.00	2.00	2.00	2.67	3.00	3.00	3.00	3.00	121.70	75.10	70.10	3.00	70.61	67.67
51	MLN26	1.33	1.67	1.67	2.33	2.33	2.33	2.00	2.00	96.30	59.47	38.50	2.00	56.78	69.78
52	MLN27	1.33	1.33	1.00	1.33	2.00	2.00	2.33	2.67	82.80	51.13	67.90	2.67	62.59	70.43
53	MLN28	1.00	1.67	1.33	2.00	2.33	2.33	2.67	3.00	98.80	61.01	83.60	3.00	55.31	74.00
54	MLN29	2.00	2.00	1.33	2.00	2.67	2.67	2.67	2.33	106.80	65.95	41.20	2.33	62.84	67.92
55	MLN30	1.67	1.67	1.33	2.00	2.33	2.00	1.67	1.67	87.20	53.81	23.90	1.67	70.37	63.45
56	MLR-1	1.00	2.00	2.33	2.33	2.67	3.04	2.54	3.04	119.10	73.52	74.90	3.07	63.78	72.28
57	MLR-2	1.00	1.67	1.00	1.33	1.67	2.00	2.00	2.00	76.80	47.43	45.40	2.00	70.61	68.33
58	MLR-3	2.04	2.04	3.04	3.04	3.04	2.54	3.54	4.04	139.80	86.32	93.60	4.07	59.39	63.69
59	MLR-4	2.00	2.00	2.67	3.33	3.33	3.00	3.33	3.00	138.80	85.70	90.60	3.00	70.83	65.69
60	MLR-5	1.94	1.44	2.44	2.94	2.94	2.94	2.94	2.94	124.40	76.77	76.70	2.87	59.00	54.67
61	MLR-6	1.00	1.67	2.33	2.67	3.00	2.67	2.67	2.67	115.80	71.50	73.60	2.67	60.78	61.53
62	MLR-7	0.44	1.94	1.44	1.44	2.44	2.44	2.44	2.94	94.90	58.56	68.90	2.87	64.81	62.67
63	MLR-8	1.33	1.67	2.33	2.67	2.67	2.67	2.67	2.33	113.50	70.06	56.40	2.33	60.00	70.33
64	MLR-9	1.00	2.00	2.00	2.67	2.67	3.00	3.00	3.00	119.30	73.66	85.60	3.00	64.58	56.53
65	MLR-10	0.92	1.92	1.92	1.92	2.91	2.91	2.91	2.91	112.30	69.31	74.00	2.86	60.31	50.28
66	MLR-11	0.67	1.33	1.33	2.00	2.00	2.00	2.00	2.00	82.70	51.03	29.70	2.00	68.11	63.67
67	MLR-12	1.54	1.54	1.54	2.04	2.54	2.54	2.04	2.54	98.80	61.02	58.50	2.57	58.00	68.00
68	MLR-13	0.67	2.00	1.67	2.00	2.33	2.33	2.33	2.33	97.30	60.08	53.90	2.33	59.39	61.53
69	MLR-14	0.67	1.67	2.00	2.67	3.00	3.00	3.33	3.33	121.80	75.21	93.90	3.33	62.59	70.60
70	MLR-15	0.67	1.67	2.33	2.00	2.67	2.67	3.00	2.67	110.00	67.90	75.40	2.67	59.00	62.33
71	MLR-16	1.33	1.67	2.33	3.00	3.00	2.67	2.67	2.67	119.30	73.66	75.00	2.67	62.08	56.03
72	MLR-17	1.33	2.00	2.33	2.67	2.67	2.67	2.67	2.00	116.80	72.12	63.60	2.00	62.59	60.94
73	check	1.33	2.33	2.00	2.33	2.67	2.67	2.33	2.33	111.00	68.52	50.00	2.33	62.33	50.00
Least significant difference										31.5	19.5	47.0	1.2	8.19	14.65
%Coefficient of variation										5.3	5.3	12.4	8.8	1.10	1.30

*=Significant difference at 5%; MLN Severity: was assessed based CIMMYT scale (1-5) where 1 = No MLN symptoms and 5 = Dead heart symptoms/ complete plant death; AUDPC: area under the disease progress curve calculated from the weekly MLN severity scores based on Wilcoxson *et al*. (1975) equation; rAUDPC: relative Area Under Disease Progress Curve calculated as a percentage of the AUDPC; % MLN incidence: percentage of the number of leaves with MLND infection; DTS= Days to 50% silking, DTP= Days to 50% Pollen shed

Table 6. Weekly MLN disease progression in season 2 and other MN disease parameters

Entry	Genotype	Weekly MLN severity scores (1 – 5)							AUDPC	rAUDPC	FS	rFS	%MLN	DTP	DTS
		week1	week2	week3	week4	week5	week6	week7					incidence		
1	MLN1	1.09	1.09	2.09	2.09	2.09	2.09	4	143	48	4	4	43	93.5	89.1
2	MLN2	1.92	1.92	2.92	2.92	2.92	2.92	4	187	63	4	4	97	85.3	78.6
3	MLN3	2.00	2.00	2.00	2.00	2.33	3.00	4	172	58	4	4	98	92.7	87.3
4	MLN4	2.00	2.00	2.00	2.00	2.00	3.00	4	167	56	4	4	81	90	83
5	MLN5	2.00	2.00	2.00	2.00	2.00	3.00	4	176	59	4	4	97	89.5	90
6	MLN6	1.09	1.09	1.09	1.09	1.09	2.59	3	130	44	3	3	63	84	80.6
7	MLN7	1.92	2.92	3.42	3.42	3.42	4.42	4	241	81	4	4	97	85.8	97.3
8	MLN8	1.16	2.16	2.16	2.16	3.16	3.16	3	179	60	3	3	83	85.8	80.9
9	MLN9	1.33	1.33	1.33	1.33	1.67	2.67	3	135	45	3	3	55	88.7	83
10	MLN10	1.59	2.09	2.09	2.09	2.09	3.09	3	162	54	3	3	69	85.4	85.6
11	MLN11	2.33	3.00	3.00	3.00	3.33	3.67	4	217	73	4	4	100	84	84.3
12	MLN12	1.01	1.01	1.01	1.01	2.01	2.01	3	123	41	3	3	26	93.7	94.3
13	MLN13	2.09	2.09	2.09	2.09	3.09	3.59	4	193	65	4	4	100	87.5	85.1
14	MLN14	1.66	1.91	2.04	2.04	2.27	2.94	3	165	56	3	3	74	85.8	80.9
15	MLN15	1.50	1.50	1.50	1.50	2.00	2.50	3	147	49	4	4	47	92.1	87.8
16	MLN16	3.16	3.16	3.16	3.16	3.16	4.16	4	239	80	4	4	74	85.8	91.9
17	MLN17	1.50	1.50	1.50	1.50	1.50	2.50	2	126	42	3	3	27	92.6	89.8
18	MLN18	0.92	1.42	1.42	1.42	1.42	2.42	3	126	42	3	3	34	92.3	89.1
19	MLN19	1.33	1.33	1.67	1.67	1.67	2.33	3	127	43	3	3	38	95	92.7
20	MLN20	1.92	1.92	1.92	1.92	2.42	3.42	3	175	59	3	3	97	88.3	89.1
21	MLN21	2.00	2.33	2.33	2.33	2.67	3.33	4	191	64	4	4	75	86	82
22	MLN22	1.01	1.01	2.01	2.01	2.01	3.01	4	162	54	4	4	80	93.7	90.3
23	MLN23	1.66	1.91	2.04	2.04	2.27	2.94	3	165	56	3	3	74	85.8	80.9
24	MLN24	1.59	2.09	2.09	2.09	2.09	2.59	3	153	51	3	3	66	93.3	83.6
25	MLN25	1.33	1.67	2.00	2.00	2.33	2.67	3	147	49	3	3	61	88.7	82
26	MLN26	1.33	2.33	2.33	2.33	2.67	3.00	3	169	57	3	3	79	86.8	81.7
27	MLN27	1.67	2.00	2.00	2.00	2.00	2.67	3	151	51	3	3	69	90	84
28	MLN28	1.50	1.50	1.50	1.50	2.00	2.00	3	131	44	3	3	56	90.9	87.8
29	MLN29	1.00	1.33	1.33	1.33	1.33	2.00	2	109	36	2	2	51	88.7	85.3
30	MLN30	1.33	2.00	2.00	2.00	2.00	3.00	3	158	53	3	3	94	90.3	84
31	MLR1	1.33	1.33	1.67	1.67	1.67	2.33	3	137	46	3	3	44	86.7	82.7
32	MLR2	1.59	1.59	1.59	1.59	2.09	3.59	5	188	63	5	5	93	89.7	82.1
33	MLR3	1.33	1.33	2.00	2.00	2.00	3.00	4	160	54	4	4	92	77.3	67.7
34	MLR4	1.33	2.00	2.00	2.00	2.00	2.33	3	141	47	3	3	29	90.1	82.8
35	MLR5	2.00	3.33	3.33	3.33	4.00	4.33	4	246	83	4	4	100	81.1	72.3
36	MLR6	1.67	1.67	1.67	1.67	2.00	3.00	3	154	52	3	3	97	74.7	70
37	MLR7	2.00	2.33	2.67	2.67	3.00	3.33	4	194	65	4	4	84	88.7	80.7
38	MLR8	1.33	1.67	1.67	1.67	2.00	2.33	3	144	48	3	3	67	83	79.7
39	MLR9	1.33	1.33	1.33	1.33	2.00	2.67	3	145	49	3	3	88	77.3	66.3
40	MLR10	2.00	2.00	2.00	2.00	2.00	3.00	4	178	60	5	5	94	87.1	79.3
41	MLR11	2.09	2.59	2.59	2.59	2.59	3.09	4	185	62	4	4	90	79	71.1
42	MLR12	2.00	2.00	2.33	2.33	2.33	2.67	3	161	54	3	3	58	83.3	73.3
43	MLR13	1.33	1.33	1.67	1.67	2.00	2.67	3	147	49	3	3	75	78.7	72
44	MLR14	2.00	2.33	2.33	2.33	2.67	3.67	4	193	65	4	4	89	73.5	67.6
45	MLR15	3.00	3.33	3.33	3.33	3.33	4.00	4	235	79	4	4	94	80.7	73.3
46	MLR16	1.67	2.00	2.00	2.00	2.00	3.00	3	161	54	3	3	97	77.3	67.3
47	MLR17	2.00	2.00	2.00	2.00	2.00	2.50	2	141	47	3	3	70	81.6	70.3
48	MLR18	1.33	1.67	1.67	1.67	2.00	2.67	3	149	50	3	3	75	71.3	66.3
Least significant difference									21.02	7.05		0.47	14.14	6.62	8.623
%Coefficient of variation									6.90	6.90		6.50	11.30	1	2.4

*=Significant difference at 5%; MLN Severity: was assessed based CIMMYT scale (0-1) where 0 = No MLN symptoms and 5 = Dead heart symptoms/ complete plant death; AUDPC: area under the disease progress curve calculated from the weekly MLN severity scores based on Wilcoxson *et al*., (1975) equation; ; rAUDPC: relative Area Under Disease Progress Curve calculated as a percentage of the AUDPC; % MLN incidence: percentage of the number of leaves with MLND infection; LSD=Least significant difference, CV= Coefficient of variation DTS= Days to 50% silking, DTP= Days to 50% Pollen shed

Table 7. Correlation among the traits across two seasons

Trait	AUDPC	DTP	DTS	FS	% DI	week1	week2	week3	week4	week5	week6	Week7
AUDPC	-											
DTP	0.43*	-										
DTS	0.47*	**0.90***	-									
FS	**0.85***	0.31*	0.35*	-								
%DI	**0.64***	0.11	0.16*	**0.64***	-							
week1	**0.51***	-0.09	-0.02	0.40*	0.42*	-						
week2	**0.57***	-0.11	-0.07	0.40*	0.38*	**0.73***	-					
week3	**0.54***	-0.23*	-0.20*	0.43*	0.40*	**0.64***	**0.84***	-				
week4	**0.59***	-0.16*	-0.14*	0.47*	0.45*	**0.60***	**0.77***	**0.90***	-			
week5	**0.66***	-0.09	-0.04	**0.53***	0.48*	**0.61***	**0.77***	**0.88***	**0.92***	-		
week6	**0.82***	0.20*	0.22*	**0.69***	**0.60***	**0.57***	**0.61***	**0.64***	**0.72***	**0.75***	-	
week7	**0.84***	0.36*	0.36*	**0.86***	**0.56***	0.44*	0.45*	0.46*	**0.54***	**0.60***	**0.81***	-

*=Significant difference at 5%; MLN Severity: was assessed based CIMMYT scale (0-1) where 0 = No MLN symptoms and 5 = Dead heart symptoms/ complete plant death; AUDPC: area under the disease progress curve calculated from the weekly MLN severity scores based on Wilcoxson et al. (1975) equation; % MLN incidence: percentage of the number of leaves with MLN infection; DTS= Days to 50% silking, DTP= Days to 50% Pollen shed

4. Discussion and Conclusion

Continuous efforts to identify resistant sources of MLN for introgression into the adapted maize genotypes are imperative in combating the sporadic nature of MLN causal agents especially in the face of climate change. The current research which involved assessing the response of assorted maize genotypes to the MLN disease has revealed the reaction of the genetically divergent maize genotypes. The plants exhibited clear mosaic symptoms on leaves, systemic in nature and which were indicative of susceptibility to MLN. Significant differences were reported among the genotypes with response to the different MLN assessment parameters. When a virus infects a plant, a signal transduction leads to physiological changes in the host plant implying that the genetic structure of the plants play a critical role in the infection and spread of viruses (Salaudeen and Aguguom, 2014). The significant and positive correlation coefficients noted between the MLN disease parameters validated their use in the assessment of the genotypes for response to MLN. Previous studies have identified susceptible and resistant genotypes by using the same parameters (Zambrano *et al*., 2013).

More than 50% of the genotypes screened in the two seasons were susceptible to the disease, validating the risk that MLN poses to maize production in Kenya and its food security status. These findings corroborate with reports by Gowda *et al.* (2015) on the high susceptibility of Kenyan maize germplasm to the MLN especially under artificial MLN infections. The MLN infection was induced by the artificial inoculation of SCMV and MCMV suggesting that the two viruses increased the viral load leading to the symptomatic effects which are both additive and lethal (Marçon *et al*., 1997). This study involved CIMMYT germplasm previously depicted as resistant in other studies. In this study, some lines still exhibited resistant responses namely MLN1, MLN15, MLN16, MLN17, MLN19, MLN18 and MLN12 which had low MLN severity ranging from 2-3 and also statistically low AUDPC, rAUDPC and % MLN incidence values. However, most of the other CIMMYT lines succumbed to the MLN disease.

Clear symptoms were observed among the susceptible MLN lines. Symptoms arise from interactions of the host with the virus and are as a result of compatible interaction which lead to the diversion of assimilates from the host plant to favour the virus cellular processes like its replication and multiplication (Revers *et al*., 1999). The resistance on the other hand could imply an incompatible interaction which could have been stimulated by the rapid necrosis at the foci of virus entry preventing its further spread and this could probably explain the partial resistance observed among some of the maize genotypes in this research work (Ronde *et al*., 2014). Previous studies have reported intense susceptibility to MLN in East Africa (EA) among the pre-commercial and commercial maize varieties (Jumbo *et al*., 2015; Semagn *et al*., 2015). It can be deduced that the use of germplasm labelled as resistant or moderately resistant should be done with caution and there is need for validation through repeat experiments over several seasons with reliable inoculations (CIMMYT, 2013; Gowda *et al*., 2015).

Among the farmer varieties, MLR-10, MLR-13 and MLR-17 MLR4, MLR6, MLR9, MLR18 and MLR16 were superior for MLN resistance These genotypes combined low AUDPC values which implies that the plant defense mechanism against the viruses could be mediated by resistance (R) genes which are observed as complete resistance or extreme resistance (ER) and that the virus replication could have been hindered or gone

undetectable among the infected cells (Ingvardsen *et al*., 2010). The farmer varieties are highly heterogeneous due to out-crossing within the farmers' fields. The presence of some resistance among these genotypes could offer the much-needed alternative to resource-constrained Kenyan farmers in combating the MLN threat.

This study also revealed that none of the genotypes was immune to the MLN disease across the two seasons of evaluation. However, some genotypes showed clear hypersensitive responses and necrotic symptoms. Previous studies by Zambrano *et al*. (2014) have reported presence of some resistance to multiple viruses in the family potyviridae. The presence of passive and active defense mechanisms hinders virus multiplication and spread influencing either the susceptibility or the resistance of germplasm (Zambrano *et al*., 2014).

The weekly MLN progression among the maize genotypes gave a great insight into the virus dynamics. Among the most susceptible genotypes, there was high AUDPC values coupled with high MLN scores as the weeks progressed. Revers *et al*. (1999) explained that the Potyviruses tend to follow the sink to source criteria in photo-assimilate partitioning. The plants viruses are known to gain access to the plant followed by the viral interaction with the host cells. This leads to the manipulation of the host cell pathways into viral factories (Sharma and Misra, 2011). Further on, the systemic infection of the viruses from the primary infection point and its invasion of the distal regions through the mesophyll into the bundle sheath cells, phloem parenchyma, and companion cells into phloem sieve elements is through passive translocation in the phloem leading to further infection and spread (Revers *et al*., 1999). However, among some genotypes, the symptoms plateaued while in others there was increased MLN severity with time. The MLN causal viruses cause systemic infections and the virus translocation from the point of inoculation depends on the cell-to-cell movement of its particles after the viral replication and establishment (Salaudeen and Aguguom, 2014). The resistant genotypes with low AUDPC values on the other hand could have had the inherent ability to retard the virus infection by inhibiting the movement of the virus inside the host cells (Gowda *et al*, 2015).

The superior maize genotypes identified in this research could serve as potential donors to improve the adapted maize varieties to combat the MLN threat in Kenya. However, the low frequency of resistance sources is an issue of great concern and this affects the nutritional and food security status of Kenya which is highly dependent on maize as a key staple food crop. Further evaluation of these elite genotypes for response to the singular viruses and establishment of the genetics of the MLN resistance will enhance their efficient utilization in breeding programs. Through genetic studies, the nature of the genes conditioning resistance to the MLN and its causal virus will help to elucidate further the viruses' dynamics.

Acknowledgements

This work was jointly supported by the Alliance for Green Revolution in Africa (AGRA) and the Association for Strengthening Agricultural Research in Eastern and Central Africa (ASARECA). The authors acknowledge the immense support from KALRO and CIMMYT for the provision of the maize germplasm.

References

Adams, I. P., Miano, D.W., Kinyua, M. Z., Wangai, A., Kimani, E., Phiri, N., … Boonham, N. (2013). Use of next-generation sequencing for the identification and characterization of Maize chlorotic mottle virus and Sugarcane mosaic virus causing maize lethal necrosis in Kenya. *Plant Pathology. 62*, 741-749. https://doi.org/10.1111/j.1365-3059.2012.02690.x

Cabanas, D., Watanabe, S., Higashi, C. H. V., & Bressan, A. (2013). Dissecting the Mode of Maize Chlorotic Mottle Virus Transmission (Tombusviridae: Machlomovirus) by Frankliniella williamsi (Thysanoptera: Thripidae). *J Econ Entomol, 106*, 16-24. https://doi.org/10.1603/EC12056

CABI., (2015). Invasive species compendium, Datasheets, Maps, Images, Abstracts and full-text invasive species of the world. http://www.cabi.org/isc/

CIMMYT. (2013). Kiboko Crops Research Station: A brief and visitors' guide. CIMMYT.

FSNWG. (2012). Regional Food Security Situation and Outlook. Food Security and Nutrition Working Group, http://www. disasterriskreduction.net/east-central-africa/ fsnwg.

Gowda, M., Das, B., Makumbi, D., Babu, R., Kassa Semagn, K., Mahuku, G., Olsen, M.S., Bright, M. J., Beyene, Y., & Prasanna, M. B. (2015). Genome‐wide association and genomic prediction of resistance to maize lethal necrosis disease in tropical maize germplasm.*TheorAppl Genet, 127*, 867-880. https://doi.org/10.1007/s00122-015-2559-0

Ingvardsen, C. R., Xing,Y., Frei, U. K., & Lübberstedt, T. (2010). Genetic and physical Wne mapping of *Scmv2*, a potyvirus resistance gene in maize. *Theor Appl Genet, 120*, 1621-1634.

https://doi.org/10.1007/s00122-010-1281-1

Jones, M. W., Boyd, E. C., & Redinbaugh, M. G. (2011). Responses of maize (Zea mays L.) near isogenic lines carrying Wsm1, Wsm2, and Wsm3 to three viruses in the Potyviridae. *Theor Appl Genet, 123*, 729-740. https://doi.org/10.1007/s00122-011-1622-8

Jumbo, M. B., Makumbi, D, Kimunye, J. N., Mahuku, G., Bekunda, M., & Hoeschle-Zeledon, I. (2015). Integration of maize lethal necrosis disease management in crop-livestock intensification to enehance productivity of smallholder agricultural production systems in East Africa-An Africa RISING approach. Poster prepared for the International conference on Integrated Systems Research, Ibadan, Nigeria, 3-6 March 2015. Nairobi, Kenya: CIMMYT.

Karyeija, R. F., Kreuze, J. F., Gibson, W. R., & Valkonen, J. P. T. (2000). Synergistic Interactions of a Potyvirus and a Phloem-Limited Crinivirus in Sweet Potato Plants. *Virology, 269*, 26-36. https://doi.org/10.1006/viro.1999.0169

Keya, S., & Rubaihayo, P. (2013). Progresson on-farm production and productivity in East Africa Community; 50 years after independence. Kilimo trust technical paper No.8. International symposium on agriculture, EAC partner states at 50 years. 5-7 November, 2013.

Kiruwa, H. F., Feyissa, T., & Ndakidemi, A. P. (2016). Insight of maize lethal necrotic disease. A major constraint to maize production in East Africa: *African journal of microbiology Research, 10*(9), 271-279. https://doi.org/10.5897/AJMR2015.7534

Marçon, A., Kaeppler, S. M., & Jensen, S. G. (1997). Genetic variability among maize inbred lines for resistance to the high plains virus–wheat streak mosaic virus complex. *Plant Dis., 81*, 195-198. https://doi.org/10.1094/PDIS.1997.81.2.195

Mbega, E. R., Ndakidemi, P. A., Mamiro, D. P., Mushongi, A. A., Kitenge, K. M., & Ndomba, O. A. (2016). Role of potyviruses in synergistic interaction leading to maize lethal necrotic disease on maize. *International journal of current microbiology and applied sciences, 5*(6), 85-96. https://doi.org/10.20546/ijcmas.2016.506.011

Melchinger, A. E., Kuntze, L.,Gumber, R. K., Lu¬ bberstedt, T., & Fuchs, E. (1998). Genetic basis of resistance to sugarcane mosaic virus in European maize germplasm. *Theor Appl Genet, 96*, 1151-1161. https://doi.org/10.1007/s001220050851

Miano, F., Kabaki, J., & Viollet, D. (2013). Controlling Maize Lethal Necrosis Disease via Vector Management. AFSTA

Nelson, S., Brewbaker, J., & Hu, J. (2011). Maize Chlorotic Mottle Virus. *Plant Disease, 79*, 1-6.

Olsen, M., Yao, N., Tadesse, B., Das, B., Gowda, M., Semagn, K., Jumbo, M., & Killian, A. (2016). Mapping genetic regions associated with MLND using QTL-Seq. Biosciences eastern and central Africa.

Onyango, C. M., Harbinson, J., Imungi, J. K., Onwonga, R. N., & Kooten, O. (2012). Effect of Nitrogen Source, Crop Maturity Stage, and Storage Conditions on Phenolics and Oxalate Contents in Vegetable Amaranth (Amaranthus hypochondriacus). *Journal of Agricultural Science, 4*(7), 219-230. https://doi.org/10.5539/jas.v4n7p219

Orawu, M., Melis R., Laing M., & Derera J. (2013). Genetic inheritance of resistance to cowpea aphid-borne mosaic virus in cowpea. *Euphytica, 189*, 191-201. https://doi.org/10.1007/s10681-012-0756-3

Redinbaugh, M. G., Seifers, D. L., Meulia, T., Abt, J. J., Anderson, R. J., Styer, W. E., Ackerman, J., Salomon, R., Houghton, W., Creamer, R.,Gordon, D. T., & Hogenhout, S. A. (2002). Maize fine streak virus, a new leafhopper-transmitted rhabdovirus. *Phytopathology, 92*, 1167-1174. https://doi.org/10.1094/PHYTO.2002.92.11.1167

Redinbaugh, M. G., Jones, M. W., & Gingery, R. E. (2004). The genetics of virus resistance in maize (Zea mays L.). *Maydica, 49*, 187-190.

Revers, F., Le Gall, O., Candresse, T., & Maule, A. J. (1999). New Advances in Understanding the Molecular Biology of Plant/Potyvirus Interactions. *MPMI, 12*(5), 367-376. https://doi.org/10.1094/MPMI.1999.12.5.367

Ronde, D., Butterbach, P., & Kormelink, R. (2014). Dominant resistance against plant viruses.

Salaudeen, M. T., & Aguguom, A. (2014). Identification of some cowpea accessions tolerant to cowpea mild

mottle virus. *I.J.S.N. 5*(2), 261-267.

Semagn, K., Beyene, Y., Babu, R., Nair S., Gowda, M., Das, B., Tarekegne A., Mugo S., Mahuku, G., Worku M., Warburton L. M., Olsen, M., & Prassana, B. M. (2015). Quantitative Trait Loci Mapping and molecular breeding for Developing stress resilient maize for Sub-Saharan Africa. *Crop Sci., 55*, 1-11. https://doi.org/10.2135/cropsci2014.09.0646

Sharma, K., & Misra, R. S. (2011). Molecular approaches towards analyzing the viruses infecting maize (*Zea mays* L.). *Journal of General and Molecular Virology, 3*(1), 1-17.

Shi, X. M., Miller, H., Verchot, J., Carrington, J. C., & Vance, V. B. (1997). Mutations in the Region Encoding the Central Domain of Helper Component-Proteinase (HC-Pro) Eliminate Potato Virus X/Potyviral Synergism. *Virology, 231*, 35-42. https://doi.org/10.1006/viro.1997.8488

Wangai, A. W., Redinbaugh, M. G., Kinyua, Z. M., Miano, D. W., Leley, P. K., Kasina, M., Mahuku, G., Scheets, K., & Jeffers. (2012). First Report of Maize chlorotic mottle virus and Maize Lethal Necrosis in Kenya. *Plant Disease, 96*, 1582. https://doi.org/10.1094/PDIS-06-12-0576-PDN

Wilcoxson, R. D., Skovmand, B., & Atif, A. H. (1975). Evaluation of wheat cultivars for ability to retard development of stem rust. *Annual Applied Biology, 80*, 275-281. https://doi.org/10.1111/j.1744-7348.1975.tb01633.x

Wu, L., Wang, S., Chen, X., Wang, X., Wu, L., & Zu, X. (2013). Proteomic and Phytohormone Analysis of the Response of Maize (Zea mays L.) Seedlings to Sugarcane Mosaic Virus. *PLoS ONE, 8*(7), e70295. https://doi.org/10.1371/journal.pone.0070295

Xu, M. L., Melchinger, A. E., & Lübberstedt, T. (2000). Origin of Scm1 and Scm2 – two loci conferring resistance to sugarcane mosaic virus (SCMV) in maize. *Theor Appl Genet, 100*, 934-94. https://doi.org/10.1007/s001220051373

Yang, Z. N., & Mirkov, T. E. (1997). Sequence and relationships of sugarcane mosaic and sorghum mosaic virus strains and development of RTPCR–based RFLPs for strain discrimination. *Phytopathology, 87*, 932-939. https://doi.org/10.1094/PHYTO.1997.87.9.932

Zambrano, J. L., Francis, D. M., & Redinbaugh, M. G. (2013). Identification of resistance to *Maize rayado fino virus* in maize inbred lines. *Plant Dis., 97*, 1418-1423. https://doi.org/10.1094/PDIS-01-13-0037-RE

Zambrano, J. L., Jones, M. W., Brenner, E., Francis, D. M., Tomas, A., & Redinbaugh, M. G. (2014). Genetic analysis of resistance to six virus diseases in a multiple virus‐resistant maize inbred line. *Theor Appl Genet, 127*, 867-880. https://doi.org/10.1007/s00122-014-2263-5

Journal of Plant Studies; Vol. 6, No. 2; 2017
ISSN 1927-0461 E-ISSN 1927-047X
Published by Canadian Center of Science and Education

Effects of *Piliostigma reticulatum* on the Vegetation Dynamic in Sudanian Zone of Burkina Faso

Barthélémy Yélémou[1], Abdoulaye Tyano[2], Babou André Bationo[3], Bassiaka Ouattara[4], Jonas Koala[5] & Jeanne Millogo Rasolodimby[6]

[1]Institut de l'Environnement et de Recherches Agricoles (INERA)-Saria, Département Gestion des Ressources Naturelles et Systèmes de Production (GRN/SP), BP 10 Koudougou, Burkina Faso

[2]Centre Universitaire Polytechnique de Dédougou (CUPD), Université Ouaga I, Pr Joseph Ky Zerbo, Ouagadougou, 03 BP 7021 Ouagadougou 03, Burkina Faso

[3]Institut de l'Environnement et de Recherches Agricoles (INERA), Département Environnement et Forêts (DEF), 01 BP 476 Ouagadougou 01, Burkina Faso

[4]Centre Universitaire Polytechnique de Fada N'Gourma, Université de Ouagadougou, 03 BP 7021 Ouagadougou 03, Burkina Faso

[5]Institut de l'Environnement et de Recherches Agricoles (INERA)-Saria, Département Environnement et Forêts (DEF), BP 10 Koudougou, Burkina Faso

[6]Université Ouaga I, Pr Joseph Ky Zerbo, 03 BP 7021 Ouagadougou 03, Burkina Faso

Correspondence: Barthélémy Yélémou, Institut de l'Environnement et de Recherches Agricoles (INERA)-Saria, Département Gestion des Ressources Naturelles et Systèmes de Production (GRN/SP), BP 10 Koudougou, Burkina Faso. Tel: 226-7052-9060. E-mail: yelbart@hotmail.com

Received: March 23, 2017 Accepted: June 23, 2017 Online Published: July 20, 2017

doi:10.5539/jps.v6n2p77 URL: https://doi.org/10.5539/jps.v6n2p77

Abstract

This study aims at identifying the effect of *P. reticulatum* on the vegetation regeneration dynamic in Sudanian fallows of Burkina Faso. Two fallows of about twenty years old have been considered. The point quadrat method was used for herbaceous inventory. Aboveground biomass has been estimated. Moreover, effect of *P. reticulatum* on the regeneration of others woody species has been studied under, at the limit and out of the shrub canopy. In north Sudanian zone, inventory recorded 39 herbaceous species of which 23 species under the canopy and 16 in open grassland, distributed in 12 families and 22 genera. In south Sudanian zone, species diversity is 41 species from which 23 under the canopy and 18 out of, spread in 16 families and 26 genera. Species higher than 80 cm have been observed only under *P. reticulatum* canopy in south and north Sudanian zone. In addition, no species of striga met in open sunlight has been observed under the shrub canopy. East and West directions recorded the important proportions of species with individuals belonging to the stratum superior to 100 cm (3.13 and 4.81 % in north direction, 1.47 and 1.73% in south directions).

Keywords: *Piliostigma reticulatum*, dynamic, trees, herbaceous, Burkina Faso

1. Introduction

Piliostigma reticulatum is protected from cuts for decades in agricultural landscape of the central plateau of Burkina Faso (Yélémou, Bationo, Yaméogo, & Millogo-Rasolodimby, 2007). At the beginning of the rainy season, its leaves are frequently cut to serve as mulch in the crusty area in the fields (Yélémou et al., 2007) while the pods are harvested by shepherds to feed cattle at the end of rainy season. *P. reticulatum* is subjected to an increasing anthropization due to its high presence in the agricultural landscape in Sahelo-Sudanian zone of Burkina Faso.

During these last years with regression of traditional agroforestry species due to climatic risks, excessive exploitation, and their low ability to regenerate, *P. reticulatum* is more and more adopted by the populations of the central plateau as agroforestry species (Yélémou et al., 2007). Competition relationship between trees and herbaceous has been often reported in functioning models and management of savanna (Akpo & Grouzis, 2009). Several authors showed that in semi-arid areas, tree promote not only climatic factors but increase also diversity

of woody regeneration and the diversity and the production of herbaceous stratum (Apko, Banoin & Grouzis, 2003; Akpo & Grouzis, 2009; Diallo et al., 2015). Nevertheless, the effect of tree on the herbaceous dynamic and woody regeneration could depend on the rainfall characteristic of the study site. For Yélémou, Yameogo, Bationo, Millogo/Rasolodimby et Hien, (2008), *P. reticulatum,* due to its bushy nature and its abundant leave biomass, contributes to reduce water and wind erosion and promotes vegetation regeneration. *P. reticulatum* should be of great importance in the sustainable management policy of soils in the Sahelo-sudanian zones through a better understanding of its function in the mechanism of environmental regeneration.

This study, conducted in two Sudanian ecosystem of Burkina Faso (north Sudanian and south Sudanian), has for goal to determine on one hand, the influence of tree on species structure of the herbaceous layer and the above ground phytomass production, and on the other hand on the state of woody regeneration.

2. Material and Methods

2.1 Study Sites

The study is carried out both at the research station of INERA in Saria, located in north Sudanian zone and at Sala in south Sudanian climatic zone in Burkina Faso (Figure 1)

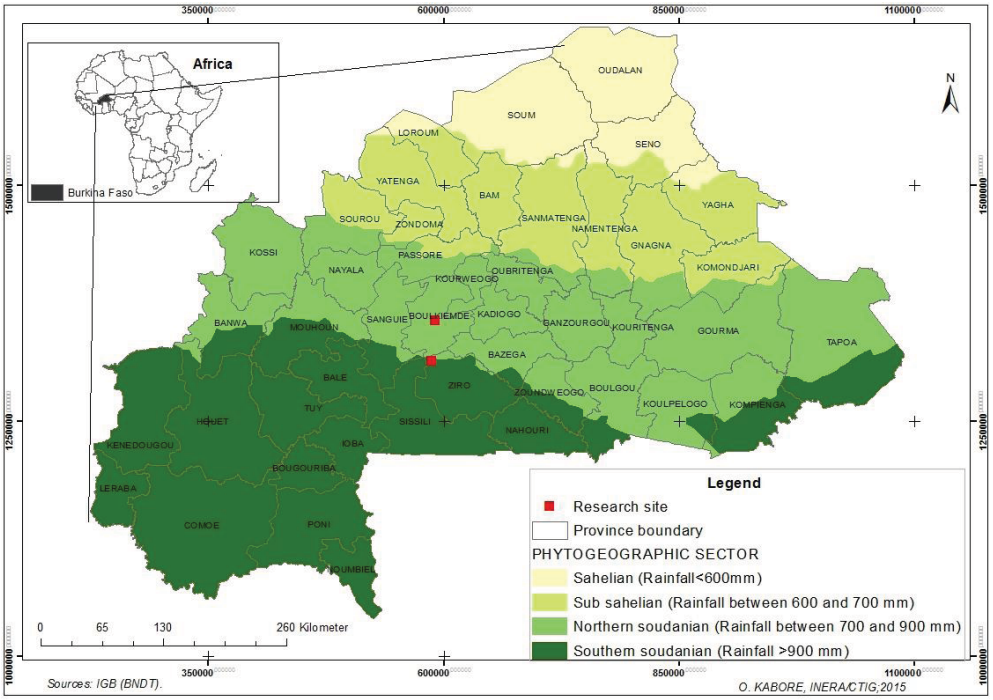

Figure 1. Site location map

North Sudanian zone is characterized by a long dry season from October to April (7 months) and a short rainy season from May to September (5 months). Harmattan wind is cold and dry and blows during the dry season and the monsoon is the dominant wind during the rainy season. Annual rainfall in the past decade ranged between 626.4 and 980.7 mm with an average of 852.03 mm in Saria.

South Sudanian part is characterized by a dry season from November to April (6 months) and a rainy season from May to October (six (6) months). The prevailing wind in rainy season is the continental trade wind.

The temperature is about 35.8°C at Saria and 28°C at Sala (Yélémou et al., 2007). In Saria, maximum temperature (40 °C) is reached in March-April and the minimum (15 °C) in December. In the south Sudanian zone, The thermal amplitudes in south Sudanian zone is relatively lower than the one of north Sudanian due mostly to vegetation cover which forms a buffer system on the climate, reducing temperature

The site in Saria is a protected fallow with monospecific vegetation of *P. reticulatum*, while in Sala site it is an open fallow, with multispecies vegetation. The two fallows are over 20 years old. Vegetation in south Sudanian zone is characterized by *Isoberlinia doka* Craib & Stapf, which forms tree stands in woodlands of Burkina Faso. Savanna woodlands in Sala are dominated by *Detarium microcarpum* Guill.&Perr., *Combretum glutinosum* Guill. & Perr., *Gardenia erubecens* Stapf. & Hucth. et *Parina ricuratellifolia*. The graminaceae stratum is dominated

by *Andropogon gayanus* Kunth, *Andropogon ascinodis* C.B.Clarke in old fallows, *Eragrostis tremula* Hochst. *Penissetum pedicellutum* Trin, *Dactyloctenium aegyptium*, *Andropogon pseudapricus* Stapf., *Loudetia togoensis* (Pilg.) C.E.Hubb., in recent fallow.

2.2 Floristic Inventory of Herbaceous Stratum

The floristic inventory of the herbaceous stratum was achieved using the method of quadrat point of Godron et al., (1969). This method is recognized for its accuracy, easness use and its non-destructive nature of natural environment.

In practice, it consisted to check off all the herbaceous species at the vertical of regular points (each 20 cm) along of a graduate twine of 20 m long above the grass layer. Then, for each line, we have 100 lecture points. Several species can be counted by lecture point, but by convention, each species has been counted only one time. Then, this alows to characterize the importance of each species in the vegetation layer measuring its cover by the obervation of frequencies (floristic analysis). Herbaceous inventory has been conducted on four lines in each site from which two lines crossed at least two *P. reticulatum* canopy and the others two lines didn't cross any *P. reticulatum* crown. The lines were randomly spread following the prescription of Boudet (1984). Then, for each site we had a sample of 400 lecture points. The number of lecture points is important for the accuracy of the results, then the exactness of the sampling is obtained by the calculation of the confidence interval (I.C) of which 5% value allows to eliminate random effect (Boudet,1984).

$$I.C = \pm\sqrt{\frac{n\,(N-n)}{N^3}}$$

N = cumulative number of contacts of all the species

n= cumulative number of contacts of the dominant species.

The inventories were achieved at the beginning of October. This period corresponds to active vegetation, heading-fructing of dominant species and when the species are most discernible (Sawadogo, 2009).

2.2.1 Study of the Vertical Structure of Herbaceous Cover

Vertical structure allows to visualize the differents stand layers. Study of the stratification of herbaceous cover was achieved through plot method. So, 9 square plots of 1 m^2 each were designed under each shrub of *P reticulatum* (Fig 2). Plots were replicated 4 times and were designed as follow:

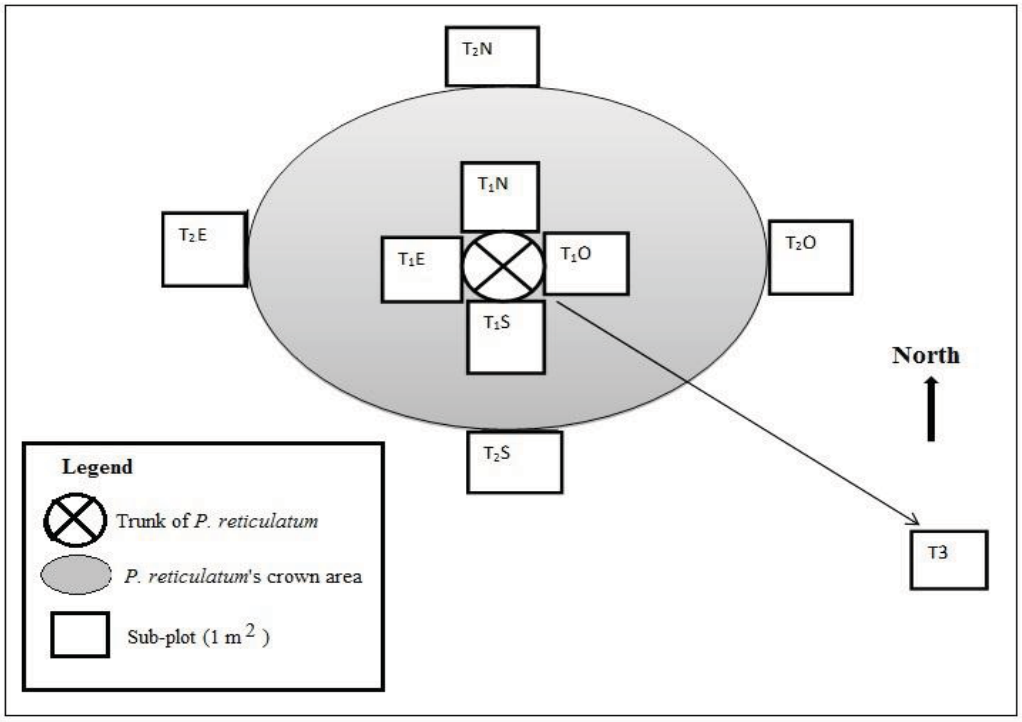

Figure 2. Experimental design for the study of vertical structure of herbaceous

P_1E: under *P. reticulatum* shrub, East side, **P_1O**: under *P. reticulatum* shrub, West side, **P_1N**: under *P. reticulatum* shrub, North side, **P_1S**: under *P. reticulatum* shrub, South side, **P_2E**: at the limit of the crown of *P. reticulatum,* East side, **P_2O**: at the limit of the crown of *P. reticulatum,* West side, **P_2N**: at the limit of the crown of *P. reticulatum,* North side, **P_2S**: at the limit of the crown of *P. reticulatum,* South side, **P_3**: out of the crown of *P. reticulatum*

P_1, under *P. reticulatum* shrub; the plot P_1 has 4 variantes that are P_1E, P_1O, P_1N and P_1S (for the four cardinal directions East, West, North and South respectively) ;

P_2, at the limit of the canopy of *P. reticulatum* shrub; the plot P_2 has also 4 variantes P_2E, P_2O, P2N and P_2S (for the four cardinal directions East, West, North and South respectively)

P3, out of the crown of *P. reticulatum* shrub, in open sunligth

In each plot, herbaceous species were recorded according to the following stratums : 0-20 cm, 20-40 cm, 40-60 cm, 60-80 cm, 80-100 cm and > 100 cm

2.2.2 Assement of the Aboveground Phytomass

The assesment of herbaceous biomass was achieved through complete harvest method (Ouédraogo, 2003). Herbaceous in the square plots of 1 m^2 have been cut, and a manual screening allows to separate the different herbaceous species.

Each species sample was immediatly weighted using an electronic scale (Mettler PM 4000, d= 0,01, e =0,1) in order to determine its contribution to the herbaceous biomass in the corresponding pot. Samples were packed in biodegradable plastic bag and labeled. Then, sample were sun dry and afterward oven dry until constant dry weight and values of dry matter have been determined.

The quantities of dry phytobiomass were afterward gathered into three forage types according to the following biological forms:

-the annual graminaceae (Ga) perennial graminaceae (Gv): they constitute the most abundant forage type in tropical regions (Daget & Godron, 1995);

- the leguminous (Le) : they are characterised by their ability to fixe atmospheric nitrogen and so by a great nitrogen content;

- and at last the others species (Au) or forbs

The assesment of phytobiomass was achieved at first October and in the same plots that allow studying the vertical herbaceous structure. This period corresponds to the phenological stage of maximal production of biomass. Likewise, forage are mown at this period. A total of 36 plots have been installed in each site according to Boudet (1984) who recommands a minimum of 20 plots to obtain an accuracy of 5%.

Study of woody regeneration

The inventories of woody regeneration have concerned four (04) *P. reticulatum* shrub. For each shrub, nine (09) square plots of 1 m^2 were designed as the plots used for the study of vertical structure of herbaceous (fig 2). In these plots, all the woody species in regeneration have been recorded. Dendrometric variables like total height, collar diameter, diameter of the great crown and diameter of the small crown have been recorded. Measures of height have been achieved using a pole as well as measure of great crown and small crown. The collar diameter was recorded with a vernier calliper.

Statistical analysis

The following variables, characteristic of the vegetation, defined by Daget and Poissonnet (1971) have been determined.

The species richness (S) that represents the number of species met in a given area.

The species frequence of species i (FSi) that corresponds to the ratio of the number of points where species I has been recorded (Boudet, 1984) to the total number of points.

The centesimal frequence of the species i (FCi) that corresponds to the ratio in percentage of the species i frequence and the number of point (N) sampled. It expresses the species cover corresponding to proportion of soil surface covered by a vertical projection of aboveground organs of this species:

$$\mathbf{FC_i} = \frac{FSi}{N} X100$$

The specific contribution of the species i (CS_i) is defined as the ratio of FCi to the sum of FCi of all the species recorded. It expresses the contribution of the species to the aboveground congestion.

The formula is:

$$CS_i = \frac{FCi}{\sum FCi}$$

A species is considered as productive if its specific contribution is higher than 5% (Sawadogo, 1996). These species contribute significantly to the global recovery of the vegetation and to the phytomass production.

Variables of species diversity have been computed as:

- Shannon diversity index (H), Piélou equitability index (E): it represents the expression of the balance in the repartition of individuals among species. Its value tends to 0 when there is a predominance phenomenon and to 1 when all the species have almost the same trend.

$$H = -\sum_{i=1}^{N} pi.lnpi \qquad Hmax = lnN \qquad E = \frac{H}{H\,max}$$

pi = relative proportion of the species (i), N = number of species, ln = Neperian Logarithm

In the order to appreciate the stability of the herbaceous grouping, "J" curve of Raunkaier (Savadogo, 2007) have been represented. This curve informs on the stability of the flora. The knowledge of the number of species and their frequencies allow establishing this curve by grouping the species in the five classes of frequencies as below:

A = 0-20%, B = 21-40%, C = 41-60%, D = 61-80%, E = 81-100%. The grouping is said:

stable if A>B>C≥ ≤D<E, this corresponds to a unimodal curve ;

disturbed if this equality isn't respected, the curve is bimodal or plurimodal.

In addition, data of herbaceous biomass have been subjected to a one-way ANOVA using the test of least squares of Fischer (LSD) in order to compare the means of the different variables under and out of the crown of *P. reticulatum* at 5% level. The statistical analysis have been achieved using XLSAT sotfware, 2007 edition.

3. Results

3.1 Characteristic of Grass Layer of P. Reticulatum Formations

3.1.1 Floristic Composition

In the north Sudanian zone, 39 herbaceous species belonging to 12 families and 22 genera were inventoried. The family of graminaceae with 14 species corresponding to 35% of the species is the most represented followed by Fabaceae family (15%), Cesalpiniaceae family and Acanthaceae family each 7.5%. The less represented families are Polygalaceae, Scrofulariaceae and Sterculiaceae, each family with 2.5% of inventoried species.

Under *P. reticulatum* crowns, 23 herbaceous species belonging to 19 families have been identified whereas 16 species belonging to 9 families have been identified out of the crown, at open grassland. The family of graminaceae is most dominant under and out of the crown of *P. reticulatum* where its represents 33.33% and 37.5% recovery rate respectively. However, it is recorded that Papilionaceae family represented under the crown of *P. reticulatum* by Alysicarpus ovalifolius (Schum Et Thon.), and Indigofera Suffructicosa Mill., is absent out of the crown. On the contrary, the family of Scropheulariaceae represented out of the crown by Striga hermontica (Del.) Benth., is absent under the crown of *P. reticulatum*.

A total of 41 grass species belonging to 16 families and 26 genera have been inventoried in the south Sudanian zone. In this zone, it is also the family of graminaceae that is dominant with 36.58% of the species. Afterward, follow families of Acanthaceae, Fabaceae and Malvaceae each corresponding to 7.32% of the species. The less represented families are Cesalpiniaceae, Asteraceae, Cyperaceae, and Labieae with 2.44% of species each.

Grass species richness out of the canopy of *P. reticulatum* is 18 whereas it is 23 under the crown. The 23 species inventoried under the crown belongs to 14 families and the 18 species inventoried out of the crown to 11 families. Three families under the crown have not been observed out of the crown: the family of Asteraceae with *Aspilia bussei* O. Hoffm. Elmusch, the family of Labiaea with *Englerastrum gracilium* Th. C.E. Fries and the family of Polygalaceae with *Polygala arenarea* Willd. On the contrary, the families of Cyperaceae with *Cyperus iria* Linn., of Oxalidaceae with *Biophyton petertianum* Klotzoch in Peters are present out of the crown and absent under the crown of *P. reticulatum*.

Table 1 presents the productive species, their specific frequencies (FSi), their centesimal frequencies (FCi) and their specific contribution (CSi). Under the crown of *P. reticulatum*, in the north Sudanian zone, six species are productive from which the most important are *Zornia glochidiata* Reighb.ex DC., and *Pennisetum pedicelatum* Trin., with recoveries of 54% and 45.5% and CSi of 25.84% and 21.77% respectively. The others productive species are: *Microchloa indica* Beauv., *Tephrosia verticilata* Bak. and *Stylosanthes erecta* with recoveries of 33.5 ; 14 and 13% and CSi of 16.03 ; 6.69 and 6.22% respectively. From herbaceous under the crown of *P. reticulatum*, four species are productive from which 2 have a high productivity, *Microchloa indica* and *Zornia glochidiata* with 36.69% and 31.26% of recovery and present 94.5% and 80.5% of CSi respectively. Afterward, we have *Andropogon ascinodis* C.B. CI and *Stylosanthes erecta* with recoveries of 23 and 19.5% and CSi of 8.93 and 7.57%. Under the crown of *P. reticulatum* in south Sudanian zone, four species are the most productive, *Tephrosia verticilata* and *Microchloa indica* with recoveries of 65% and 53% and CSi of 31.4% and 25.66 % respectively. *Pennisetum pedicelatum* and *Setaria pumula* (poïr.)Roem. et Schult are the species that follow with CSi of 11.62 and 10.65% and recoveries of 24 and 22% respectively. Out of the crown, *Microchloa indica*, *Tephrosia verticilata* and *Setaria pumula* (poïr.)Roem. et Schult. with respectively recoveries of 72%, 59.5% and 50.5% and CSi of 32.57% ; 26.92%, 22.85% are the most productive

Table 1. Frequencies and specific contributions of producing species according to the treatment and the site.

Sites	Nbr of species	Producing species	F.B	FSi	Fci (%)	Csi (%)
		Zornia glochidiata	Le	108	54	25.84
		Pennisetum pedicelatum	Ga	91	45.5	21.77
		Microchloa indica	Ga	67	33.5	16.03
SH-NS	23	*Stylosanthes erecta*	Le	28	14	6.69
		Tephrosia verticilata	Le	26	13	6.22
		Microchloa indica	Ga	189	94.5	36.69
		Zornia glochidiata	Le	161	80.5	31.26
HH-NS	16	*Andropogon ascinodis*	Gv	46	23	8.93
		Stylosanthes erecta	Le	39	19.5	7.57
		Tephrosia verticilata	Le	130	65	31.4
SH-SS	23	*Microchloa indica*	Ga	106	53	25. 66
		Pennisetum pedicelatum	Ga	48	24	11. 62
		Setaria pumula	Ga	44	22	10. 65
		Microchloa indica	Ga	144	72	32.57
HH-SS	18	*Tephrosia pedicelleta*	Le	119	59.5	26.92
		Setaria pumula	Ga	101	50.5	22.85

FB: Biologica form; **FS_i**: Specific frequence; **FC_i**: Centesimal frequence; **CS_i: Specific** contribution; **Ga** : annual graminaceae; **Gv** : perennial graminaceae; **Le** : leguminous ; **SH-NS**: under the crown of *P. reticulatum* in north Sudanian zone, **HH-NS** :out of the crown of *P. reticulatum* in the north Sudanian zone, **SH-SS** : under the crown of *P. reticulatum* in south Sudanian zone, **HH-SS** : out of the crown of *P. reticulatum* in south Sudanian zone

3.2 Floristic Diversity

Diversity index (Shannon-Wiener index, Simpson index and equitability index of Piélou) are presented in relation to the phytogeographical zone (Table 2).

Table 2. Floristic diversity according to the phytogeographical zone and treatment

Area/Treatments	**Number of species**	**H' (Shannon-Wiener)**	**Hmax**	**R (Pielou)**
SH-NS	23	2.28	2.77	0.72
HH-NS	16	1.80	3.17	0.65
SH-SS	23	2.07	3.13	0.66
HH-SS	18	1.73	2.89	0.60

SH-NS: under the crown of *P. reticulatum* in north Sudanian zone, **HH-NS** : out of the crown of *P. reticulatum* in the north Sudanian zone, **SH-SS** : under the crown of *P. reticulatum* in south Sudanian zone, **HH-SS** : out of the crown of *P. reticulatum* in south Sudanian zone

Values of Shannon-Wiener index varied from 1.73 to 2.28. The index is higher under the crown of *P. reticulatum* compare to its value out the crown of *P. reticulatum*.

3.3 Structure

The forage spectrums present large variations according to the phytogeographical area (Fig 3).

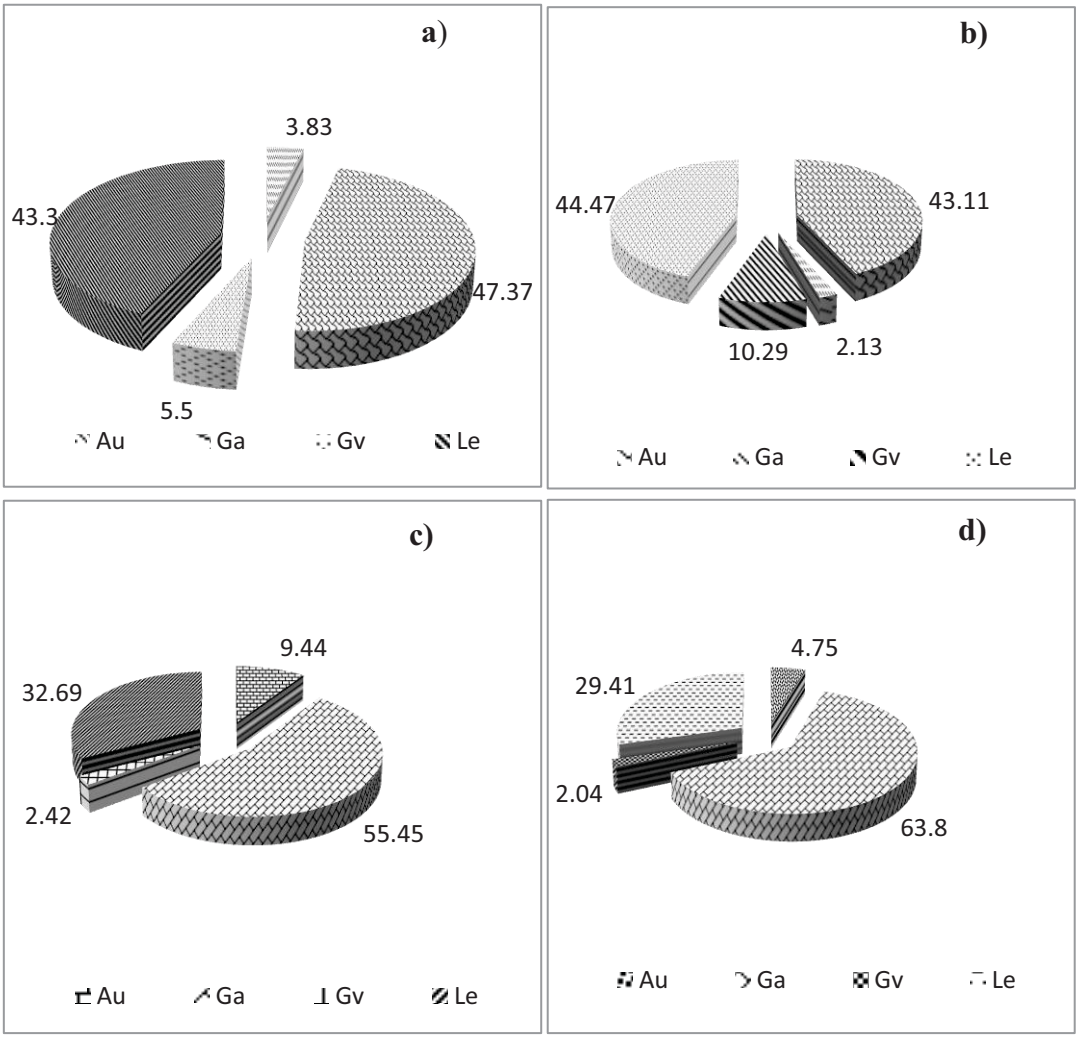

Figure 3. forage spectrums (a) under canopy and (b) out of canopy in north sudanian zone ; (c) under canopy and (d) out of canopy in south sudanian zone

In the same phytogeographical area, fodder types present low variation of CSi. Curves "J" of Raunkiaer, in the different climatic zones and independently to the treatment under and out of the crown, present variations linked to the number of species in the class of frequency 0 to 20% (Fig. 4). However, they all indicate the stability of the grass cover of *P. reticulatum* formations.

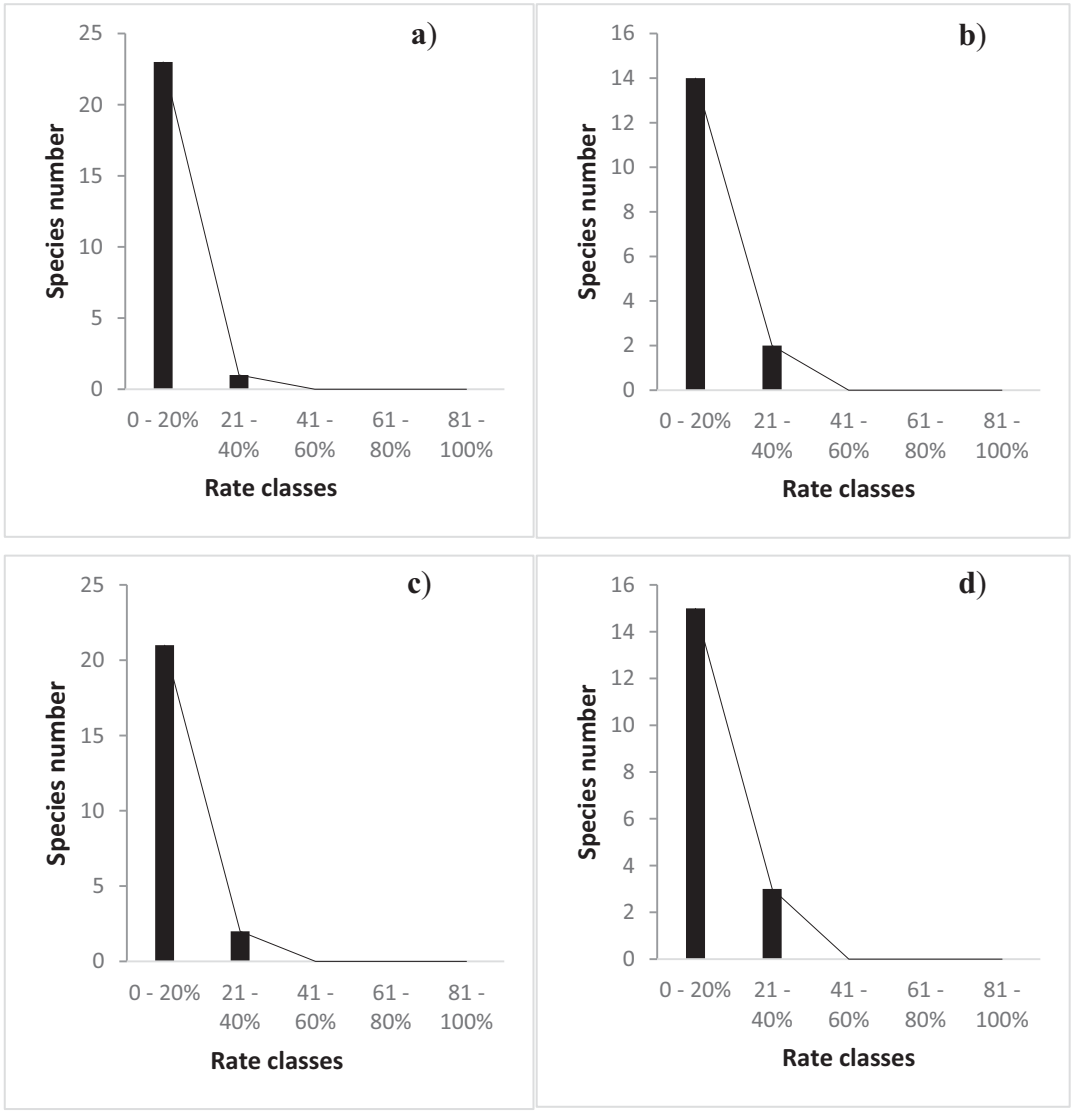

Figure 4. Raunkiaer J curve (a) under canopy and (b) out of canopy in north sudanian zone ; (c) under canopy and (d) out of canopy in south sudanian zone

The analysis of forage spectrum shows the dominance of annual graminaceae on all the two sites independently to the treatment except that out of the canopy of *P. reticulatum* at Saria where leguminous have a slight dominance. Among the 16 graminaceae recorded, 13 are annual representing 81% of the species encountered. Under the crown of *P. reticulatum* in the north Sudanian zone, a total of 23 herbaceous species have been recorded. The leguminous are the most represented (8 species) follow by the annual graminaceae (7 species). Nevertheless, annual graminaceae present the higher CSi of 47.37% compared to 43.3% for leguminous. The high CSi of Leguminous is largely due to *Zornia glochidiata* (with a CS_i of 25.84%), follow by *Tephrosia pedicelleta* and *Stylosanthes erecta* (6.22 and 6.70% of CS_i respectively). For the annual graminaceae, the high value of CSi is due to *Pennisetum pedicelatum* and *Microchloa indica* (21.77 and 16.02% respectively). The perennial graminaceae and forbs recorded the lowest CSi with 5.5 and 3.83% respectively. The grass layer of this biotope is stable as showed by the unimodal "J" curve of Raunkiaer.

Out of the crown of *P. reticulatum* in the north zone, five of the species recorded are annual graminaceae and five are leguminous. Afterward, forbs are the most represented with 4 species.

Only two species recorded are perennial graminaceae. Leguminous and annual graminaceae have almost the same CSi, 44.47% and 43.11% respectively. *Zornia glochidita* is responsible of the high contribution of leguminous whereas the high contribution of annual graminaceae is due to *Microchloa indica.* The flora of these areas is stable according to the unimodal "J" curve of Raunkiaer. In the south Sudanian zone, the forage

spectrums show a clear dominance of annual graminaceae.

Under the crown of *P. reticulatum,* 8 of the 23 species inventoried are annual graminaceae. They have a CSi of 54.45% from which *Microchloa indica* and *Pennisetum pedicelatum* (25.66 and 11.62% of CSi respectively) are the most represented. Afterward, we have leguminous with species and a CSi of 32.69% mostly due to *Tephrosia pedicelleta* which counts alone a CS_i of 31.47%. The leguminous are follow by forbs which count 9 species and a CSi of 9.44% showing that a biological form can be presented by high number of species and have a low CSi. Perennial graminaceae are the lowest represented (in term of species) and have a CSi of 2.42% for 3 species.

Annual graminaceae dominate out of the crown of *P. reticulatum* with 8 species among 18 inventoried and a CSi of 63.8%. This high value of CSi is due to *Microchloa indica* which present a CSi of 32.58%. Annual graminaceae are followed away by the leguminous with 3 species and a CSi of 29.41%. The perennial graminaceae are low represented with only 2 species and a CSi of 4.75%. The forbs are represented by 5 species but present a low CSi (2.04%).

3.4 Grass Height Stratification

The herbaceous distribution according to vertical structure shows that species having individuals with height higher than 80 cm are only represented under the canopy of *P. reticulatum* independently to the phytogeographic area (Fig. 5).

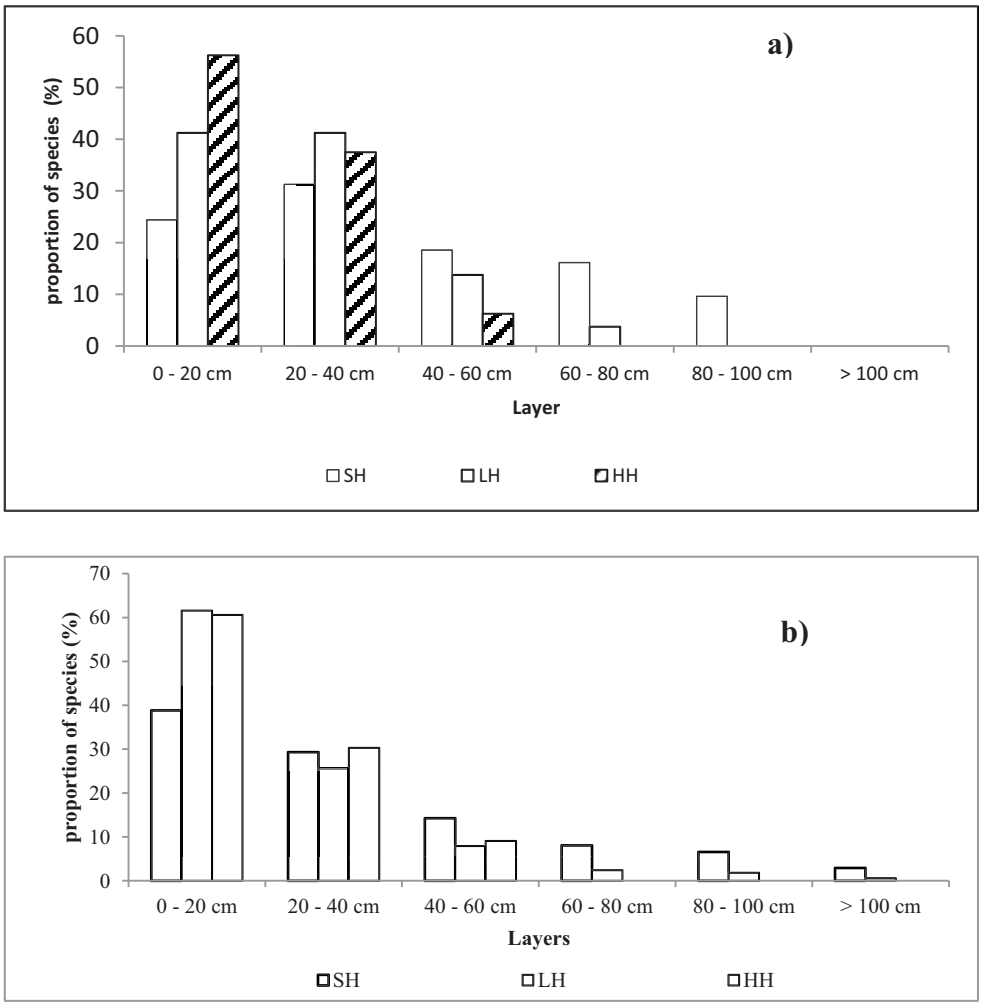

Figure 5. Distribution of herbaceous according to height classes in north (a) and south (b) Sudanian zone.

SH: under the crown of *P. reticulatum*, **LH** : at the limit of the crown of P. reticulatum, **HH** : out of the crown of *P. reticulatum*

Under the *P. reticulatum* shrub, 24.4 ; 31.27 ; 18.56 ; 16.15 and 9.62 % of the species belong to the layers 0 – 20 ; 20 – 40 ; 40 - 60 ; 60 – 80 and 80 – 100 cm respectively in the north Sudanian zone. In the plots located at the

limit of the cover of *P. reticulatum,* the proportions of species are 41.25; 41.25; 13.75 and 3.75 % for the layers 0 – 20; 20 – 40; 40 - 60 et 60 – 80 respectively.

At open grassland, only low layers are represented: 56.25; 37.5 and 6.25% of species for the layers 0 – 20; 20 – 40; 40 - 60 cm respectively. No herbaceous with a higher than 60 cm has been observed in the control plots (out of the crown of *P. reticulatum*). Under the *P. reticulatum* shrub, the cardinal directions seem to have an effect on the herbaceous height (Table 3). The East and West directions record the higher proportions of species presenting individuals belong to the layer higher than 100 cm (3.13 and 4.81% compared to 1.47 and 1.73% for the North and the South directions respectively).

Table 3. Proportion of the different grass layer (%) under *P. reticulatum* shrub in the north Sudanian zone

Treatments / Layer	P1E	P1O	P1N	P1S
0 – 20 cm	26.74	28.36	20	22.06
20 – 40 cm	24.42	20.90	40	41.18
40 – 60 cm	20.93	19.40	17.14	16.18
60 – 80 cm	17.45	19.40	14.29	13.23
80 – 100 cm	10.46	11.94	8.57	7.35

P_1E: under the *P. reticulatum* shrub, East side, **P_1O**: under the *P. reticulatum* shrub, West side, **P_1N**: under the *P. reticulatum* shrub, north side, **P_1S**: under the *P. reticulatum, south side*.

In the south Sudanian zone, independently to the treatment (under and out of the cover of *P. reticulatum*), the proportion of individuals decreases from low layers to the high layers. Under the *P. reticulatum* shrub in the south Sudanian zone 38.83 ; 29.31 ; 14.28 ; 8.06 ; 6.59 ; 2.93 % of the species have individuals belonging to the layers 0 – 20 ; 20 – 40 ; 40 - 60 ; 60 – 80 ; 80 – 100 and superior to 100 cm respectively. The layers 60 – 80 and 80 – 100 cm are not observed in the plots under the canopy of *P. reticulatum.* The herbaceous higher than 100 cm have only been observed in plots located under the crown of *P. reticulatum.* The cardinal direction has an effect on the height of herbaceous under the crown of *P. reticulatum.* The proportion of species having individuals reaching 100 cm height are 3.13 and 4.81% respectively for the East and West direction compared to 1.47 and 1.73% for the north and south directions respectively (Table 4).

Table 4. Proportion of different grass layers (%) under the *P. reticulatum* shrub in the south Sudanian zone

Treatments / Layers	P1E	P10	P1N	P1S
0 – 20 cm	50	28.92	38.23	41.37
20 – 40 cm	29.69	28.92	30.88	27.58
40 – 60 cm	7.80	19.28	16.19	12.08
60 – 80 cm	4.69	8.43	8.82	10.35
80 – 100 cm	4.69	9.64	4.41	6.89
>100 cm	3.13	4.81	1.47	1.73

P_1E: under the *P. reticulatum* shrub, East side, **P_1O**: under the *P. reticulatum* shrub, West side, **P_1N**: under the *P. reticulatum* shrub, north side, **P_1S**: under the *P. reticulatum, south side*.

3.5 Effect of P. reticulatum on the Production of the Herbaceous Phytomass

In the north Sudanian zone, the evolution of herbaceous phytomass varies according to the cardinal direction (Table 5). In addition, if we consider the treatments under and out of the crown, in north Sudanian zone the production of phytomass is enhanced in T_1E and T_2E treatments at 524.18% and 63.39% respectively compared to their values recorded out of the crown (control). In south Sudanian zone, the evolution of the phytomass production according to the two treatments, under and out of the crown, is low. However, the trend is always the same, we have a better production under the canopy compared to the production at the limit of the crown.

Table 5. Aboveground production (g/m^2) under the shrub, at the limit and out of the cover of grass layer in the two sites

Aboveground biomass (g/m^2)		
Treatments	**North Sudanian zone**	**South Sudanian zone**
P_1E	477.5± 95.95 ^{c}	168.25 ±37.03 ^{ab}
P_1O	474.50 ± 111.95 ^{c}	218.00 ± 133.24 ^{ab}
P_1N	345.25 ± 139.83 ^{abc}	215.75 ± 81.50 ^{b}
P_1S	394.75 ± 93.95 ^{ab}	229.25 ± 70.06 ^{b}
P_2E	125.00 ± 19.86 ^{ab}	108.50 ± 56.44 ^{a}
P_2O	162.25 ± 19.84 ^{ab}	151.00 ± 37.04 ^{ab}
P_2N	161.00 ± 37.72 ^{ab}	179.25 ± 44.61 ^{ab}
P2S	132.50 ± 37.06 ^{ab}	149.00 ± 27.47 ^{ab}
P_3	76.50 ± 21.18 ^{a}	145.50 ± 61.22 ^{ab}
P > F	**0.0021**	**< 0.023**
Significativity	**S**	**s**

In the same phytogeographical area, values with the same are not significantly different at 5% level according to Fischer test. **P_1E** : under the *P. reticulatum* shrub, East side, **P_1O** : under the *P. reticulatum* shrub, West side, **P_1N** : under the *P. reticulatum* shrub, north side, **P_1S** : under the *P. reticulatum, south side,* **P_2E** : at the limit of *P. reticulatum* crown, East side, **P_2O** : at the limit of *P. reticulatum* crown West side, **P_2N** : at the limit of *P. reticulatum* crown north side, **P_2S** : at the limit of *P. reticulatum* crown south side, **P_3** : out of the crown of *P. reticulatum*

3.6 Effect of P. reticulatum on the Quality of Grass Phytomass

In the north Sudanian zone, plots under the crown of *P. reticulatum* show a clear dominance of annual graminaceae. They count for 79.89; 73.87; 76.25 and 69.60% in plots P_1E, P_1O, P_1N and P_1S respectively (Fig. 6). Afterward, we have leguminous which have the largest contributions 14.27; 11.69; 17.96 and 19.5% in plots P_1E, P_1O, P_1N and P_1S respectively. The forbs and the perennial graminaceae contribute very low to the composition of the abovegroung phytomass. In the plots located at the limit of the crown of *P. reticulatum,* the contribution of leguminous to the composition of herbaceous biomass become important. It is of 36.6; 32.35; 77.02 and 70.56% in the plots P_2E, P_2O, P_2N and P_2S respectively. So, it can be said that when we go away from the crown of *P. reticulatum,* the annual graminaceae decrease to the benefit of leguminous. This remark is confirmed in the control where 76.48% of the phytomass is constituted by leguminous.

In the south Sudanian zone, annual graminaceae have the largest contribution to total biomass independently to the treatment and the cardinal direction (Fig. 6). However, the contribution of leguminous progressively increases when we go away from the crown of *P. reticulatum.* The contribution is 16.79; 14.1; 17.56 and 29.29 % in plots P1E, P1O, P1N and P_1S respectively and reaches 33.87% in the plot P_2E and 29.89% for the control.

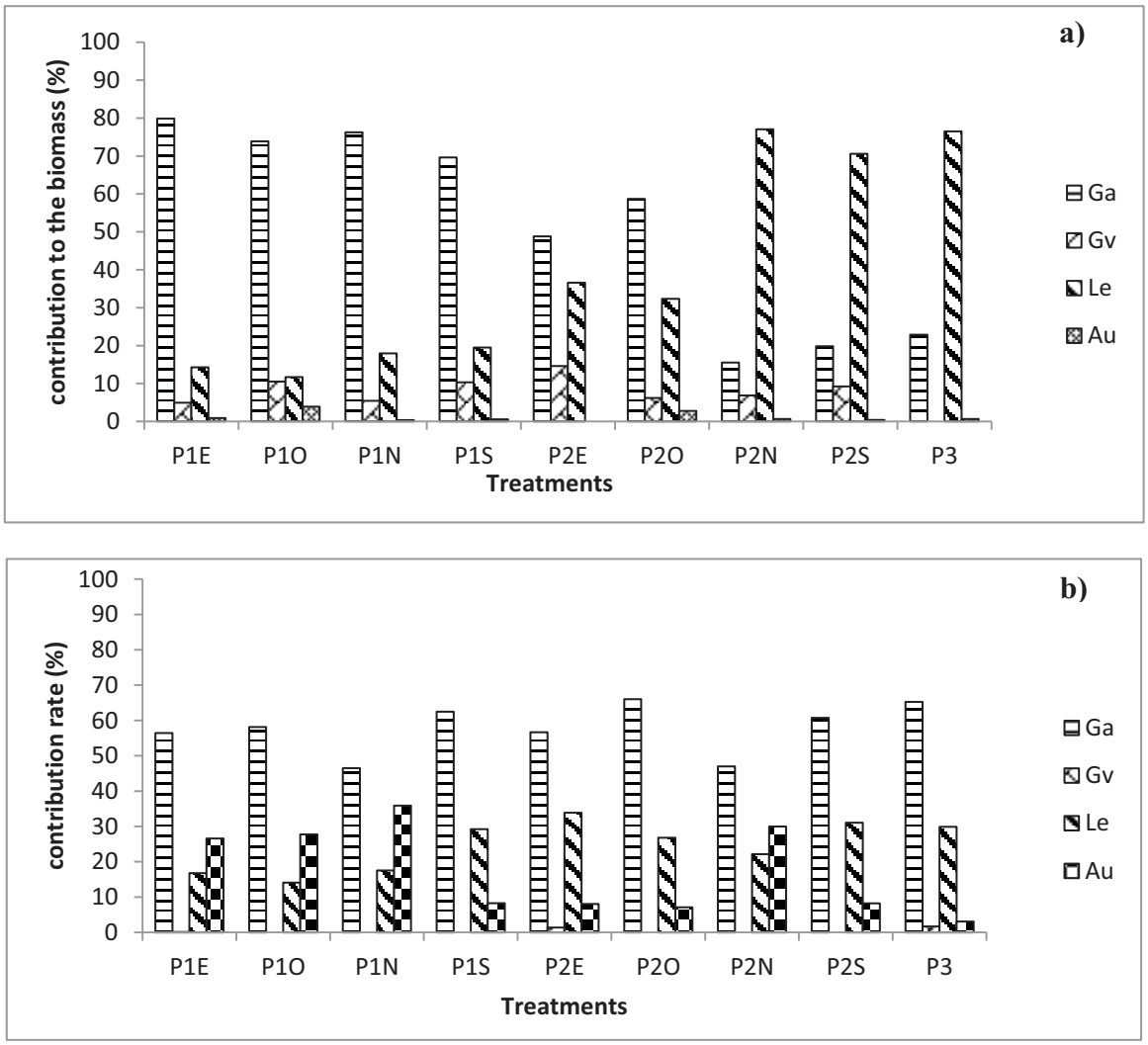

Figure 6. Contribution of forage species to vegetation biomass in the north (a) and south (b) Sudanian zone

P_1E: under the *P. reticulatum* shrub, East side, **P_1O**: under the *P. reticulatum* shrub, West side, **P_1N**: under the *P. reticulatum* shrub, north side, **P_1S**: under the *P. reticulatum, south side,* **P_2E**: at the limit of *P. reticulatum* crown, East side, **P_2O**: at the limit of *P. reticulatum* crown West side, **P_2N**: at the limit of *P. reticulatum* crown north side, **P_2S** : at the limit of *P. reticulatum* crown south side, **P_3**: out of the crown of *P. reticulatum,* **Ga**: annual graminaceae; **Gv** : perennial graminaceae; **Le**: leguminous, **Au:** forb

3.6 Effect of P. reticulatum on the Woody Regeneration

3.6.1 Diversity Index

The values of Shannon index varies from 0.69 to 1.87 (table 6). Independently to the Sudanian zone, the values of Shannon index under the cover of *P. reticulatum* are always higher compared to values recorded out of the cover (control). In the north Sudanian zone, the Shannon index is 1.3 under *P. reticulatum* shrub compared to 0.69 recorded out of the cover (control). The values are 1.71 compared to 1.27 respectively in the south Sudanian zone. The values of Piélou index vary from 1 to 0.56. The value of Piélou index out of the cover is always higher compared to which recorded under the cover. In the north Sudanian zone, it is of 1 out of the cover and 0.81 under the cover of *P. reticulatum.* It is of 0.56 and 0.92 under the shrub and out of the cover of *P. reticulatum* respectively in the south Sudanian zone.

Table 6. Diversity index of woody regeneration

Measures of diversity	SH-NS	LH- NS	HH-NS	SH-SS	LH-SS	HH-SS
H (Shannon Wiener)	1.3	0.69	0.69	1.71	1.87	1.27
R (Equitability of Piélou)	0.81	1	1	0.56	0.66	0.92

3.6.2 State of Woody Regeneration

In all the sites, woody species regeneration is most important under the crown of *P. reticulatum* compared to plots out of the crown (control). The most represented species in the regeneration are *Guiera senegalensis* J.F.Gmel., for the north Sudanian zone, *Dichrostachys cinerea* (L.) Wight & Arn., *Combretum glutinosum* Perr. et *Piliostigma reticulatum* (DC.) Hochst for the south Sudanian zone.

3.6. 3 Structure into Diameter Classes of Woody Regeneration

The distribution into diameter classes of young populations present an irregular trend according to the phytogeographic zone and the treatments (Fig. 7). In the north Sudanian zone, the look of the curve presents large variations between sites: reversed "J" under the crown, (L) at the limit of the crown and "J" out of the crown. Individuals with diameters higher than 15 mm have been only observed under the crown of *P. reticulatum.*

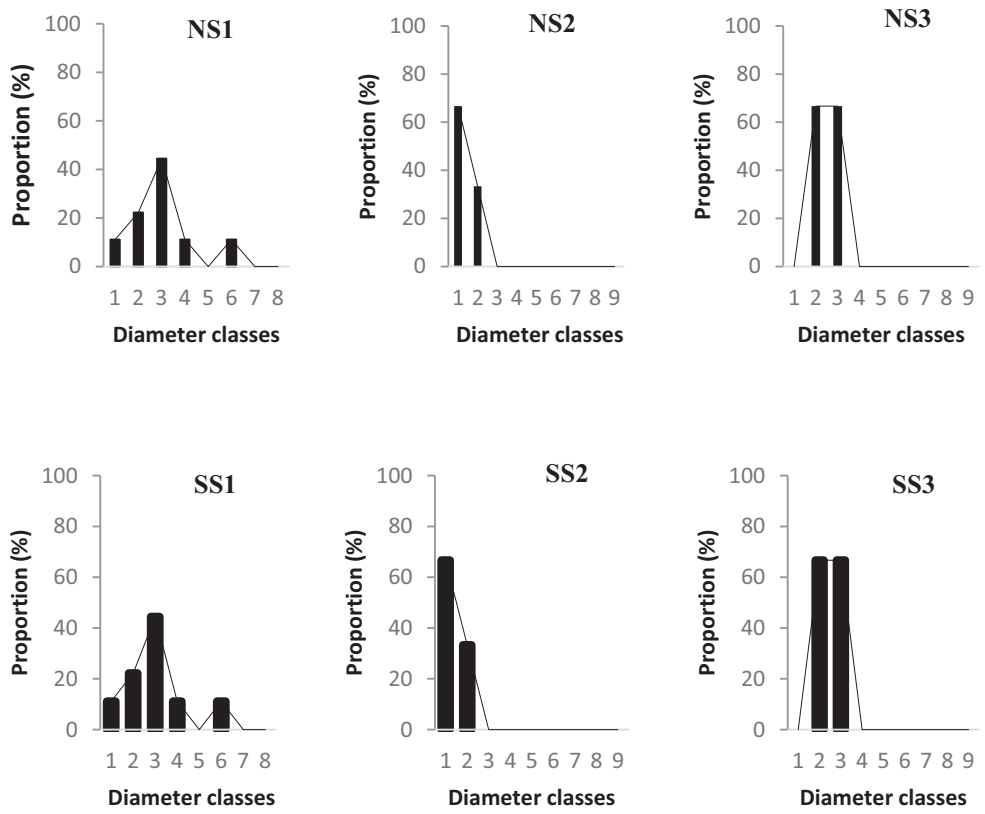

Figure 7. Collar diameter classes distribution of sapling under (1), at the limit (2) and out of the crown (3) in north and southern Sudanian zones. Diameter classes in mm: 1 = [0-5[, 2 = [5-10[, 3 = [10-15[, 4 = [15-20[, 5 = [20-25[, 6 = [25-30[, 7 = [30-35[, 8 = [35-40[, 9 = *D≥40*

In the south Sudanian zone, there is a variation in the curve looks according to the treatment (Fig. 7). Under the crown of *P. reticulatum* and at the limit of the crown reversed "J" curve forms have been recorded. The individuals of the class ([0-5 mm [) represent 57.14 to 75% of individuals under the crown of *P. reticulatum* and at the limit of the crown respectively. The individuals with collar diameter superior to 25 mm are not observed under the crown of *P. reticulatum.* In the plots out of the crown (control), no individual has more than 10 mm

collar diameter.

3.6.4 Structure into Height Classes of Woody Regeneration

The distribution of woody regeneration into height classes allows to understand the vertical structure of young individuals. The structure into height classes of the repartition of young species varies between phytogeographical zones and between treatments (Fig. 8).

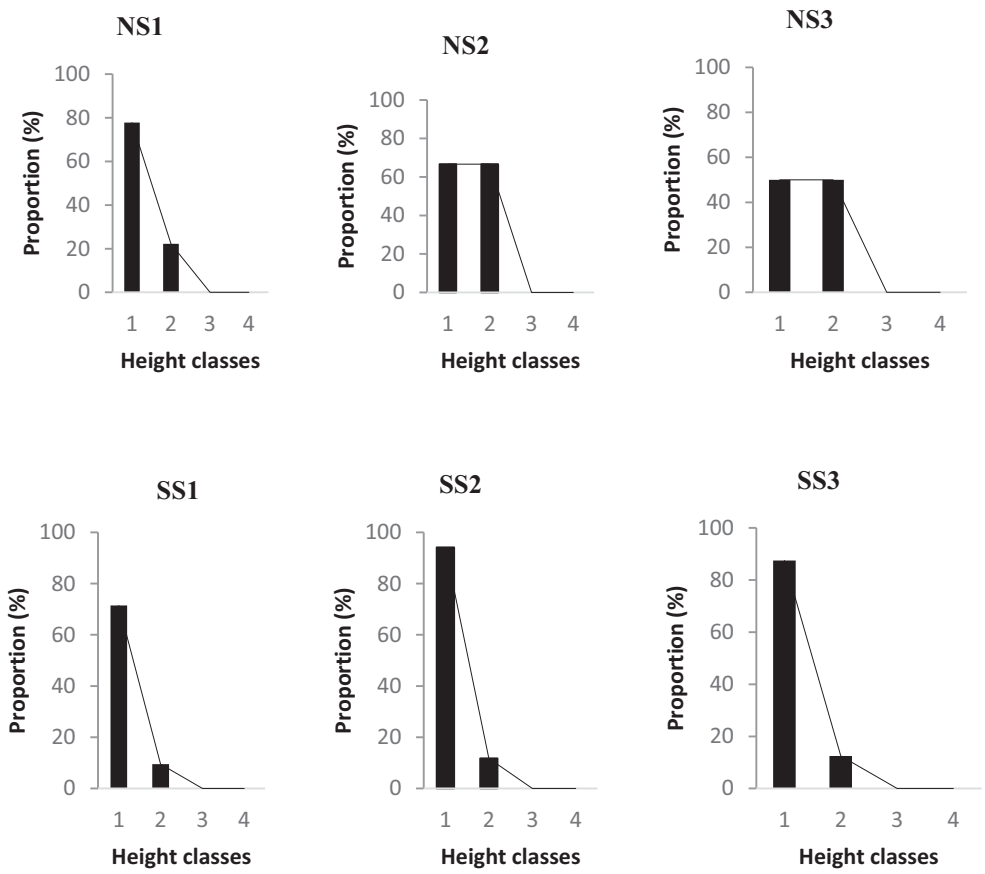

Figure 8. Vertical structure of sapling under (1), at the limit of the crown (2) and out of the crown (3) in the north and south Sudanian zones (NS and SS). *Height class in cm: 1=] 0-100[, 2= [100-200[, 3=H≥200s*

In the north Sudanian zone under the crown of *P. reticulatum,* most of the woody regeneration is represented into height class [0-1m [with 77.77% of individuals, followed by class [1-2m [with 22.22% of individuals. No regeneration more than 2 m has been recorded under the crown of *P. reticulatum* nor out of the crown. It has been observed that more we go away from the crown of *P. reticulatum,* more the proportion of individuals belonging to the height class [0-1m [decreases. This proportion, that is 77.77% under the crown of *P. reticulatum* becomes 66.66% at the limit of the crown and is less than 50% in plots out of the crown (control).

In the south Sudanian zone, it is also the height class [0-1m [that recorded most of the woody regeneration. Then, 71.43%; 94.12%; 87.5% of regeneration under the *P. reticulatum* shrub, at the limit of the crown and out of the crown respectively belong to [0-1m [height class. In this zone also, no sapling did not have height higher than 2 m (Fig. 8).

4. Discussion

4.1 Characteristics of Grass Layer of P. reticulatum Formation

4.1.1 Floristic Composition

Independently to the Sudanian zone, floristic richness is higher under the canopy of *P. reticulatum* compared to that recorded in open grassland. The floristic richness is the number of species recorded in a given area

(Botoni/Liehoun, Daget & César, 2006).

Each species growths on sites presenting conditions corresponding to that of its fundamental niche defined as the area of species tolerance to the main environmental factors (Fournier, 1991, Fournier, Floret & Gnahoua, 2001). Tree canopy constitutes a favorable area to the grass layer based both on the microclimatic and soil status (Apko & Grouzis 2004, 2006). On the microclimatic basis, woody cover reduces solar radiation, air temperature and wind speed then potential evapo-transpiration (PET) is reduced. On the soil status basis, it appears that tree increases soils fertility, at less in the superficial horizon. The species characteristic of the woody cover, generally sciaphytes and hygrophytes, are in their majority, dicotyledons or monocotyledons with broad-leaves. The species characteristics of uncovered areas, generally xerophytes, mostly belong to Poaceae family with narrow leaves roughly rolled. According to Grego, Di Mattia, Moscatelli and Cacciari (2000), *Alysicarpus ovalifolius*, *Indigofera Suffructicosa, Aspilia bussei, Englerestrum gracilium,Polygala arenarea, Biophyton petertianum* are severe sciaphytes species that explains the fact that they are only observed under the crown. They have an excellent forage quality. Ours results on the herbaceous diversity under and out of the crown of *P. reticulatum* are consistent to those obtained by others authors (Apko & Grouzi*,* 2004; Diallo et al. 2015) on other trees. Indeed, Apko and Grouzis (2006) found in the Senegalese Ferlo that floristic richness of herbaceous under the cover of *Acacia raddiana* (Savi) Brenan is significantly greater than that outside. Diallo and al., (2015) found that floristic diversity under the cover of *Balanites aegyptiaca* (L.) Del., *Acacia tortilis* subsp. *raddiana* (Savi) Brenan, *Acacia senegal* (L.) Willd, *Boscia senegalensis* (Pers.) Lam. ex Poir. et *Sclerocarya birrea* (A. Rich.) Hochst., are higher compared to that recorded outside (control). Likewise, Bationo (1994) recorded an important presence of certain herbaceous as *Pennisetum pedicelatum* under *Guiera senegalemensis* in the south center (south Sudanian zone) of Burkina Faso.

Our results show values of Piélou index changing from 0.60 to 0.72. These values tend rather to 1 indicating an absence of predominance event. Independently to the Sudanian zone, Shannon index under the cover of *P. reticulatum* is higher compared to that outside, 2.28 compared to 1.8 and 2.07 compared to 1.73 in the north and south Sudanian zones respectively. These results indicate the existence of a gradient of herbaceous diversity from the crown of *P. reticulatum* to the open grassland: far we go away from the crown of *P. reticulatum,* more the herbaceous diversity decreases. The important floristic diversity under the crown of *P. reticulatum* has to be linked to soil richness in organic matter, total nitrogen and total phosphorus directly influenced by tree.

4.2 Structure

The analysis of all the "J" curves of Raunkiaer shows that *P. reticulatum* stand have a stable cover (all the curves are unimodal). Annual graminaceae are predominant on all the forage spectrums. That could be related to their ability to grow on low soil fertility (Ouédraogo, 2008). Graminaceae are species that resist to different disturbances due to their ability to develop a strategy allowing them to remain and to growth in a disturbed environment (Breman & De Ridder, 1991). Others authors also highlighted this predominance of annual graminaceae in the vegetation of Sudanian zones (Bremann & De Ridder, 1991; Daget *&* Godron, 1995; Ouédraogo, 2008). The contribution of perennial graminacea is low on all of our inventories (5.5 and 10.29% under and out of the crown of *P. reticulatum* respectively in the north Sudanian zone and 2.42 and 4.75% under and out of the crown of *P. reticulatum* respectively in the south Sudanian zone). This situation allows to predict a low capacity of these formations to give regrowths during the dry season especially after fires and at first rains. In north Sudanian zone (Saria) where fallow is protected (again bush fire and pasture), CSi of perennial herbaceous is higher compared to that of the south Sudanian zone (Sala). Human practices observed in the management of traditional soils negatively impact the development of herbaceous vegetation (Ouédraogo, 2008). The climatic factors, particularly low rainfall and rain distribution along the year, low relative humidity during a long period of the year and biotic factors (low degradation of organic matter) are all defavorable conditions to the growth of perennial herbaceous species (Ousseina, Ricardo, Fortina, Marichatou & Yenikoye, 2013). We have to highlight that man negative actions is more perceptible on the degradation of the vegetation compared to climatic factors. This low contribution of perennial graminaceae in the herbaceous cover in Sudanian zone has been mentioned by Ouédraogo, (2008).

Considering especially *Microchloa indica* species, we found that independently to the Sudanian zone, its CSi is higher out of the crown of *P. reticulatum* compared to the value recorded under the crown. In the north Sudanian zone, we have recorded a CSi of 16.03 and 36.69% under and out of the crown of *P. reticulatum* respectively. Referring to the five successive steps in the evolution of a savanna subjected to pasture (Botoni/Liehoun *et al.,* 2006), it appears that the apparition of the small annual graminaceae *Microchloa indica* corresponds to the fifth step. This step is characterized by the degradation of the plant cover. It is an ultimate step that forecasts the total denudation of the soil. The crown of *P. reticulatum,* reducing the CSi of *Microchloa indica,* constitutes an

important actor of fighting soil denudation then enhancing pasture.

4.3 Influence of P. reticulatum on the Production of Grass Phytomass

The annual production of grass layer is always higher under the cover compared to outside independently to the experimental site. For several arid and semi-arids regions, similar results have been reported (Weltzin & Coughenou, 1990; Apko & Grouzis, 2004, 2006). In return, these results are not consistent to those recorded in sub humid zones where it has been reported that the woody cover has depressive effect on herbaceous production compared to the production in open grassland (Akpo *et al*., 2003). The effect of the tree on the production is more favorable in ecological zone with low rainfall compared to zones with great rainfall and where woody density is higher (Akpo & Grouzis, 2004; Apko *et al* 2003). This explains that in north Sudanian zone the difference in herbaceous production between the cover of *P. reticulatum* and production in outside is largest compared to the difference in south Sudanian zone. Analyzing several works achieved in Africa under different bioclimats (from 150 mm to 1200 mm of annual rainfall), Akpo & Grouzis (2000) sets the rainfall threshold (100-800 mm) and the threshold of woody recovery (60%) at which the effect of tree is null. However, our results didn't sustain this threshold sets by Akpo & Grouzis (2000) because the rainfall in our sites is higher than 800 mm though the benefit of tree on the herbaceous production is effective. The morphology of the crown of *P. reticulatum* could explain our results.

4.4 Effect of P. reticulatum on Woody Regeneration

Our results show a low diversity of woody regeneration of *P. reticulatum* formations. However, independently to the Sudanian zone, the diversity index of woody regeneration are always higher under the canopy of *P. reticulatum* compared to outside. Others authors highlighted the beneficial effect of tree on woody regeneration. Akpo & Grouzis (2000) showed that tree enhances the regeneration of certain woody species: plots under canopy presenting a regeneration higher more than 7 times compared to the regeneration outside the canopy. Akpo & Grouzis, (2004) found higher lifting under *Acacia raddiana, Balanites aegyptiaca* and *Ziziphus mauritiana.*

The large woody regeneration under the crown compared to the regeneration outside could be explain by the fact that the crown constitutes a preferential area for ruminants rest and a better perch for birds then allows the dissemination (Akpo & Grouzis 2004).

5. Conclusion

In the Sudanian conditions, *P. reticulatum* enhances herbaceous diversity and production, and woody regeneration under its crown compared to the open grassland. In south Sudanian zone, except CSi of perennial herbaceous, the floristic diversity (woody and herbaceous), the height of herbaceous is higher compared to north Sudanian zone. The study undertaken on the influence of *P. reticulatum* on the functioning of grass layer and woody regeneration showed a benefit effect of tree in the Sudanian zone. The floristic diversity (Woody and herbaceous) and the production of herbaceous biomass are greater under the canopy of *P. reticulatum.* Based on the results obtained during this experimentation, *P. reticulatum* is recommanded in tree plantation processes aiming to enhance biodiversity and the herbaceous production in transhumance zones. This recommendation is all the more valuable that the clove of *P. reticulatum* is consumed by cattle.

References

Akpo, L. E., Banoin, M., & Grouzis, M., (2003). Effet de l'arbre sur la production et la qualité fourragères de la végétation herbacée : bilan pastoral en milieu sahélien. *Revue Méd. Vét., 154*(10), 619-628.

Akpo L. E., & Grouzis, M. (2000). Valeur pastorale des herbages en région soudanienne, le cas des parcours sahéliens du Nord-Sénégal. *Tropicultura*, pp. 1-8.

Akpo L. E., & Grouzis M. (2004). Interactions arbre/herbe en bioclimat semi-aride : influence de la pâture. *Sécheresse, 15*(3), 253-61

Akpo L. E., & Grouzis, M. (2006). Interactions arbre-herbe au Sahel. *Sécheresse, 17*(1-2), 318-25.

Akpo L. E., & Grouzis, M. (2009). Effet des arbres sur la diversité de la végétation herbacée dans les parcours communautaires du Nord - Sénégal (Afrique de l'Ouest), 272-293.

Bationo B. A. (1994). Etude des potentialités agroforestières, de la multiplication et des usages de Guierra senegalensis. Mémoire IDR Ouagadougou, 70 pages

Botoni/Liehoun, E., Daget, P., & César, J. (2006). Activités de pâturage, biodiversité et végétation pastorale dans la zone Ouest du Burkina Faso. *Revue Élev. Méd. vét. Pays trop, 59*(1-4), 31-38. https://doi.org/10.19182/remvt.9951

Boudet, G. (1984). Manuel sur les Pâturages Tropicaux et les Cultures Fourragères (4e éd, révisée). IEMVT : *Maisons-Alfort*, 266.

Breman, H., & De Ridder, N. (1991). Manuel sur les pâturages des pays sahéliens. *CTAACCT-Karthala, Paris*, 486p.

Daget, P., & Godron, M. (1995). Pastoralisme: Troupeaux, espaces et sociétés. *HATIER, AUPELF, UREF,* Universités francophones, 510 p.

Daget, P., & Poissonet, J. (1971). Un procédé d'estimation valeur pastorale des pâturages. Fourrages, 31-39.

Diallo, M., Ndiaye, O., Diallo, A., Saleh, M., Bassene, C., Wood, S. A., Diop, A., & Guisse, A. (2015). Influence de la litière foliaire de cinq espèces végétales tropicales sur la diversité floristique des herbacées dans la zone du Ferlo (Sénégal). *Int. J. Biol. Chem. Sci. 9*(2), 803-814. https://doi.org/10.4314/ijbcs.v9i2.20

Fournier, A. (1991). Phénologie, croissance et production végétales dans quelques savanes d'Afrique de l'ouest. Variation selon un gradient climatique. Thèse de Doctorat d'État, université Pierre et Marie Curie (Paris VI), 312 p.

Fournier, A., Floret, C., & Gnahoua, G. M. (2001). Végétation des jachères et succession post-culturale en Afrique tropicale. *John Libbey Eurotext*, 123-168.

Godron, M., Daget, P., Emberger, L., Long, G., Le, floc'h, E., Poissonet, J., Sauvage, Ch., & Wacquant, J. M. (1969). Vade-mecum pour le relevé méthodique de la végétation et du milieu*. C.N.R.S. Paris*, 170 p.

Grego, S., Di, Mattia, E., Moscatelli, M. C., Cacciari, I. (2000). Functional Diversity Of Microbial communities present in the rhizosphere of *Acacia tortilis:* an ecophysiological approach. *In* Floret Ch., Pontanier R., éd.: *La jachère en Afrique tropicale,* Paris, John Libbey Eurotext: 300-307.

Ouédraogo, D. (2008). Caractérisation des ressources fourragères et des pratiques pastorales du terroir de Kotchari à la périphérie du parc w. Mémoire d'ingénieur UPB/IDR, 87 p + annexes.

Ouédraogo, N. M. (2003). Influence de différentes herbacées sur les indicateurs chimiques et biologiques de la fertilité des sols. Mémoire de fin d'études d'Ingénieur du développement Rural (IDR), Université Polytechnique de Bobo Dioulasso, Bobo Dioulasso (Burkina Faso).

Ousseina, S., Riccardo, Fortina, R., Marichatou, H., & Yenikoye, A. (2013). Dynamique du peuplement herbacé de la station sahélienne expérimentale de Toukounous (Filingué – Niger). *Int. J. Biol. Chem. Sci. 7*(2), 657-671. https://doi.org/10.4314/ijbcs.v7i2.22

Savadogo, P. (2007). Dynamics of sudanian savanna woodland ecosystem in response to disturbances. PhD thesis. Swedish university of agricultural sciences, (Sweden).

Sawadogo, L. (1996). Evaluation des potentialités pastorales d'une forêt classée nord soudanienne au Burkina Faso (cas de la forêt classée de Tiogo). Université de Ouagadougou /FAST, Ouagadougou (Burkina Faso).

Sawadogo, L. (2009). Influence de facteurs anthropiques sur la dynamique de la végétation des forêts classées de Laba et de Tiogo en zone soudanienne du Burkina Faso. Thèse Doctorat d'Etat, Université de Ouagadougou, Ouagadougou (Burkina Faso).

Yelemou, B., Yameogo, G., Bationo, B. A., Millogo/Rasolodimby, J., & Hien, V. (2008). Biologie florale et mode de reproduction sexuée de *Piliostigma reticulatum*, (DC) Hochst., *Int. J. Biol. Chem. Sci., 2*(3), 281-291

Yélemou, B., Bationo, B. A., Yaméogo, G., & Millogo-Rasolodimby, J. (2007). Gestion traditionnelle et usage de *Piliostigma reticulatum* (D.C.) Hochst., dans le plateau central du Burkina Faso. *Bois et For. Trop., 291*, 55-65. http://bft.cirad.fr/cd/BFT_291_55-66.pdf

Weltzin, J. F., Coughenou, MU, B., (1990). Savanna tree influence on understory vegetation and soi1nutrients in northwestern Kenya. *J. Veget. Sci., 1*, 325-334. https://doi.org/10.2307/3235707

Journal of Plant Studies; Vol. 6, No. 2; 2017
ISSN 1927-0461 E-ISSN 1927-047X
Published by Canadian Center of Science and Education

Height-diameter Relationships in Longleaf Pine and Four Swamp Tree Species

Xiongwen Chen[1] & Dale G. Brockway[2]

[1]Department of Biological and Environmental Sciences, Alabama A&M University, Normal, AL 35762, USA

[2]USDA Forest Service, Southern Research Station, 521 Devall Drive, Auburn, AL 36849, USA

Correspondence: Xiongwen Chen, Department of Biological and Environmental Sciences, Alabama A&M University, Normal, AL 35762, USA. Tel: 256-372-4231. E-mail: xiongwen.chen@aamu.edu

Received: May 19, 2017 Accepted: August 4, 2017 Online Published: August 10, 2017

doi:10.5539/jps.v6n2p94 URL: https://doi.org/10.5539/jps.v6n2p94

Abstract

The scaling relationship between height and diameter is important for understanding the dynamic patterns of tree growth and estimating the accrual of tree biomass. Metabolic ecology predicts that tree growth follows a universal scaling invariant relative to the height-diameter relationship (i.e., no variation based on taxonomy or resource availability). Comparing field data for different tree species across a range of site conditions should be an informative test of that prediction. Our results indicate that the scaling exponents of height and diameter for longleaf pine (Pinus palustris Mill.) vary at the four locations across its natural range. As for swamp trees, the scaling exponents for red maple (Acer rubrum L.) and river birch (Betula nigra L.) were consistent with that predicted by metabolic ecology; however, those for water tupelo (Nyssa aquatica L.) and bald cypress (Taxodium distichum (L.) Rich) were not. Our study confirms that high plasticity and variation in allometric scaling of the tree height and diameter relationship may very well be the rule, rather than the exception.

Keywords: allometric scaling, precipitation, scaling invariant, wetland

1. Introduction

The tree height and diameter relationship has been a subject of theoretical and empirical research (Henry & Aarssen, 1999; Ducey, 2012; Forrester, Benneter, Bouriaud, & Bauhus, 2017) Tree scaling of the height-diameter relationship is very important in forestry and ecological science, because it is used to describe tree or stand growth, productivity and yield (Parresol, 1992). If the scaling algorithm is erroneous, it will result in inaccurate estimates (Kearsley et al., 2013). In forestry research, much effort has been invested in developing algorithms for scaling this relationship for various tree species and under different conditions (e.g., Zhang, Ma, & Guo, 2009). Recent developments in metabolic ecology propose that all tree species share an optimal design for the vascular system, which is related to plant physiology, biomass partitioning and population and community dynamics (Enquist, West, Charnov, & Brown, 1999; West, Brown, & Enquist, 1999). One of the important predictions and hypotheses from metabolic ecology concerning tree growth is the claimed universal scaling invariant in the tree height-diameter relationship $H \propto D^{2/3}$ (i.e., no variation based on taxonomy or resource availability).

Yet, other researchers found no evidence in their empirical studies for the universal scaling invariant (e.g., Chen & Li, 2003; Li, Han, & Wu, 2005; Ducey, 2012; Forrester et al., 2017). Tree allometry significantly differs across the United States largely because of climate (Hulshof , Swenson, & Weiser, 2015) It is possible that tree species living under frequently stressed conditions may have different scaling exponents, resulting from environmental stress or resource limitation. Trees growing in heath and peat-swamp forests exhibit differentiation in allometric relationships among their seedlings (Nishimura & Suzuki, 2001). Thus, trees having different scaling exponents are expected to exist in environments with frequent stress. This type of environment may exist for trees near the edge of their natural range or for some swamp trees with small habitat areas and frequent change in water level.

Although historically quite extensive (37 million ha) and then greatly reduced by exploitive logging (to 1.3 million ha), longleaf pine (*Pinus palustris* Mill.) forests are today making a steady recovery primarily on public lands, with somewhat slower gains on private lands. While the restoration goal is to eventually achieve an occupancy of 3.2 million ha, longleaf pine is still narrowly distributed across its native range in the southeastern United States (Fig. 1). Comparing the height-diameter relationships for trees growing in the central portion and

near the northern and southern edges of this large natural range should prove insightful, as will a similar analysis for water tupelo (*Nyssa aquatic* L.), bald cypress (*Taxodium distichum* (L.) Rich), red maple (*Acer rubrum* L.) and river birch (*Betula nigra* L.) naturally growing in the small swamps and wetlands of northern Alabama. Using tree height and diameter data from numerous sites, the objective of this study is to determine whether there are deviations in the scaling exponent (2/3) for forest trees growing in this environment, specifically (i) whether longleaf pine have a consistent scaling exponent for trees across their native range or vary between the central and boundary areas and (ii) whether the four swamp tree species have a consistent scaling exponent. Comparing these scaling relationships should be helpful in better understanding the complexity of tree growth and also provide specific information for continuing research in tree allometric scaling.

2. Materials and Methods

Tree species and study sites

Longleaf pine were measured at four sites representing the northernmost (Bankhead National Forest in northern Alabama), central (Tuskegee National Forest in central Alabama) and southernmost (Goethe State Forest and Blackwater River State Forest in northern Florida) portions of its native range (Table 1, Fig. 1). The Bankhead NF (34º15'N, 87º15'W), Tuskegee NF (32º50'N, 85º50'W) and Blackwater River SF (30º47'N, 86º44'W) are typical of mesic uplands with broad, moderately-inclined ridges and deep, well-drained sandy soils, low in organic matter and nutrients and low to moderate in water holding capacity (Weeks, Hyde, Roberts, Lewis, & Peters, 1980; USDA Forest Service, 1995). Longleaf pine at the Bankhead NF was a young forest plantation, about 15 -20 years in age. There were also some loblolly pine (*Pinus taeda* L.), vines (*Smilax* spp. L.) and shrubs in the stand, but limited broadleaved trees. At the Tuskegee NF and Blackwater River SF, overstories were dominated by longleaf pine, with lesser components of loblolly pine, shortleaf pine (*Pinus echinata* Mill.), slash pine (*Pinus elliotti* Englem.), southern red oak (*Quercus falcata* Michx.), bluejack oak (*Quercus incana* W. Bartram), post oak (*Quercus stellata* Wangenh.) and persimmon (*Diospyros virginiana* L.). The understory at the Blackwater River SF was rich in herbaceous plants, resulting from a history of frequent prescribed burning, while that at the Tuskegee NF contained somewhat greater shrub cover along with the grasses and forbs. These uplands were occupied by second-growth forest that naturally regenerated following cutover of the original forest in the early 1900s. Although most of the overstory pines ranged from 60 to 80 years in age, multiple waves of natural regeneration resulted in uneven-aged stand structures. The Goethe SF (29º13'N, 82º33'W) is characterized by a nearly-level flatwoods environment with deep, poorly-drained sands, low in organic matter and nutrients and low in water holding capacity (Slabaugh, Jones, Puckett, & Schuster, 1996). Overstory vegetation was dominated by longleaf pine, with lesser amounts of slash pine, oaks and sweetgum (*Liquidambar styraciflua* L.). The understory was dominated by saw-palmetto (*Serenoa repens* (W. Bartram) Small) and other shrubs, with little herbaceous cover. These flatwoods were also cutover in the early 20th century and naturally regenerated thereafter. Overstory pines here ranged from 48 to 74 years in age. Site index at these study sites is fairly consistent, ranging from 21 to 24 m at 50 years (Brockway & Outcalt, 2017).

Table 1. Mean height and diameter of surveyed tree species

Tree species	Location	Number of trees sampled	Mean diameter (cm) (± standard deviation)	Mean height (m) (± standard deviation)
Longleaf pine	Goethe State Forest, FL	359	30.78 (±7.05)	22.13 (±2.99)
	Blackwater River State Forest, FL	332	31.90 (±9.93)	22.18 (±5.45)
	Tuskegee National Forest, AL	40	29.22 (±15.72)	22.10 (±8.90)
	Bankhead National Forest, AL	200	10.36 (±4.78)	6.92 (±2.51)
Red maple	Wheeler Wildlife Refuge, AL	110	10.04 (± 4.66)	10.77 (± 4.13)
River birch	AAMU Agricultural Experimental Station Bradford Creek, AL	105	16.60 (± 7.38)	14.04 (± 4.99)
Water tupelo	Wheeler Wildlife Refuge, AL	107	34.90 (±17.90)	26.68 (± 7.69)
Bald cypress	Wheeler Wildlife Refuge, AL	109	47.82 (±17.00)	30.95 (± 6.96)

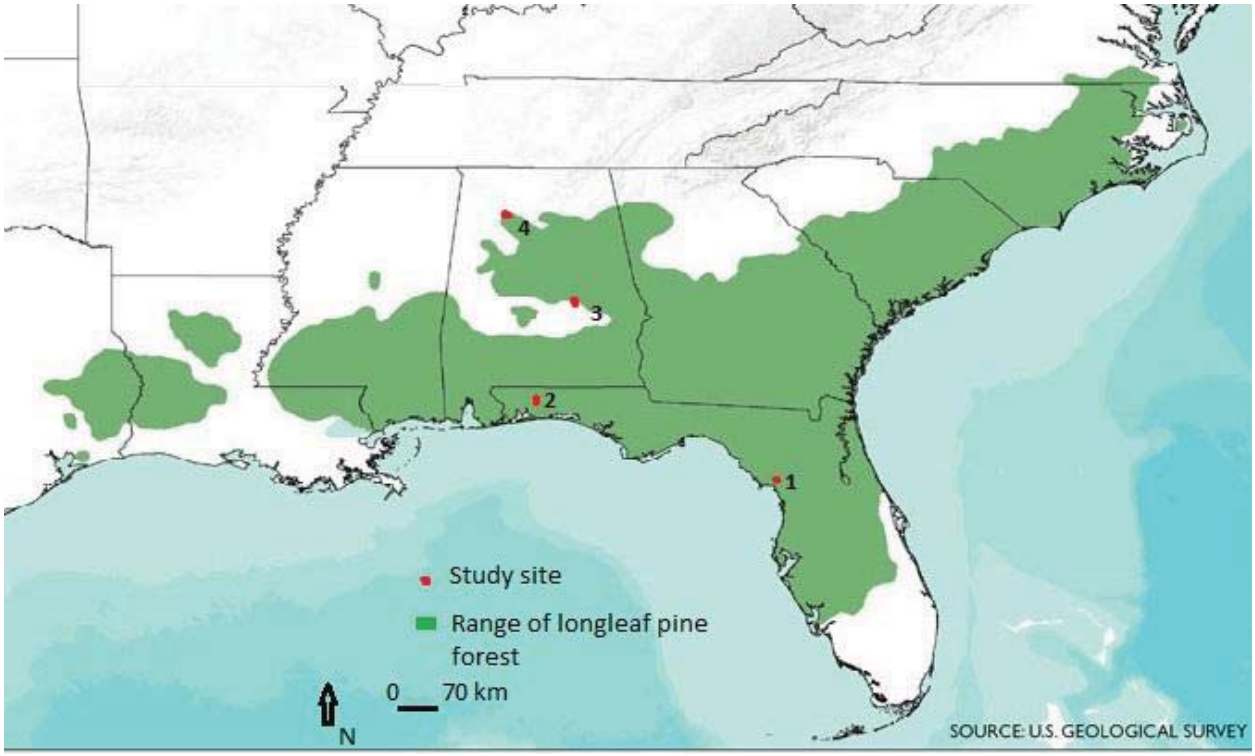

Figure 1. Natural range of longleaf pine and our study sites (1: Goethe State Forest; 2: Blackwater River State Forest; 3: Tuskegee National Forest; 4: Bankhead National Forest)

Water tupelo and red maple were measured along Beaver Dam Creek at the Wheeler Wildlife Refuge, near Madison, Alabama. Water tupelo dominated the forest and red maple co-occurred with it in a swamp environment. Bald cypress was measured near the visitor center at the Wheeler Wildlife Refuge, near Decatur, Alabama. Small seedlings of red maple were present on the floor of this bald cypress forest. River birch was measured along Bradford Creek and at the Alabama A & M University Agriculture Experimental Station in Madison, Alabama. These river birch were accompanied by southern red oak, tulip poplar (*Liriodendron tulipifera* L.), sycamore (*Platanus occidentalis* L.) and others. All these forest locations are in close proximity to one another (34º40'N, 87º00'W).

Measurements and analysis

Diameter at breast height (DBH 1.37 m above the ground) and total tree height were measured for randomly selected individuals in forests at the study sites. However, for water tupelo and bald cypress, DBH was measured at 46 cm above the flared buttress. Tree diameter was measured by using a d-tape, with accuracy to 1 mm. Tree height was measured by a Pulse Rangerfinder Hypsometer (Laser Technology Inc., Centennial, Colorado), with accuracy to 1 cm.

The exponent of $H \propto D^x$ is estimated through $\log_{10}$-$\log_{10}$ transformation. Figures illustrating $\log_{10}$ of H and $\log_{10}$ of D relationships were produced from our study data. To be consistent with early literature concerning the estimation of allometric relationships, a reduced major axis (RMA) of regression analysis Model Type II was used to determine scaling exponents (αRMA). The difference between estimated scaling exponents at each site and the theoretical value (2/3) was then statistically tested (Sokal & Rohlf, 1995). Significant differences were discerned at the $p = 0.05$ level.

3. Results and Discussion

Deviations in the scaling relationship between tree height and diameter existed for longleaf pine trees at the Goethe State Forest (0.4229) and Blackwater River State Forest (0.713) (Fig. 2), but scaling exponents at the Tuskegee National Forest (0.6866) and Bankhead National Forest (0.6442) were not different from 2/3. Overall, the scaling exponent for longleaf pine at the four sites across its native range was 0.8146, which was significantly different from 2/3.

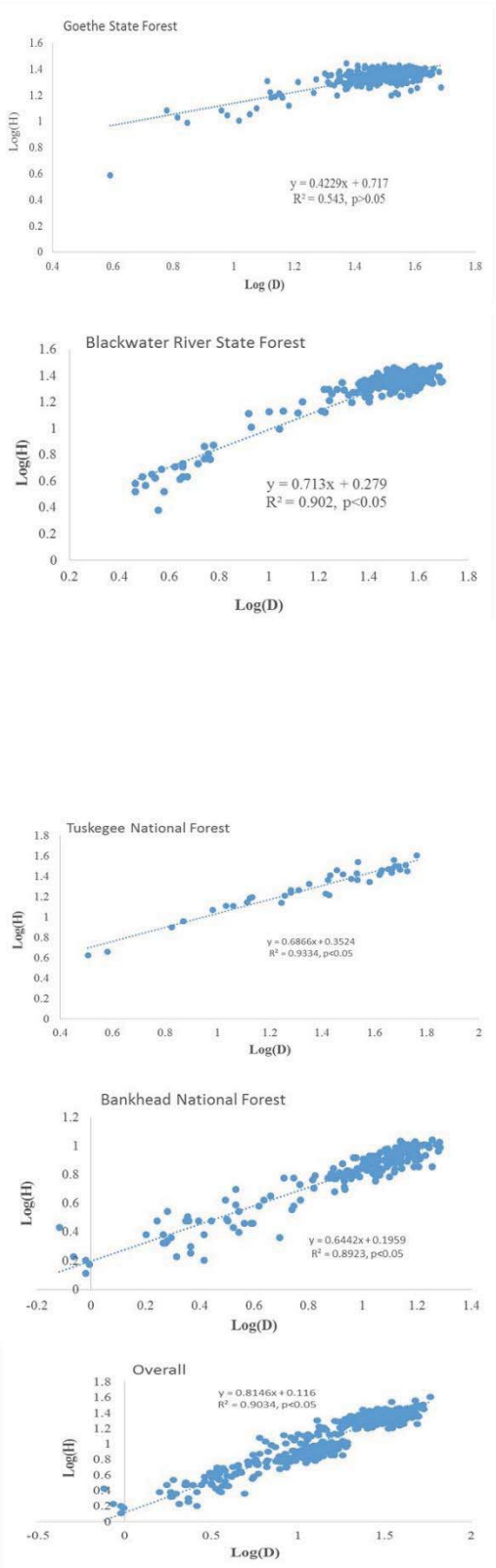

Figure 2. Allometric scaling of height and diameter for longleaf pine at different locations across its native range

Scaling exponents of height and diameter for red maple (0.6556) and river birch (0.6489) were not different from 2/3 (Fig. 3). But, the scaling exponents for water tupelo (0.3117) and bald cypress (0.5252) were significantly different from 2/3. The overall scaling exponent of height and diameter for all trees of these four species was 0.4396, this value was significantly low than 2/3.

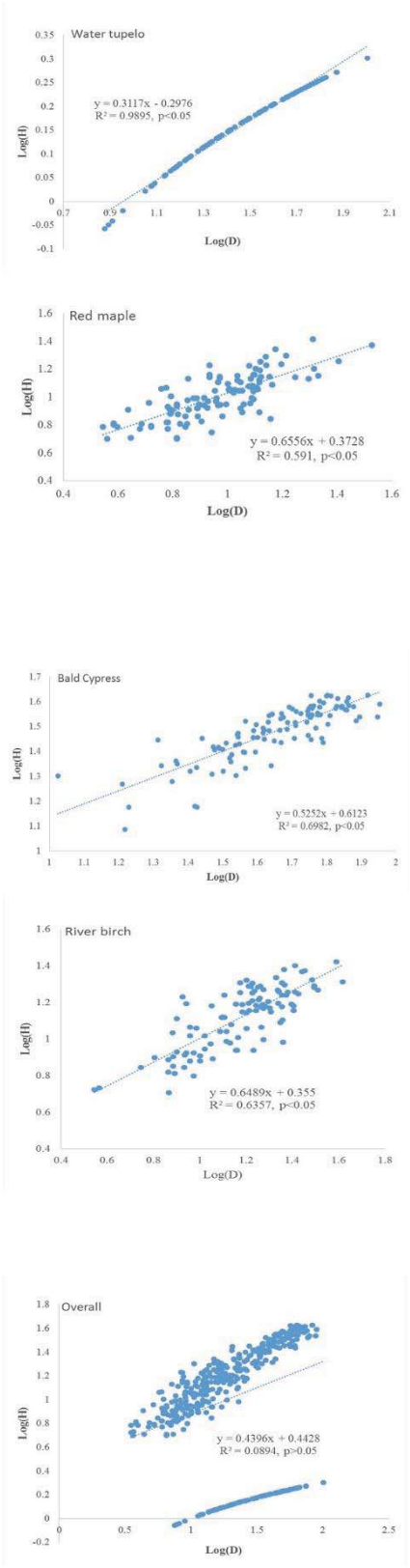

Figure 3. Allometric scaling of height and diameter for water tupelo, red maple, bald cypress and river birch in northern Alabama

We found spatial variations in the scaling exponents for longleaf pine trees at the four study sites across its natural range. The overall scaling exponent also deviated from the theoretical prediction of 2/3. Based on the

assumption that larger geographic distances might result in the greatest disparity, scaling exponents for longleaf pine trees at the Goethe State Forest (southern portion of range) and Bankhead National Forest (northern edge of range) might be expected to deviate most from 2/3. However, scaling exponent deviations were observed instead at the Blackwater River State Forest and Goethe State Forest, both in the southern portion of the native range. Since annual precipitation is lowest at the Goethe State Forest (~ 127 cm) and highest at the Blackwater River State Forest (~ 158 cm), the scaling exponent may be related to annual precipitation. Among these four longleaf pine sites, there was a positive correlation between annual precipitation and scaling exponents (Fig. 4). Hulshof et al. (2015) suggested that tree height is negatively influenced by decreasing mean precipitation. Thus, height-diameter scaling for longleaf pine may vary across its natural range because of differing amounts of precipitation (and evapotranspiration) across this extensive geographic area.

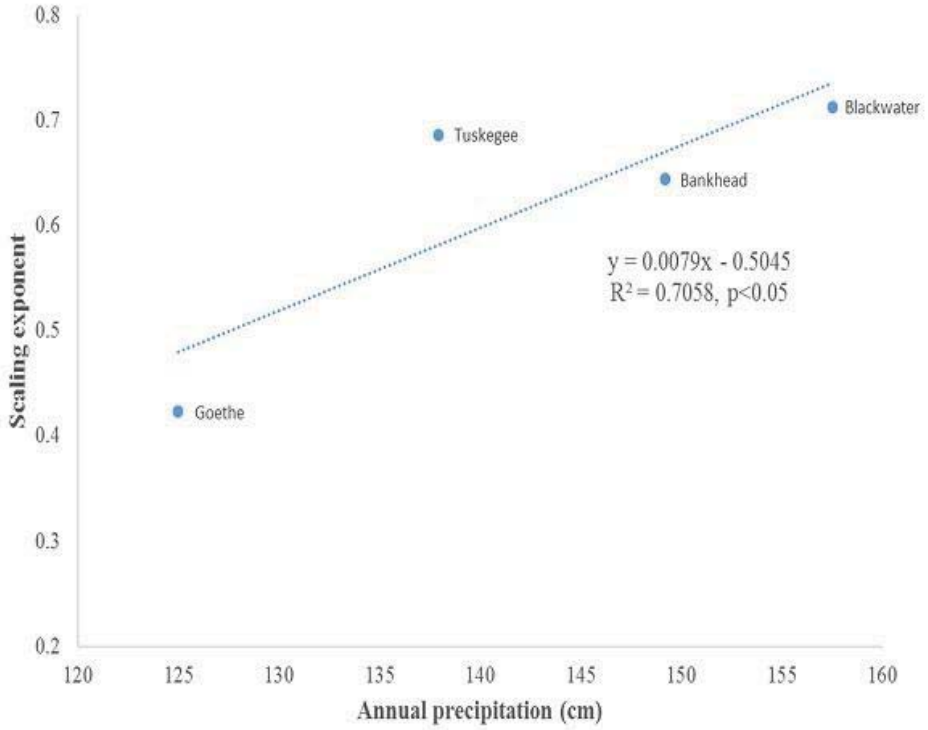

Figure 4. Correlation between mean annual precipitation and the scaling exponent of height and diameter

Our findings for red maple and river birch supported the exponent predicted by metabolic ecology; however, the results for water tupelo and bald cypress did not. Both scaling exponents of water tupelo and bald cypress were significantly less than the predicted 2/3. These two tree species can live in flooded conditions for prolonged periods and are characterized by swollen trunks called “buttresses” or “knees”. One function of a swollen lower trunk is to provide enhanced stability by physically supporting a tree on a larger-diameter base and keeping it standing upright in wet soil. Another function attributed to a swollen trunk is that of providing oxygen to roots which grow in an environment of low dissolved oxygen. Otherwise, the tree would be expected to die from suffocation, since water-saturated soils contain less oxygen than well-aerated, better-drained soils. But, there is little actual evidence for this assertion (Angelov et al., 1996). Metabolic ecology postulates a power law with an invariant exponent, because all tree species share an optimal design for their vascular system, which is related to plant physiology (Enquist et al., 1999; West et al., 1999). However, trees may not exhibit the most efficient hydraulic architecture, because of limitations related to mechanical safety (Sperry, Meinzer, & McCulloh, 2008) and/or environmental stress. Despite no consensus on the role of the swollen trunks, their construction must consume energy and photosynthate, which could otherwise be used for increasing tree height. Thus, the scaling exponent for height and diameter was lower for water tupelo and bald cypress.

We conclude that the height-diameter scaling relationship for longleaf pine was not consistent across its natural range, most likely because of varied patterns of precipitation and the locally adaptive response of this species to water availability across the varied environments, which comprise the vast geographic area in which it can occur.

Although two of the swamp tree species, red maple and river birch, conformed to the scaling invariant of 2/3 predicted by metabolic ecology, bald cypress (another conifer) and water tupelo, both species observed to form buttresses at their lower trunks, did not support that prediction. Other studies have indicated that this scaling relationship can also be affected by light, tree health condition and others (Ducey, 2012; Ishihara, Konno, Umeki, Ohno, & Kikuzawa, 2016; Swetnam, O'Connor, & Lynch, 2016; Forrester et al., 2017). This study puts forth additional data supporting the concept of a universal height-diameter scaling invariant of 2/3 for some tree species, while providing a strong argument for deviation by other tree species directly related to possible environmental stresses that cause them to adapt to unique localized conditions throughout their range. Our findings confirm that high plasticity and variation across environments in the allometric scaling of tree height and diameter may very well be the rule, rather than the exception.

Acknowledgements

The authors express appreciation to Matthew Shaw, Ferhat Kara, David Jones, Bryan Bulger, Jason O'Shell and Eric Neiswanger for field assistance. This study was partially supported by USDA National Institute of Food and Agriculture McIntire Stennis project (1008643).

References

Angelov, M. N., Sung, S-J. S., Doong, R. L., Harms, W. R., Kormanik, P. P., & Black, C. C. Jr. (1996). Long- and short-term flooding effects on survival and sink–source relationships of swamp-adapted tree species. *Tree Physiology, 16*, 477-484. https://doi.org/10.1093/treephys/16.5.477

Brockway, D. G., & Outcalt, K. W. (2017). Influence of reproduction cutting methods on structure, growth and regeneration of longleaf pine forests in flatwoods and uplands. *Forest Ecology and Management, 389*, 249-259. https://doi.org/10.1016/j.foreco.2017.01.002

Chen, X., & Li, B-L. (2003). Testing the allometric scaling relationships with seedlings of two species. *Acta Oecologica, 24*, 125-129. https://doi.org/10.1016/S1146-609X(03)00062-6

Ducey, M. J. (2012). Evergreenness and wood density predict height–diameter scaling in trees of the northeastern United States. *Forest Ecology and Management, 279*, 21-26. https://doi.org/10.1016/j.foreco.2012.04.034

Enquist, B. J., West, G. B., Charnov, E. L., & Brown, J. H. (1999). Allometric scaling of production and life-history variation in vascular plants. *Nature, 88*, 907-911. https://doi.org/10.1038/44819

Forrester, D. I., Benneter, A, Bouriaud, O., & Bauhus, J. (2017). Diversity and competition influence tree allometric relationships - developing functions for mixed‐species forests. *Journal of Ecology, 105*, 761-774. https://doi.org/10.1111/1365-2745.12704

Henry, H. A. L., & Aarssen, L. W. (1999). The interpretation of stem diameter-height allometry in trees: biomechanical constraints, neighbor effects or biased regression? *Ecology Letters, 3*, 89-97. https://doi.org/10.1046/j.1461-0248.1999.22054.x

Hulshof, C. M., Swenson, N. G., & Weiser, M. D. (2015). Tree height-diameter allometry across the United States. *Ecology and Evolution,* 5, 1193-1204. https://doi.org/doi/10.1002/ece3.1328

Kearsley, E., de Haulleville, T., Hufkens, K., Kidimbu, A., Toirambe, B., Baert, G., … Verbeeck, H. (2013). Conventional tree height–diameter relationships significantly overestimate aboveground carbon stocks in the Central Congo Basin. *Nature Communication, 4*, 2269. https://doi.org/doi/10.1038/ncomms3269

Ishihara, M. I., Konno, Y., Umeki, K., Ohno, Y., & Kikuzawa, K. (2016). A new model for size-dependent tree growth in forests. *PLOS One, 11*, e0152219. https://doi.org/doi/10.1371/journal.pone.0152219

Li, H-T., Han, X-G., & Wu, J. G. (2005). Lack of evidence for ¾ scaling of metabolism in terrestrial plants. *Journal of Integrative Plant Biology, 47*, 1173-1183. https://doi.org/doi/10.1111/j.1744-7909.2005.00167.x

Nishimura, T. B., & Suzuki, E. (2001). Allometric differentiation among tropical tree seedlings in heath and peat-swamp forests. *Journal of Tropical Ecology, 17*, 667-681. https://doi.org/10.1017/S0266467401001493

Parresol, B. R. (1992). Baldcypress height-diameter equations and their prediction confidence intervals. *Canada Journal of Forest Research, 22*, 1429-1434. https://doi.org/10.1139/x92-191

Slabaugh, J. D., Jones, A. O., Puckett, W. E., & Schuster, J. N. (1996). *Soil Survey of Levy County, Florida*. Washington, DC: USDA-NRCS, U.S. Govt. Printing Office.

Sokal, R. R., & Rohlf, F. J. (1995). *Biometry*. Third ed. New York, NY: W.H. Freeman and Company.

Sperry, J. S, Meinzer, F. C., & McCulloh, K. A. (2008). Safety and efficiency conflicts in hydraulic architecture: scaling from tissues to trees. *Plant, Cell and Environment, 31*, 632-645. https://doi.org/10.1111/j.1365-3040.2007.01765.x

Swetnam, T., O'Connor, C. D., & Lynch, A. M. (2016). Tree morphologic plasticity explains deviation from metabolic scaling theory in semi-arid conifer forests, southwestern USA. *PLOS One, 11*, e0157582. https://doi.org/10.1371/journal.pone.0157582

USDA Forest Service. (1995). *Land Type Associations of the Tuskegee National Forest.* Resource Management Report, Southern Region. Montgomery, AL: National Forests in Alabama.

Weeks, H. H., Hyde, A. G., Roberts, A., Lewis, D., & Peters, C. R. (1980). *Soil Survey of Santa Rosa County, Florida*. Washington, DC: USDA-SCS, U.S. Govt. Printing Office.

West, G. B., Brown, J. H., & Enquist, B. J. (1999). A general model for the structure and allometry of plant vascular systems. *Nature, 400*, 664-667. https://doi.org/10.1038/23251

Zhang, L., Ma, Z., & Guo, L. (2009). An evaluation of spatial autocorrelation and heterogeneity in the residuals of six regression models. *Forest Science, 55*, 533-548.

Journal of Plant Studies; Vol. 6, No. 2; 2017
ISSN 1927-0461 E-ISSN 1927-047X
Published by Canadian Center of Science and Education

Inhibition of Advanced Glycation End Products Formation by *Mangifera indica* Leaf Extract

Kimihisa Itoh[1], Kazuya Murata[2], Nao Sakaguchi[2], Kohei Akai[2], Tomoka Yamaji[2], Kohsuke Shimizu[1], Kaoru Isaki[3],Tetsuya Matsukawa[1, 3], Shin'ichiro Kajiyama[3], Masahiko Fumuro[1], Morio Iijima[1, 4] & Hideaki Matsuda[1, 2]

[1]The Experimental Farm, Kindai University, Wakayama, Japan

[2]Faculty of Pharmacy, Kindai University, Osaka, Japan

[3]Faculty of Biology-Oriented Science and Technology, Kindai University, Wakayama, Japan

[4]Faculty of Agriculture, Kindai University, Nara, Japan

Correspondence: Kimihisa Itoh, The Experimental Farm, Kindai University, 2355-2 Yuasa, Yuasa-cho, Arida-gun, Wakayama 643-0004 Japan. Tel: 81-737-622-953. E-mail: itoh_k@nara.kindai.ac.jp

Received: June 16, 2017 Accepted: July 24, 2017 Online Published: August 12, 2017

doi:10.5539/jps.v6n2p102 URL: https://doi.org/10.5539/jps.v6n2p102

Abstract

The purpose of this study was to examine an inhibitory effect of mango leaf extracts on advanced glycation end products (AGEs) formation and to identify these active ingredients, and also to investigate a relationship between leaves maturation and the inhibitory activity. A methanolic extract of old dark green mango leaf extract (OML-ext) exhibited an inhibitory activity of AGEs formation in nonenzymatic glycation of albumin. The inhibitory activity of OML-ext was attributable to 3-C-*β*-D-glucosyl-2,4,4',6-tetrahydroxybenzophenone (**1**), mangiferin (**2**) and chlorophyll. Inhibitory effect of young dark reddish brown mango leaf extract (YDL-ext) on AGEs formation was similar to that of OML-ext. The inhibitory activity of YDL-ext was attributable to **1** and **2**, in addition, a part of the the activity of YDL-ext due to anthocyanins whose content is highest in young dark reddish brown mango leaves. Considering the amounts of leaves obtained from pruning, old dark green leaves may be a reasonable natural resource for the preparation of ingredients with inhibitory activity of AGEs formation.

Keywords: advanced glycation end products (AGEs) formation inhibition, anthocyanin, chlorophyll, 3-C-*β*-D-glucosyl-2,4,4',6-tetrahydroxybenzophenone, glycation, *Mangifera indica*, mangiferin

1. Introduction

Glycation is a non-enzymatic browning reaction caused by amino-carbonyl reactions between reducing sugars and amino groups of proteins and lipids (Tsuji-Naito, Saeki, & Hamano, 2009). By glycation of these compounds, advanced glycation end products (AGEs) are irreversibly synthesized in the body (Huebschmann, Regensteiner, Vlassara, & Reusch, 2006), and the accumulation of AGEs in organs is induced by hyperglycemia and is one of the causes of diabetic complications (Sourris, Harcourt, & Forbes, 2009). Moreover, AGEs accumulate in the skin of non-diabetics and are correlated with skin aging (Dyer et al., 1993). The AGEs accumulation in the skin induce cross-linking of collagen and reduce skin degradability and dermal regeneration (Wondrak, Roberts, Jacobson, & Jacobson, 2002). In addition, AGEs induce fibroblast apoptosis by adducting to AGE receptors on the cell (Pageon, Bakala, Monnier, & Asselineau, 2007). These phenomena are also thought to be related to skin aging (Lohwasser, Neureiter, Weigle, Kirchner, & Schuppan, 2006). Therefore, in recent years, the role of AGEs has been increasingly discussed in the skin aging, and the inhibition of AGEs formation can be one of the effective strategies for direct alleviation of the development of novel antiaging cosmeceutical ingredients.

An AGEs formation inhibitor, namely aminoguanidine (Pimagedine®) (Dyer et al., 1993) was under development in U.S.A. as a drug for the treatment of diabetic complications such as diabetic nephropathy, however the clinical trial on aminoguanidine has been discontinued due to adverse reactions such as anemia, liver injury and vitamin B6 deficiency. In order to find new and safe AGEs formation inhibitors from natural resources, pharmacological screening of plant is considered as one of strategies. Hitherto, several plant, such as *Thymus vulgaris* whole grass (Morimitsu, Yoshida, Esaki, & Hirota, 1995), *Chrysanthemum morifolium* and

Chrysanthemum indicum corolla (Tsuji-Naito et al., 2009), *Alpinia zerumbet* rhizomes (Chompoo, Upadhyay, Kishimoto, Makise, & Tawata, 2011), *Derris indica* stem bark (Anusiri, Choodej, Chumriang, Adisakwattana, & Pudhom, 2014) and *Ribes nigrum* fruit (Chen et al., 2014, Xu et al., 2016), have been reported to have AGEs formation inhibitory activity.

In our preceding paper (Itoh et al., 2016), we reported that mango (*Mangifera indica* Linne) leaf extracts exhibited pancreatic lipase inhibitory activities, and a part of the activity of leaf extract was attributable to C-glucosyl-polyphenols, such as 3-C-*β*-D-glucosyl-2,4,4',6-tetrahydroxybenzophenone (**1**) and mangiferin (**2**), and that dark green mango leaf which was obtained by summer pruning may be a reasonable natural resource for the preparation of ingredients with lipase inhibitory activity. For finding another utility value of pruned mango leaves, we examined the inhibitory effects of mango leaf extracts on AGEs formation. In this paper, we report AGEs formation inhibitory activity of mango leaf extracts, and also discuss a relationship between leaves maturation and the inhibitory activity.

2. Materials and Methods

2.1 Plant Materials

Three kinds of Mango leaves (old dark green leaf, young dark reddish brown leaf, and young yellow leaf, Figure 1) of *M. indica* (cv. Irwin) were collected according to the preceding paper (Itoh et al., 2016). In order to describe accurately the color of young mango leaves, we describe the color of the leaves as dark reddish brown in this paper instead of dark brown in the preceding paper (Itoh et al., 2016).

1-a; Young dark reddish brown leaves 1-b; Young yellow leaves 1-c; Old dark green leaves

Figure 1. Photographs of typical mango leaves at various stages of development

2.2 Extraction

Methanolic extracts of young dark reddish brown leaves (this extract is abbreviated as YDL-ext throughout this paper), young yellow leaves (YYL-ext), and old dark green leaves (OML-ext) were obtained according to the preceding paper (Itoh et al., 2016).

2.3 Reagents

Aminoguanidine hydrochloride (Lot #: MKCB3580), Bovine serum albumin (BSA, fraction V, Lot #: SLBQ4710V) and authentic **1** and **2** were purchased from Sigma-Aldrich Japan (Tokyo, Japan). Authentic chlorophyll was purchased from Tokyo Chemical Industry Co., Ltd. (Tokyo, Japan). Other chemical and biochemical reagents were of reagent grade and were purchased from Wako Pure Chemical Industries, Ltd. (Osaka, Japan) and/or Nacalai Tesque, Inc. (Kyoto, Japan) unless otherwise noted.

2.4 In vitro AGEs Formation Inhibition Assay by Incubation of Glucose and Albumin

AGE formation activity was measured according to the method of Shimoda et al. (2011) with minor modification. The test sample was dissolved with dimethyl sulfoxide (DMSO) and diluted with sodium phosphate buffer (PBS, 0.2 M KH_2PO_4, 0.2 M NaOH, pH 7.2) to a final DMSO concentration of 5% v/v. The reaction mixture of glucose (10% w/v) and bovine serum albumin (BSA, 1% w/v) dissolved in PBS (900 μl) was incubated for 48 h at 60ºC in microtube (2 ml) with or without a test solution. After incubation, the reaction mixture was diluted with distilled water (1:7 v/v), the fluorescence (***F***) associated with AGEs was monitored at an excitation wavelength of 370 nm and emission of 450 nm using a multi-label counter (PerkinElmer 2030 ARVO X4，PerkinElmer Life and Analytical Sciences). Aminoguanidine hydrochloride was used as a reference agent. The inhibitory ratio of the sample was calculated using the following formula:

$$\% \text{ inhibition} = 1 - [(\boldsymbol{F} \text{ sample} - \boldsymbol{F} \text{ sample blank}) / (\boldsymbol{F} \text{ control} - \boldsymbol{F} \text{ normal})] \times 100$$

where ***F*** control is the fluorescence with PBS containing glucose and BSA; ***F*** normal is the fluorescence with PBS containing glucose and BSA without incubation (stored at 4ºC); ***F*** sample is the fluorescence with sample solution in PBS containing glucose and BSA, ***F*** sample is blank the fluorescence with sample solution in PBS.

Each assay was performed in triplicate (P value < 0.01). IC_{50} value represents the concentration required to inhibit 50% of AGEs formation by incubation of glucose and albumin.

*2.5 Isolation of 3-C-β-D-glucosyl-2,4,4',6-tetrahydroxybenzophenone (**1**) and Mangiferin (**2**)*

The OML-ext (5.4 g) was submitted to a silica gel column chromatography with a stepwise gradient elution with $CHCl_3$/MeOH (10:0 v/v) to (0:10 v/v). Inhibition of AGEs formation at 25 μg/ml of each fraction was assayed. Fraction I (fr. 1-6) eluted firstly with $CHCl_3$ showed a significant activity. Fraction I was dark green, and it seemed to contain green pigments, such as chlorophyll as one of active constituents. Fraction II (fr. 7-25) eluted with $CHCl_3$/MeOH 30:1 v/v, 10:1 v/v, 5:1 v/v and 0:10 v/v also showed potent activity. Further purification of fraction II by a preparative HPLC led to isolation of **1** and **2** as described in the preceding paper (Itoh et al., 2016).

*2.6 Content of Chlorophyll, Total Anthocyanin, **1** and **2** in Mango Leaf Extracts*

In this paper, determination of each compound in leaf extracts was performed in triplicate, and values represent the mean ± standard deviation. Spectrophotometric determination of the content of chlorophyll (mg/g extract) was carried out with 80% acetone aqueous solution containing 2.5 mM sodium phosphate buffer (pH 7.8) according to the method of Porra et al. (Porra, Thompson, & Kriedemann, 1989). The content of total anthocyanin (μg/g extract) in each leaf extract was determined by the following HPLC analysis and shown as μg/g extract in which weight (μg) was calculated as that of an external standard, cyanidin-3-*O*-glucoside chloride. The extract was dissolved in 10% MeOH aqueous solution containing 10% acetic acid, followed by centrifugation at 12,000 G for 10 min. Resulting supernatant was applied to a HPLC system. The HPLC system consisted of LC-20A pump and SPD-20A photodiode array detector (Shimadzu, Kyoto, Japan). The samples were analyzed by using an Inertsil ODS-3 reverse phase column (4.6 × 150 mm, GL Sciences, Tokyo, Japan) and gradient elution with MeOH aqueous solution at a constant flow rate of 0.8 ml/min. The elution was carried out using linear gradient condition as follows; initial condition was set at 5% MeOH and maintained for 5 min, followed by a linear gradient from 5% to 40% MeOH for 35 min. The column temperature was set at 40ºC, and eluted compounds were detected at 520 nm. Total anthocyanins content was determined using total 520 nm peak areas from linear calibration curves made from an external standard, cyanidin-3-*O*-glucoside chloride. Linear calculation curves in the range of 0.02 to 0.1 nmol were made from the peak areas analyzed at 520 nm, and the correlation coefficient was 0.992. The HPLC determination of **1** and **2** in each leaf extract was described in the preceding paper (Itoh et al., 2016).

2.7 Statistical Analysis

The experimental data were evaluated for statistical significance using Bonferroni/Dunn's multiple-range test with GraphPad Prism for Windows, Ver. 5 (GraphPad Software Inc., 2007).

3. Results and Discussion

3.1 Identification of AGEs Formation Inhibitory Active Ingredients of OML-ext

In the preliminary evaluation of mango leaf extract on inhibitory activity of AGEs formation in nonenzymatic glycation of albumin, the OML-ext inhibited AGEs formation with the IC_{50} value of 43 μg/ml. To identify the active constituents, we carried out activity-guided fractionation of OML-ext using AGEs formation inhibitory assay. Silica gel column chromatographic fractionation of OML-ext gave two active fractions, fraction I and fraction II. The dark green color of fraction I suggested that this fraction may contain green pigments such as chlorophyll as an active ingredient.

Table 1. Inhibitory activities of 3-C-β-D-glucosyl-2,4,4',6-tetrahydroxybenzophenone (**1**), mangiferin (**2**), chlorophyll and cyanidin-3-*O*-glucoside chloride on AGEs formation

Samples	IC_{50} values [a)] (μM or μg/ml or mM)
3-C-β-D-glucosyl-2,4,4',6-tetrahydroxybenzophenone (**1**)	85 μM
Mangiferin (**2**)	18 μM
Chlorophyll	41 μg/ml
Cyanidin-3-*O*-glucoside chloride	32 μM
Aminoguanidine hydrochloride	0.9 mM

Aminoguanidine hydrochloride was used as reference compound. a); IC_{50} value represents the concentration required to inhibit 50% of AGEs

formation.

Further purification of another active fraction II led to isolation of **1** and **2** as active constituents. The IC_{50} values (Table 1) of **1** and **2** were 85 and 18 μM, respectively. As shown in Table 1, the IC_{50} value of aminoguanidine hydrochloride as a reference compound was 0.9 mM (= 99 μg/ml) in accordance with the reported IC_{50} value (138 μg/ml) (Shimoda et al., 2011). Thus, a part of the AGEs formation inhibitory activity of OML-ext is attributable to these two compounds. To the best of our knowledge, this is the first report on AGEs formation inhibitory activity of **1**. Mahali et al. (Mahali, Verma, & Manna, 2014) reported **2** inhibited AGE-mediated reactive oxygen intermediate generation and inhibited ERK and IKK activity, thereby suppression of sterol regulatory element binding protein activity and lipogenesis. Hou et al. (2016) described mangiferin reduced AGE formation and decreased the mRNA and protein expression of receptor for AGEs in diabetic cardiomyopathy model rats. In addition, Suchal et al. (2017) reported **2** attenuated ischemia-reperfusion induced myocardial injury in streptozotocin-induced diabetic rats by modulation of AGE-receptor/MAPK pathways which further prevented oxidative stress, inflammation and apoptosis in the myocardium. From the view point of structure-activity relationship, we will attempt to examine whether **1** and **2** have a similar inhibitory mechanism of AGEs formation because **1** and **2** belong to C-glucosyl-polyphenols.

3.2 A Relationship between Leaves Maturation and AGEs Formation Inhibitory Activity

We examined a relationship between leaves maturation and inhibitory activity of AGEs formation. The collected leaves were visually classified by the color of leaf into three groups as shown in Figure 1.

As shown in Table 2, OML-ext exhibited an inhibitory activity of AGEs formation with the IC_{50} value of 43 μg/ml. The IC_{50} values of young dark reddish brown mango leaf extract (YDL-ext) and young yellow leaf extract (YYL-ext) were 40 and 66 μg/ml, respectively (Table 2). The activity of YDL-ext was similar to that of OML-ext. The inhibitory activity of YYL-ext showed slightly decreased compared to those of OML-ext and YDL-ext. HPLC analysis revealed that the contents of **1** and **2** in these leaf extracts were high as described in the preceding paper (Itoh et al., 2016). Taking account of the inhibition data of **1** and **2**, and high contents of **1** and **2** in the extracts, the inhibitory activities of these extracts would be partly attributable to these compounds.

Table 2. Inhibitory activities of MeOH extracts of young dark reddish brown and young yellow leaves and old dark green mango leaves on AGEs formation

Samples	**IC_{50} values [a)] (μg/ml or mM)**
Young dark reddish brown leaf extract (= YDL-ext)	40 μg/ml
Young yellow leaf extract (= YYL-ext)	66 μg/ml
Old dark green leaf extract (= OML-ext)	43 μg/ml
Aminoguanidine hydrochloride	0.9 mM

Aminoguanidine hydrochloride was used as reference compound. a); IC_{50} value represents the concentration required to inhibit 50% of AGEs formation.

On the other hand, we can not exclude a hypothesis that other ingredients may also contribute to the activity. Ali et al. (1999) reported that young dark reddish brown mango (cv. Irwin) leaves contain anthocyanin, however, anthocyanin rapidly disappears and chlorophyll content increases with an increase in area after unfolding. Sami & Shakoori (2011) have isolated cyanidin-3-*O*-glucoside as an anthocyanin with cellulase inhibitory activity from mango leaves. These reports prompted us to evaluate inhibitory effects of chlorophyll and cyanidin-3-*O*-glucoside on AGEs formation, considering with the assumption that the dark green fraction I contained green pigments, such as chlorophyll as one of active ingredients as described above. As shown in Table 1, the IC_{50} values of chlorophyll and cyanidin-3-*O*-glucoside chloride were 41 μg/ml, 32 μM, respectively. Although AGEs formation inhibitory activity of anthocyanins including its inhibitory mechanism has been reported (Chen et al. 2014), there is no report on AGEs formation inhibitory effect of chlorophyll. The content of chlorophyll in each leaf extract was spectrophotometrically determined by the method of Porra et al. (1989). The content of total anthocyanin in each leaf extract was determined by a HPLC analysis. As a result, the content of chlorophyll in YDL-ext was 0.85 mg/g. The corresponding content data of other two leaf extracts were as follows; YYL-ext, 2.18 mg/g, and OML-ext, 4.34 mg/g. The content of chlorophyll in leaf extract were increased

with leaves enlargement. The contents of total anthocyanins in these leaf extracts were as follows; YDL-ext, 7.38 ± 0.24 μg/g; YYL-ext, 5.80 ± 0.59 μg/g; OML-ext, not detected of any anthocyanins. These data are in accordance with the reported data of Ali et al. (Ali, Koeda, & Nii, 1999). Considering with the content of chlorophyll and total anthocyanin in leaf extracts, the inhibitory activity of OML-ext was attributable to **1**, **2** and chlorophyll. The inhibitory activities of YDL-ext and YYL-ext were attributable to **1** and **2**, in addition, a part of the inhibitory activity of YDL-ext and YYL-ext was due to anthocyanins whose content is high in young dark reddish brown and young yellow mango leaves. On the other hand, to fully identify other active ingredients and to reveal the inhibitory mechanisms of **1** and chlorophyll, further studies are required, and now undergoing.

From the view point of utility of mango leaves, old dark green leaves obtained by summer pruning may be a reasonable natural resource for the preparation of ingredients with inhibitory activity of AGEs formation.

4. Conclusion

YDL-ext, YYL-ext and OML-ext exhibited inhibitory activities of AGEs formation in nonenzymatic glycation of albumin. The inhibitory activity of YDL-ext was similar to that of OML-ext, and YYL-ext was less potent than YDL-ext and OML-ext, this is the first report to reveal a relationship between leaves maturation and inhibitory activity of AGEs formation. The inhibitory activity of OML-ext was attributable to 3-C-*β*-D-glucosyl-2,4,4',6-tetrahydroxybenzophenone (**1**), mangiferin (**2**) and chlorophyll. Whereas the inhibitory activity of YDL-ext and YYL-ext were attributable to **1** and **2**, in addition, a part of the inhibitory activity of YDL-ext and YYL-ext was due to anthocyanins whose content is high in young dark reddish brown and young yellow mango leaves. This is the first report on AGEs formation inhibitory activity of **1** and chlorophyll. Hitherto, pruned mango leaves were unworthy and discarded during the cultivation process of mango fruit, these findings suggested that pruned mango leaves may be a useful resource for the preparation of ingredients for skin aging or diabetic complications such as diabetic nephropathy with having lipase inhibitory activity. However, further investigations are required to examine administration safety and the mechanisms involved and to reveal other active constituents.

Acknowledgment

We are grateful to all technical staffs of Yuasa Experimental Farm, Kindai University for the collection of mango leaves. I am deeply grateful to Dr. Shunsuke Naruto for his invaluable guidance and advice.

References

Ali K., Koeda K., & Nii, N. (1999). Changes in anatomical features, pigment content and photosynthetic activity related to age of 'Irwin' mango leaves. *Journal of the Japanese Society for Horticultural Science*, *68*(6), 1090-1098. https://doi.org/10.2503/jjshs.68.1090

Anusiri, P., Choodej, S., Chumriang, P., Adisakwattana, S., & Pudhom, K. (2014). Inhibitory effects of flavonoids from stem bark of *Derris indica* on the formation of advanced glycation end products. *Journal of Ethnopharmacology*, *158*, 437-441. https://doi.org/10.1016/j.jep.2014.10.053

Chen, X. Y., Huang, I. M., Hwang, L. S., Ho, C. T., Shiming, L., & Lo, C. Y. (2014). Anthocyanins in blackcurrant effectively prevent the formation of advanced glycation end products by trapping methylglyoxal. *Journal of functional foods*, *8*, 259-268. https://doi.org/10.1016/j.jff.2014.03.025

Chompoo, J., Upadhyay, A., Kishimoto, W., Makise, T., & Tawata, S. (2011). Advanced glycation end products inhibitors from *Alpinia zerumbet* rhizomes. *Food Chemistry*, *129*, 709-715. https://doi.org/10.1016/j.foodchem.2011.04.034

Dyer, D. G., Dunn, J. A., Thorpe, S. R., Bailie, K. E., Lyons, T. J., McCance, D. R., & Baynes, J. W. (1993). Accumulation of Maillard reaction products in skin collagen in diabetes and aging. *Journal of Clinical Investigation*, *91*, 2463-2469. https://doi.org/10.1172/JCI116481

Hou, J., Zheng, D., Fung, G., Deng, H., Chen, L., Liang, J., … Hu, Y. (2016). Mangiferin suppressed advanced glycation end products (AGEs) through NF-κB deactivation and displayed anti-inflammatory effects in streptozotocin and high fat diet-diabetic cardiomyopathy rats. *Canadian Journal of Physiology and Pharmacology*, *94*(3), 332-340. https://doi.org/10.1139/cjpp-2015-0073

Huebschmann, A. G., Regensteiner J. G., Vlassara H., & Reusch J. E. B. (2006). Diabetes and advanced glycoxidation end products. Diabetes Care, *29*(6), 1420-1432. https://doi.org/10.2337/dc05-2096

Itoh, K., Murata, K., Nakagaki, Y., Shimizu, A., Takata, Y., Shimizu, K., … Matsuda, H. (2016). Inhibitory activity of *Mangifera indica* leaf extract on pancreatic lipase. Journal of Plant Studies, *5*(2), 72-78. https://doi.org/10.5539/jps.v5n2p72

Lohwasser, C., Neureiter, D., Weigle, B., Kirchner, T., & Schuppan, D. (2006). The receptor for advanced glycation end products is highly expressed in the skin and upregulated by advanced glycation end products and tumor necrosis factor-alpha. *Journal of Investigative Dermatology*, *126*(2), 291-299. https://doi.org/10.1038/sj.jid.5700070

Mahali, S. K., Verma, N., & Manna, S.K. (2014). Advanced glycation end products induce lipogenesis: regulation by natural xanthone through inhibition of ERK and NF-κB. *Journal of Cellular Physiology*, *229*(12), 1972-1980. https://doi.org/10.1002/jcp.24647

Morimitsu, Y., Yoshida, K., Esaki, S., & Hirota, A. (1995). Protein glycation inhibitors from thyme (*Thymus vulgaris*). *Biosci Biotechnol Biochem.*, *59*(11), 2018-2021. https://doi.org/10.1271/bbb.59.2018

Pageon, H., Bakala, H., Monnier, V. M., & Asselineau, D. (2007). Collagen glycation triggers the formation of aged skin in vitro. *European Journal of Dermatology*, *17*(1), 12-20. https://doi.org/10.1016/j.plantsci.2013.12.014

Porra R. J., Thompson W. A., & Kriedemann P. E. (1989). Determination of accurate extinction coefficients and simultaneous equations for assaying chlorophylls *a* and *b* extracted with four different solvents: verification of the concentration of chlorophyll standards by atomic absorption spectroscopy. *Biochimica et Biophysica Acta*, *975*, 384-394. https://doi.org/10.1016/S0005-2728(89)80347-0

Sami, A. J., & Shakoori, A. R. (2011). Cellulase activity inhibition and growth retardation of associated bacterial strains of *Aulacophora foviecollis* by two glycosylated flavonoids isolated from *Mangifera indica* leaves. *Journal of Medicinal Plants Research*, *5*(2), 184-190.

Shimoda, H., Nakamura, S., Morioka, M., Tanaka, J., Matsuda, H., & Yoshikawa, M. (2011). Effect of cinnamoyl and flavonol glucosides derived from cherry blossom flowers on the production of advanced glycation end products (AGEs) and AGE-induced fibroblast apoptosis. *Phytotherapy Research*, *25*, 1328-1335. https://doi.org/10.1002/ptr.3423

Sourris, K. C., Harcourt, B. E., & Forbes, J. M. (2009). A new perspective on therapeutic inhibition of advanced glycation in diabetic microvascular complications: common downstream endpoints achieved through disparate therapeutic approaches? *American Journal of Nephrology*, *30*, 323-335. https://doi.org/10.1159/000226586

Suchal, K., Malik, S., Khan, S. I., Malhotra, R. K., Goyal, S. N., Bhatia, J., … Arya, D. S. (2017). Protective effect of mangiferin on myocardial ischemia-reperfusion injury in streptozotocin-induced diabetic rats: role of AGE-RAGE/MAPK pathways. *Scientific Reports*, *7*, 1-11. https://doi.org/10.1038/srep42027

Tsuji-Naito, K., Saeki, H., & Hamano, M. (2009). Inhibitory effects of *Chrysanthemum* species extracts on formation of advanced glycation end products. *Food Chemistry*, *116*, 854-859. https://doi.org/10.1016/j.foodchem.2009.03.042

Wondrak, G. T., Roberts, M. J., Jacobson, M. K., & Jacobson, E. L. (2002). Photosensitized growth inhibition of cultured human skin cells: mechanism and suppression of oxidative stress from solar irradiation of glycated proteins. *Journal of Investigative Dermatology*, *119*, 489-498. https://doi.org/10.1046/j.1523-1747.2002.01788.x

Xu, Y., Liu, G., Yu, Z., Song, X., Li, X., Yang, Y., … Dai, J. (2016). Purification, characterization and antiglycation activity of a novel polysaccharide from black currant. *Food Chemistry*, *199*, 694-701. https://doi.org/10.1016/j.foodchem.2015.12.078

Journal of Plant Studies; Vol. 6, No. 2; 2017
ISSN 1927-0461 E-ISSN 1927-047X
Published by Canadian Center of Science and Education

Reviewer Acknowledgements

Journal of Plant Studies wishes to acknowledge the following individuals for their assistance with peer review of manuscripts for this issue. Their help and contributions in maintaining the quality of the journal are greatly appreciated.

Journal of Plant Studies is recruiting reviewers for the journal. If you are interested in becoming a reviewer, we welcome you to join us. Please find the application form and details at http://www.ccsenet.org/reviewer and e-mail the completed application form to jps@ccsenet.org.

Reviewers for Volume 6, Number 2

Ahmed Ghannam, University of Strasbourg, France

Alfredo Benavente, Consejería de Agricultura, Pesca y Medioambiente, Spain

Ami Lokhandwala, University of Mississippi, Department of Biology, USA

Bingcheng Xu, Chinese Academy of Sciences and Ministry of Water Resources, China

Chrystian Iezid Maia e Almeida Feres, Tocantins Federal University, Brazil

Estelle Dumont, université Aix-Marseille, France

Homa Mahmoodzadeh, Department of Biology, Mashhad Branch, Islamic Azad University, Mashhad, Iran

Khyati Hitesh Shah, Stanford University, United States

Kinga Kostrakiewicz-Gieralt, Institute of Botany, Jagiellonian University, Poland

Konstantinos Vlachonasios , Aristotle University of Thessaloniki, School of Biology, Greece

Martina Pollastrini, University of Florence, Italy

Massimo Zacchini, National Research Council of Italy (CNR), Italy

Melekber Sulusoglu, Arslanbey Vocational School Kocaeli University, Turkey

Mohamed Trigui, Sfax Preparatory Engineering Institute and CBS, Tunisia

Rajiv Ranjan, T. P. Varma College, India

Rajnish Sharma, Dr YS Parmar University of Horticulture & Forestry, Solan (HP), India

Rakesh Ponnala, Zoetis Inc, United States

Rocío Deanna, Instituto Multidisciplinario de Biología Vegetal, Argentina

Said Laarabi, University Mohammed V/Ministry of National Education, Morocco

Slawomir Borek, Adam Mickiewicz University, Poland

Suheb Mohammed, University of Virginia, United States

Tomoo misawa, Donan Agricultural Experiment Station, Hokkaido Research Organization, Japan

The journal is peer-reviewed
The journal is open-access to the full text
The journal is included in:

AGRICOLA
BASE (Bielefeld Academic Search Engine)
CABI's full text
Chemical Abstracts Service (CAS)
EZB–Elektronische Zeitschriftenbibliothek – Universitätsbibliothek Regensburg
Google Scholar
Index Copernicus
InfoBase Index
Journal Impact Factor
JournalTOCs
LOCKSS
PKP Open Archives Harvester
SHERPA/RoMEO
Standard Periodical Directory
WorldCat

Journal of Plant Studies
Semiannual

Publisher Canadian Center of Science and Education
Address 1120 Finch Avenue West, Suite 701-309, Toronto, ON., M3J 3H7, Canada
Telephone 1-416-642-2606
Fax 1-416-642-2608
E-mail jps@ccsenet.org
Website http://jps.ccsenet.org

ISSN 1927-0461